Design, synthesis and evaluation of novel endoprotease-activated prodrugs and fluorogenic probes with theranostic applications in chemotherapy

Yao Ding

Thesis submitted in partial fulfilment of the requirements of Edinburgh Napier University for the degree of Doctor of Philosophy

January 2014

Abstract of Thesis

Proteolytic degradation of the extracellular matrix (ECM) by overexpressed endoproteases, notably the matrix metalloproteinase MMP-9 and legumain (human asparaginyl endopeptidase), contributes to the invasive and migratory phenotype of cancer cells and promotes metastases. These proteases represent valid biological targets in cancer for diagnostic and therapeutic purposes.

In this research programme, novel MMP-substrate oligopeptide prodrugs of potent anticancer agents have been rationally designed for activation selectively in the tumour microenvironment. Prodrugs of experimental colchicine-based cytotoxic and vascular disrupting agents, experimental anthraquinone-based agents or clinically-active drugs, including epirubicin, have been synthesised by both solution- and solid-phase peptide methods, and characterised. Results of the preliminary cytotoxic and DNA-binding properties of examples of active agents are reported.

Furthermore, the approach has been extended to legumain, which is overexpressed in colon, breast and ovarian cancers and is capable of extracellular proteolytic activity. A series of novel substrates of legumain has been designed and characterised by high resolution mass spectrometry. The new peptide substrates have been developed as fluorogenic molecular probes of legumain for diagnostic applications in the early detection of cancer. The novel substrates exploit the proteolytic activity of legumain to cleave uniquely at the C-terminus of asparagine residues. The new peptide substrates, exemplified by prototype fluorogenic probe TL11 (FAM-Pro-Ala-Asn-Leu-PEG-AQ) are efficient FRET substrates in which fluorescein-based (donor) fluorescence is fully quenched by an aminoanthraquinone residue (acceptor). Proof of principle has been demonstrated by use of recombinant human legumain which cleaves the substrate library efficiently as shown by fluorescence spectroscopic methods. The tetrapeptide sequence pro-X-asn↓-leu was shown to be sensitive when X= ala, ser or thr (wherein ↓indicates the legumain cleavage 'hotspot'). The approach was also shown to be extendable to a therapeutic prodrug approach with the potential to selectively deliver potent agents to the tumour microenvironment.

It is hereby declared that this thesis and the research work upon which it is based were conducted by the author.

Yao Ding

Contents

Acknowledgements

Preface

Results from this research programme have been reported, in part, in the following publications:

Ding, Y., Lam, T., Turnbull, A. and Mincher, D. J. (2013) Exploiting the 'dark side' of the tumour associated, putative biomarker legumain (human asparaginyl endoprotease) in the detection and drug-targeting of tumours. *Joint 34th EORTC-PAMM-BACR Winter Meeting*, National Museum Cardiff, Wales, UK, 23rd-26th January. Abstract. P10

Ding, Y., Van Valkenborgh, E., Lavado, A., Vanderkerken, K., Turnbull, A., Bibby, M. C. and Mincher, D. J. (2013) Selective cellular activation of vascular disrupting and cytotoxic agents in the microenvironment of murine and human multiple myeloma. *Joint 34th EORTC-PAMM-BACR Winter Meeting*, National Museum Cardiff, Wales, UK, 23rd-26th January, Abstract. P27

Finlay, C., **Ding, Y.**, Turnbull, A., Stevens, C. and Mincher, D. J. (2013) Design of novel theranostic, vascular disrupting prodrug substrates of legumain: applications in cancer treatment and detection. *Proceedings of the APS Pharm Sci 2013 Conference: The Science of Medicines*, Heriot-Watt University, Edinburgh, UK 2nd – 4th September 2013 (oral and poster presentation) Abstract. 202

Mincher, D. J., **Ding, Y.**, Lam, T., MacCallum, J. and Turnbull, A. (2012) Design activation of novel fluorogenic oligopeptide substrate probes of legumain with theranostic applications in breast and ovarian cancer. *8th NCRI Cancer Conference*, BT Convention Centre, Liverpool, UK, November 4-7. NCRI 2006-2012, Abstract. B60. Available at: http://conference.ncri.org.uk/abstracts/2012/abstracts/B60.html

Graphical Abstract Concept Diagrams

Chapter 1. MMP9-Targeted Prodrugs and Fluorogenic Substrate Probes: Design Strategy

Chapter 1 presents the results and discussion of experiments directed to the synthesis of Matrix Metalloproteinase (MMP)-activated fluorogenic substrate probes (in part) <u>and</u> principally, novel prodrugs of anticancer agents designed to release the active agents in the tumour microenvironment by exploiting the proteolytic action of overexpressed proteases. The active agents were either experimental colchicine-based vascular disrupting agents or clinically useful drugs, e.g. epirubicin.
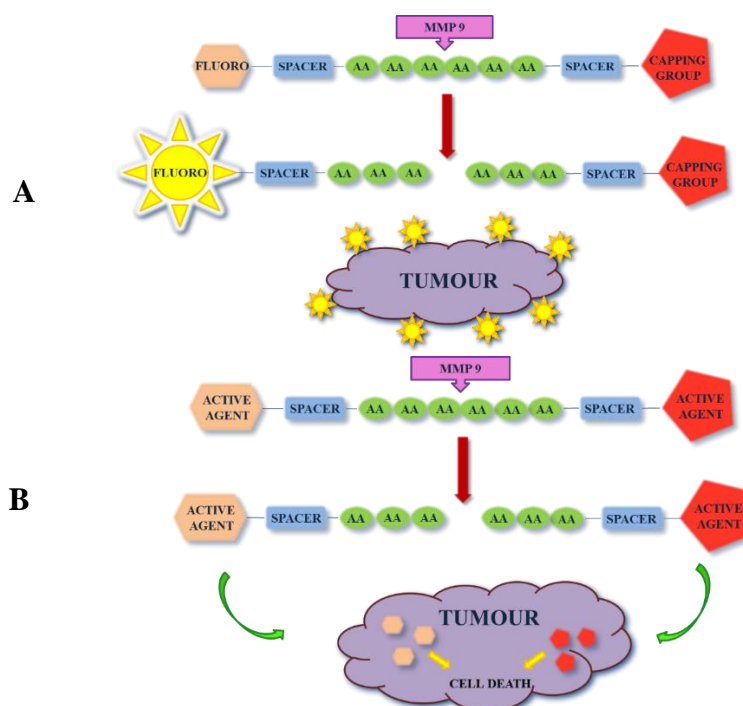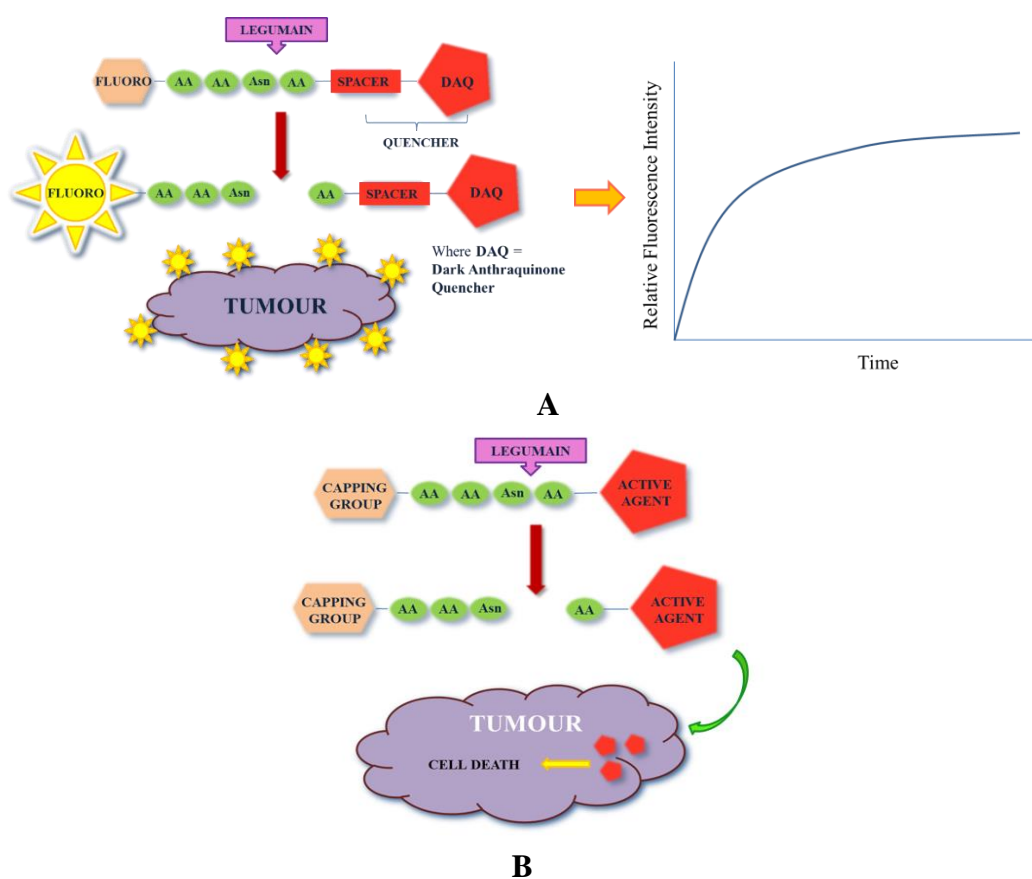

Figure P1. Design strategy for MMP9 fluorogenic probes (A) and prodrugs (B)

In **Figure P1**, **(A)** illustrates that once a latent fluorogenic FRET probe(s) is cleaved by MMP9 at the preferred cleavage site, the fluorophore may then be released from its 'dark' (aminoanthraquinone) quencher with restoration of its fluorescence. Hence, the fluorescence would indicate the presence of tumour cells and protease markers for diagnostic purposes; **(B)** shows a therapeutic twin-prodrug approach in which released active agents may enter into tumour cells and lead to cell death after prodrug cleavage by MMP9 at its designed cleavage site.

Chapter 2. Legumain-Targeted Prodrug and Molecular Probe Design

Chapter 2 presents the results and discussion of a major study directed to the design, synthesis and characterisation of novel fluorogenic substrates of the tumour-associated endoprotease legumain, a putative cancer biomarker, for diagnostic applications in the early detection of cancer. The approach is also extendable to a therapeutic prodrug approach to selectively deliver potent agents to the tumour microenvironment. In each case, the design strategy relies upon exploiting the unique strict substrate specificity of legumain for cleavage at the *C*-terminus of asparagine residues.


A

B

Figure P2. General design of legumain fluorogenic substrate probes (A) and prodrugs (B)

In **Figure P2**, **(A)** illustrates the general design strategy for activation of legumain fluorogenic probes. Once the latent fluorogenic FRET probe is cleaved at the *C*-terminus of asparagine, the released fluorescence will detect the biomarker or location of tumour cells; **(B)** shows the design of legumain specific prodrugs, with active agent and a capping group (which may be replaced by a second active agent) for tumour-specific targeting.

Chapter 3. DNA Binding Study on Novel Anthracenediones: Active agents (prodrug 'warheads') and Dark Quenchers (in Fluorogenic Substrates)

This study focuses on the synthesis and physicochemical properties of some anthraquinone amino acid conjugates which a members of a wider series, related to the anticancer drug mitoxantrone, and which were variously chosen to act as active agents and/or quenchers in the main aspects of the research; namely, the design of endoprotease-activated protease prodrugs and substrates.
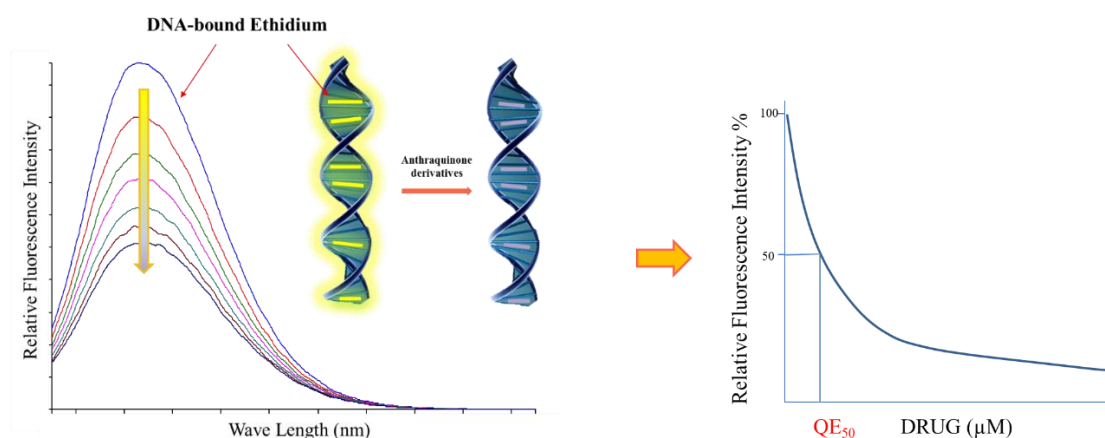

Figure P3. Ethidium bromide-DNA binding displacement study

Various anthraquinone-based active agents, capable of incorporation as 'warheads' in either of the endoprotease-mediated activation of substrate probes or prodrugs (of MMPs or legumain) were compared by using an ethidium bromide-DNA binding displacement assay, as shown in **Figure P3**. DNA-ethidium complexes are fluorescent was replaced with anthraquinone derivatives, its fluorescence would decrease. Hence, by measuring the decease of DNA-bound ethidium fluorescence, it is possible to determine an active agent's DNA binding ability within a closely related series.

Nomenclature

The structures below represent the compounds prepared in this study in their simplest format.
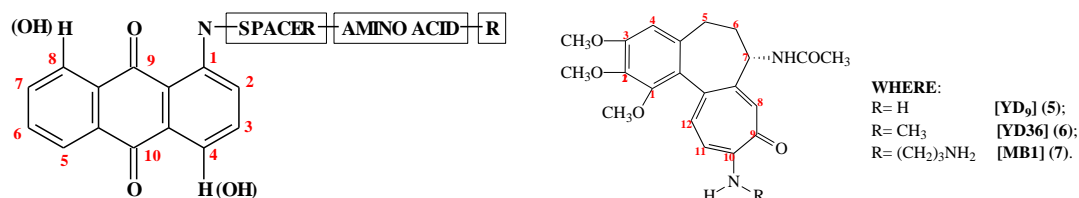
Figure P4. General structures of anthraquinone conjugates and colchicine derivatives

The terms anthraquinone, anthra-9,10-quinone, anthracenedione and anthracene-9,10-dione have been used interchangeably, since they are all in common usage. The anthraquinones (aminated anthraquinones or conjugates of amino acids or peptides) synthesised in this study are regarded fundamentally as anthraquinones i.e. anthraquinones substituted with amino ($RNH-$ or R_1R_2N-) side-chains in either the 1- or 2- position. As such, anthraquinone amino acid/ peptide conjugates derived from simple aminoalkylamino spacer groups have been named as substituted anthraquinones, according to the numbering system shown in the figure. Aminoalkylamino groups have been abbreviated to, for example, 'propyl' or 'propyl-spacer' in terminology representing the species $-NH-(CH_2)_3-NH-$ when set in the context of spacer linked conjugates and are convenient descriptors for the simpler spacer groups in these molecules. The spacer (or linker) groups have been further abbreviated for convenience (in chapter 1), for example, the species $-NH-(CH_2)_3-NH-$ is denoted as APA (aminopropylamino); this system has been adopted to simplify the description of relatively complex prodrugs containing active agents connected to a peptide carrier via spacer groups (consistent with practices exemplified in the Literature). It is anticipated that the meaning of these descriptors facilitates communication and will be obvious from the context.

Example A: 4-hydroxy-1-[3-(*N*-tertiarybutoxycarbonylglycylamino)propylamino] anthraquinone
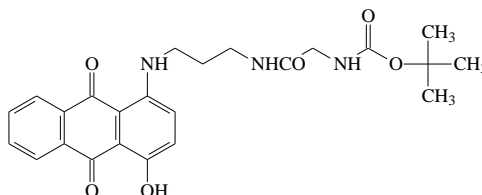
4-hydroxy-1-(Boc-Gly-[Propyl Spacer])-AQ YD3 **(16) [Chapter 3]**

More generally, the example may be described as 'an *N*-protected, propyl-linked glycine conjugate' wherein *propyl* is a shorthand description for the spacer moiety.

Example B: 1-{2-[2-(2-(*N*-5(6)-carboxyfluoresceinylcarbonyl-L-prolyl-L-alanyl-L-asparaginyl-L-leucylamino)ethoxy)ethoxy]ethylamino}anthracene-9,10-dione
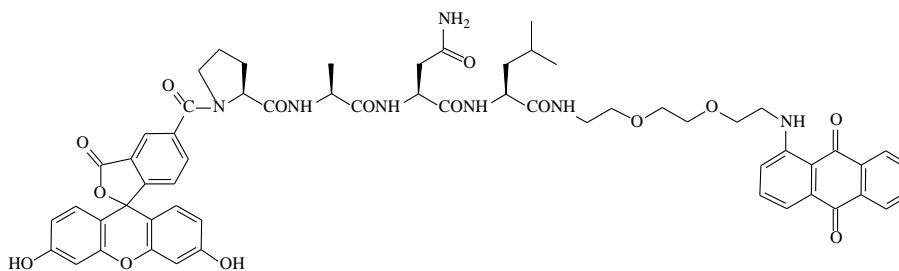
5(6)-FAM-Pro-Ala-Asn-Leu-[PEG Spacer]-AQ [TL11] **(3) [Chapter 2]**

In example B, descriptors for the aminoacyl residues derived from the component amino acids are conveniently used to describe B as: an L-prolyl-L-alanyl-L-asparaginyl-L-leucyl PEG spacer tetrapeptide conjugate. [The peptide is thus described conventionally, with the *N*-terminus 'to the left'].

Example C: A 'non-identical twin' hexapeptide prodrug with colchicine- and anthraquinone- based active agents (showing piperazine and dimethylpiperazine spacer residues)
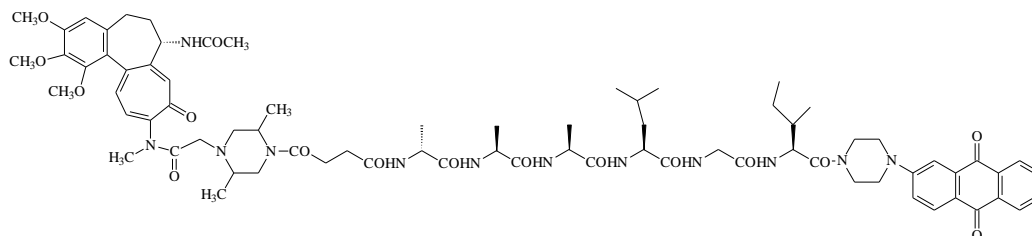
YD36-DMPIP-SUCC-D-Ala-Ala-Ala-Leu-Gly-Ile-PIP-AQ (YD 42) **(29) [Chapter 1]**

Note: During discussion of anthraquinone-oligopeptide conjugates of this type, particularly during enzyme studies of Example B, it was convenient to describe molecules as having residual amino acid fragments attached to the anthraquinone-spacer [AQ-SP] compounds, as in a (truncated) e.g. AQ-SP-Leu-Asn dipeptide conjugate, wherein it was understood that neither the amino acid sequence was altered nor the amino terminus reversed [i.e. that Asn was the amino terminus and that the correct interpretation would be unambiguous from the context in which these passages occurred].

Note: With regard to the **spacer group**, EXAMPLES of convenient descriptors have been adopted:

SPACER RESIDUE	DESCRIPTOR
	APA (aminopropylamino)
	PEG (polyethylene glycol-like spacer)
	PIP (piperazinyl-spacer)
	DMPIP (dimethylpiperazinyl-spacer)
	SUCC (succinyl/succinate)

Abbreviations

ADEPT	antibody-directed enzyme prodrug therapy
AEP	asparaginyl endopeptidase (legumain)
AMC	7-amino-4-methylcoumarin
APMA	4-aminophenyl mercuric acetate
AQ	anthraquinone
Boc (or ^{t}Boc)	tertiarybutoxycarbonyl
CEA	carcinoembryonic antigen
CT	cytoplasmic tail
DCC	dicyclocarbodiimide
DCU	dicyclohexylurea
DIPEA	*N,N*-diisopropylethylamine
DMAP	4-(*N,N*-dimethylamino)pyridine
DMF	*N,N*-dimethylformamide
DMSO	dimethyl sulphoxide
EB	ethidium bromide
ECM	extracellular matrix
EPR	enhanced permeability and retention
ER	estrogen receptor
ESI	nanoelectrospray ionisation
ETR	electron transfer reagent
FAM	carboxyfluorescein
FCS	foetal calf serum
FITC	fluorescein isothiocyanate isomer I
Fmoc	fluorenylmethoxycarbonyl
FRET	fluorescence resonance energy transfer
HBTU	*N,N,N′,N′*-tetramethyl-*O*-(1H-benzotriazol-1-yl)uronium hexafluorophosphate
HE4	human epididymis protein 4
HOBt	1-hydroxybenzotriazole
HPLC	high-performance liquid chromatography
IGF	insulin like growth factor
INT	2-(4-iodophenyl)-3-(4-nitrophenyl)-5-phenyltetrazolium chloride
IC$_{50}$	lethal concentration, 50%
LD$_{50}$	lethal dose, 50%
LDH	lactate dehydrogenase
LEG-3	*N*-succinyl-β-alanyl-L-alanyl-L-asparaginyl-L-leucyl-doxorubicin
LEG-4	*N*-succinyl-L-alanyl-L-asparaginyl-L-leucyl-doxorubicin
Leu-Epi	*N*-L-leucyl-Epirubicin
Leu-Dox	*N*-L-leucyl-Doxorubicin
LPS	lipopolysaccharide
mAbs	monoclonal antibodies
MCF-7	Michigan Cancer Foundation-7 (breast cancer cell line)
MES	2-(*N*-morpholino)ethanesulfonic acid
MM	multiple myeloma
mmol	millimole(s)
MMPs	matrix metalloproteinases
MTD	maximum tolerable dose

MT-MMPs	membrane-type MMPs
MTS	3-(4,5-dimethylthiazol-2-yl)-5-(3-carboxymethoxyphenyl)-2-(4-sulfophenyl)-2H-tetrazolium
MTT	3-(4,5-dimethylthiazol-2-yl)-2,5-diphenyltetrazolium bromide
NAD$^+$	nicotinamide adenine dinucleotide
NADH	nicotinamide adenine dinucleotide (reduced form).
NMR	nuclear magnetic resonance
NU:UB	Napier University: University of Bradford (compound codes)
O^{t}Bu	*O-tert*-butyl
OPFP	*O*-pentafluorophenolate
OSu	succinimidyl
PBS	phosphate buffered saline
PDEPT	polymer-directed enzyme prodrug therapy
PEG	polyethylene glycol
PFP	pentafluorophenyl
PMS	phenazine methosulfate
PMSF	phenylmethanesulphonyl fluoride
ppm	parts per million
pro	pro-domain
PyBOP	(benzotriazol-1-yloxy)tripyrrolidinophosphonium hexafluorophosphate
R$_f$	retention factor
RFU/I	relative fluorescence unit/intensity
RT	room temperature
SPPS	solid phase peptide synthesis
ss	signal sequence
TAMs	tumour associated macrophages
TBTU	*O*-(benzotriazol-1-yl)-*N*,*N*,*N'*,*N'*-tetramethyluronium tetrafluoroborate
TC	tetracycline
TFA	trifluoroacetic acid
TGF	transforming growth factor
THF	tetrahydrofuran
TLC	thin layer chromatography
TMEAP	tumour microenvironment activated prodrug
TM	transmembrane domain
Trt	trityl
TSTU	*O*-(*N*-succinimidyl)-1,1,3,3-tetramethyluranium tetrafluoroborate
VEGF	vascular endothelial growth factor
VPE	vacuolar processing enzyme
Z-AAN-AMC	benzyloxycarbonyl-Ala-Ala-Asn-7-amido-4-methylcoumarin

Contents

Chapter I. MMP9-Targeted Prodrugs and Fluorogenic Substrate Probes

1.1 INTRODUCTION

1.1.1 Aim

The principal aim of this research is to design systems for the selective targeting of the microenvironment of tumours (and potentially, bacteria-infected tissues) using a prodrug approach and exploiting the proteolytic action of overexpressed enzymes (proteases) in the extracellular matrix (ECM); ultimately, to improve therapeutic index and reduce side effects for patients.

Figure 1.1. General structure of prodrugs in this project

Figure 1.1 outlines the general structure of prodrugs which were designed and synthesised in this project. Generally, these prodrugs have three parts: the oligopeptide carrier which can be cleaved off once the prodrug binds to proteolytically active forms of enzymes (proteases); the active agents on both ends of the prodrug are ideally twin active drugs (identical or non-identical) that can target tumours (or bacteria-infected tissues); and also the linker, usually an ester or amide-containing group, which connects the active agent onto the oligopeptide carrier. In these approaches, the targeted proteases are associated with the extracellular matrix (ECM). The main focus of the project is to incorporate vascular disrupting agents (VDAs) into novel substrates targeted to human MMP-9.

1.1.2 Extracellular matrix (ECM)

The extracellular matrix (ECM) is a network of molecules separating and supporting tissues, which is constituted by structural components, for instance proteoglycans, glycoproteins and collagens. Timely degradation of the ECM is essential for reproduction, morphogenesis, and tissue resorption and remodelling. However, excessive degradation of the ECM may lead to various pathologies such as arthritis, cancer, chronic ulcers, fibrosis and cardiovascular diseases. Several kinds of proteinases are involved in ECM degradation, but matrix metalloproteinases (MMPs) are the primary enzymes in the degradation of the ECM (McCawley and Matrisian, 2000; Nagase *et al.*, 2006; Vargová *et al.*, 2012). Excess breakdown of the matrix is a crucial step of tumour progression [**Figure 1.2**].
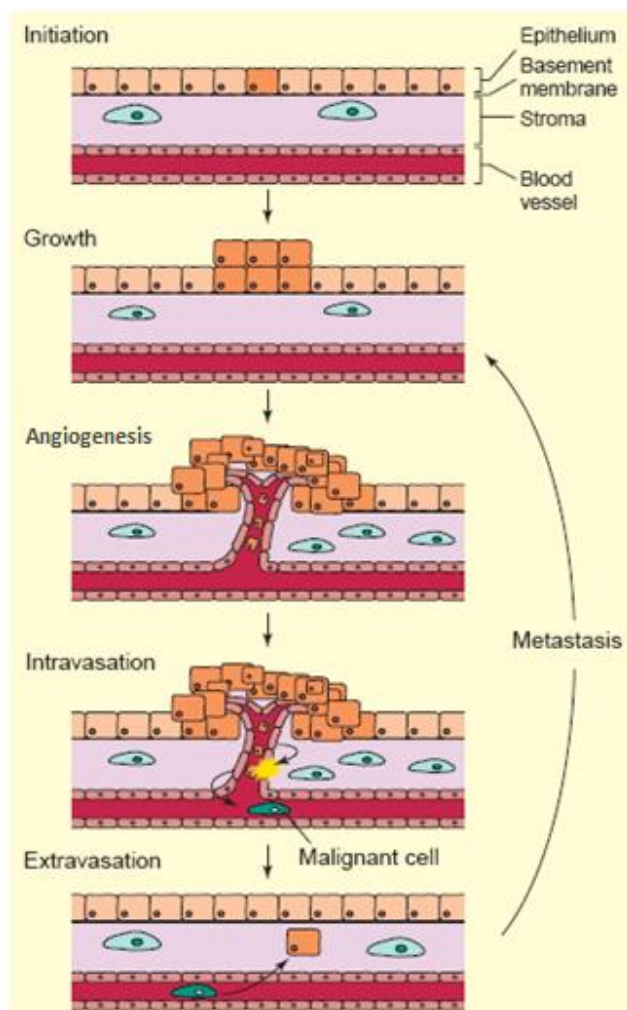
Figure 1.2. Process of tumour progression. (McCawley and Matrisian, 2000)

A single tumour cell needs nutrients supply from angiogenesis for further growth. The tumour cell must pass through the basement membrane for its invasion and metastasis. It then enters the circulation to a distant site where it has to leave the circulation, pass through the host tissue, and penetrate the basement membrane again. Metastases are established if tumour cells can grow at this new distant site.

1.1.3 Matrix Metalloproteinases (MMPs)

Matrix Metalloproteinases (MMPs), also called matrixins, are a family of secreted and membrane-associated zinc-dependent proteinases and peptide hydrolases, which once activated have the ability to degrade a variety components of the extracellular matrix (Birkedal-Hansen *et al*., 1993; Stetler-Stevenson, 1999; Hidalgo and Eckhardt, 2001; Tallant *et al*., 2010). Most MMPs have very low activities in the normal tissues; MMPs were first discovered a half century ago by Gross and Lapiere, who tried to explain how the tail came off from a metamorphosing tadpole (Gross and Lapiere, 1962). Since then a number of matrix metalloproteinases have been discovered in several physiological remodelling processes (i.e. embryonic development, bone and growth plate remodelling, ovulation, wound healing), and in some important disease processes such as tumour invasion (Woessner, 1991; Dufour and Overall, 2013).

1.1.4 Human MMPs domain structure

Twenty six human MMP enzymes have been found in the past four decades and they are classified in five groups (collagenases, gelatinases, stromelysins, membrane-type MMPs and others), which are based on their primary structure, substrate specificity and cellular location (Birkedal-Hansen *et al*., 1993; Clark *et al.*, 2008; Verma and Hansch, 2007; Vargová *et al.*, 2012).

There are three collagenases: MMP-1 (collagenases-1), MMP-8 (collagenases-2) and MMP-13 (collagenases-3). Propeptide, catalytic and hemopexin domains can be found in these three collagenases. The cooperation between catalytic and hemopexin domains is regarded as an essential part of these three collagenases' collagenolytic activity. These collagenases can make a single cleavage to give ¾ and ¼ of the length of triple-helical collagen (Birkedal-Hansen *et al*., 1993; Chung *et al*., 2004; Tallant *et al*., 2010).

MMP-2 (gelatinase A) and MMP-9 (gelatinase B) are both type IV collagenases but because they perform much better in cleaving gelatin, they were named gelatinases. Both gelatinases have three repeats of a fibronectin type II motif for gelatin binding in the catalytic domain (Birkedal-Hansen *et al*., 1993). The size difference between the two gelatinases is gelatinase B (92kDa) has a longer hinge region than gelatinase A (72kDa) (DeClerck, 2000).

Three stromelysins have been identified: MMP-3 (stromelysin-1) and MMP-10 (stromelysin-2) have nearly the same function, degrading fibronectin, laminin, and gelatin of the ECM (Birkedal-Hansen *et al*., 1993). Although MMP-11 (stromelysin-3) has very weak activity toward ECM proteins (Murphy *et al*., 1993), it can degrade serpin (serine proteinase inhibitor) and antitrypsin (α_1-antiproteinase inhibitor) (Birkedal-Hansen *et al*., 1993; Van Valckenborgh *et al*., 2004). Both MMP-3 and MMP-10 are secreted in the form of inactive proMMPs (zymogens) from the cells, while MMP-11 is activated by furin intracellularly and secreted as an active enzyme (Pei and Weiss, 1995).

MMP-7 (matrilysin 1) and MMP-26 (matrilysin 2) do not have a hemopexin domain and MMP-7 is the smallest one (28kDa) among the MMP family. Research showed that it can digest ECM molecules and also degrade cell surface molecules into soluble forms. Different from other MMPs, MMP-7 is expressed by tumour cells other than stromal cells (Liu *et al*., 2007). MMP-26 is expressed in both carcinomas and normal epithelial cells and degrades ECM components (Marchenko *et al*., 2004).

Membrane-type MMPs (MT-MMPs) are not secreted, but attached to the cell surface by 24 amino acids from their transmembrane domain. MT-MMPs also have a short cytoplasmic domain that could help MT-MMPs move to the front edge of the cells (Lehti *et al*., 2000). There are two types of MT-MMPs: MMP-14,-15,-16 and -24 (type I

transmembrane proteins) and MMP-17 and -25 (glycosylphosphatidylinositol-anchored proteins). All MT-MMPs can activate proMMP-2, except MT4-MMP (MMP-17) (English *et al.*, 2001). ProMMP-13 can be activated on the cell surface by MT1-MMP (MMP-14) (Knäuper *et al.*, 1996).
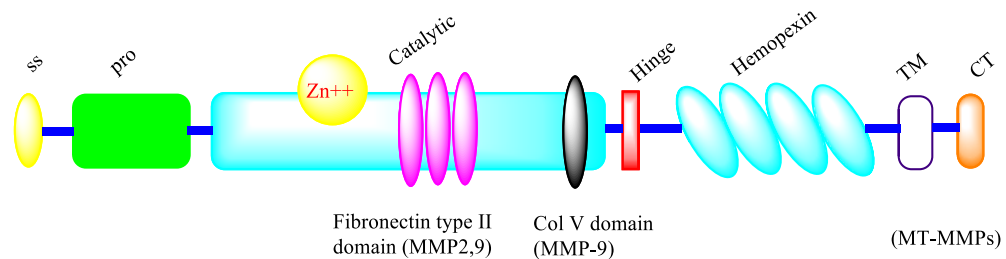
Figure 1.3. MMPs domain structure. signal sequence (ss); pro-domain (pro); transmembrane domain (TM); cytoplamic tail (CT) (Adapted from Zucker *et al*., 2002).

Figure 1.3 shows the basic structure of MMPs, which typically have five domains (from the *N* terminus): a signal peptide domain, a propeptide domain that has a "cysteine switch", a catalytic domain, a hinge region, and a hemopexin-like domain. However, there are some exceptions in the domain structure: there is no linker peptide and hemopexin-like domain in MMP-7 (matrilysin 1), MMP-26 (matrilysin 2) and MMP 23; two additional inserts at the *C* terminus are found in MT-MMPs, which are transmembrane domain and cytoplasmic domains. Only MT-MMPs and MMP-11 contain the furin-consensus sequence; MMP-2 and MMP-9 also have a fibronectin-like domain; a collagen-V-like domain can be found in MMP-9; MMP-23 also has cysteine rich and Ig domain (Zucker *et al*., 2002; Murphy and Nagase, 2008; Vargová *et al.*, 2012).

1.1.5   <u>Activation of MMPs</u>

Most MMPs, apart from MT-MMPs and MMP-11, MMP-21, MMP-23, MMP-28, are secreted in inactive forms and are activated by dissociating the *N*-terminal propeptide domain (Yu and Woessner, 2000; Cunningham *et al*., 2005). The *N*-terminal prosequence,

also called propeptide domain, is about 80 amino acids large and performs as an internal inhibitor and keeps the enzyme in an inactivated form. In the inactive MMPs, the unpaired cysteine thiol group in the propeptide binds to a Zn atom in the active site. Upon activation, as shown in **Figure 1.4**, the cysteine-zinc bonding has to be disrupted by a water-zinc interaction (the cysteine switch) (Birkedal-Hansen, 1995). *In vitro*, MMPs can be activated by two general methods: applying proteolysis or chemical activators such as 4-aminophenyl mercuric acetate (APMA). The propeptide domain which has cysteine residue can be degraded by proteolytic treatment. While in the activation with APMA, it can modify cysteine, hence APMA can disconnect cysteine-zinc bonding permanently (Van Wart and Birkedal-Hansen, 1990; Nagase and Woessner, 1999).

Cysteine switch mechanism for activation of metalloproteinases
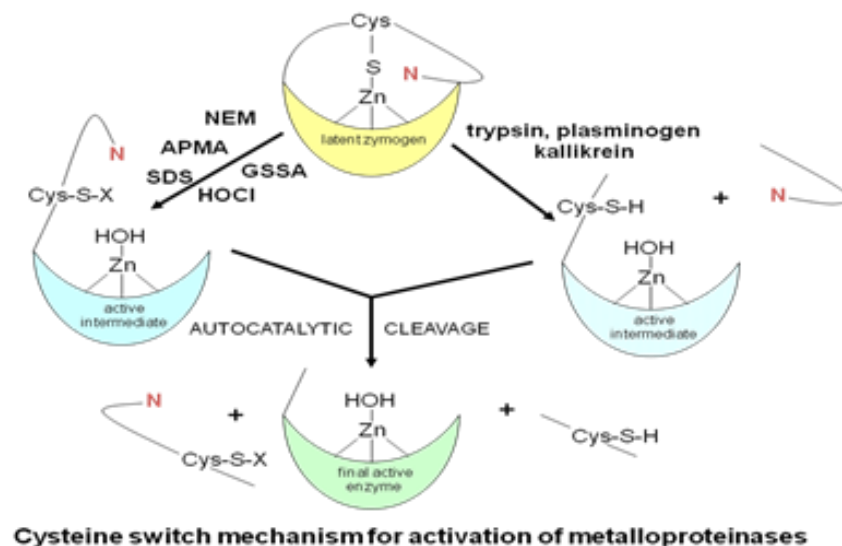
Figure 1.4. Adapted from Birkedal-Hansen, 1995

Some studies proved that gelatinase A (MMP-2) could be activated by a trimolecular complex of activated MT-MMP, TIMP-2 and progelatinase A. On the cell surface, TIMP-2 binds to MT1-MMP, and then the *C*-terminal domain of progelatinase A binds to the *C* terminus of TIMP-2 to form a trimolecular complex. A second MT1-MMP on the cell surface can cleave progelatinase A; hence activate gelatinase A (MMP-2) (Butler *et al*., 1998). TIMP-2 acts as an inhibitor or adaptor depending on its concentration vis-à-vis MT1-MMP and proMMP-2 (DeClerck, 2000; Hadler-Olsen *et al.*, 2013).

1.1.6   Inhibition of MMPs

Once activated, MMPs can be inhibited by some natural inhibitors, especially TIMPs (tissue inhibitors of matrix proteases) and α_2-macroglobulin (α_2M) (Birkedal-Hansen *et al*., 1993).

Water molecule entry responsible for hydrolysis of the peptide bond could be blocked by binding MMPs' catalytic domains to the *N*-terminal domains of TIMPs (Chau *et al*., 2003). Four TIMPs have been discovered so far and they are cross-linked by six disulfide bridges. TIMP-1 (28 kDa), TIMP-2 (21 kDa) and TIMP-4 (22 kDa) are soluble proteins and can be found in the body fluids, while TIMP-3 (24 kDa) is insoluble and can be found bound to the ECM. TIMP-1 has been found that it has a very poor ability to inhibit MT-MMPs that are attached to the cell surface. TIMP-2 and TIMP-3 can inhibit all MMPs to different degrees. TIMP-4 has been reported to inhibit MMP-1, -2, -3, -7, and –9 (Birkedal-Hansen *et al*., 1993; Liu *et al*., 1997). Although TIMPs can inhibit most MMPs, they have a short half-life (Curran & Murray, 2000).

The other endogenous MMP inhibitor is α_2-macroglobulin, which is a non-specific protease inhibitor produced by the liver. α_2M is a large size protein, of 750kDa, that is normally spread throughout plasma and serum. Aspartyl-, cysteine-, metallo- and serine-proteases can all be inhibited by α_2M. Because α_2M usually functions in blood and tissue fluids, where the MMPs are often inactive in this environment, α_2M has less effect on MMPs (Zucker *et al*., 1999). However, Kolodziej *et al*. (2002) three years later discovered that inactive MMPs could be captured by α_2M as well.

Endostatin is the third known natural inhibitor of MMPs, which is generated by type XVIII collagen during its cleavage. It has been found that the level of endostatin could be increased during cancer progression. This may be because of increases in MMPs'

activities, but details are still unknown (Klein *et al*., 2004). *In vitro*, it has been proved that endostatin has the ability to inhibit proMMP-2 activation and MMP-2 activity and form a complex with MMP-2 (Kim *et al*., 2000).

1.1.7 MMPs in Tumour Angiogenesis and Tumour Growth

Angiogenesis is a process to form new blood vessels from existing vessels. It is essential for tumour growth and it can be found in primary and secondary tumours (Giavazzi and Taraboletti, 2001). Without further supply of oxygen and nutrients, tumour cells normally would not grow beyond $2mm^3$ (Zetter, 1998). As angiogenesis is a prerequisite for tumour growth and metastatic spread, it would be an advantage to deliver toxic agents selectively to attack newly formed vessels to the tumour or inhibit outgrowth of capillary sprouts. There are some benefits to attacking tumour vasculature instead of tumour cells: (1) as endothelial cells are more stable than tumour cells, so drug resistance could be decreased by attacking endothelial cells; (2) it would be easy for agents to reach tumour vasculature during circulation; (3) as antiangiogenic therapy focuses on tumour vasculature, so it could apply to many different kinds of tumours (Koop and Voest, 2002; Klein *et al*., 2004).

In order to form new blood vessels, initially MMPs are required to degrade the basement membrane of the ECM for the migration of endothelial cells (Moses, 1997). Among all MMPs, MMP-2 and MMP-9 have been studied the most in cancer and metastasis. MMP-2 and –9 have been linked to increased metastasis and tumour stage in some studies. Vacca *et al.* (1999) discovered that in the patients with active multiple myeloma (MM), there was a bigger area of microvessels and a higher level of MMP-2 and MMP-9 than those with inactive MM. Endothelial cells separated from the bone marrow of MM patients secrete more MMP-2 and MMP-9 than human umbilical vein endothelial cells

(HUVECs) (Vacca *et al.*, 2003). In the treatment of MM mice, SC-964, an MMP inhibitor, controlled angiogenesis—outgrowth of blood vessels was dramatically decreased. In this research project, prodrugs were initially designed against MMP-9 (see also **section 1.1.10**).

During degradation of the basement membrane of the ECM, some growth factors, which are secreted and kept in an inactive form bound to the ECM, could be released to target their receptors. Hence, MMPs can also release or activate growth factors, like transforming growth factor (TGF)-α, TGF-β and insulin like growth factor (IGF). Imai *et al.* (1997) had proved that MMP-2, -3 and -7 can release TGF-β during cleavage of the matrix molecule decorin. TGF-α and IGF may also have the ability to cause the tumour to grow without angiogenesis (Klein *et al*., 2004; Hadler-Olsen *et al.*, 2013). MMP-9 can release vascular endothelial growth factor (VEGF) from the ECM (Bergers *et al*., 2000) and generate tumstatin, an angiogenesis inhibitor, by degrading type IV collagen (Hamano *et al*., 2003).

It also has been found that some fragments of ECM (e.g. tumstatin), fragments of plasminogen (e.g. angiostatin) and fragments of MMPs (e.g. PEX) could lead to a negative effect on tumour angiogenesis (Klein *et al.*, 2004). Tumstatin was found capable of inhibiting tumour angiogenesis by inhibiting proliferation of endothelial cells and endothelial cell apoptosis promotion, while endostatin inhibited migration of endothelial cells (Sudhakar *et al*., 2003). MMP-3,-7,-9 and −12 can produce angiostatin from plasminogen and their activity was found to inhibit tumour angiogenesis (Vihinen and Kähäri, 2002). PEX, a noncatalytic MMP-2 fragment, has been found to inhibit activity and cell surface localization of MMP-2, which leads to a positive effect on inhibiting angiogenesis *in vitro* and *in vivo* (Cao, 2001; Brooks *et al*., 1998).

1.1.8 Development of MMP inhibitors

Based on the studies of the relationship between MMP expression in tumour tissues and tumour progression, it suggested that tumour dissemination could be inhibited by using MMPs as pharmacological targets (Stetler-Stevenson, 1996). The imbalance between TIMPs and MMPs can cause degradation of the ECM. It has been reported that increased levels of TIMPs can decrease tumourigenicity and angiogenesis (Giavazzi and Taraboletti, 2001). As MMP-inhibition could lead to inhibition of angiogenesis, tumour growth, invasion and metastasis, and TIMPs are not suitable for clinical use because of their complex function and large molecular size, many research studies have been focused on developing small molecule MMP-inhibitors (or MMPIs). Many inhibitors of MMPs have been synthesised and have undergone clinical trials. In the MMPI structure, there should be a metal-binding group (a carboxyl, hydroxamate, sulphydryl or thiol), which can bind to the zinc atom at the active site of the MMPs (Drummond *et al.*, 1999). Most synthetic MMP-inhibitors can be separated into four groups: collagen peptidomimetics; non-peptidomimetics; tetracycline derivatives; and bisphosphonates (Giavazzi and Taraboletti, 2001; Klein *et al*., 2004; Newby, 2012). Sulphonamides have also been suggested as a potential class of MMPIs (Jain *et al.*, 2013; Mori *et al.*, 2013)

Instead of focusing on designing MMP-inhibitors, in this project the focus was on exploiting MMPs' peptide hydrolysis ability to activate newly designed and synthesised prodrugs in the tumour microenvironment.

1.1.9 Prodrug strategies

Prodrugs are compounds which are initially in inactive form, but after administration can be converted into the active form in the body by normal metabolic processes. They are typically very useful to solve problems such as poor membrane permeability, drug

toxicity, side effects, bad taste and instability (Patrick, 2009), but in this project, the prodrug is designed to be tumour-targeted. There are two basic targeting modes for prodrug strategies: active and passive targeting. Active targeting is based on the interaction between carrier-linked prodrugs and markers on the tumour cell surface. Passive targeting relies on the differences of physiology and biochemistry between normal healthy and tumour tissue (Kratz *et al.*, 2008).

1.1.9.1 <u>Active targeting</u>

Active targeting depends on the differences of antigens or receptors on the cell surface between healthy and tumour tissues. Ideal active targeting carrier-linked prodrugs should be able to load and release drugs at specific targets; have long term circulation, high affinity to the antigen or receptor on the tumour cell surface, lower toxic and lower drug level in healthy tissue (Juillerat-Jeanneret and Schmitt, 2007; Lu *et al*., 2006).

However, some drawbacks could affect the delivery of active targeting prodrugs: **1)** Some antibodies and receptor-affinity ligands are not only just binding to tumour cells, but also reacting with normal tissue and may cause systemic toxicity (Kratz *et al.*, 2008); **2)** Because the inside of solid tumours, is normally poorly vascularised and blood flow is relatively slow, both factors could prevent macromolecular prodrugs reaching inner regions of tumours (Jain, 1999); **3)** Tumour cells often express heterogeneity in the antigen or receptor, hence it could reduce active targeting prodrugs binding to tumour cells (Kratz *et al.*, 2008); **4)** Some antigens and receptors are secreted into the circulation, so they can bind to prodrugs in the circulation instead of on the surface of tumour cells, hence restrict the binding between prodrugs and tumour cells (Kratz *et al.*, 2008); **5)** Most active targeting prodrugs are evaluated based on human tumour translated mouse models.

However, even if the prodrugs can be activated effectively in mouse models, it does not mean they will have the same results in humans (Oriuchi *et al.*, 1998).

1.1.9.1.1 Antibody-directed enzyme prodrug therapy (ADEPT)

Antibody-directed enzyme prodrug therapy (ADEPT) was introduced by Bagshawe and Senter *et al.* (Bagshawe, 1987; Senter *et al.*, 1988) to overcome the above problems. ADEPT has a two-step mechanism which is outlined in **Figure 1.5**:

1) Monoclonal antibodies (mAbs) and drug-activating enzyme conjugates are administered into patients i.v., then the mAbs of the conjugate will bind to a specific antigen that is expressed on the surface of the tumour cell;

2) After nearly all conjugates have bound to the tumour cells, low-molecular-weight prodrugs are applied and activated by the enzyme from the mAbs-enzyme conjugates. Then cytotoxic drugs will be released and cause tumour cell death.
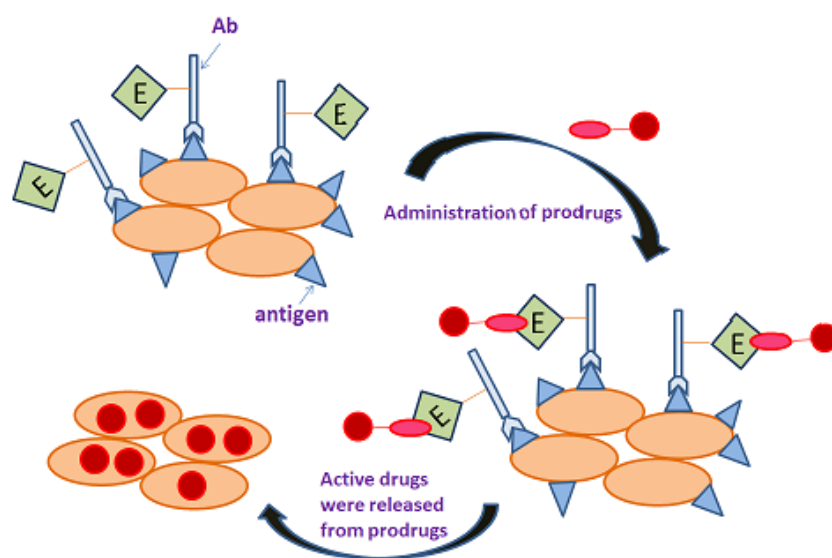
Figure 1.5. ADEPT (Adapted from Kratz *et al.*, 2008).

1.1.9.2   **Passive targeting**

Passive targeting prodrugs usually apply large molecules (biopolymers or synthetic) or nanoparticles (nanospheres, liposomes) as inert carriers, which do not react with tumour cells but can accumulate in tumour tissue to influence the drug's biodistribution.

1.1.9.2.1   **EPR effect (enhanced permeability and retention)**

New blood vessels that are formed during tumour angiogenesis process are always in an irregular shape and dilated and leaky. Widened intercellular spaces in tumour vessels, overlapping endothelial cells and absent or abnormal smooth-muscle layer make tumour tissue permeable to macromolecules and nanoparticles (Maeda *et al*., 2006; Kratz *et al.*, 2008). The diameter size of tumour microvessels has been reported between 100nm to 1200nm (Yuan *et al.*, 1995; Hobbs *et al.*, 1998). However, in most healthy tissue, junctions between endothelial cells of microvessels are less than 2nm in diameter [except postcapillary venules (up to 6nm) and liver, spleen, and kidney (up to 150nm)] (Jang *et al.*, 2003). Macromolecule carriers in macromolecular prodrugs are normally from 2nm to 10nm; hence prodrugs with macromolecule carriers could enter into tumour tissue instead of normal healthy tissue (Kratz *et al.*, 2008). If the molecular weight is below 40kDa, it could be cleared from the tumour very quickly, while large molecular entities are retained (Noguchi *et al.*, 1998), this is because there is poor or no functional lymphatic drainage inside tumour tissue. So, the explanation for the accumulation of macromolecules in solid tumours is the combination of enhanced permeability and retention (EPR) as outlined in **Figure 1.6** (Matsumura and Maeda, 1986).
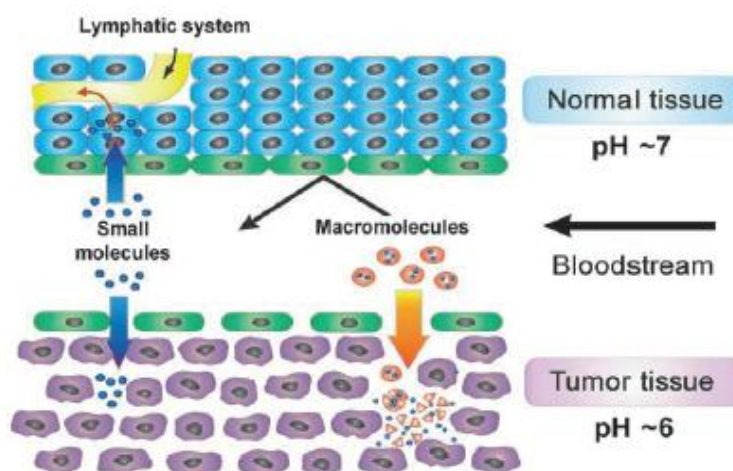
Figure 1.6. The EPR effect (Adapted from Kratz *et al.*, 2008).

As there are extensive vascular areas in large tumours, so they have less EPR active than small tumours. On the other hand, at the pre-angiogenic stage, macromolecular prodrugs are hard to target on small metastases (Jang *et al.*, 2003). Apart from the EPR effect, macromolecular prodrugs have been reported to have enhanced retention with longer plasma half-lives, because they cannot be cleared from kidneys easily. Venturoli and Rippe reported that negatively charged or uncharged macromolecules (>40kDa) could escape renal clearance successfully (Venturoli and Rippe, 2005). Many models showed tumour size-dependent accumulation. Smaller tumours have higher tumour localisation than larger tumours, and this may due to angiogenic activity is higher in smaller tumours, while in larger tumours, blood supply is reduced or absent in the hypoxic regions and tumour interstitial fluid pressure is higher than in smaller tumours (Duncan *et al.*, 2013).

1.1.9.2.2   Polymer-directed enzyme prodrug therapy (PDEPT)

The basic passive targeting strategy PDEPT— polymer-directed enzyme prodrug therapy, as it illustrated in **Figure 1.7**, is similar to ADEPT, needs both administrations of macromolecular prodrug and polymer-enzyme conjugate which can combine with each other and hence release anti-cancer agent at the tumour site. The difference between ADEPT and PDEPT is that during polymer-directed enzyme prodrug therapy, the polymer-prodrug needs to be administrated into the patient's body initially and after it reaches the tumour target site, then the polymer-enzyme conjugate is applied. Since the

polymeric prodrug only stays in plasma for a comparatively short time, the prodrug will not be activated until the polymer-enzyme conjugate is administrated and both polymer conjugates combine inside the tumour [**Figure 1.7**] (Satchi *et al.*, 2001; Kratz *et al.*, 2008).
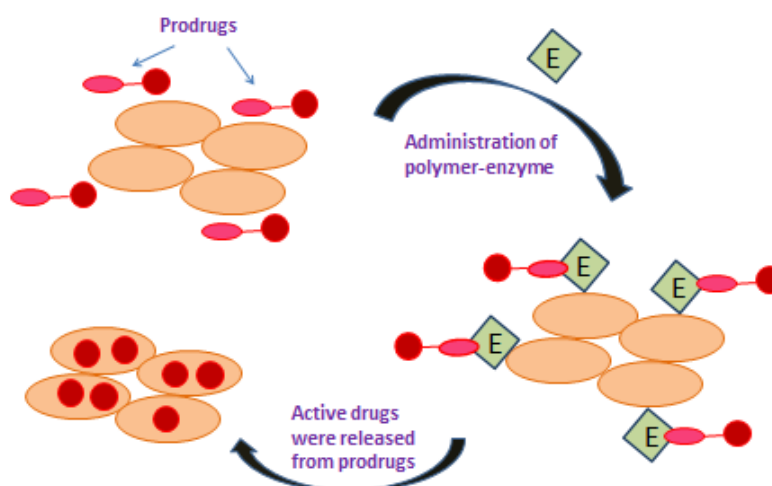
Figure 1.7. PDEPT— polymer-directed enzyme prodrug therapy (Adapted from Kratz *et al.*, 2008).

Compared with ADEPT, PDEPT has two potential advantages:

1) In ADEPT, an antibody-enzyme conjugate often has long plasma half-life which makes it difficult to design an optimal dosing schedule for the administration of prodrug subsequently. If a prodrug is administrated when there is still a high level of antibody-enzyme conjugate in the plasma, it would be activated in the normal tissue instead of tumour site (Bagshawe, 1994; Satchi *et al.*, 2001). While, in PDEPT, due to passive accumulation of polymeric prodrug after initial administration, polymeric prodrug is only presents in plasma for a relatively short time. Following administration, the polymer-enzyme conjugate mostly binds and activates prodrug at the tumour site (Kratz *et al.*, 2008).

2) Compared to the antibody-enzyme conjugates in ADEPT, the polymer-enzyme conjugates in PDEPT could reduce potential enzymes' immunogenicity (Satchi *et al.*, 2001).

1.1.10 Design strategy of new prodrugs for activation by MMP 9

1.1.10.1 Early development of MMP 9 prodrug substrates
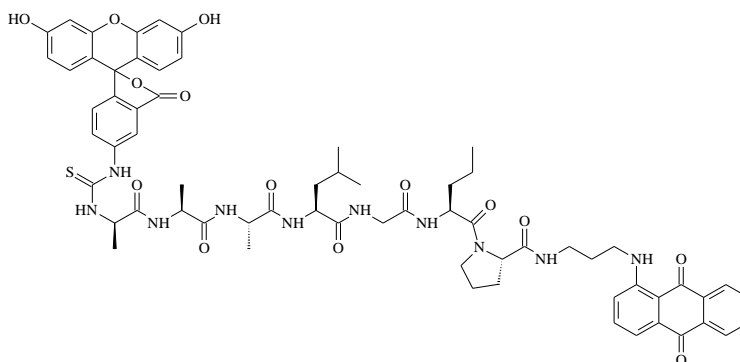
Figure 1.8. Structure of EV1-FITC (1)

The above structure is the prototype (synthesised earlier in this laboratory) which forms the basis of the present study. The MMP 9-targeted prodrug EV1-FITC **(1)** [**Figure 1.8**], is an FITC-containing heptapeptide-1-(3-aminopropylamino)anthraquinone conjugate, for which it was shown that cleavage between glycine and norvaline by MMP 9, which was produced by 5T33MM *vv* murine myeloma cells, with the result of fluorescence release which indicated the activation of this prodrug. Van Valckenborgh *et al.* showed that in the 5T33MM mouse model, EV1-FITC **(1)** gave a higher fluorescence release by the MMP 9-rich isolated spleen and bone marrow (BM) cells of diseased animals compared to this prodrug in healthy animals. This suggested MMP 9-activatable prodrugs can be used to target multiple myeloma (MM), an incurable B-cell cancer located in the bone marrow (Van Valckenborgh *et al.*, 2005). This proof of principle in the animal model is used as the starting point for extending the design of optimised MMP-targeted prodrugs in this project.

1.1.10.2 Outline strategy for new prodrugs in this research project

In this research project, a series of single agent or twin (identical or non-identical) prodrugs with optimised peptide sequences have been synthesised with the combination

16

of an oligopeptide as carrier and attached on each end: either dual antivascular agents (such as a colchicine series of compounds) or dual cytotoxic agents (such as a clinically-used agent, like epirubicin (**2**)) or combined antivascular and cytotoxic agents. Illustrative examples are outlined below.
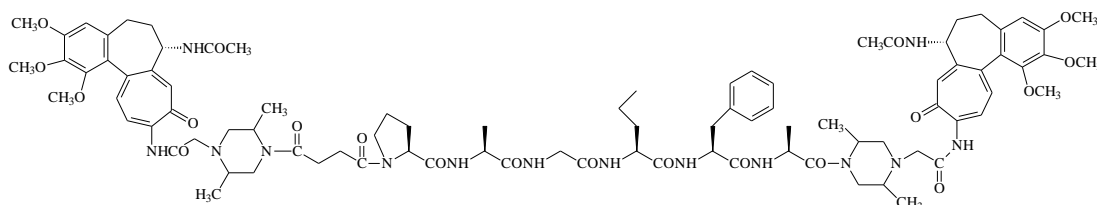
Figure 1.9. YD9-DMPIP-SUCC-Pro-Ala-Gly-Nva-Phe-Ala-DMPIP-YD9 (YD 55) (3)

Identical twin prodrug YD 55 (**3**) [**Figure 1.9**], has the same antivascular 'warheads' on both ends of the MMP9 substrate hexapeptide, and an MMP9 cleavage 'hotspot' at the Gly~Nva junction. Similar to EV1-FITC (**1**), the hexapeptide carrier was designed to be cleaved off between glycine and norvaline (the MMP9 cleavage 'hotspot') when this prodrug binds to MMP 9, hence to release double doses of colchiceinamide (the active cytoxic and vascular disrupting agent) to target tumour blood vessels.
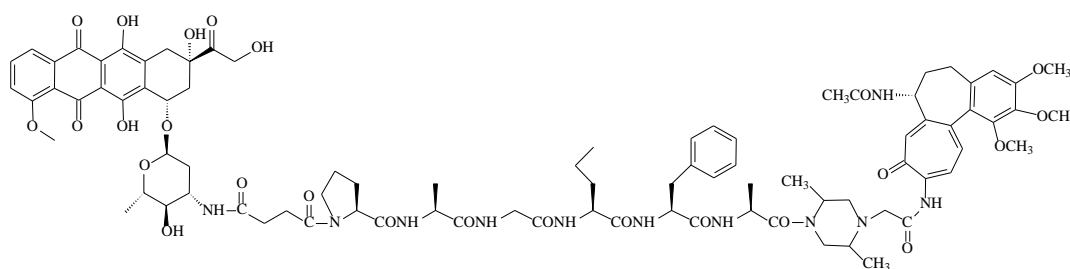
Figure 1.10. Epi-SUCC-Pro-Ala-Gly-Nva-Phe-Ala-DMPIP-YD9 (YD 61) (4)

Figure 1.10 outlines the structure of a non-identical twin prodrug YD 61 (**4**), which was designed similarly to identical prodrug YD 55 (**3**), and has the same hexapeptide sequence, the same colchiceinamide compound at one end, but clinically-used cytotoxic agent epirubicin (**2**) was chosen for the second active agent for this twin prodrug.

1.2   RESULTS AND DISCUSSION

1.2.1   Target compounds

The series of 'twin prodrugs' were designed with a combination of an oligopeptide as carrier and on its ends attaching: either dual antivascular agents (including colchicine series compounds) or dual cytotoxic agents (such as clinically-used agents, like epirubicin (**2**); experimental anticancer agents, including anthraquinone series compounds, like the NU:UB series of compounds) or antivascular and cytotoxic agents in combination. The general structure is shown in **Figure 1.11**:
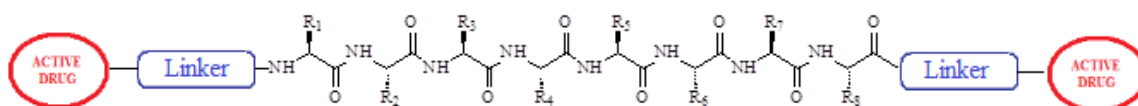
Figure 1.11. Structure of 'twin drugs' prodrug

In the 'traditional' way, prodrugs are designed to solve problems such as poor membrane permeability, drug toxicity, side effects and instability (Patrick, 2009). Tumour targeting prodrugs are also designed to target particular enzymes or antigens which are over expressed on tumour tissue cells when compared with normal tissue cells (Han and Amidon, 2000), so that the active drugs would only be released at the tumour site; hence this could greatly increase selectivity and decrease side effects which active drugs would cause to normal tissue. This kind of 'twin drug' prodrugs [**Figure 1.11**], theoretically, can bind to MMPs and be cleaved at the 'hot spot', hence release active drugs from both ends. Thus, these kinds of prodrug can produce two doses of active drugs during one prodrug activation, hence it can increase the overall potency. Moreover, complementary agents may work by a synergistic mechanism. The 'twin prodrugs', which were synthesised in this laboratory, were composed of three crucial parts: 1) active drugs which have pharmacological effects on tumour cells; 2) two chemical linkers (often

18

ester, amine and thioether or thiourea bonds that can be metabolised easily in the body) that can connect active drugs with oligopeptide spacers; 3) the oligopeptide carrier which was designed to be enzymatically cleavable by specific proteases (focus on MMP9) to release the active drugs at the tumour site.
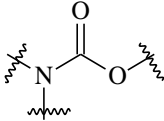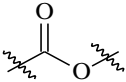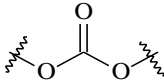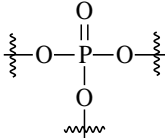
1.2.1.1 Active drugs

Three different kinds of combinations of active drugs or agents were used in this research project, they are:

1) Antivascular agents, the colchicine compounds: colchiceinamide and *N*-methylcolchiceinamide;

2) Cytotoxic agents, such as clinically-used epirubicin **(2)** and experimental agents (with proven activity), notably: anthraquinone compounds (such as: 1-(4-hydroxypiperidyl)anthraquinone and 1-(3-aminopropylamino)anthraquinone, or 2-piperazinylanthraquinone) or amino acid conjugates thereof;

3) Antivascular and cytotoxic active drugs and agents in combination.

1.2.1.2 Chemical linker

Commonly, an ester is the first choice for simple prodrug design, not only because it is easy to synthesise, but also in the body, esterases are distributed widely. After administration, ester bonds are ready to be hydrolysed by esterases in the liver, blood and other organs. Different ester structures, as shown in **Table 1.1**, exhibit various stabilities in the body. Compared with carboxyl ester, carbonate ester and phosphate ester, carbamate ester is the most stable 'ester' bond in the body (Mahato *et al*., 2011). In general, linkers between active drugs and an oligopeptide should stay stable in the body until it reaches the target(s).

Linker:	Carbamate ester	Carboxyl ester	Carbonate ester	Phosphate ester
Structure:				

Table 1.1: Chemical structures of common ester bonds (Adapted from Mahato *et al*., 2011).

The purposes of adding a 'linker' between active agent and oligopeptide are: **1)** the linker compounds act as a 'glue' to link active drugs onto the oligopeptide. Oligopeptides at least at the *N*-terminus cannot add directly onto active amino-containing drugs, as two amine groups will not react, so it is necessary to make short linkers typically, pentafluorophenyl esters or succinate compounds for further reactions; **2)** adding linkers between active drugs and an oligopeptide can make sure that the 'twin drug' conjugates are 'masked' peptides which will become less susceptible to spontaneous hydrolysis, hence to increase the stability of the prodrugs. Additionally, linkers are sometimes required to distance the drug from the peptide to make it easier for a protease to gain access to the cleavage site.

1.2.1.3 <u>Oligopeptide chain</u>

In order to reduce the side effects caused by active drugs attacking normal tissue cells, it requires active drugs or agents to be selectively released at tumour sites. Hence, the stability of oligopeptide chains in 'twin drug' prodrugs is very important for the design of this kind of prodrugs: the oligopeptide should be stable enough in the circulation to carry active drugs or agents till they reach tumour sites, and also should easily bind to and be cleaved off by MMPs once they are at tumour sites to release the active drugs.

In **Figure 1.12**, to the left of the 'cleavage hot-spot'— the scissile bond, the amino acid substrate residues are named P1, P2, P3 etc; to the right of scissile bond, they are named P1', P2', P3' etc. Similarly, as the protein subsites (S), to the left of scissile bond, they

20

are non-primed (S1, S2, S3); to the right of scissile bond, they are primed (S1', S2', S3') (Atlas *et al.*, 1970).
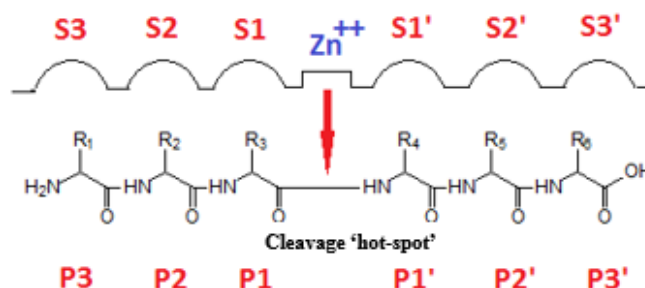
Figure 1.12. Relationship between substrate residues and protein subsites (Adapted from Atlas *et al.*, 1970)

As S1' is a deep hydrophobic pocket, so both gelatinases (MMP-2 and -9) prefer a leucine (or isoleucine) residue at this position in natural substrates. In general, MMP-2 favours more hydrophobic substrate residues at positions on the right of the scissile bond than the ones on the left (Massova *et al.*, 1997). McGeehan *et al*. showed that the hydrophobic amino acids with long straight chain residues (such as unnatural norleucine or norvaline) would be the best choice for the S1' pocket, or amongst the proteinogenic ones, the branched amino acids, such as Leu, Ile and Val; however, MMP-9 can also accept some branching at the β-carbon and the γ-carbon. S1 is a shallow pocket and not many residues can fit in, overall, glycine is the first choice for the S1 pocket (McGeehan *et al.*, 1994). The S2' pocket, the last important recognition site for substrate binding to MMP-9, has a small hydrophobic surface. It is very tolerant for most amino acids which have large hydrophilic or small hydrophobic side chains. The unique five-membered ring structure of Pro is preferred for the S3 pocket which has a cambered surface (Kridel *et al.*, 2001). Chen *et al*. found in MMP-2, smaller amino acid residues would easily fit in the S2 pocket. The P2 position is the key distinct position of the substrate to separate MMP-2 and MMP-9 subsite preferences; if Glu is replaced by Asp at the P2 position, the original specific substrates for MMP-2 would be changed to that for MMP-9 instead (Chen *et al.*, 2002; Chen *et al.*, 2003). Research also showed that Arg can hardly be

21

found at the P2 position in MMP-2 substrates, so the selectivity might shift away from MMP-2 to MMP-9 by choosing Arg at the P2 position. Substrate Arg at the P2 position can significantly increase hydrolysis by MMP-9, but considerably decrease hydrolysis by MMP-2 (Chen *et al.*, 2002).

	Substrate sequence				
	P3	**P2**	**P1**	**P1'**	**P2'**
MMP subsites properties	Hydrophobic pocket	Broad specificity	Small, shallow surface.	Straight chain residues are the best choice. Some specificity for braches at β and γ carbon.	Very broad specificity for both collagenase and gelatinase, however, with exclusion of acidic amino acids and imino acids.
MMP 2 Preferred substrates	Pro	Ser/ Lys/ Ala/Glu	Ala/Gly	Leu/ Ile	Val/ Leu/ Ile
MMP 9 Preferred substrates	Pro	Arg/ Asp	Gly/ Ala/ Ser/ Thr	Leu/ Ile	Ser/ Thr

Table 1.2. MMP-substrate specificity table amongst the proteinogenic amino acids (Adapted from McGeehan *et al.*, 1994; Kridel *et al.*, 2001)

1.2.2 <u>Synthesis of 'warheads' (active agents)</u>

Colchicine **(5)** [**Figure 1.13**], an alkaloid extracted from plant *Colchicum Autumnale*, has been used as anti-inflammatory drug to treat gouty arthritis and familial Mediterranean fever (Cerquaglia *et al.*, 2005). As an antimitotic drug, colchicine **(5)** has a high affinity to its principal cellular receptor tubulin, a subunit protein of microtubules

(Andreu and Timasheff, 1982; Farrell and Wilson, 1980). Most colchicine **(5)** biological functions are related to its binding with tubulin, hence leading to disruption of microtubule polymerization substoichiometrically (Uppuluri *et al.*, 1993). Colchicine binds to a limited number of soluble tubulin dimers first, and then these colchicine-tubulin dimer complexes attach to the assembling ends of microtubules during assembly and prevent further tubulin dimer addition (Margolis and Wilson, 1977). Colchicine and its active analogues can act as spindle poisons in cancer cells, hence the cell cycle can be impeded at the M-phase and lead to cell death (Jordan and Wilson, 1998). Although colchicine and its analogues showed positive antitumour properties *in vitro*, due to their extreme toxicities, there is no FDA approved drug available on the market that belongs to colchicine related microtubule-interacting agents (Raspaglio *et al.*, 2005; Lee and Gewirtz, 2008).

Microtubules, made of α- and β-tubulin heterodimers, are crucial polymers of eukaryotic cells and they are involved in several cellular functions, such as cell division, motility, polarity and signalling (Avila, 1990). Microtubule dynamics is very slow during interphase, however, it can be increased by 20- to 100-fold during mitosis. Hence, based on its crucial function during mitosis, microtubule processing is an attractive target for anti-cancer compounds development (Combeau *et al.*, 2000).

In its tricyclic chemical structure [**Figure 1.13**], colchicine **(5)** has a trimethoxyphenyl ring (A ring), a seven membered ring (B ring) which has an acetamide at the C-7 position and a tropolonic ring (C ring). The counterclockwise helicity form of A- and C-rings in the colchicine chemical structure as shown in **Figure 1.13** presents biological activity.
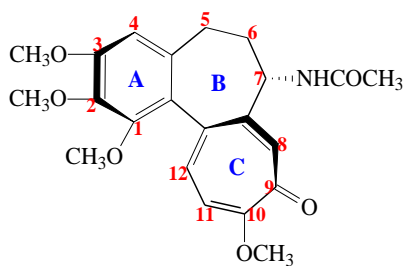
Figure 1.13. Chemical structure of Colchicine (5).

The binding of colchicine (**5**) to tubulin is a slow process that has a two-step mechanism. The first binding step is fast, reversible and shows low binding affinity by fitting its tropolone ring (C ring) into the tubulin binding site through hydrogen bonding or ring stacking. Then the initial binding process is followed by rearrangement of tubulin structure in order to form a proper position for the trimethoxyphenyl ring (A ring) to fit in place. The binding of the trimethoxyphenyl ring is slow and shows high binding affinity (Andreu and Timasheff, 1982; Medrano *et al.*, 1989). Colchicine does not fluoresce in aqueous or organic solvent, however, once it binds with tubulin, fluorescence can be detected with an excitation maximum at 362nm and an emission maximum at 435nm. Based on this fact, fluorescence measurement offers a convenient method to detect derivatives of colchicine and whether they can bind to tubulin or not (Bhattacharyya and Wolff, 1974). Colchicine analogue studies showed both A- and C-rings of colchicine structure are crucial for its high affinity binding to tubulin. However, several changes in the C-ring are tolerated, such as substitutions at the C-10 position or a change of the seven-membered ring to a six-membered ring (Bhattacharyya and Wolff, 1974; Hastie, 1989). Three methoxy groups in the A-ring are crucial for binding to tubulin and demethylation would lead to decreasing binding affinity. The acetamide group at the C-7 position in the B-ring can be substituted by a range of amides and tubulin binding potency is retained. Removing the methoxy group at C-10 position in the C-ring causes inactivation; however, it can be replaced with SCH_3 or NR_2 to increase potency [**Figure 1.14**] (Cerquaglia *et al.*, 2005).

24
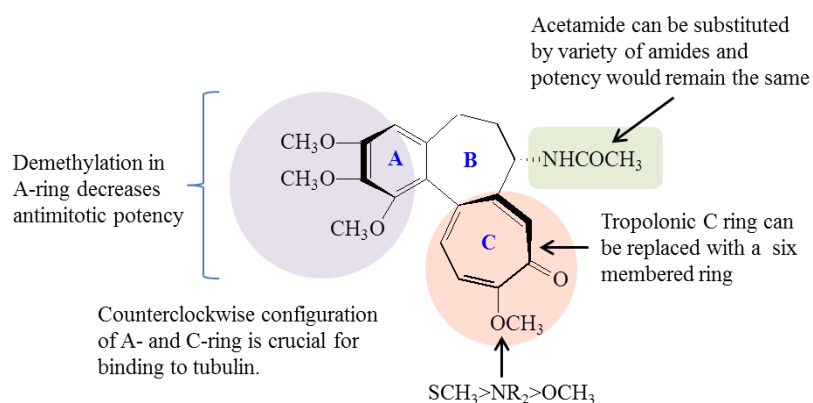
Figure 1.14. Relationship of colchicine analogues' structures and tubulin binding activity

Guan *et al.* reported that even though demethylcolchiceinamide analogues do not have any antimitotic activity [**Figure 1.14**], they are a new class of DNA topoisomerase II inhibitors. The trihydroxy A-ring is a determinant for these novel topoisomerase II inhibitors having topoisomerase II inhibitory activity (Guan *et al.*, 1998).

Due to the fact that colchicine (**5**) has a very narrow therapeutic index, using colchicine as a therapeutic drug has been limited. It has been reported that when *N*-substituted colchiceinamides are compared to colchicine, they have more potency and less toxicity (Hartwell *et al.*, 1952; Davis, 1981). So in this research programme, colchicine (**5**) was converted to *N*-substituted colchiceinamides. Crucially, this also provides a starting point (functional group) for the coupling of an oligopeptide carrier as a key part of the target prodrugs.
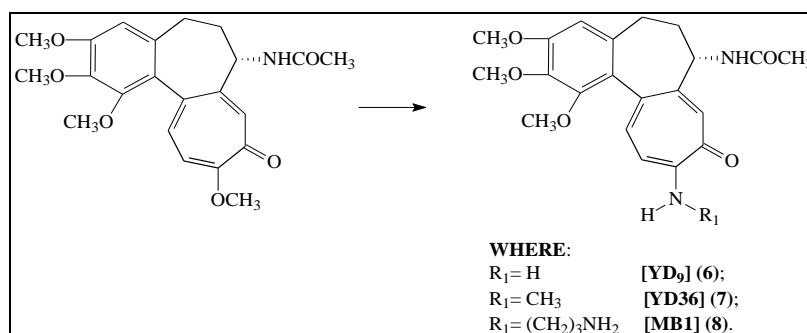
Reagents and conditions: ammonia, DMF, RT, 4 days (YD 9); methylamine, RT, 15min (YD 36); 1,3-diaminopropane, RT, 15min (MB1).

Scheme 1.1. Synthesis of colchicine analogues YD 9 (6), YD 36 (7) and MB1 (8).

1.2.2.1   Synthesis of colchiceinamide (YD 9) (6)

Colchiceinamide **(6)** has been shown to have similar potency to colchicine **(5)** (unpublished data from this laboratory in collaboration with the University of Bradford) as an antivascular agent with less toxicity when compared to *N*-methylcolchiceinamide (YD 36) **(7)** and colchicine **(5)** (Hartwell *et al.*, 1952; Davis, 1981)**.** In its chemical structure, it has a free amino group for attachment of peptide carriers.
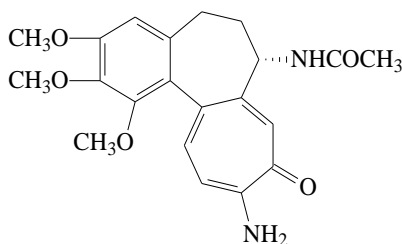
Figure 1.15. Structure of colchiceinamide (YD 9) (6)

The synthesis of YD 9 **(6)** [**Figure 1.15**] is outlined in **Scheme 1.1**. Colchiceinamide (YD 9) **(6)** was synthesised by reacting ammonia with a stirred solution of colchicine **(5)** in DMF. This reaction was very slow and could take three or four days at room temperature. Then, the reaction solution was evaporated to dryness to give a pale yellow solid compound.

The structure of colchiceinamide (YD 9) **(6)** was confirmed by signals in its ^{1}H-NMR spectrum, for example, three three-proton singlets at 3.42, 3.72 and 3.77ppm were assigned to C1, C2 and C3 methoxy protons. The amide proton at C7 was found at 8.53ppm.

1.2.2.2   Synthesis of *N*-methylcolchiceinamide (YD 36) (7)

N-methylcolchiceinamide (YD36) **(7)** (Muller and Poittevin, 1966) was also considered as a suitable 'warhead' for antivascular prodrugs (having comparable potency to colchicine as a vascular disrupting agent).

26
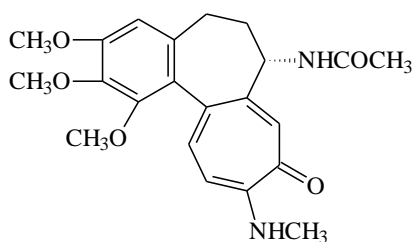
Figure 1.16. *N*-methylcolchiceinamide (YD 36) (7)

The synthesis of YD 36 **(7)** is shown in **Scheme 1.1**. Unlike the synthesis of colchiceinamide **(6)**, the first step of the synthesis of *N*-methylcolchiceinamide (YD 36) **(7)** [**Figure 1.16**] was fast, taking 10-15 minutses to react instead of 3 to 4 days when compared with the synthesis of colchiceinamide **(6)**. Also, during the reaction, there was no need of DMF as a solvent. The pale yellow precipitated solid was filtered and washed with ice-cold water, and then dried *in vacuo*. The structure of *N*-methylcolchiceinamide (YD 36) **(7)** was confirmed by the expected signals in its ^{1}H-NMR spectrum which could all be assigned, for example, a three-proton doublet centred at 3.03ppm was assigned to the methyl protons from methylamino group. Three three-proton singlets at 3.56, 3.83 and 3.88ppm were assigned to C1, C2 and C3 methoxy protons. A one proton quartet centred at 7.18ppm was assigned to the secondary amine proton from methylamino group. The amide proton can be found at 7.95ppm.

1.2.2.3 Synthesis of 10-(3-aminopropyl)amino-10-demethoxycolchicine (MB1) (8)

The 'warhead' MB1 **(8)** had an extended amino substituent compared to colchiceinamide **(6)**.
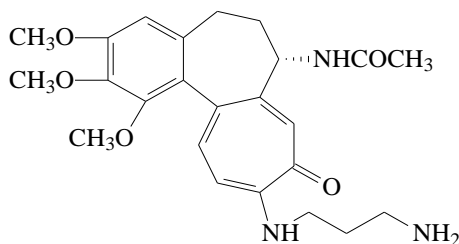
Figure 1.17. 10-(3-aminopropyl)amino-10-demethoxycolchicine (MB1) (8)

27

The synthesis of MB1 (**8**) [**Figure 1.17**] is illustrated in **Scheme 1.1**. Colchicine **(5)** was mixed with 1,3-diaminopropane. The whole mixture was stirred well at room temperature for 3 hours, and then the whole reaction mixture was transferred to an evaporating basin to evaporate at room temperature. The dried mixture was re-dissolved in dichloromethane from which some white unknow compound could be precipitated from MB1 (**8**). The structure of MB1 (**8**) was confirmed by ^{1}H NMR spectrum (in d_6-DMSO), which showed, for example, a two proton triplet centred at 1.70ppm was assigned to the primary amine protons and a one proton triplet centred at 7.78ppm was assigned to the secondary amine proton from aminopropylamino group. A six-proton broad singlet at 3.40ppm was assigned to the methanediyl group from aminopropylamino group. The colchicine protons were all successfully assigned; C1, C3 and C2 methoxy protons gave three-proton singlets at 3.45, 3.74 and 3.81ppm respectively. The C5 and C6 protons were present at 1.95-2.20ppm and C7 proton can be found at 4.43ppm. The amide proton can be found at 8.53ppm.

1.2.3   Synthesis of 'warhead'-spacer/ linker compounds

Scheme structures and labels:

Colchiceinamide **[YD 9] (6)** ; *N*-methylcolchiceinamide **[YD 36] (7)**

N-chloroacetylcolchiceinamide **[YD 10] (9)** ; *N*-chloroacetyl methylcolchiceinamide **[YD 38] (13)**

Colchiceinamide—Dimethylpiperazine Spacer **[YD 11] (10)** ; *N*-methylcolchiceinamide—Dimethylpiperazine Spacer **[YD 39] (14)**

Colchiceinamide—Dimethylpiperazine Spacer—Boc **[YD 31] (11)** ; *N*-methylcolchiceinamide—Dimethylpiperazine Spacer—Boc **[YD 40] (15)**

[YD 33] (12) ; **[YD 41] (16)**

Reagents and conditions: (i) chloroacetyl chloride, NaHCO₃, DMF was used as solvent in YD 10 **(9)** reaction and THF was used as solvent in YD 38 **(13)** reaction; (ii) trans-2,5-dimethylpiperazine, DMF was used as solvent in YD 11 **(10)** reaction and THF: DMSO (10:1) mixture was used in YD 39 **(14)** reaction; (iii) (Boc)₂O, Dry methanol; (iv) TFA, RT, 30min.

Scheme 1.2. Synthesis of colchiceinamide and *N*-methylcolchiceinamide spacer conjugates.

1.2.3.1 Synthesis of YD9-DMPIP (YD 11) (10)

Figure 1.18. YD9-DMPIP (YD 11) (10)

The synthesis of YD 11 **(10)** [**Figure 1.18**] is shown in **Scheme 1.2**: sodium bicarbonate was added into colchiceinamide **(6)** in DMF and the suspension was stirred over an ice bath for 10 minutes before adding chloroacetyl chloride drop wise. 24 hours later, after checking by TLC, the whole reaction mixture was transferred to an ice-water mixture dropwise. The new yellow target compound *N*-chloroacetylcolchiceinamide (YD 10) **(9)** immediately precipitated in the ice-water mixture once every drop of reaction mixture was added in. The precipitate was filtered and evaporated to dryness. *N*-chloroacetylcolchiceinamide and trans-2,5-dimethylpiperazine were both dissolved in DMF separately, and the solution of *N*-chloroacetyl colchiceinamide was added into a well-stirred solution of trans-2,5-dimethylpiperazine drop wise and slowly to make sure that *N*-chloroacetyl colchiceinamide would only react with one secondary amine end of trans-2,5-dimethylpiperazine, instead of both sides. Then the reaction mixture was partitioned between chloroform and water. Diethyl ether was also applied finally to give a precipitate of the desired compound. It had been noticed that trans-2,5-dimethylpiperazine would not easily dissolve in DMF. At room temperature, it would take up to 3 or 4 hours to dissolve. However, if the suspension mixture was warmed to 40°C, trans-2,5-dimethylpiperazine dissolved in DMF very easily in less than 15 minutes; consequently, this procedure was adopted.

1.2.3.2   Synthesis of YD9-DMPIP [TFA] (YD 33) (12)

Figure 1.19. YD9-DMPIP [TFA] (YD 33) (12)

Colchiceinamide dimethylpiperazine spacer YD 11 **(10)** was dissolved in dry methanol and the solution was kept stirring well at 0°C. Di-*t*-butyl-dicarbonate was dissolved in dry methanol separately, and then it was added into cooled, stirred YD 11 **(10)** solution drop wise slowly and the whole reaction mixture was kept in the dark. *N-*tBoc protected conjugate YD 31 **(11)** was purified by loading the concentrated reaction mixture onto a flash chromatography column. Dried chromatographically pure *N-*tBoc protected conjugate YD 31 **(11)** was treated with trifluoroacetic acid for 30 minutes at room temperature, and then the reaction solution was evaporated to near dryness and re-evaporated with methanol twice. Addition of diethyl ether gave a precipitate of yellow final compound colchiceinamide dimethylpiperazine spacer *N*-terminal trifluoroacetate salt YD 33 **(12)** [**Figure 1.19**].

1.2.3.3   Synthesis of YD36-DMPIP (YD 39) (14)
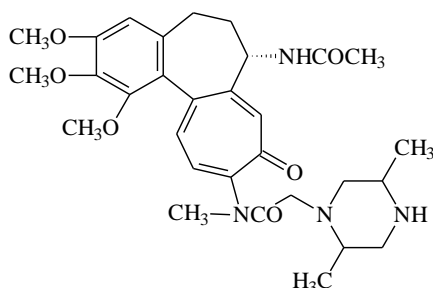
Figure 1.20. YD36-DMPIP (YD 39) (14)

Synthesis of YD 39 **(14)** [**Figure 1.20**] is illustrated in **Scheme 1.2**: chloroacetyl chloride was added dropwise into a cooled (0°C), well-stirred suspension mixture of sodium

bicarbonate and *N*-methylcolchiceinamide (YD 36) **(7)** in THF. For this reaction, at the first attempt, DMF was used as solvent, but the reaction was slow (several days) and in the end, on the TLC plate, it was a bit messy. When using THF as a solvent on the other hand, the reaction was faster (3 hours); there was only one yellow spot on the TLC plate; a high yield of final compound (over 90%) and also THF was easier to remove than DMF. As *N*-chloroacetylmethylcolchiceinamide (YD 38) **(13)** was also soluble in water, a method different from purification of *N*-chloroacetylcolchiceinamide was required; it cannot be purified by simply adding reaction mixture into ice-water mixture dropwise. *N*-chloroacetylmethylcolchiceinamide (YD 38) **(13)** reaction mixture was filtered to remove solid sodium bicarbonate, and then it was partitioned between chloroform and water to remove THF and extra chloroacetyl chloride. In the synthesis of *N*-methylcolchiceinamide dimethylpiperazine spacer conjugate YD 39 **(14)**, four different solvents were used and compared, and they were: DMF, THF, THF: DMSO (10:1) and CH_3CN. Results showed using DMF and THF as solvent, both reactions were quite slow (five days reacting by using DMF and two days by using THF), and on TLC plates, both were quite messy mixtures of products. It seemed that by using THF: DMSO (10:1) and CH_3CN as solvent the speed of this reaction could be improved. However, TLC plates showed complex mixtures by using CH_3CN as solvent. So, THF: DMSO (10:1) was the best solvent for this reaction among the four different solvents. [Because DMSO has a very low melting point, if the room temperature is lower than 18°C, DMSO may form white/clear crystals in the *N*-methylcolchiceinamide dimethylpiperazine spacer conjugate YD 39 **(14)** reaction mixture].

1.2.3.4   Synthesis of YD36-DMPIP [TFA] (YD 41) (16)
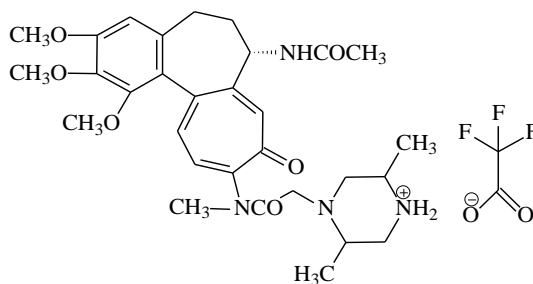
Figure 1.21. YD36-DMPIP [TFA] (YD 41) (16)

Di-*t*-butyl-dicarbonate was dissolved in dry methanol separately, and then it was added into cooled, stirred YD 39 **(14)** solution drop wise slowly and the whole reaction mixture was kept in the dark. *N*-*t*Boc protected *N*-methylcolchiceinamide spacer conjugate YD 40 **(15)** was purified by loading the reaction mixture onto a flash chromatography column. Chromatographically pure dried YD 40 **(15)** was treated with trifluoroacetic acid for 45 minutes at room temperature, and then the reaction solution was evaporated to near dryness and re-evaporated with methanol twice. Addition of diethyl ether gave a precipitate of yellow final compound colchiceinamide piperazine spacer *N*-terminal trifluoroacetate salt YD 41 **(16)** [**Figure 1.21**]. The structure of this methylcolchiceinamide spacer trifluoroacetate salt was confirmed by its ES(+) mass spectrum which gave a signal at m/z 553.4 for $(M+H)^+$ and its ES(-) mass spectrum which had a base peak at m/z 113.0 for the presence of the trifluoroacetate anion.

1.2.3.5   Synthesis of MB1-SUCC (YD 56) (17)

Any warhead spacer or peptide conjugates that have primary or secondary amine ends can react with succinic anhydride in DMF under basic (DIPEA) conditions to give the required extended linkers [**Scheme 1.3**].
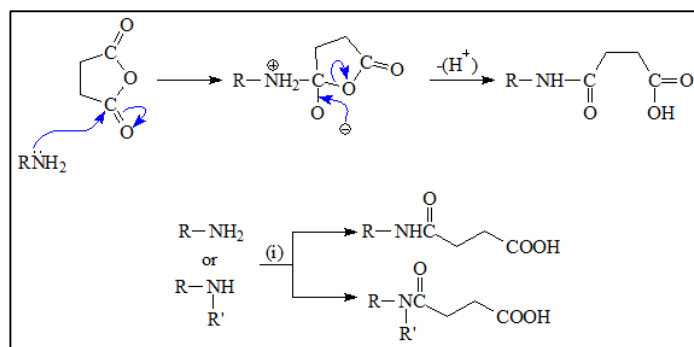
Reagents and conditions: (i) succinic anhydride, DMF and DIPEA, RT, 12~48h.

Scheme 1.3. Formation of succinate compounds

Succinic acid has carboxylic acid ends on both sides (an α, ω-diacid), so it is an ideal linker for connecting warhead spacer and oligopeptide together from their amine ends. The reaction would take a small number of hours or typically at most one or two days, and extra succinic acid could be removed by washing with water or purifying the reaction mixture on a silica gel column. Litmus blue test paper and bromocresol green were applied to detect whether there was any succinic acid left in the compound mixture, because if any extra succinic acid was carried through to the next step, it would cause impurity, low yield and even react with the starting materials. When synthesising colchiceinamide spacer oligopeptide succinate compound YD 54 (**18**), it was noticed that YD 54 (**18**) could dissolve in dichloromethane while succinic acid could not. So if any succinate compounds were soluble in dichloromethane, excess succinic acid could be simply removed by filtering off from the compounds' dichloromethane solutions.
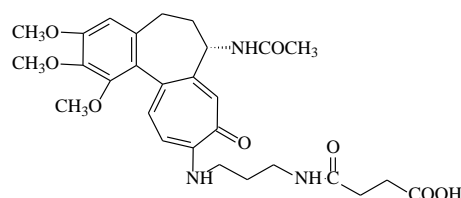
Figure 1.22. MB1-SUCC (YD 56) (17)

MB1-SUCC (YD 56) (**17**) [**Figure 1.22**] was synthesised by reacting MB1 (**8**) with succinic anhydride in DMF under basic (DIPEA) conditions, following the general method outlined in **Scheme 1.3**. Overnight, after checking by TLC, the whole reaction

34

mixture was transferred to an evaporating basin to evaporate till dryness. As the succinate compound YD 56 **(17)** was soluble in water, excess succinic acid could not be washed away by water. On the TLC plate, it showed that even if it was eluted with dichloromethane: methanol (5:1), succinic acid would not be removed at all. So the succinate compound YD 56 **(17)** was then applied onto a very fine silica gel chromatography column, eluted with dichloromethane: methanol (5:1). After chromatography, YD 56 **(17)** was checked by TLC again; bromocresol green was applied on the starting line on the TLC plate for detecting any remaining succinic acid in the final compound. There was a bright yellow spot which showed up against a blue background which meant there was some succinic acid remaining in the mixture, so the whole final compound and remaining succinic acid mixture was put on a very fine silica gel chromatography column again. After re-chromatographing twice, when the YD 56 **(17)** TLC plate was treated with bromocresol green, there was still a tiny yellow spot showed up against blue background, but it was very weak. Then the whole compound solution was evaporated to dryness to afford a sample sufficiently chromatographically pure for further use.

1.2.3.6   Ile-PIP-AQ [TFA] NU:UB 234 (19)
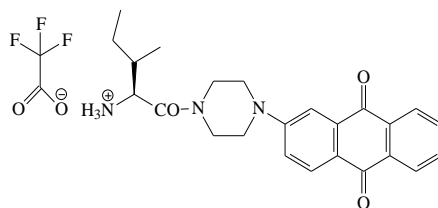
Figure 1.23. Ile-PIP-AQ [TFA] NU:UB 234 (19)

Spacer-linked anthraquinone-amino acid conjugate NU:UB 234 **(19)** [**Figure 1.23**] was designed in this laboratory (Mincher, Turnbull and Kay, 2003) as a topoisomerase inhibitor. In NU:UB 234 **(19)**, the spacer group was chosen as a relatively rigid,

conformationally restricted, piperazine ring system; anthraquinone and isoleucine parts were attached to the piperazine via the nitrogen atoms in the 1- and 4-positions. Connection of the spacer to the anthraquinone was in the C-2 position. It has been shown that NU:UB 234 **(19)** is a dual topoisomerase I and II inhibitor and it can inhibit topoisomerase II α- and II β- mediated relaxation of DNA at concentration of 50 μM. Topoisomerase cleavage assays indicated that NU:UB 234 **(19)** was inactive in topoisomerase I mediated DNA cleavage assay even with a concentration up to 100 μM. On the other hand, the optimum concentrations of NU:UB 234 **(19)** that can stimulate topoisomerase II α- and II β- mediated DNA cleavage were 50 μM and 5 μM, respectively (Young, 2006).

1.2.4   Synthesis of model compounds (model prodrugs)

At the early stages of this research project, a few model compounds were synthesised first, in order to find the best reaction conditions for some later crucial reactions involving sensitive drugs, including epirubicin.

During the synthesis of YD 20 **(20)** [**Figure 1.24**], it had been shown that epirubicin **(2)** can be successfully coupled onto an OPFP ester to form amide-linked derivatives. Later on, it proved that epirubicin **(2)** can be coupled successfully onto an OPFP ester which had a longer peptide during the synthesis of YD 67 **(21)** as well. And then, colchicine spacer conjugate MB1 **(8)** and 6-aminofluorescein **(22)** were both shown to react with the same OPFP ester YD 62 **(23)** by the same method. Hence, based on this discovery, the rest of the prodrugs synthesised in this project that contained epirubicin **(2)** were all achieved with the same method to couple epirubicin **(2)** with an OPFP ester critically at the last step of the synthesis.

1.2.4.1 Synthesis of Epi-SUCC-Pro-APA-AQ (YD 20) (20)
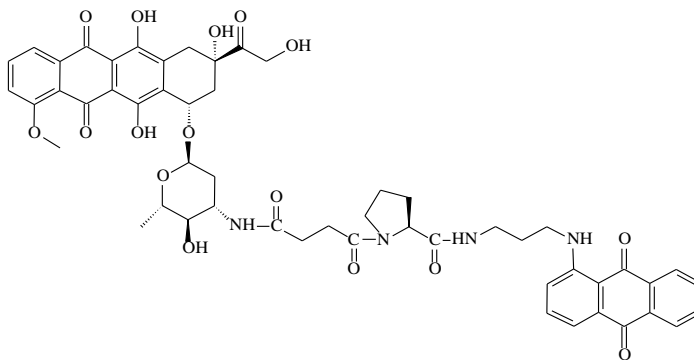
Figure 1.24. Epi-SUCC-Pro-APA-AQ (YD 20) (20)

The motivation for synthesis of 'twin prodrug' YD 20 **(20)**, as shown in **Figure 1.24**, was a trial experiment to find the optimum reaction conditions for coupling epirubicin **(2)** with anthraquinone 'warhead' compounds. As strong base cannot be used for the reaction with epirubicin **(2)**, in the beginning, sodium hydrogen carbonate was used as base for this reaction. However, after 3 hours, it showed nothing had happened. So instead, one equivalent of DIPEA was introduced in this reaction [**Scheme 1.4**].
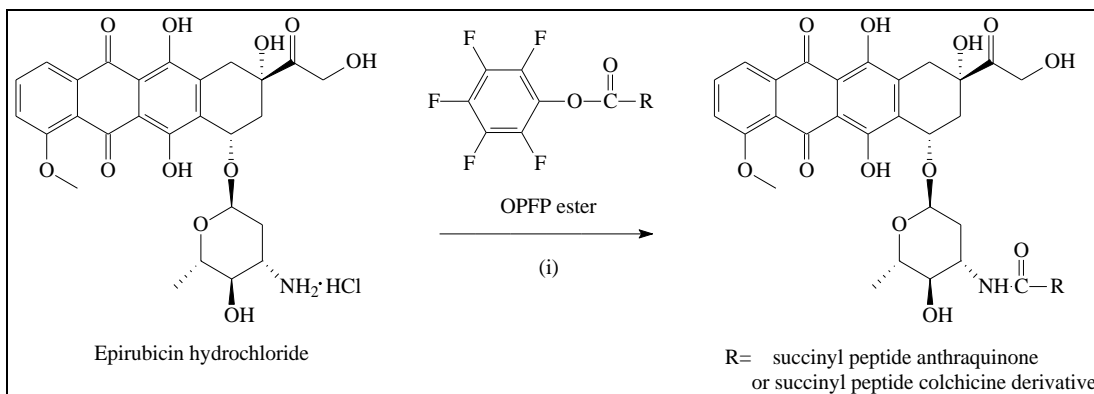
Reagents and conditions: (i) DMF, DIPEA, RT, 3 to 12h.

Scheme 1.4. **General synthesis of epirubicin (2) conjugates**

'Twin prodrug' YD 20 **(20)** was synthesised by reacting anthraquinone conjugate pentafluorophenyl ester YD 19 **(24)** with epirubicin hydrochloride in DMF with one equivalent of DIPEA as base by following the general method which is outlined in **Scheme 1.4**. Overnight, after checking by TLC, the solution was evaporated to almost dryness before it was applied onto a silica gel chromatography. The structure of YD 20

37

(20) was confirmed by both its ES(-) mass spectrum which had a a strong signal at m/z 1001.3449 for the species $(M-H)^-$ and its ES(+) mass spectrum which had a strong peak at m/z 1025.3418 for $(M+Na)^+$.

1.2.4.2 Synthesis of Epi-SUCC-MB1 (YD 59) (25)
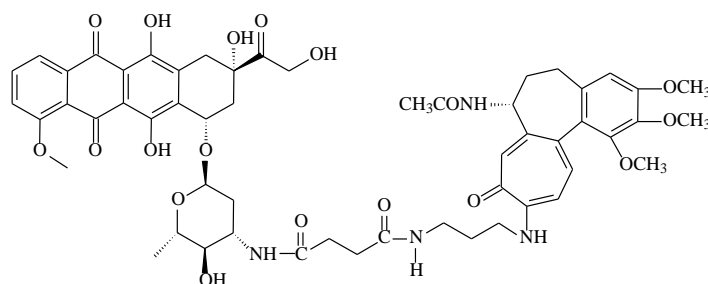
Figure 1.25. Epi-SUCC-MB1 (YD 59) (25)

The motivation for the synthesis of dual prodrug YD 59 **(25)** [**Figure 1.25**] was another trial experiment to find out whether epirubicin **(2)** could be coupled with a colchicine succinate compound by the same reaction conditions as for dual prodrug YD 20 **(20)**.

Dual prodrug Epi-SUCC-MB1 YD 59 **(25)** was synthesised by reacting MB1-SUCC-OPFP YD 57 **(26)** with epirubicin hydrochloride in DMF under basic (DIPEA) condition for overnight by following the general method outlined in **Scheme 1.4**. Because of the potential for YD 59 **(25)** to go into water layers during partition between dichloromethane and water, the whole reaction solution was evaporated to near dryness and purified by applying the residue onto thick-layer silica gel chromatography plates. Fractions containing the major product were combined, filtered and evaporated to afford the title compound. The structure of YD 59 **(25)** was confirmed by its ES(+) mass spectrum which gave, for example, a signal at m/z 1067.4127 for the species $(M+H)^+$.

1.2.5   Synthesis of target prodrugs

1.2.5.1   Synthesis of YD9-DMPIP-SUCC-ᴅ-Ala-Ala-Ala-Leu-Gly-Ile-PIP-AQ (YD 34) (27): a twin prodrug of active agents NU:UB 234 (19) and the colchiceinamide derivative (YD33) (12)
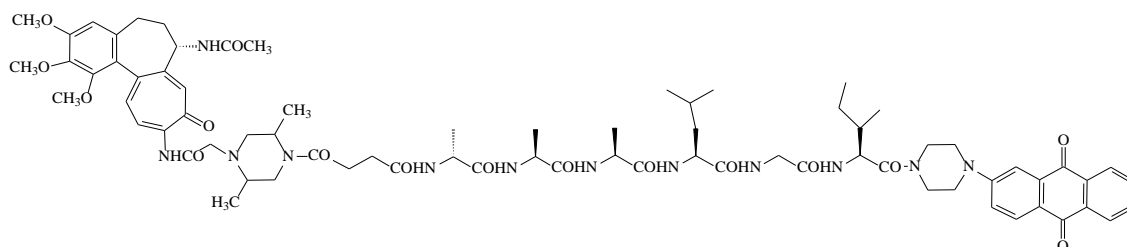
Figure 1.26. YD9-DMPIP-SUCC-ᴅ-Ala-Ala-Ala-Leu-Gly-Ile-PIP-AQ (YD 34) (27)

The synthesis of YD 34 **(27)** [**Figure 1.26**] is illustrated in **Scheme 1.5**:

Scheme 1.5. Synthesis of YD9-DMPIP-SUCC-ᴅ-Ala-Ala-Ala-Leu-Gly-Ile-PIP-AQ (YD 34) (27)

'Twin prodrug' colchiceinamide spacer hexapeptide anthraquinone conjugate YD 34 **(27)** was synthesised by reacting anthraquinone spacer oligopeptide conjugate succinate YD 30 **(28)** (already available as the hexapeptide succinate from the solution-phase sequential addition of amino acids onto an anthraquinone-spacer compound) with *N*-

colchiceinamide spacer trifluoroacetate salt YD 33 **(12)**, mixed with coupling reagents PyBOP and HOBt in DMF under basic conditions (DIPEA) for two hours, then the reaction solution was concentrated and purified by thick layer chromatography. The electrospray (+) mass spectrum of the chromatographically pure principal product gave a signals at m/z 1409.7136 for the presence $(M+H)^+$ and at m/z 1431.7 for the species $(M+Na)^+$.

1.2.5.2 Synthesis of YD36-DMPIP-SUCC-ᴅ-Ala-Ala-Ala-Leu-Gly-Ile-PIP-AQ (YD 42) (29): a twin prodrug of active agents NU:UB 234 (19) and the *N*-methylcolchiceinamide derivative (YD41) (16)
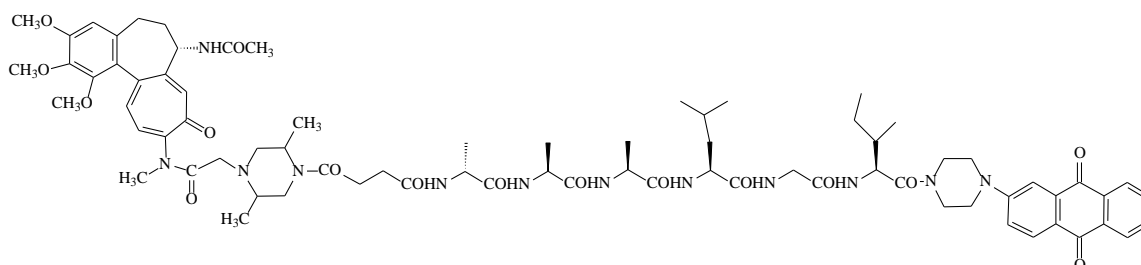
Figure 1.27. YD36-DMPIP-SUCC-ᴅ-Ala-Ala-Ala-Leu-Gly-Ile-PIP-AQ (YD 42) (29)

The synthesis of YD 42 **(29)**, as shown in **Figure 1.27**, is outlined in **Scheme 1.6**:
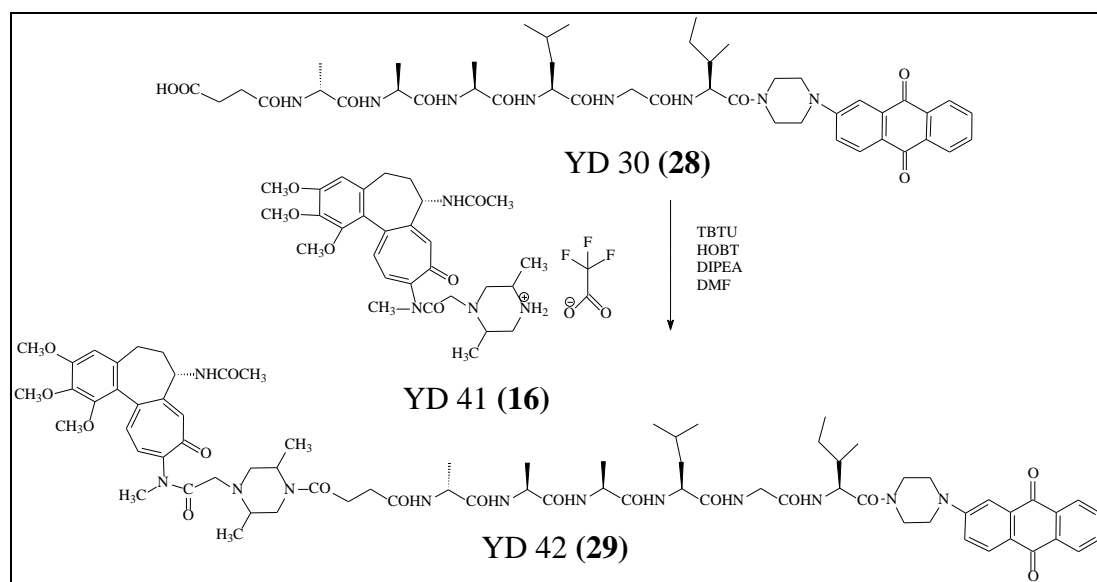
Scheme 1.6. Synthesis of YD36-DMPIP-SUCC-ᴅ-Ala-Ala-Ala-Leu-Gly-Ile-PIP-AQ (YD 42) (29)

'Twin prodrug' YD36-DMPIP-SUCC-ᴅ-Ala-Ala-Ala-Leu-Gly-Ile-PIP-AQ (YD 42) **(29)** was similar to the colchiceinamide spacer hexapeptide anthraquinone conjugate YD

40

34 **(27)**, the only difference is that colchiceinamide was replaced by *N*-methylcolchiceinamide in prodrug YD 42 **(29)**. It was synthesised by reacting anthraquinone spacer oligopeptide conjugate succinate YD 30 **(28)** and *N*-methylcolchiceinamide spacer trifluoroacetate salt YD 41 **(16)** with coupling reagents under basic conditions (DIPEA) in DMF for 3 hours. It was purified by loading onto a thick layer TLC plate. There were two orange bands on thick layer TLC plate. Both bands were collected and sent for mass spectrometry. Mass spectral results showed that only the second orange band (the lower one) was the right compound. On TLC, there was a tiny spot in the middle part of TLC plate, which could be seen under UV light was from compound YD 41 **(16)**. After comparing with *N*-methylcolchiceinamide on TLC, it proved that the tiny spot from compound YD 41 **(16)** was *N*-methylcolchiceinamide (YD 36) **(7)**. The first orange band ran at nearly the same level as that tiny spot, so this may explain why the first orange band was not the right compound: NU:UB 363 **(30)** succinate could have reacted with *N*-methylcolchiceinamide (YD 36) **(7)** while reacting with YD 41 **(16)**. The structure of this dual prodrug was confirmed by its ES(+) mass spectrum which had a peak at m/z 1423.7272 for the species (M+H)$^+$.

1.2.5.3 Synthesis of MB1-SUCC-D-Ala-Ala-Ala-Leu-Gly-Ile-PIP-AQ (YD 58) (31): a twin prodrug of active agents NU:UB 234 (19) and the colchicine derivative (MB1) (8)
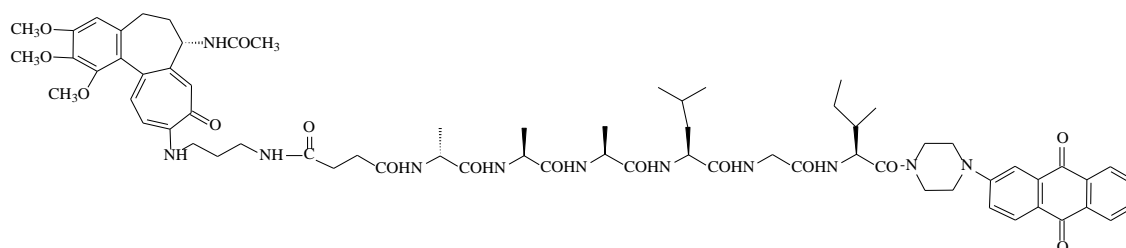
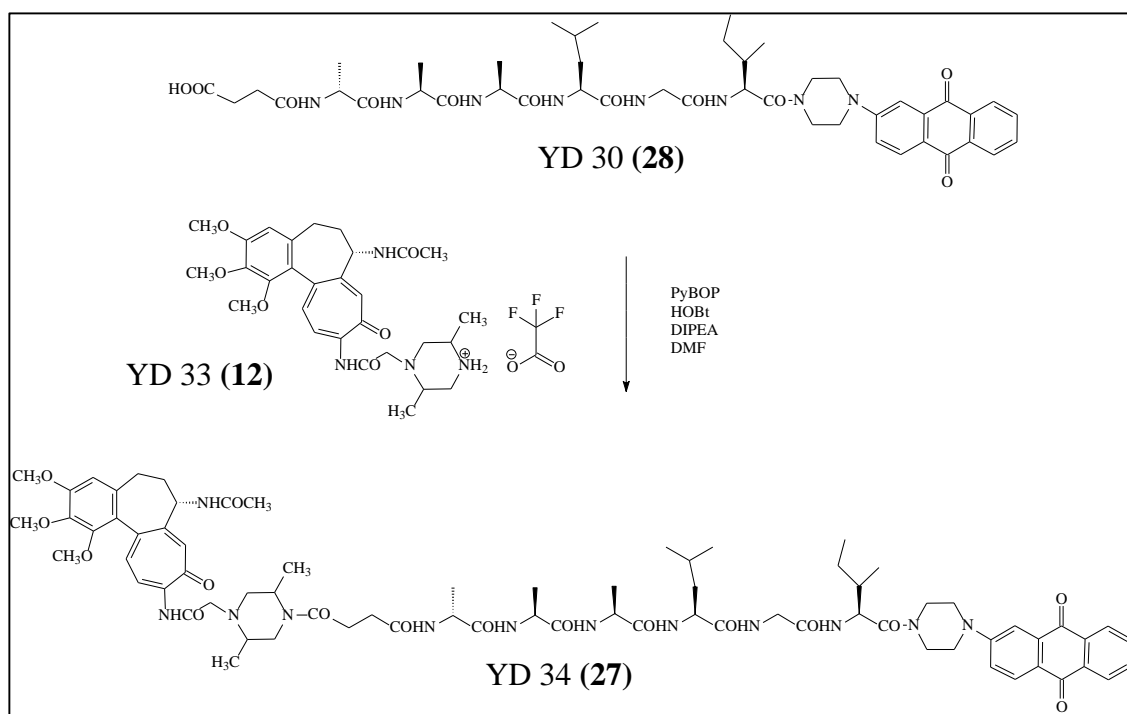**Figure 1.28. MB1-SUCC-D-Ala-Ala-Ala-Leu-Gly-Ile-PIP-AQ (YD 58) (31)**

In **Scheme 1.7**, is shown the first attempted synthesis of YD 58 **(31)** [**Figure 1.28**]:
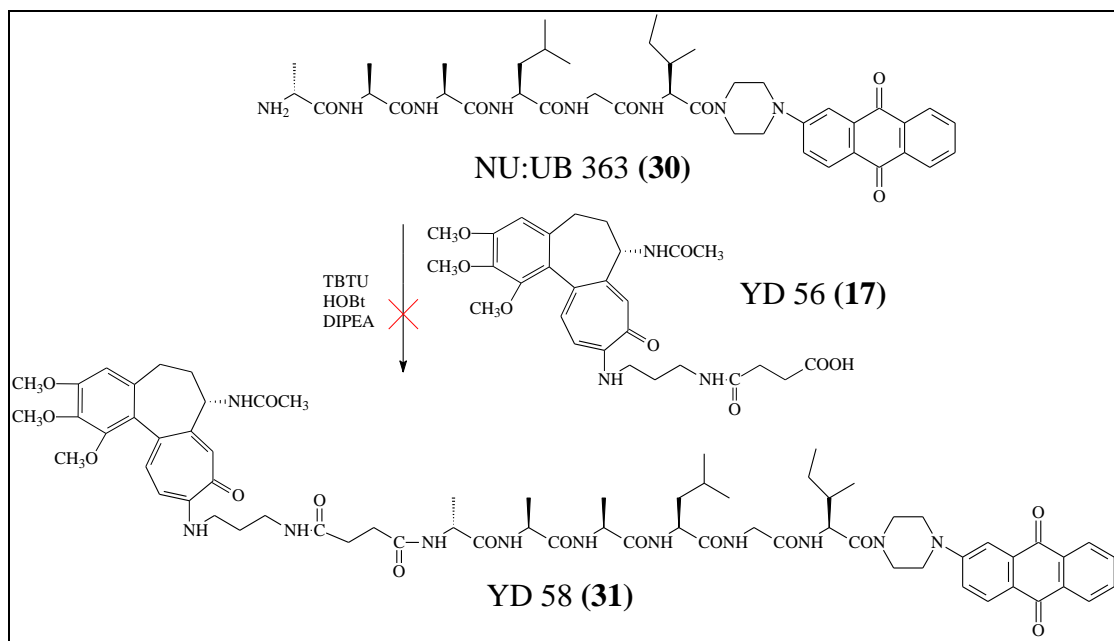
Scheme 1.7 Attempted synthesis of MB1-SUCC-D-Ala-Ala-Ala-Leu-Gly-Ile-PIP-AQ YD 58 (31)

This colchicine derivative spacer hexapeptide anthraquinone conjugate YD 58 **(31)** was similar to the previous two colchicine derivative spacer hexapeptide anthraquinone conjugates YD 34 **(27)** and YD 42 **(29)**, the only difference is that colchicine derivative 10-(3-aminopropyl)aminocolchiceinamide MB1 **(8)** was chosen in prodrug YD 58 **(31)**. The synthesis of 'twin prodrug' YD 58 **(31)** [**Scheme 1.7**] was first attempted by reacting anthraquinone conjugate NU:UB 363 **(30)** and MB1-SUCC (YD 56) **(17)** in DMF with coupling reagents TBTU and HOBt under basic (DIPEA) condition. It was purified by silica gel chromatography, eluting with dichloromethane: methanol 7:1. However, the TLC showed that the compound collected from the chromatography column was just NU:UB 363 succinate. The mass spectrum result showed a very weak signal of YD 58 **(31)**, the strong signal was assigned to NU:UB 363 succinate. This was because after synthesising MB1-SUCC (YD 56) **(17)**, excess succinic acid was very difficult to remove, so NU:UB 363 **(30)** reacted with succinic acid instead of MB1-SUCC (YD 56) **(17)** to create the linker between the warheads.

42
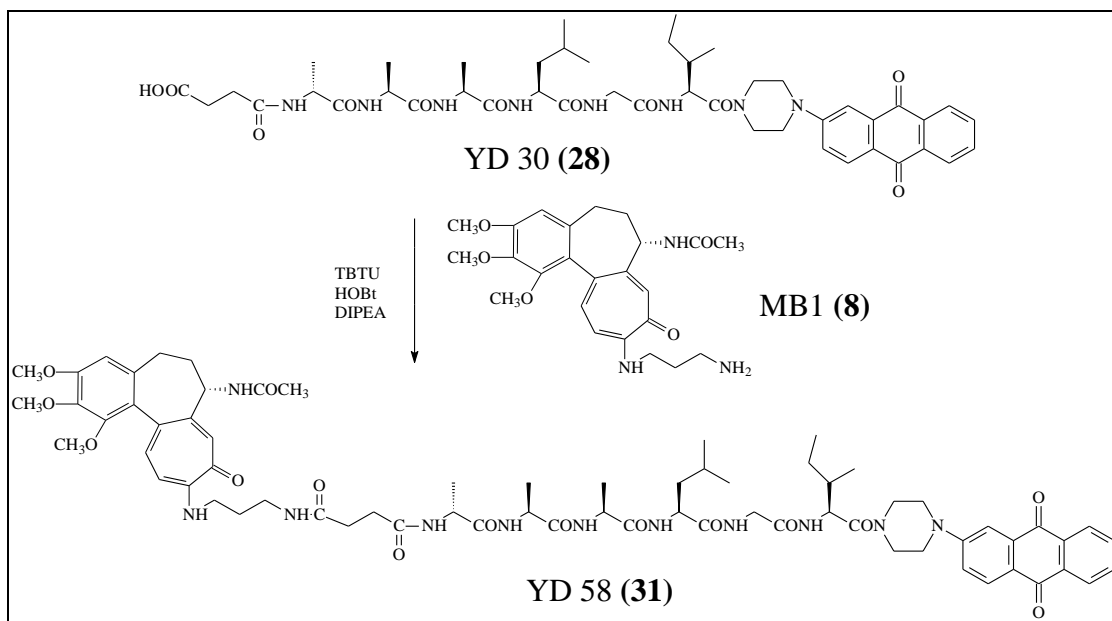
Scheme 1.8. Synthesis of MB1-SUCC-D-Ala-Ala-Ala-Leu-Gly-Ile-PIP-AQ (YD 58) (31)

However, 'twin prodrug' YD 58 **(31)** was sucessfully synthesised by coupling MB1 **(8)** with NU:UB 363 succinate YD 30 **(28)** in DMF at room temperature for 2 hours [**Scheme 1.8**]. The final product from the reaction mixture was purified using a thick layer chromatography plate which was eluted with dichloromethane: methanol 7:1. The ES(+) mass spectrum confirmed the structure of this 'twin drug' prodrug: a signal for the doubly charged ion $[(M+2H)/2]^{2+}$ was found at m/z 656.8336. A signal at m/z 1312.6671 was for the species $(M+H)^{+}$ and a signal at m/z 1334.6471 was for $(M+Na)^{+}$.

1.2.5.4 Synthesis of YD9-DMPIP-SUCC-D-Ala-Ala-Ala-Leu-Gly-Leu-Nva-Gly-PIP-AQ (YD 18) (32): a twin prodrug of active agents NU:UB 347 and the *N*-colchiceinamide derivative (YD11) (10)
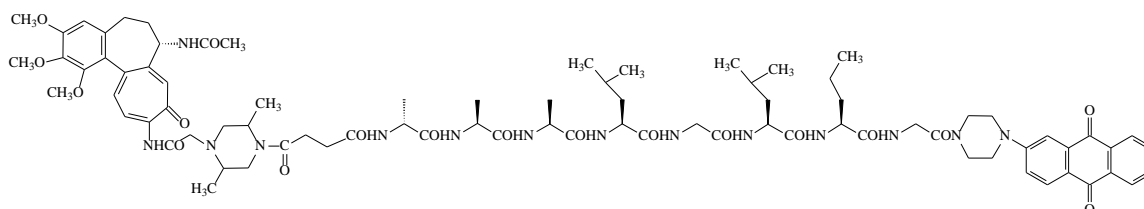
**Figure 1.29. YD9-DMPIP-SUCC-D-Ala-Ala-Ala-Leu-Gly-Leu-Nva-Gly-PIP-AQ (YD 18) (32)**

Scheme 1.9 illustrates the synthesis of YD 18 **(32)** [**Figure 1.29**]:
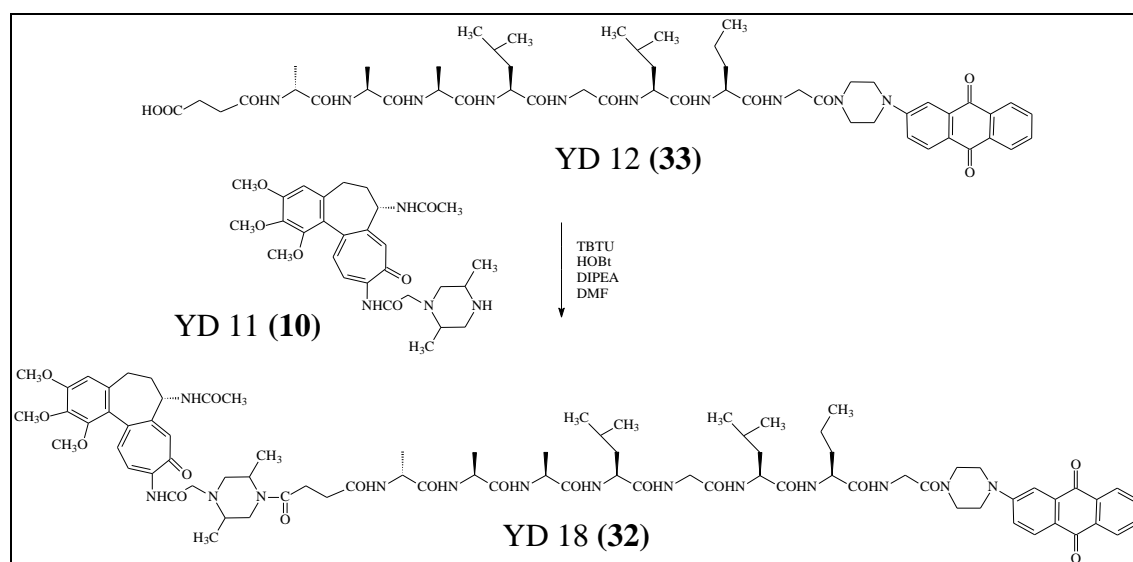
Scheme 1.9. Synthesis of YD9-DMPIP-SUCC-D-Ala-Ala-Ala-Leu-Gly-Leu-Nva-Gly-PIP-AQ (YD 18) (32)

The motivation for this synthesis of 'twin drugs' prodrug colchiceinamide spacer octapeptide anthraquinone conjugate YD 18 **(32)** was to synthesise an anticancer active agent that has two different 'warheads', one is the antivascular agent—a colchicine compound and the other one is a cytotoxic agent—the experimental anthraquinone compound. The 'cleavage hot spot' in the oligopeptide is between Gly and Leu. Once this prodrug has been cleaved by MMPs at the 'hot spot', both colchicine and anthraquinone compounds would be released.

Colchicine and anthraquinone 'twin drug' prodrug YD 18 **(32)** was synthesised by reacting colchiceinamide spacer YD 11 **(10)** with anthraquinone oligopeptide compound YD 12 **(33)**, using coupling reagents TBTU, HOBt and DIPEA in DMF. After three hours reaction, the compound was purified by column chromatography. Followed by further purification by the successful use of thick-layer (semi-preparative) TLC plates. The structure of this 'twin drug' prodrug was confirmed by its ES(+) mass spectrum at m/z of 1588.0 for the fragment of $(M+Na)^+$ corresponding to a molecular mass of 1565 Daltons.

1.2.5.5 Synthesis of YD9-DMPIP-SUCC-Pro-Ala-Gly-Nva-Phe-Ala-DMPIP-YD9 (YD 55) (3): an identical twin prodrug of the *N*-colchiceinamide derivative (YD11) (10)
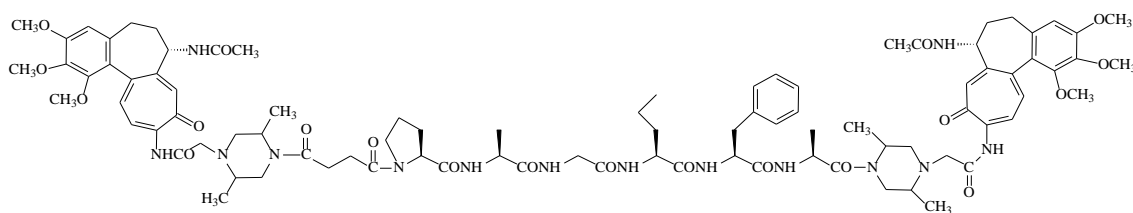
Figure 1.30. YD9-DMPIP-SUCC-Pro-Ala-Gly-Nva-Phe-Ala-DMPIP-YD9 (YD 55) (3)

The motivation for synthesis 'twin prodrug' YD 55 (**3**), as shown in **Figure 1.30**, was to make a prodrug that had exactly the same antivascular 'warheads' on both ends of hexapeptide ('identical twin'). The 'cleavage hot spot' on this hexapeptide was designed to be between Gly and Nva, as the S1' pocket is very deep, so Nva should fit in easily; and the S1 pocket is very specific to bind with Gly. The S3 pocket is a curved pocket, so the Pro five-membered ring should fit in well. The synthesis of YD 55 (**3**) is outlined in **Scheme 1.10**:
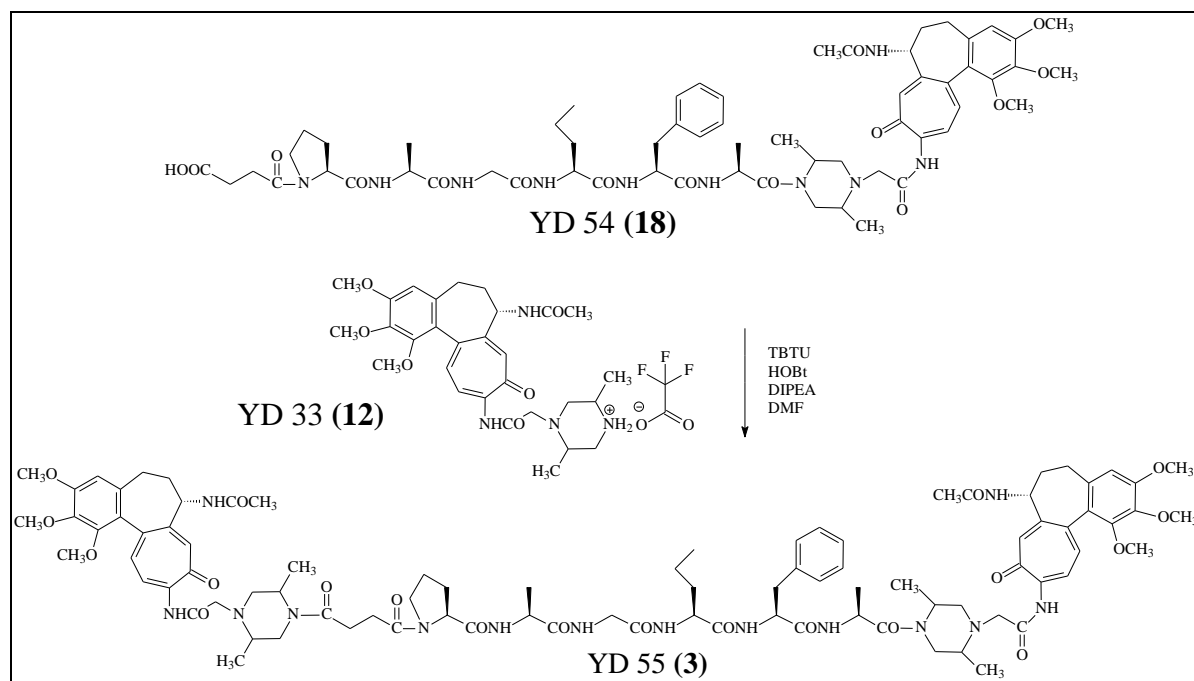
Scheme 1.10. Synthesis of YD9-DMPIP-SUCC-Pro-Ala-Gly-Nva-Phe-Ala-DMPIP-YD9 (YD 55) (3)

45

'Twin prodrug' bis-(colchiceinamide-spacer)hexapeptide conjugate YD 55 **(3)** was synthesised by reacting *N*-colchiceinamide spacer trifluoroacetate salt YD 33 **(12)** and *N*-colchiceinamide spacer oligopeptide succinate compound YD 54 **(18)** in DMF with coupling reagents TBTU and HOBt under basic (DIPEA) condition. Due to its low yield, it was purified by chromatography on a thick-layer TLC plate. The structure of this dual vascular disrupting agent prodrug was confirmed by its ES(+) mass spectrum which had a signal at m/z 1701.8528 which corresponded to (M+H)$^+$.

1.2.5.6 Synthesis of MB1-SUCC-Ala-Gly-Leu-Pro-Ala-Ala-APA-AQ (YD 63) (34): a twin prodrug of Ala-APA-AQ and colchiceinamide derivative (MB1) (8)
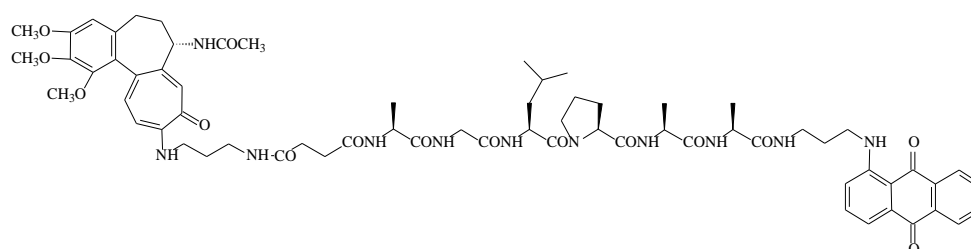
Figure 1.31. MB1-SUCC-Ala-Gly-Leu-Pro-Ala-Ala-APA-AQ (YD 63) (34)

The synthesis of YD 63 **(34)** [**Figure 1.31**] is outlined in **Scheme 1.11**:
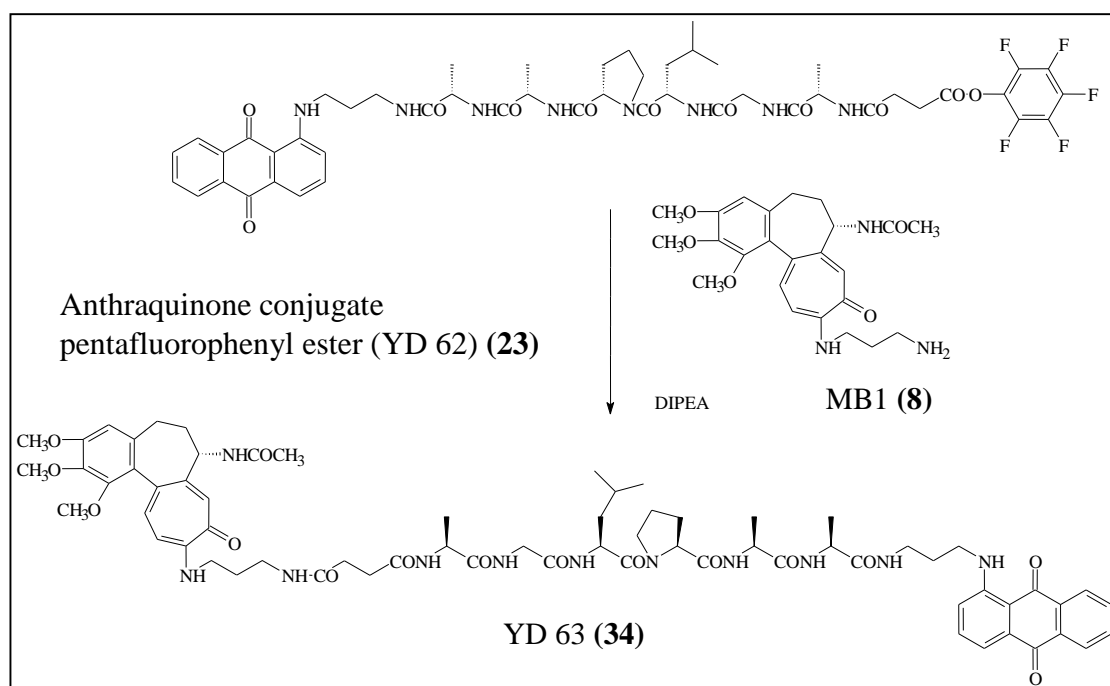
Scheme 1.11. Synthesis of MB1-SUCC-Ala-Gly-Leu-Pro-Ala-Ala-APA-AQ (YD 63) (34)

For the synthesis of the non-identical twin prodrug YD63, the anthraquinone conjugate pentafluorophenyl ester YD 62 **(23)** and 10-(3-aminopropyl)amino-10-demethoxy colchicine (MB1) **(8)** were dissolved in DMF; DIPEA was added into this reaction mixture afterwards [**Scheme 1.11**]. The reaction was relatively slow, two days later, some starting materials remained and it seemed it would not go any further, so the reaction mixture was partitioned between chloroform and water, the organic layer washed with saturated sodium bicarbonate solution and water, dried, filtered and evaporated to near dryness, and then purified by thick layer chromatography, eluting with chloroform: methanol 6:1. The lower red band was collected from the plate, washed with methanol, filtered and evaporated to dryness. The structure of this prodrug containing two experimental cytotoxics was confirmed by its ES(+) mass spectrum which had a signal at m/z 642.8182 for the species $[(M+2H)/2]^{2+}$.

1.2.5.7 <u>Synthesis of AF-SUCC-Ala-Gly-Leu-Pro-Ala-Ala-APA-AQ (YD 64) (35):</u>
<u>a FRET probe of 6-aminofluorescein (22) and its quencher APA-AQ</u>
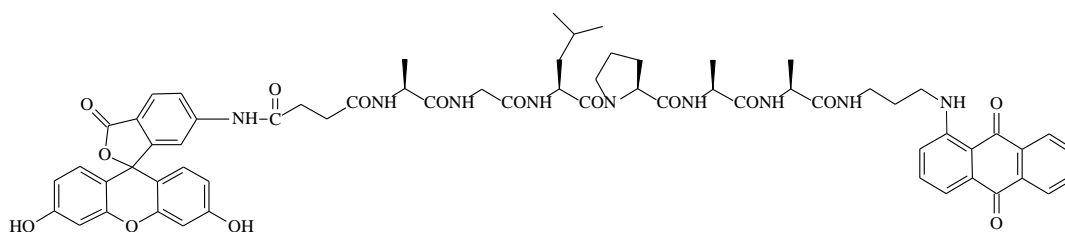
Figure 1.32. AF-SUCC-Ala-Gly-Leu-Pro-Ala-Ala-APA-AQ (YD 64) (35)

The synthesis of a new FRET probe for MMP-9, YD 64 **(35)** [**Figure 1.32**] is shown in **Scheme 1.12**:
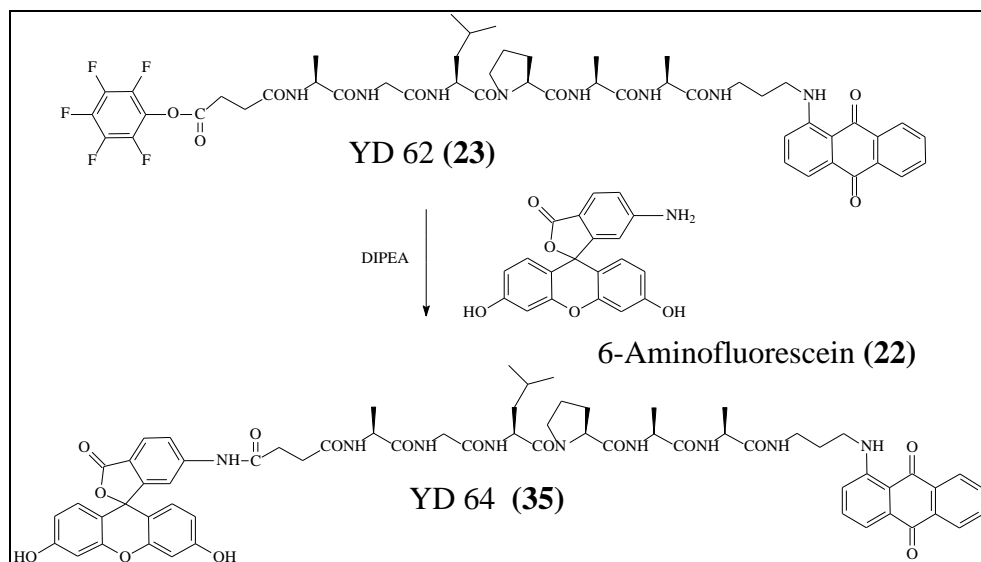
Scheme 1.12. Synthesis of AF-SUCC-Ala-Gly-Leu-Pro-Ala-Ala-APA-AQ (YD 64) (35)

YD 64 **(35)** was designed as a new potential FRET probe of MMP-9 and as a test of the potential of this substrate sequence to be of use in later prodrug syntheses. Also, it represented a departure from labelling an amino group at the terminus of a peptide (typically with FITC or 5,6-FAM), by introducing a succinate linker to use aminofluorescein to label the peptide substrate at a free carboxylic acid terminus. YD 64 **(35)** was synthesised by mixing anthraquinone conjugate pentafluorophenyl ester YD 62 **(23)** and 6-aminofluorescein **(22)** in DMF with one equivalent DIPEA as base. After two days of reaction at room temperature, the reaction mixture was concentrated and re-dissolved in methanol before applying onto thick-layer plates, eluted with chloroform: ethyl acetate: methanol (5:2:1). The dark brown band was collected, washed with methanol, and filtered. However, on TLC (eluted with chloroform: methanol 6:1), there were still traces of one purple spot on the top of the major product brown spot and a yellow spot on the bottom, so the product was re-chromatographed, eluting with chloroform: methanol (6:1). The brown product band from the middle of the plate was isolated in a chromatographically pure form. The structure of this FRET probe was confirmed by its ES(+) mass spectrum which gave a signal at m/z 1212.4 for the species of $(M+Na)^+$ and one at m/z 1228.4 for $(M+K)^+$.

48

Prior to the synthesis of YD 64 (**35**) described above, two separate 'mini' reactions were carried out in ethanol and DMF on a 10 mg of YD 62 (**23**) scale. One hour later, it was found out that YD 62 (**23**) did not dissolve sufficiently well in ethanol and on TLC, the new product brown spot was weaker when compared with the one from the reaction in DMF. Although, ethanol could have been very easily evaporated, poor solubility for YD 62 (**23**) and poor yield for the new compound dictated that DMF was chosen as solvent for the YD 64 (**35**) synthesis reaction.

1.2.5.8 Synthesis of Epi-SUCC-ᴅ-Ala-Ala-Ala-Leu-Gly-Ile-PIP-AQ (36): a twin prodrug of active agents NU:UB 234 (19) and epirubicin (2)
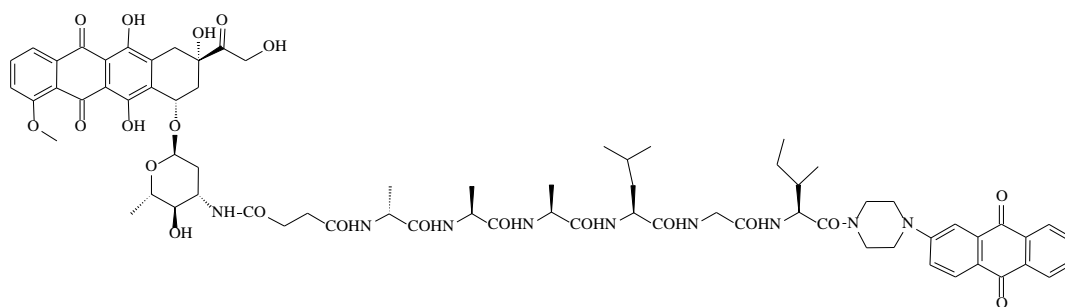
Figure 1.33. Epi-SUCC-ᴅ-Ala-Ala-Ala-Leu-Gly-Ile-PIP-AQ (YD 35) (36)

The motivation for the synthesis of dual cytotoxic prodrug YD 35 (**36**), as shown in **Figure 1.33**, was to combine an experimental anticancer active agent 2-piperazineanthraquinone and clinical anticancer drug epirubicin (**2**) together through a hexapeptide succinate linker.

Epi-SUCC-ᴅ-Ala-Ala-Ala-Leu-Gly-Ile-PIP-AQ (YD 35) (**36**) was synthesised by reacting anthraquinone piperazine spacer hexapeptide succinyl OPFP ester YD 32 (**37**) with epirubicin hydrochloride in DMF; one equivalent DIPEA was added into the reaction solution afterwards, following the general method outlined in **Scheme 1.4**. Overnight, after checking by TLC, the reaction solution was partitioned between dichloromethane and water, purified by flash chromatography and thick-layer chromatography. The

structure of this dual prodrug was confirmed by its ES(+) mass spectrum which had a distinct signal at m/z 1431.6349 for the species $(M+NH_4)^+$.

1.2.5.9 Synthesis of Epi-SUCC-Pro-Ala-Gly-Nva-Phe-Ala-DMPIP-YD9 (YD 61) (4): a twin prodrug of active agents the *N*-colchiceinamide derivative (YD11) (10) and epirubicin (2)
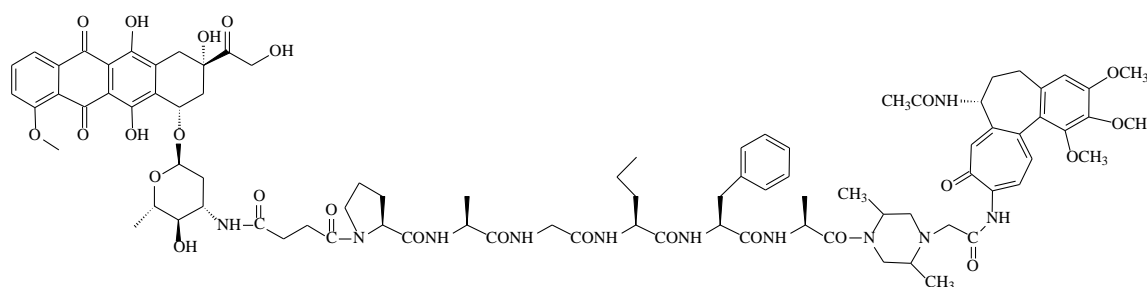
Figure 1.34. Epi-SUCC-Pro-Ala-Gly-Nva-Phe-Ala-DMPIP-YD9 (YD 61) (4)

The motivation for the synthesis of dual prodrug YD 61 **(4)** [**Figure 1.34**] was to combine a vascular disrupting colchicines derivative with the clinically used epirubicin to afford potentially a dual-acting agent with increased synergy (drugs working by two different mechanisms). The colchiceinamide conjugate pentafluorophenyl ester YD 60 **(38)** and clinical anticancer active agent epirubicin **(2)** were linked together through a hexapeptide succinate linker. The hexapeptide is the same as the one successfully applied in the synthesis of YD 55 **(3)**; from previous work, it was decided that the amine bond between Gly and Leu would provide an ideal concensus 'cleavage hot spot' for MMPs.

'Twin prodrug' YD 61 **(4)** was synthesised by reacting the colchicine-derived conjugate pentafluorophenyl ester YD 60 **(38)** with epirubicin hydrochloride in DMF with basic conditions; DIPEA for two hours (following the general method outlined in **Scheme 1.4**). After checking on TLC, DMF was evaporated to dryness, and then the compound was purified by applying onto a thick-layer chromatography plate. The dark red new product band was collected and washed with dichloromethane and methanol, and then it

was filtered and evaporated to dryness. The ES(+) mass spectrum confirmed the structure of this dual prodrug YD 61 **(4)**: for example, a signal at m/z 1706.7479 for the species (M+H)⁺.

1.2.5.10   Synthesis of Epi-SUCC-Ala-Gly-Leu-Pro-Ala-Ala-APA-AQ (YD 67) (21): a twin prodrug of active agents Ala-APA-AQ and epirubicin (2)
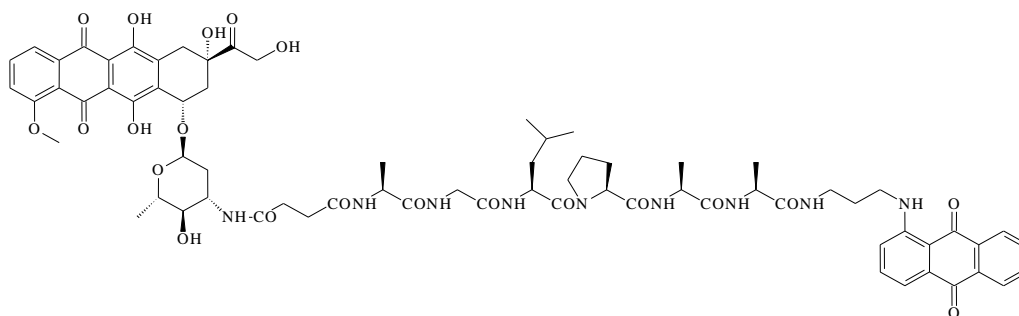
Figure 1.35. Epi-SUCC-Ala-Gly-Leu-Pro-Ala-Ala-APA-AQ (YD 67) (21)

This twin prodrug YD 67 **(21)** is similar to the prodrug YD 63 **(34)**, the only difference is that epirubicin was chosen as an active agent in YD 67 **(21)** instead of colchiceinamide derivative MB1 **(8)** in prodrug YD 63 **(34)**. Anthraquinone conjugate pentafluorophenyl ester YD 62 **(23),** which incorporated an alanine-anthraquinone conjugate cytotoxic agent and epirubicin hydrochloride were mixed together and dissolved in DMF. DIPEA was added into this reaction solution afterwards (following the same method outlined in **Scheme 1.4**). The product was isolated by thick layer chromatography using similar conditions to the above epirubicin-containing conjugates and the structure of this twin drug prodrug YD 67 **(21)** [**Figure 1.35**] was confirmed by its ES(+) mass spectrum which had a base peak at m/z 1386.5755 for the anticipated species (M+H)⁺.

1.2.5.11　Synthesis of Epi-SUCC-Pro-Ala-Gly-Leu-Ala-Ala-PIP-AQ (YD 75) (39): a twin prodrug of active agents Ala-PIP-AQ and epirubicin (2)
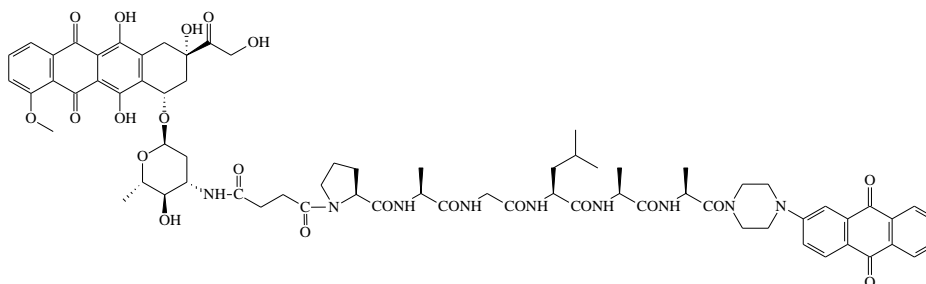

Figure 1.36. Epi-SUCC-Pro-Ala-Gly-Leu-Ala-Ala-PIP-AQ (YD 75) (39)

The motivation for the synthesis of dual prodrug YD 75 **(39)**, as shown in **Figure 1.36**, was to combine experimental anticancer active agent 2-piperazineanthraquinone and clinical anticancer drug epirubicin **(2)** together through the MMP-9 sensitive hexapeptide succinate linker. It is similar to dual prodrug YD 35 **(36)**, but with a different peptide sequence.

Pro-Ala-Gly-Leu-Ala-Ala-PIP-AQ [TFA] (HZ 14) **(40)** was reacted with succinic anhydride in DMF overnight at room temperature to form SUCC-Pro-Ala-Gly-Leu-Ala-Ala-PIP-AQ (HZ 15) **(41)** by following the general method outlined in **Scheme 1.3**. The completion of this reaction was monitored by TLC, and then the reaction mixture was partitioned between dichloromethane and water to remove DMF and excess succinic acid. When the succinate compound HZ 15 **(41)** was almost dry, it was purified by chromatography. Pentafluorophenyl ester compound YD 74 **(42)** was synthesised by reacting the succinate ester HZ 15 **(41)** with pentafluorophenol, DCC and DMAP in dichloromethane. When the PFP-derivative was formed, with no further purification (of DCU), it was reacted with epirubicin hydrochloride by following the general method outlined in **Scheme 1.4**. The progress of synthesis of dual prodrug YD 75 **(39)** was monitored by TLC. When the synthesis was completed, the product was obtained in a chromatographically homogeneous form from thick-layer chromatography. The

structure of this dual prodrug YD 75 **(39)** was confirmed by its electrospray (+) mass spectrum which had a strong signal at m/z 1415.6036 corresponding to the species $(M+NH_4)^+$.

1.2.5.12 <u>Synthesis of FITC-Ala-Nva-Gly-Leu-Pro-Aib-(oxypiperidine)-AQ (YD 17) (43): a FRET probe of FITC and its quencher 1-(4-hydroxypiperidyl) anthraquinone (44)</u>
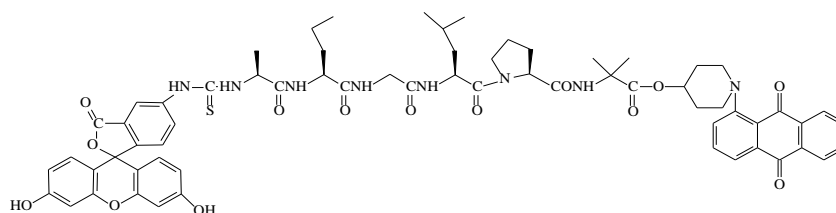
Figure 1.37. FITC-Ala-Nva-Gly-Leu-Pro-Aib-(oxypiperidine)-AQ (YD 17) (43)

The aim of the synthesis of an FITC-anthraquinone oligopeptide conjugate FRET probe, YD 17 **(43)** [**Figure 1.37**] was to test the quenching phenomenon in this prodrug model with an anthraquinone spacer quencher compound at one end before replacement of the fluorophore with another active agent. The anthraquinone residue in this conjugate, in addition to acting as a quencher of fluorescein fluorescence, would act as cytotoxic once it has been released at the tumour side. The pentapeptide acts as a linker to combine two 'warheads' together, and in the middle of this pentapeptide, Gly-Leu is the preferred 'cleavage hot spot' for MMPs. The peptide represented the smallest in this series, since typically hexa- or hepta-peptides had been used in earlier MMP substrates. The FITC label in this prodrug does not function as an active anticancer agent, but an indicator for the proteolytic cleavage of this pentapeptide and release of anthraquinone compound (model drug). Once the prodrug conjugate was cleaved by MMPs, the anthraquinone and FITC residues would no longer be combined together, hence fluorescence of the FITC label would be released which should be straightforward to detect (Van Valckenborgh *et al.*, 2005). In addition to the shorter peptide sequence, this model system was

important because for the first time, a cyclic spacer was attached to the anthraquinone. Thus, model probe/prodrug YD 17 (**43**) was synthesised in order to determine if this Ala-Nva-Gly-Leu-Pro pentapeptide would be cleavable by MMPs, and hence release the anthraquinone compound and free the fluorescence of the FITC label. **Schemes 1.13, 1.14**, and 1.**15** show the synthesis of this FRET probe YD 17 (**43**):
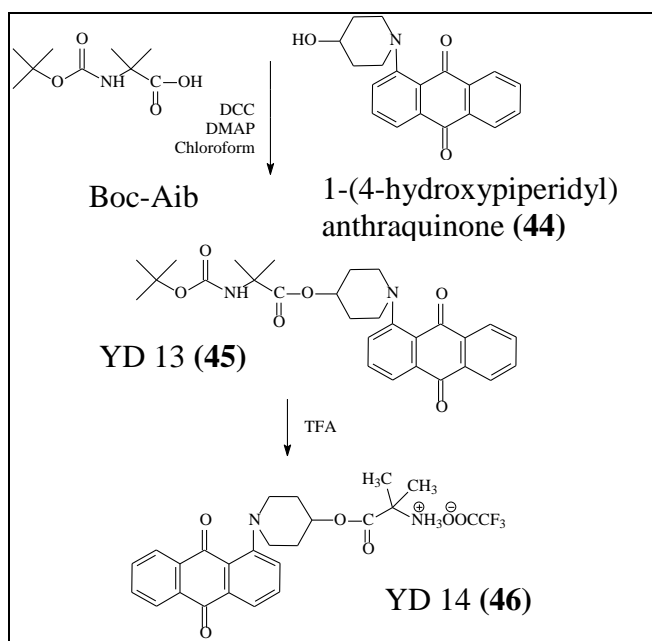
Scheme 1.13. Synthesis of Aib-(oxypiperidine)-AQ [TFA] YD 14 (46)

*N-^{t}*Boc-protected anthraquinone spacer conjugate YD 13 (**45**) was synthesised by reacting 1-(4-hydroxypiperidyl)anthraquinone (**44**) with *N*-α-*t*-Boc-α-aminoisobutyric acid (Boc-Aib), followed by adding coupling reagent dicyclohexylcarbodiimide under basic (DMAP) conditions in chloroform. Overnight, some white crystals of *N,N'*-dicyclohexylurea (DCU) were filtered off from the reaction solution. The rest of the reaction solution was partitioned between chloroform and water, washed with saturated sodium bicarbonate solution and water, dried (MgSO$_4$), filtered and evaporated to dryness. Then YD 13 (**45**) was treated with trifluoroacetic acid at room temperature for 20 minutes to remove the Boc protecting group to form an *N*-terminal trifluoroacetate salt YD 14 (**46**).
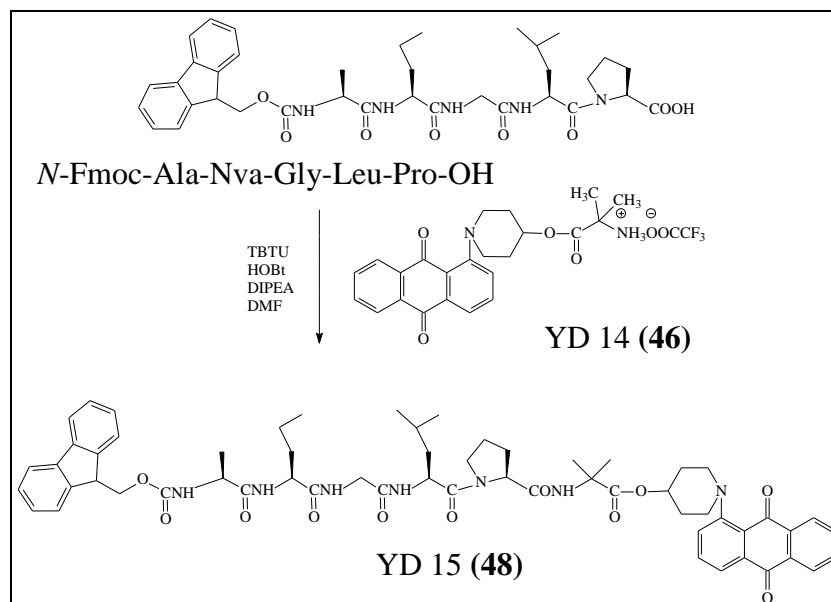
Scheme 1.14. Synthesis of Fmoc-Ala-Nva-Gly-Leu-Pro-Aib-(oxypiperidine)-AQ YD 15 (48)

Then, this *N*-terminal trifluoroacetate salt YD 14 **(46)** was further reacted with Fmoc-Ala-Nva-Gly-Leu-Pro-OH **(47)** in DMF with coupling reagents TBTU and HOBt under basic conditions (DIPEA) at room temperature for two hours. The reaction mixture was then partitioned between chloroform and water, and then evaporated to near dryness before it was loaded onto a silica gel chromatography column, which was eluted with chloroform: methanol (9:1).
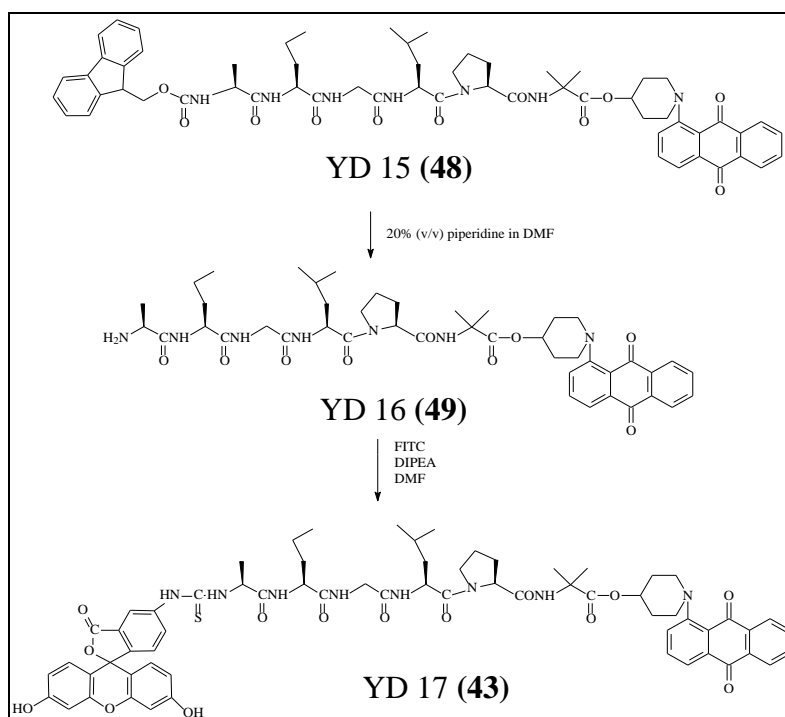
Scheme 1.15. Synthesis of FITC-Ala-Nva-Gly-Leu-Pro-Aib-(oxypiperidine)-AQ (YD 17) (43)

After purification, the pentapeptide conjugate YD 15 **(48)** was dissolved in 20% (v/v) piperidine in DMF and kept stirred for 10 minutes, in order to remove the Fmoc protecting group. Once the compound was dry, it was reacted with fluorescein isothiocyanate in DMF in the presence of DIPEA for four hours. Then the reaction solution was partitioned between chloroform and water, and purified by flash chromatography. The structure of this anthraquinone FITC probe (model for a prodrug) was confirmed by its ESMS(-) mass spectrum which had a signal at m/z 1217.7 for the species (M-H)$^-$.

1.2.6   Synthesis of miscellaneous compounds including prodrug intermediates

1.2.6.1   Synthesis of SUCC-D-Ala-Ala-Ala-Leu-Gly-Leu-Nva-Gly-PIP-AQ (YD 12) (33)
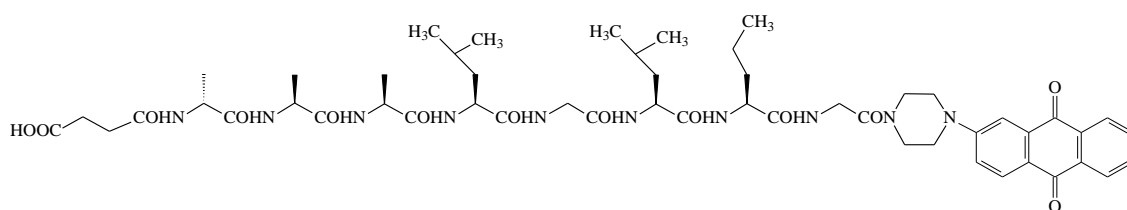
Figure 1.38. SUCC-D-Ala-Ala-Ala-Leu-Gly-Leu-Nva-Gly-PIP-AQ (YD 12) (33)

YD 12 **(33)** is an *N*-trifluoroacetate salt of an octapeptide-anthraquinone conjugate required for the synthesis of some of the above-reported main synthetic targets of this project, namely the twin drug MMP substrate prodrugs. On treatment with base, the trifluoroacetate acid salt would be neutralised and the amine end would be exposed freely for further reaction. Because most warhead spacer conjugates have free amine ends too, in order to couple warhead spacer conjugates onto NU:UB 349 **(50)**, succinic acid with two carboxyl acid ends was applied as a linker.

Succinate compound YD 12 **(33)**, as shown in **Figure 1.38**, was synthesised by reacting NU:UB 349 **(50)**, an anthraquinone-spacer-octapeptide conjugate, with succinic anhydride in DMF under basic (DIPEA) conditions overnight by following the general method outlined in **Scheme 1.3**. After checking by TLC, the whole reaction mixture was

56

evaporated to dryness. Distilled water was added to the dry compound, the mixture was transferred to three 2mL eppendorf tubes with shaking for one hour, and then they were centrifuged. The water layer was checked by the litmus blue test paper. If the litmus blue test paper turned to pink, the compound was washed with further distilled water and centrifuged again until there was no colour change showed on litmus blue test paper. Evaporation to dryness afforded chromatographically pure YD12 **(33)** whose structure was confirmed by its ES(-) mass spectrum which gave a signal at m/z 1043.5 for the species (M-H)⁻ which corresponded to the expected molecular mass of 1044 Da.

1.2.6.2   Synthesis of PFPO-SUCC-Pro-APA-AQ (YD 19) (24)
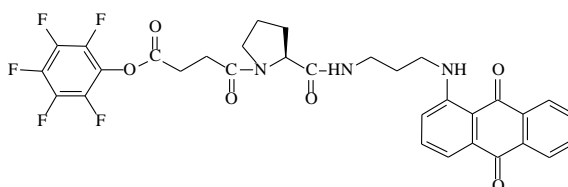
Figure 1.39. PFPO-SUCC-Pro-APA-AQ (YD 19) (24)
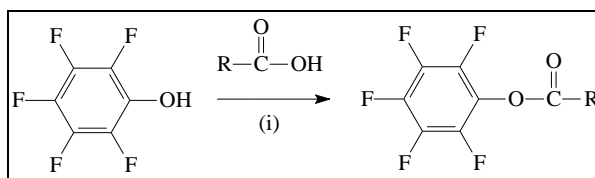
Reagents and conditions: (i) DCC, DMAP, chloroform or dichloromethane, RT, 3h.

Scheme 1.16: General synthesis of OPFP ester compounds

The pentafluorophenolate succinyl proline anthraquinone conjugate YD19 **(24)** was an important model compound to establish both the conditions for making the OPFP ester from a succinate and also to explore the reactivity of the active ester towards important 'warheads' like epirubicin. If good methods could be established with the model compound, it was considered this would provide the best starting point for the eventual synthesis of the target twin prodrugs containing longer peptide sequences.

Aside, because YD12 incorporated the aminopropyl-spaced anthraquinone proline conjugate – which is a known cytotoxic topoisomerase inhibitor – coupling to a second active agent would also afford a simple twin drug of some interest.

DCC, DMAP, pentafluorophenol and NU:UB 354 **(51)** were mixed and dissolved in dichloromethane. The whole reaction was left reacting at room temperature overnight. The progress of this reaction was monitored by TLC. When it was finished, clear/white crystalline precipitate (DCU) in the reaction solution was filtered off. The remainder was evaporated to dryness and used without further purification.

1.2.6.3   Synthesis of Fmoc-Pro-Ala-Gly-Nva-Phe-Ala-OH (YD 43) (52)
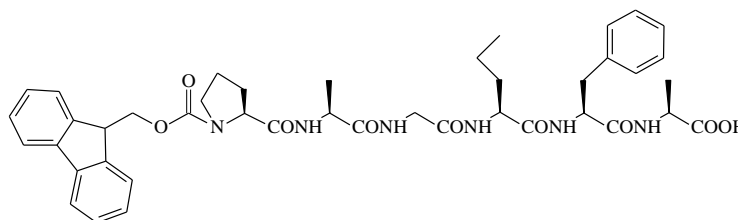
Figure 1.40. Fmoc-Pro-Ala-Gly-Nva-Phe-Ala-OH (YD 43) (52)

Fmoc-Pro-Ala-Gly-Nva-Phe-Ala-OH (YD 43) **(52)**, as shown in **Figure 1.40**, was synthesised by using solid phase peptides synthesis (SPPS).

1.2.6.4   Solid Phase Peptide Synthesis (SPPS)

The simple idea of solid phase peptide synthesis was first introduced by Merrifield in 1963. Solid phase peptide synthesis is based on adding N-α-protected-amino acids onto an insoluble polymeric support.
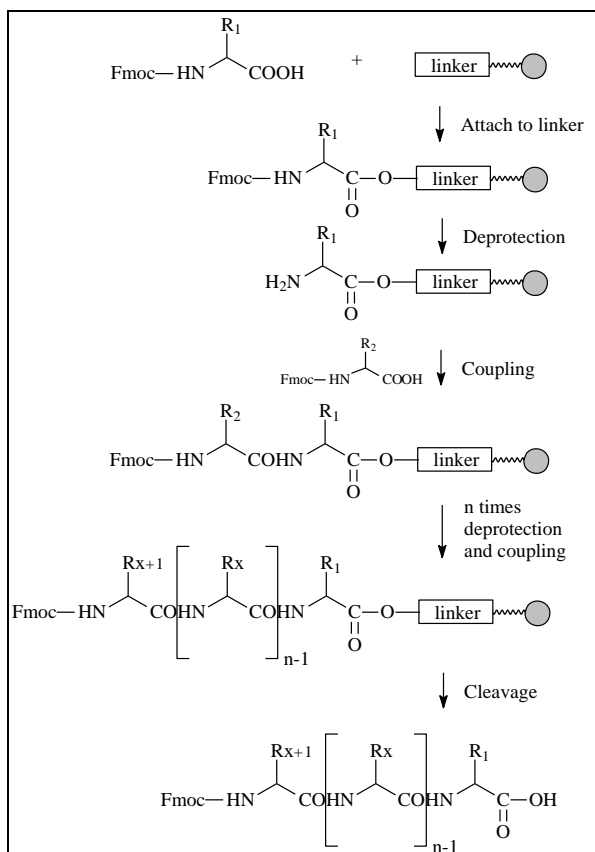
Scheme 1.17. Solid Phase Peptide Synthesis (SPPS)

Dichloromethane (DCM) and *N*,*N*-dimethylformamide (DMF) are the better solvents used for resin deprotection, coupling and washing. Fmoc protected amino acids are used more popularly than Boc protected amino acids in SPPS. In Fmoc synthesis, the Fmoc protecting group can be removed by using 20% piperidine in DMF, and TFA is only used for the final cleavage of peptide from the resin. However, in Boc synthesis, the Boc protecting group has to be removed by very dangerous HF and using expensive laboratory equipment that are not available in most labs.

Pre-loaded peptide 2-chlorotrityl resins **(53)** [**Figure 1.41**] were used for building peptide chains in this research.
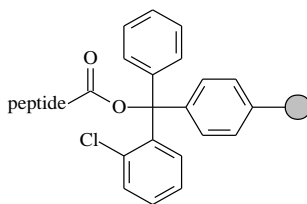
Figure 1.41. Pre-loaded peptide 2-chlorotrityl resin (53)

Using an SPPS method to synthesise particular peptide chains is fast, efficient and easy to carry out. However, if during coupling and de-protecting stages, the reaction is not totally completed, it will bring impurity problems and reduce the yield. So, the Kaiser test (for the detection of free amino groups) was introduced in SPPS to monitor the completeness during coupling and de-protecting reactions. The Kaiser test has been used widely because it is simple and quick. However, it cannot give a positive dark blue colour reliably when testing some free α-amino acids (such as serine, asparagine, and aspartic acid) and proline which is a secondary amino acid. **Scheme 1.18** outlines the general Kaiser test reaction:
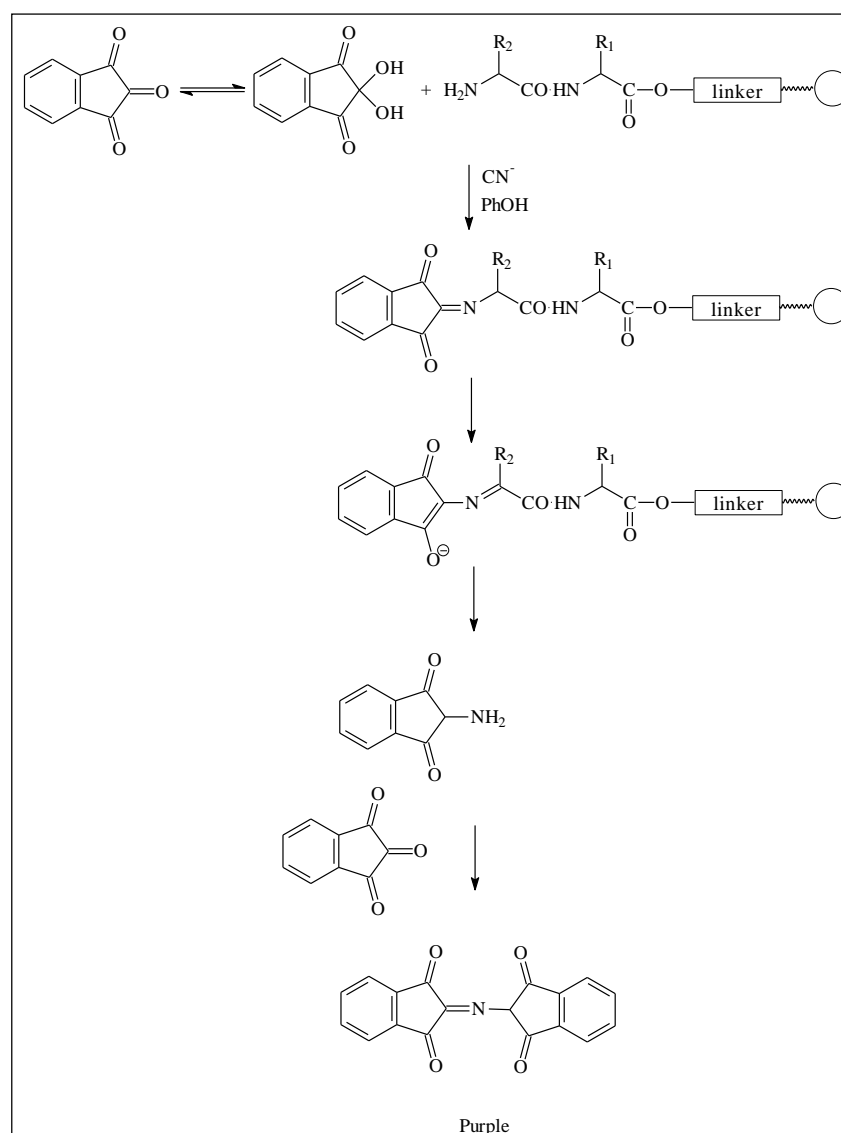
Scheme 1.18. Kaiser test (Friedman, 2004)

60

Proline pre-loaded 2-chlorotrityl resin was swelled in dichloromethane first, and then was reacted with *N*-Fmoc amino acid in the cycles of coupling and deprotection: Fmoc-Pro-Ala-Gly-Nva-Phe-Ala-OH (YD 43) **(52)** was synthesised by following sequences:

- 1st cycle: *N*-Fmoc-L-phenylalanine
- 2nd cycle: *N*-Fmoc-L-norvaline
- 3rd cycle: *N*-Fmoc-L-glycine
- 4th cycle: *N*-Fmoc-L-alanine
- 5th cycle: *N*-Fmoc-L-proline

After coupling five *N*-Fmoc-protected amino acids onto pre-loaded resins in sequence, the hexapeptide was cleaved off from resin without further purification.

After each coupling and deprotection steps, it was noticed that Kaiser test was not suitable for this peptide synthesis for some reasons. As after removing *N*-Fmoc protecting group, the Kaiser test should give a positive result—resin beads should turn to dark blue, while during this peptide synthesis, after heating at 80°C for three minutes, only the solution turned into blue colour, resin beads still remained colourless. This may suggest that during the Kaiser test, peptides were cleaved off from the resin beads. So, during each deprotection step, a solution of 20% (v/v) piperidine in DMF was added into SPPS reaction vessel for 4, 5 times, 10-15min each time, to make sure the *N*-Fmoc protecting group was fully removed. Also, an anthraquinone compound **(54)** (prepared and developed in-house) was introduced to replace the Kaiser test.
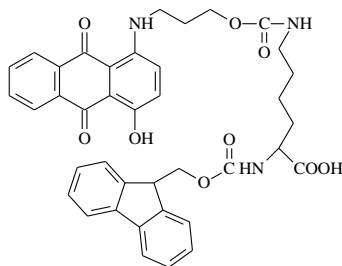
Figure 1.42. Colour test *N*-Fmoc protected anthraquinone compound (54)

In this anthraquinone compound **(54)**, as shown in **Figure 1.42**, there was an *N*-Fmoc-protected amino acid with a free acid end, so with coupling reagents and under basic condition, it could react with free amino end from a peptide on resin beads after the *N*-deprotection step. As the anthraquinone compound was dark blue, because of its 4-hydroxyl-anthraquinone part, so after this anthraquinone compound **(54)** coupling with peptide on resin beads, produced a dark blue colour, to give a positive result. The structure of this *N*-Fmoc protected peptide YD 43 **(52)** was confirmed by its ES(+) mass spectrum which had a signal at m/z 800.3979 for the species of $(M+NH_4)^+$.

During attempts to couple the *N*-Fmoc protected oligopeptide YD 43 **(52)** onto colchiceinamide piperazine spacer *N*-terminal trifluoroacetate salt YD 33 **(12)** in DMF with PyBOP and HOBt coupling reagents under basic (DIPEA) condition, even after two days, no new products were found. However, if one amino acid, like alanine, was coupled onto colchicine compound YD 33 **(12)** first, and then coupled to YD 43 **(52)** with coupling reagents under basic condition, the reaction proceeded with no difficulty. The ES(+) mass spectrum displayed a signal at m/z 1374.6753 corresponding to $(M+H)^+$, which proved its structure was correct.

1.2.6.5 <u>Synthesis of D-Ala-Ala-Ala-Leu-Gly-Ile-PIP-AQ [TFA] (NU:UB 363) (30)</u>
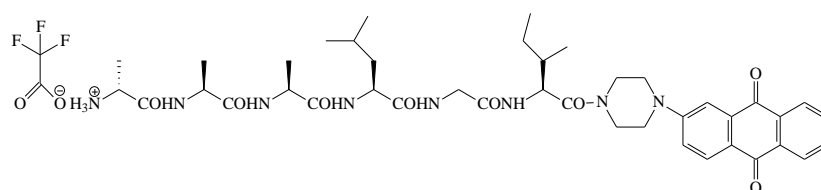
Figure 1.43. D-Ala-Ala-Ala-Leu-Gly-Ile-PIP-AQ [TFA] (NU:UB 363) (30)

The motivation for the synthesis of anthraquinone spacer oligopeptide conjugates of the type represented by the trifluoroacetate salt NU:UB 363 **(30)** [**Figure 1.43**] was to combine the experimental anticancer agent anthraquinone compound onto a hexapeptide conjugate which theoretically can bind and be cleaved at the 'hot spot' by MMPs, hence release active anticancer agent.

- In MMP-9, the S1 subsite is a very shallow pocket, so glycine at the P1 position is the preferred fit in MMPs' S1 pocket, while, in contrast, the S1' subsite is a long deep pocket, so isoleucine (or leu or long straight chains, e.g. nva or nle) at the P1' can fit well inside the S1 position. Once the oligopeptide binds with MMPs, the amine bond between glycine and isoleucine would be an ideal 'cleavage hot spot'.

- The piperazine substituent on the anthraquinone provided the secondary amino group as an anchor point for constructing the oligopeptide with the required MMP9-sensitive cleavage site.

- Finally, the whole anthraquinone oligopeptide conjugate was further modified to an *N*-trifluoroacetate salt for further coupling with other active anticancer agents, either experimental or clinical agent.

The synthesis of NU:UB 363 (**30**) is shown in **1.18**:
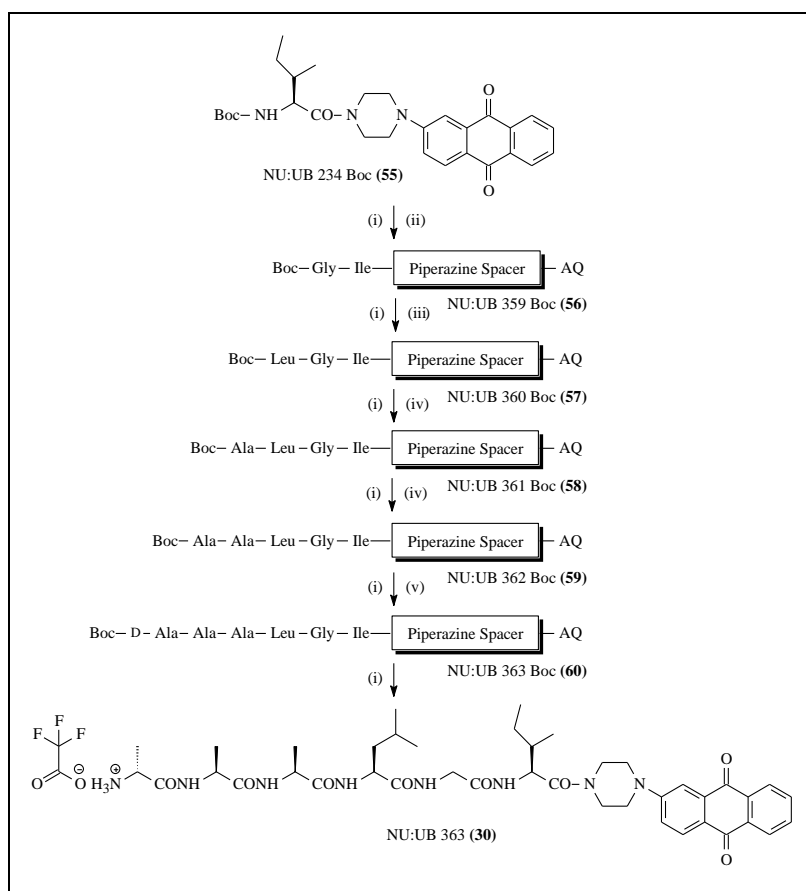
Reagents and conditions: (i) TFA, RT, 30min. (ii) Boc-Gly-OSu, DIPEA, DMF, RT, 4h. (iii) Boc-Leu-OSu, DIPEA, DMF, RT, 4h. (iv) Boc-Ala-OSu, DIPEA, DMF, RT, 2h. (v) Boc-D-Ala-OH, TBTU, HOBt, DIPEA, DMF, RT, 2h.

Scheme 1.19. Synthesis of NU:UB 363 (30)

The anthraquinone-hexapeptide conjugate *N*-trifluoroacetate salt NU:UB 363 **(30)** was synthesised (by solution methods) from *N-^tBoc* protected NU:UB 234 **(55)** [**Scheme 1.19**] by a repeating sequence of deprotection of the *N-^tBoc* protecting group by treating compounds with TFA for around 30min, and then coupling the next *N-^tBoc* protected amino acid OSu ester (in sequence: Boc-Gly-OSu, Boc-Leu-OSu, Boc-Ala-OSu, Boc-Ala-OSu, Boc-D-Ala-OSu) under basic (DIPEA) condition without any coupling reagents. The sequential intermediates were purified by flash chromatography before deprotection of *N-^tBoc* group. However, during the last step, when the *N*-trifluoroacetate salt NU:UB 362 **(61)** was reacted with Boc-D-Ala-OSu, it barely reacted even after 24h. This could have been because the Boc-D-Ala-OSu was not very fresh; some of it may have decomposed. So, instead, fresh Boc-D-Ala-OH was used to couple with NU:UB 362 **(61)** by using coupling reagents TBTU, HOBt and DIPEA. The structure of this trifluoroacetate salt was confirmed by its ES(+) mass spectrum which gave a strong signal at m/z 789.4277 for the cation $(M+H)^+$ and its ES(-) mass spectrum which had a strong signal (base peak) at m/z 113.0 for the trifluoroacetate anion.

1.2.6.6 Synthesis of SUCC-D-Ala-Ala-Ala-Leu-Gly-Ile-PIP-AQ (YD 30) (28)
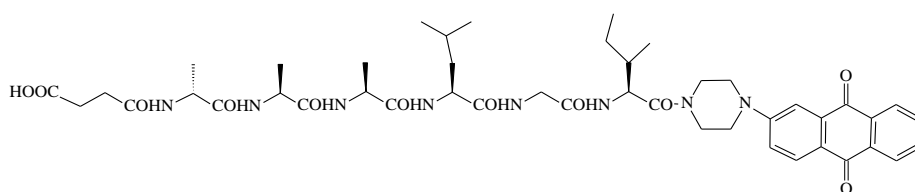
Figure 1.44. SUCC-D-Ala-Ala-Ala-Leu-Gly-Ile-PIP-AQ (YD 30) (28)

This hexapeptide spacer anthraquinone succinate conjugate YD 30 **(28)** was coupled with different colchiceinamide derivatives in the syntheses of twin prodrugs YD 34 **(27)** [**Scheme 1.5**], YD 42 **(29)** [**Scheme 1.6**] and YD 58 **(31)** [**Scheme 1.8**].

By the same method as the synthesis of succinate compound YD 12 **(33)**, in order to couple *N*-trifluoroacetate salt NU:UB 363 **(30)** with an amine containing 'warhead spacer

conjugate' to form a new 'twin drugs' prodrug, succinic anhydride was applied as a linker between these two compounds.

The hexapeptide spacer anthraquinone succinate conjugate YD 30 **(28)**, as shown in **Figure 1.44**, was synthesised by reacting NU:UB 363 **(30)**, an anthraquinone-spacer-octapeptide *N*-trifluoroacetate salt, with succinic anhydride in DMF under basic (DIPEA) conditions overnight, following the general method outlined in **Scheme 1.3**, Upon completion of the reaction, the whole mixture was evaporated to dryness. YD 30 **(28)** did not dissolve in water, thus, excess succinic acid was washed out with copious amounts of water until a negative litmus test was obtained. The succinate was used for further reaction without further purification.

1.2.6.7 Synthesis of PFPO-SUCC-D-Ala-Ala-Ala-Leu-Gly-Ile-PIP-AQ (YD 32) (37)
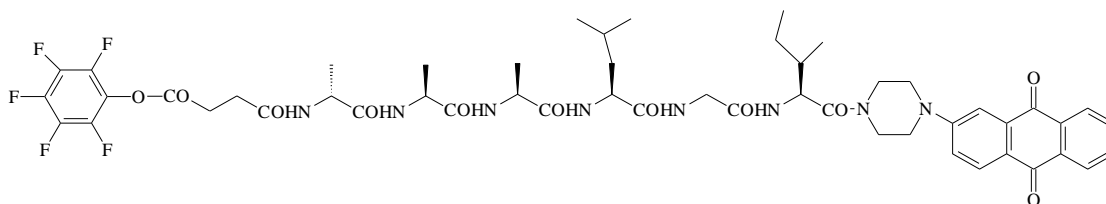
Figure 1.45. PFPO-SUCC-D-Ala-Ala-Ala-Leu-Gly-Ile-PIP-AQ (YD 32) (37)

Because epirubicin **(2)** is unstable under the general peptide (basic) reaction conditions, in order to couple epirubicin **(2)** with hexapeptide spacer anthraquinone succinate conjugate YD 30 **(28)** to form the twin prodrug YD 35 **(36)** [**Figure 1.33**], YD 30 **(28)** had to be converted into its OPFP ester YD 32 **(37)**.

PFPO-SUCC-D-Ala-Ala-Ala-Leu-Gly-Ile-PIP-AQ (YD 32) **(37)** [**Figure 1.45**] was synthesised by reacting succinate compound YD 30 **(28)** with pentafluorophenol and coupling reagents DCC, DMAP in chloroform by following the general synthesis of OPFP ester compounds outlined in **Scheme 1.16**. The first time, the attempted synthesis of YD 32 **(37)** was tried in dichloromethane with 10% DMF, but YD 30 **(28)** did not

dissolve in dichloromethane very well, so a bit more DMF was applied to help YD 30 (**28**) to dissolve in the solution. However, the mass spectrum result showed that the isolated product was not YD 32 (**37**); it was the unproductive, rearrangement product intermedia *N*-acylurea compound.
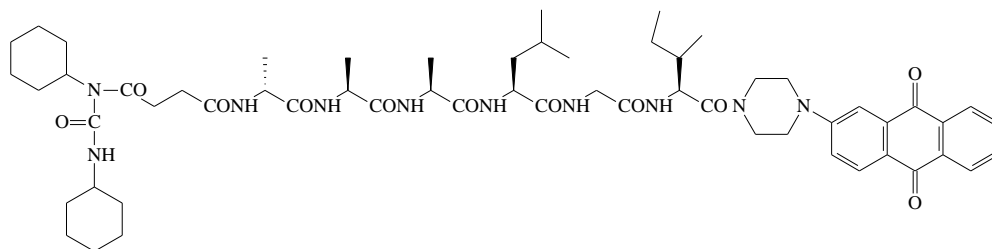
Figure 1.46. Intermediate *N*-acylurea compound (62)

This is because in the solution of DMF, it would be more likely to happen that the rearrangement of the *O*-acylisourea compound (**63**) by intramolecular reaction than further reaction of *O*-acylisourea compound (**63**) by external nucleophiles as expected (Montalbetti and Falque, 2005). This unproductive *N*-acylurea compound (**62**) [**Figure 1.46**] was confirmed by its ES(+) mass spectrum which had a peak at m/z 1095.6221 for the species $(M+H)^+$.
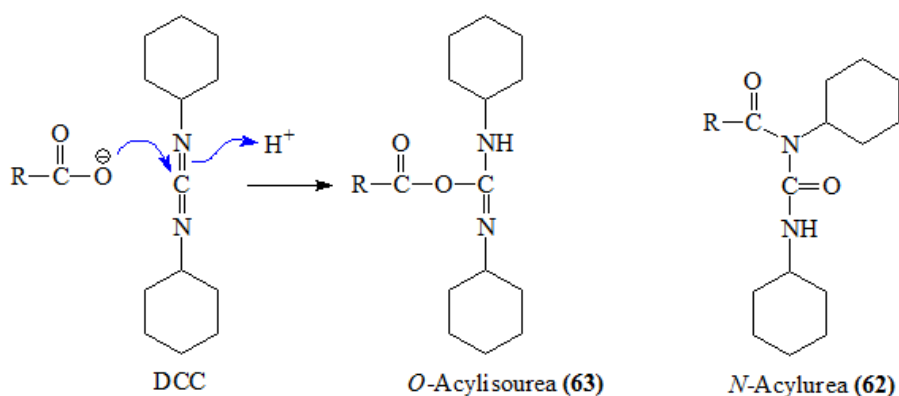
Scheme 1.20. Formation of *O*-Acylisourea (63) and *N*-Acylurea (62)

So, the choice of solution became a crucial feature in this reaction. In the synthesis of OPFP ester YD 32 (**37**), three solutions had been tested. In the beginning, dichloromethane was chosen. It took hours to dissolve YD 30 (**28**), and in the end there were two spots on the TLC plate, the lower one was stronger than the upper one. So a

mini reaction of the impure compound and YD 41 (**16**) was carried out. The TLC plate showed the upper spot disappeared and a new spot could be found lower than the original second spot. This could suggest that the upper spot was the pentafluorophenolate ester and the lower one was the less reacted *N*-acylurea compound (**62**). And then, the YD 32 (**37**) formation was repeated in chloroform. It took 1.5 hours to dissolve 90% of YD 30 (**28**), and there were two spots on the TLC plate as well, but the upper one was much more intense than the lower one. This could suggest that in chloroform, the desired *O*-acylisourea compound of this reaction would be more likely to react with external nucleophiles to form the desired pentafluorophenolate ester. Lastly, acetonitrile was chosen for this reaction, but unfortunately, no reaction took place. The activation of DCC was very dependent on the choices of solvent. Dichloromethane or chloroform were preferred. Windridge and Jorgensen (1971) also suggested that mixing the acid and DCC at 0°C first, and then adding the amine into the reaction mixture could diminish the side reaction. Also, selected nucleophiles (such as DMAP and HOBt) could prevent the side reaction, as they can react faster with DCC than the acyl transfer, and form an intermediate for further reaction.

1.2.6.8   Synthesis of Pro-Ala-Gly-Nva-Phe-Ala-DMPIP-YD9 [TFA] (YD 53) (64)
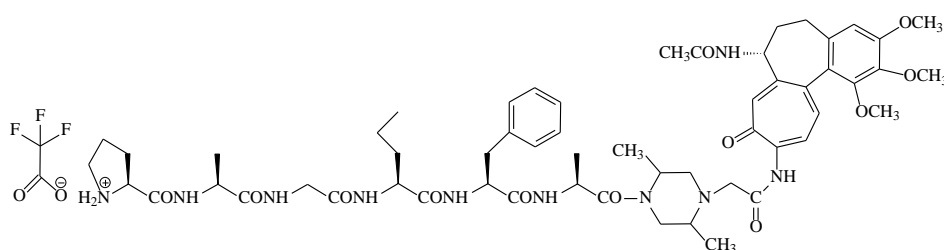
Figure 1.47. Pro-Ala-Gly-Nva-Phe-Ala-DMPIP-YD9 [TFA] (YD 53) (64)

In the beginning, it was attempted to react *N*-trifluoroacetate salt YD 33 (**12**) with YD 43 (**52**) (an *N*-Fmoc group protected hexapeptide conjugate synthesised by solid phase peptide synthesis) to form Fmoc-Pro-Ala-Gly-Nva-Phe-Ala-DMPIP-YD9, but somehow,

even after a few days, it still would not react very well. It seemed that the *N*-trifluoroacetate salt YD 33 **(12)** barely reacted with *N*-Fmoc group protected hexapeptide. Because of this unsuccessful attempt to make this Fmoc-Pro-Ala-Gly-Nva-Phe-Ala-spacer-colchiceinamide, so hexapeptide spacer colchiceinamide derivative trifluoroacetate YD 53 **(64)** was synthesised by using solution phase peptide coupling method to add each amino acid in sequence onto a pre-formed colchiceinamide spacer derivative (trifluoroacetate) YD 33 **(12)**.

The rationale of the design for *N*-trifluoroacetate salt YD 53 **(64)** [**Figure 1.47**] was similar to *N*-trifluoroacetate salt NU:UB 363 **(30)**. Instead of using a cytotoxic agent anthraquinone compound, the antivascular disrupting agent colchicine analogue was applied in this synthesis.

- Colchicine was initially converted into *N*-colchiceinamide **(6)**. As both 2,5-dimethylpiperazine and *N*-colchiceinamide **(6)** have a free amino group, so chloroacetyl chloride was used to introduce a linker, in order to couple the 'warhead agent' with the spacer compound.

- The P3 position was occupied by proline, it's five-membered ring structure can fit well in the round shape S3 pocket; glycine and norvaline can fit in shallow S1 pocket and long deep hydrophobic S1' pocket respectively (McGeehan, 1994).

The synthesis of YD 53 **(64)** is shown in **Scheme 1.21**:
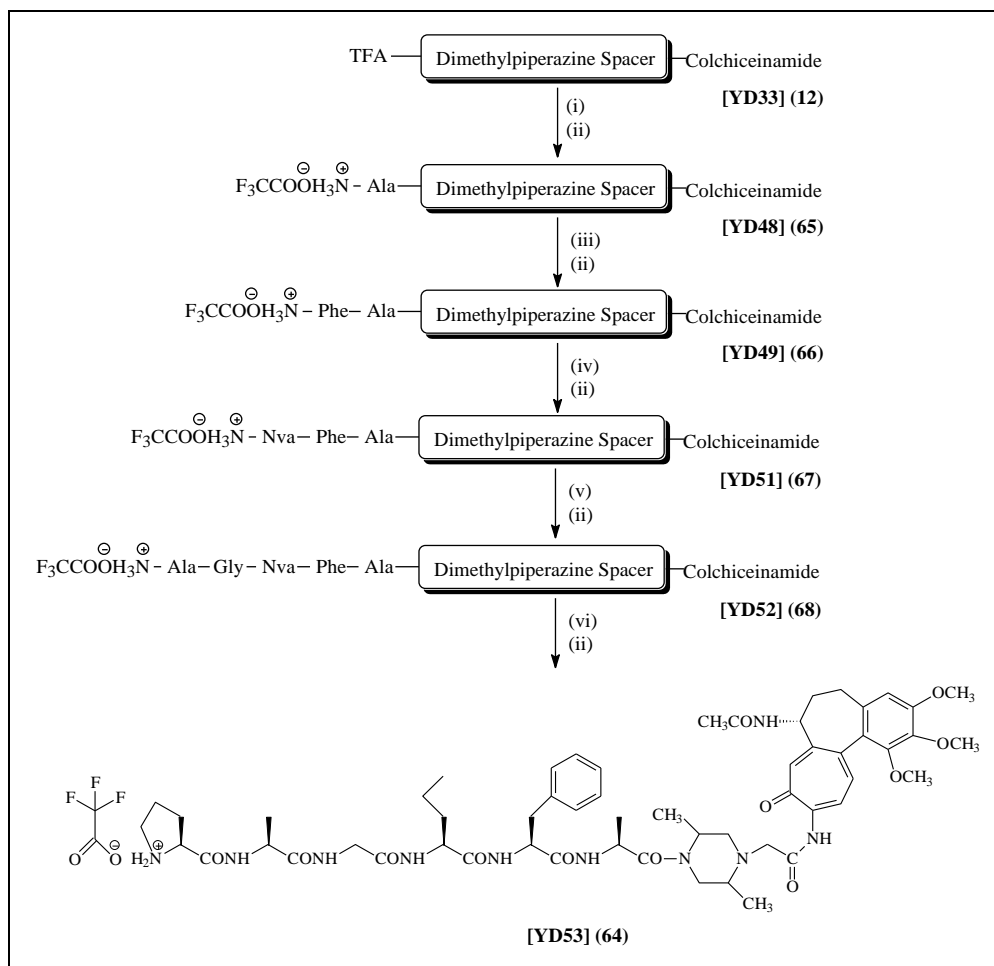
Reagents and conditions: (i) Boc-Ala-OSu, DIPEA, DMF, RT, 4h. (ii) TFA, RT, 30min. (iii) Boc-Phe-OSu, DIPEA, DMF, RT, 4h. (iv) Boc-Nva-OSu, DIPEA, DMF, RT, 4h. (v) Boc-Ala-Gly-OSu, DIPEA, DMF, RT, 4h. (vi) Boc-Pro-OSu, DIPEA, DMF, RT, 4h.

Scheme 1.21. Synthesis of Pro-Ala-Gly-Nva-Phe-Ala-DMPIP-YD9 [TFA] (YD 53) (64)

Pro-Ala-Gly-Nva-Phe-Ala-DMPIP-YD9 [TFA] (YD 53) **(64)** was synthesised from *N*-colchiceinamide spacer *N*-trifluoroacetate salt YD 33 **(12)** by repeating coupling with Boc protected amino acid or Boc protected amino acid OSu ester compounds (in sequence followed by Boc-Ala-OSu, Boc-Phe-OSu, Boc-Nva-OH, Boc-Ala-Gly-OSu, Boc-Pro-OH), purifying by loading onto a flash chromatography column, and deprotecting by using TFA for typically 30 minutes. The structure of this trifluoroacetate salt YD 53 **(64)** was confirmed by its ES(+) mass spectrum which gave a signal (base peak) at m/z 1081.5708 for the species of $(M+H)^+$.

It seemed *N*-trifluoroacetate salt YD 33 (**12**) barely reacted with *N*-Fmoc group protected hexapeptide YD 43 (**52**). It suggested that maybe because of the piperazine ring in YD 33 (**12**) compound acted as a weak base, so the solution of YD 33 (**12**) in DMF would act as a 20% (v/v) solution of piperidine in DMF in the deprotection of *N*-Fmoc protecting group, then it could remove the Fmoc group from YD 43 (**52**) instead of coupling with YD 43 (**52**). A mini test reaction was carried out to prove this suggestion. YD 33 (**12**) and YD 43 (**52**) were mixed together in DMF without coupling reagents. However, after a few days, TLC still showed that no reaction took place. Both YD 33 (**12**) and YD 43 (**52**) could be found on TLC plates separately, no other new spot(s) were detected.
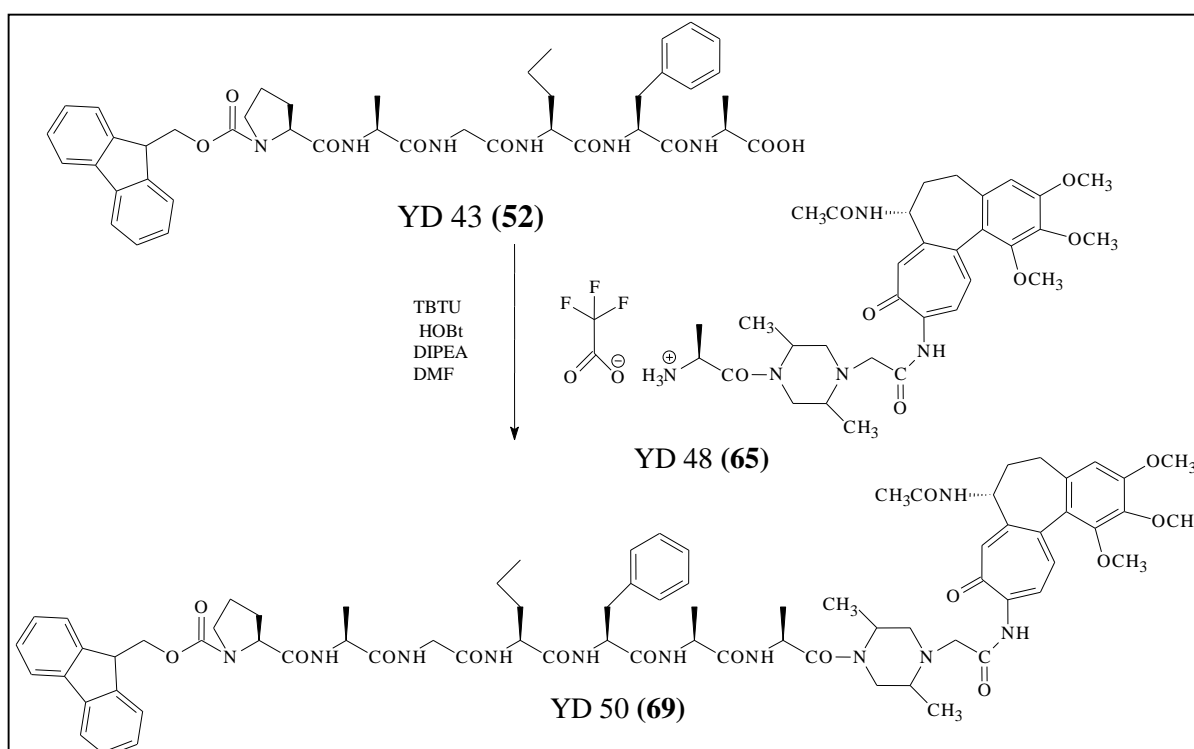
Scheme 1.22. Synthesis of Fmoc-Pro-Ala-Gly-Nva-Phe-Ala-Ala-DMPIP-YD9 (YD 50) (69)

So, it was repeated, by reacting *N*-Fmoc group protected hexapeptide conjugate YD 43 (**52**) with *N*-trifluoroacetate salt YD 48 (one amino acid, Ala, attached to the colchicine compound) (**65**) by using coupling reagents in DMF under basic (DIPEA) condition, as illustrated in **Scheme 1.22**. Within two hours, a new spot was found by TLC. The mass spectrum result confirmed this structure, ES(+) m/z: 1374.6753 (M+H)$^+$. So it suggested

that the colchicine compound might have difficulty to react with the Fmoc-protected compound directly because of the two methyl groups on the piperazinyl ring possibly blocking access to the carboxyl acid end of hexapeptide conjugate YD 43 **(52)**. However, if one amino acid was coupled onto the colchiceinamide piperazine spacer compound first, it would be more straightforward to couple with the Fmoc-protected oligopeptide. Coupling one alanine on to *N*-colchiceinamide piperazine conjugate YD 48 **(65)** will prolong the distance between the methyl groups and the carboxyl acid end of YD 43 **(52)**, hence increase the likely success of coupling the oligopeptide onto a colchiceinamide spacer conjugate.

1.2.6.9   Synthesis of SUCC-Pro-Ala-Gly-Nva-Phe-Ala-DMPIP-YD9 (YD 54) (18)
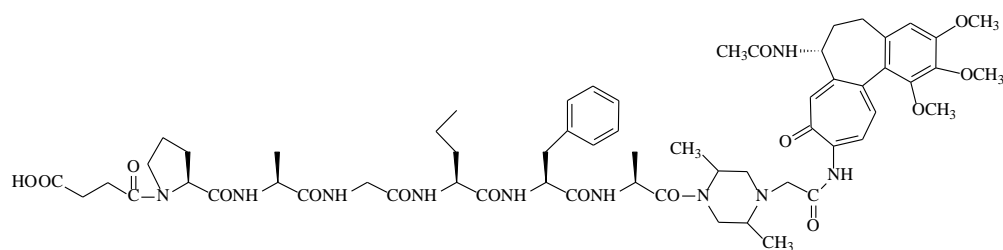
Figure 1.48. SUCC-Pro-Ala-Gly-Nva-Phe-Ala-DMPIP-YD9 (YD 54) (18)

This succinyl hexapeptide spacer colchiceinamide (YD 54) **(18)** was applied in the synthesis of bis-(colchiceinamide-spacer)hexapeptide conjugate (YD 55) **(3)** [**Scheme 1.10**]. SUCC-Pro-Ala-Gly-Nva-Phe-Ala-DMPIP-YD9 (YD 54) **(18)** [**Figure 1.48**] was synthesised by reacting *N*-trifluoroacetate salt YD 53 **(64)** with succinic anhydride in DMF under basic (DIPEA) condition, following the general method outlined in **Scheme 1.3**. Three days later, after checking on the TLC plate, then the reaction mixture was evaporated to dryness. YD 54 **(18)** compound was dissolved in dichloromethane, as extra succinic acid would not be dissolved in dichloromethane, so it was simply filtered off from YD 54 **(18)** dichloromethane solution. Then YD 54 **(18)** compound was evaporated to dryness.

1.2.6.10 Synthesis of MB1-SUCC-OPFP (YD 57) (26)
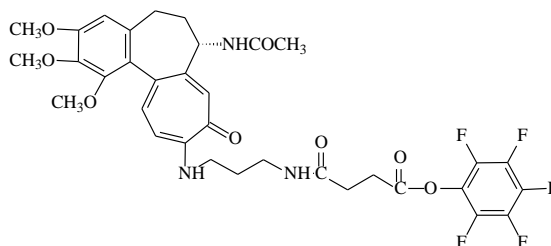
Figure 1.49. MB1-SUCC-OPFP (YD 57) (26)

MB1-SUCC-OPFP YD 57 **(26)**, as shown in **Figure 1.49**, was used to couple with epirubicin **(2)** to form the model compound Epi-SUCC-MB1 (YD 59) **(25)** [**Figure 1.25**]. This OPFP ester was synthesised by mixing colchiceinamide derivative succinate compound YD 56 **(17)** and DCC in dichloromethane first, and then followed by adding pentafluorophenol and DMAP, following the general synthesis of OPFP ester compounds outlined in **Scheme 1.16**. This reaction took nearly two days to react. White solid compound - DCU was filtered out from the YD 57 **(26)** dichloromethane solution. As pentafluorophenolate ester was not steady, so no further purification was needed to apply for YD 57 **(26)**.

Balalaie *et al.* (2008) reported that a traditional method to synthesise carboxylic acid esters with DCC/ DMAP was slow, often in low yield and sometimes could not prevent side reactions. They had found using TBTU as an efficient coupling reagent could speed up the esterification of carboxylic acids with alcohols and phenols at room temperature, and as no DCC had been used, so there would be no *N*-acylurea compound in the product. Using TBTU instead of DCC/ DMAP could give high yield and the by-product HOBt is water-soluble, which are the other two advantages of this new application.

Scheme 1.23. Synthesis of PFPO-SUCC-Pro-APA-AQ (YD 19) (24)

Before using Balalaie's method to synthesis YD 57 **(26)**, a mini test reaction was carried

out by using Balalaie's method to synthesis YD 19 **(24)**. When compared with the original

YD 19 **(24)** compound, the new OPFP ester compound YD 19 **(24)** was identical. So this

suggested Balalaie's method may be suitable for pentafluorophenyl ester YD 57 **(26)**

reaction as well. However, when a mini reaction was carried on for YD 57 **(26)** synthesis

by using Balalaie's method, nothing happened. There was only a barely weak spot on

TLC plate even after two days reaction. This may suggest that Balalaie's method was not

suitable for colchicine compound reaction to form pentafluorophenyl ester.

1.2.6.11 Synthesis of PFPO-SUCC-Pro-Ala-Gly-Nva-Phe-Ala-DMPIP-YD9 (YD 60) (38)

Figure 1.50. PFPO-SUCC-Pro-Ala-Gly-Nva-Phe-Ala-DMPIP-YD9 (YD 60) (38)

In order to synthesise the twin prodrug YD 61 **(4)**, epirubicin **(2)** has to couple with this

colchiceinamide spacer hexapeptide succinyl OPFP ester YD 60 **(38)** [**Figure 1.50**] that

was synthesised by mixing colchiceinamide spacer oligopeptide succinate compound YD

73

54 (**18**) and DCC in dichloromethane first, and then mixed with pentafluorophenol and DMAP, following the general synthesis of OPFP ester compounds outlined in **Scheme 1.16**. This reaction took nearly 4 hours to react significantly. White solid compound DCU was filtered out from YD 60 (**38**) dichloromethane solution. The whole reaction solution was evaporated to dryness and used without any further purification.

1.2.6.12   Synthesis of PFPO-SUCC-Ala-Gly-Leu-Pro-Ala-Ala-APA-AQ (YD 62) (23)
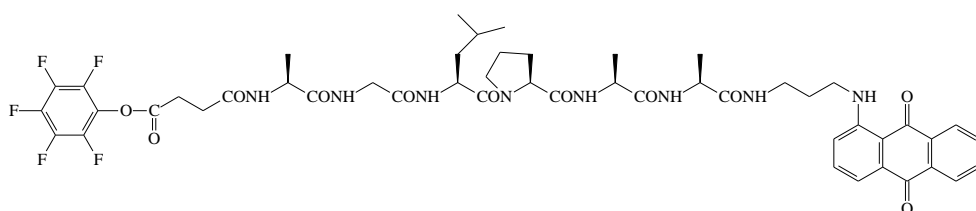
Figure 1.51. PFPO-SUCC-Ala-Gly-Leu-Pro-Ala-Ala-APA-AQ (YD 62) (23)
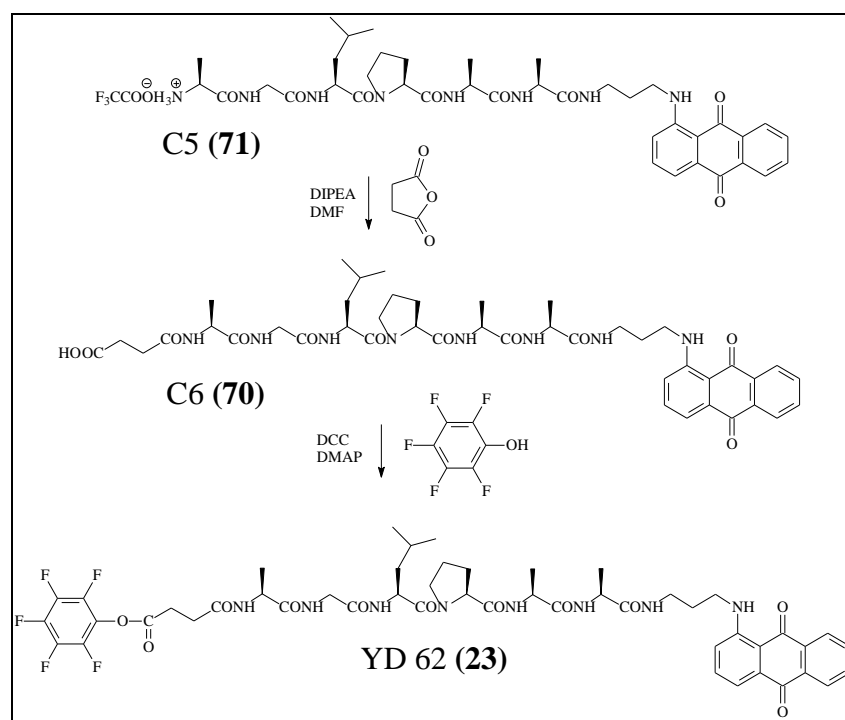
Scheme 1.24 Synthesis of PFPO-SUCC-Ala-Gly-Leu-Pro-Ala-Ala-APA-AQ (YD 62) (23)

In **Scheme 1.24**, it outlines that 1-[(3-aminopropyl)amino]anthraquinone oligopeptide succinate compound C6 (**70**) was synthesised by reacting *N*-trifluoroacetate salt C5 (**71**) and succinic anhydride in DMF under basic (DIPEA) condition, following the general method outlined in **Scheme 1.3**.

Pentafluorophenyl ester YD 62 **(23)** [**Figure 1.51**], which was required in the syntheses of twin prodrugs colchicine succinyl hexapeptide anthraquinone YD 63 **(34)** [**Scheme 1.11**], epirubicin succinyl hexapeptide anthraquinone YD 67 **(21)** [**Figure 1.35**] and FRET probe 6-aminofluorescein succinyl hexapeptide anthraquinone YD 64 **(35)** [**Scheme 1.12**], was synthesised by dissolving 1-[(3-aminopropyl)amino]anthraquinone oligopeptide succinate compound C6 **(70)** and DCC in DMF at 0°C first, then DMAP and pentafluorophenol were added into this reaction mixture. Montalbetti and Falque suggested that if mixing acid and DCC in DMF at 0°C first, then adding amine/ OPFP could minimise *N*-acylurea formation (Montalbetti and Falque, 2005) (following the general synthesis of OPFP ester compounds outlined in **Scheme 1.16**). Four hours later, the whole reaction solution was partitioned between chloroform and water, then the organic layer was washed with saturated sodium bicarbonate solution and water, dried, filtered and evaporated to dryness, to afford the target conjugates.

1.3   <u>**CONCLUSION**</u>

In this research project, three 'prodrug warheads' have been made, two model compounds and twelve target prodrugs have been designed, synthesised and characterised by spectroscopic methods, including mass spectrometry and NMR spectroscopy.

Prodrugs, which were designed and synthesised in this project, are 'twin prodrugs' that have either two identical or non-identical potent active agents binding onto designed oligopeptides. The synergy of the two active agents from 'twin prodrug' would offer greater effect in tumour chemotherapy than using prodrugs which only have one active agent.

During the synthetic stages, some conditions and methods have been improved in order to make compounds easier to synthesise and achieve higher yields of chromatographically pure products. For instance, during epirubicin **(2)** coupling stages, it was found if epirubicin **(2)** were reacted with an OPFP ester compound, these methods proved superior to in situ coupling methods. The strategy of designing and synthesising the active agents ('warheads') has been extended from potent cytotoxic agents, such as anthraquinone compounds, to antivascular agents, in the colchicine class of compounds. Hence the prodrugs which were made in this project, not only have the potential to cause a cytotoxic effect on tumours cells, but also can potentially target and shrink tumour blood vessels in order to cut off the oxygen and nutrition supplies to tumour cells, as a consequence of their vascular disrupting properties.

1.4 <u>FUTURE WORK</u>

Immediate future work, in conjunction with collaborating laboratories, should focus on in vitro testing of prodrug activation in a panel of cancer cell lines which express MMP-9 and, for any promising conjugates, preliminary *in vivo* work. *In vitro* metabolism studies could be carried out using recombinant MMP-9, cell lysates or tumour homogenates by HPLC-MS methods.

In new work, it would be of interest to determine whether or not the prodrug approach can be translated (from cancer) to the delivery of potent antibacterials to define a preferred oligopeptide carrier sequence containing cleavage 'hotspots' for bacterial proteases, similar to but distinct from the human equivalent and to determine the biological potency of active agents and their respective prodrug forms against a panel of bacterial proteases.

In infected mammals, surface-located or soluble extracellular proteases are crucial in the process of bacterial resistance against the immune system. Bacterial proteases (in common with mammalian MMPs) can degrade host structures, such as the extracellular matrix; hence, bacteria can migrate in the host without barriers (Haiko *et al.*, 2009).

PgtE is an endoprotease and an important factor for survival of *Salmonella* in the host; Ramu *et al.* showed that removal of PgtE can decrease the survival of bacterial in murine macrophages and human serum (Ramu *et al.*, 2007, Ramu *et al.*, 2008). The *Salmonella* surface protease PgtE has been found have the ability to degrade gelatin and also can activate human proMMP-9 (Haiko, 2009).

Based on above observations, it would be very interesting to clone the salmonella derived cell surface protease and to screen a library of potential MMP-9 substrate prodrug compounds (containing antibacterial agents in latent form) for their cleavage sensitivity towards PgtE protease.

1.5 STRUCTURE LIBRARY

1.5.1 'Warheads' (active agents)
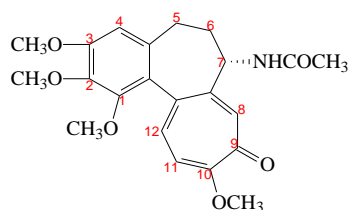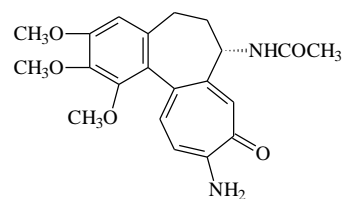
Colchicine (5)

Colchiceinamide (YD 9) (6)
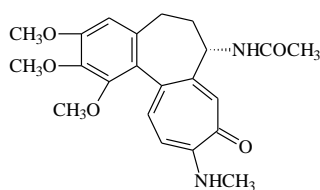
N-methylcolchiceinamide (YD 36) (7)
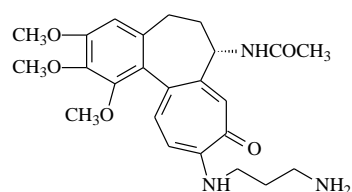
10-(3-aminopropyl)amino-10-demethoxycolchicine (MB1) (8)
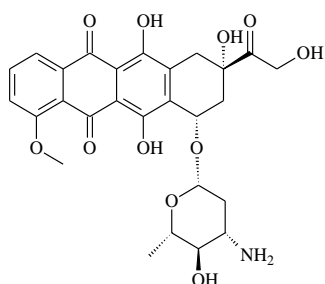
Epirubicin (2)
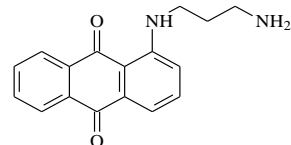
APA-AQ (72)

1.5.2 'Warheads'-spacer/ linker compounds
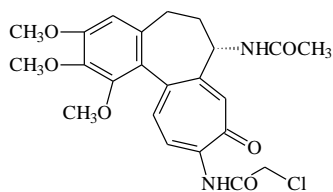
N-chloroacetylcolchiceinamide (YD 10) (9)
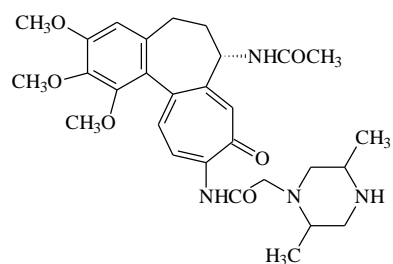
YD9-DMPIP (YD 11) (10)
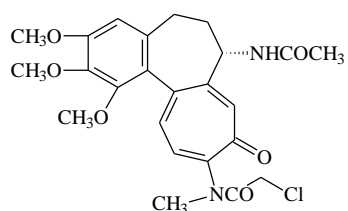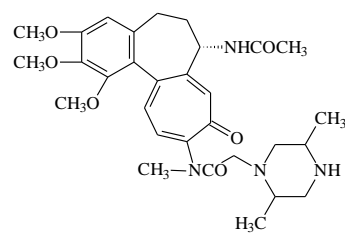
N-chloroacetylmethylcolchiceinamide (YD 38) **(13)**   YD36-DMPIP (YD 39) **(14)**
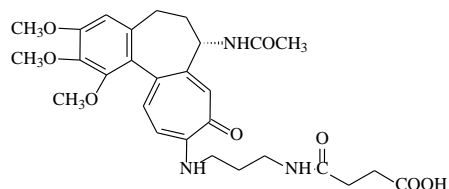
MB1-SUCC (YD 56) **(17)**

1.5.3 Model compounds (Model prodrugs)
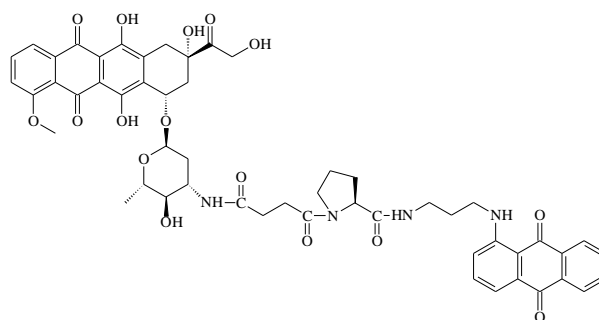
Epi-SUCC-Pro-APA-AQ (YD 20) **(20)**
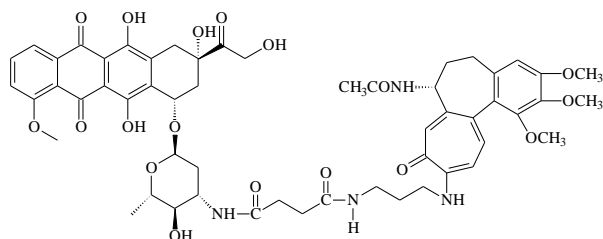
Epi-SUCC-MB1 (YD 59) **(25)**

1.5.4 Target prodrugs
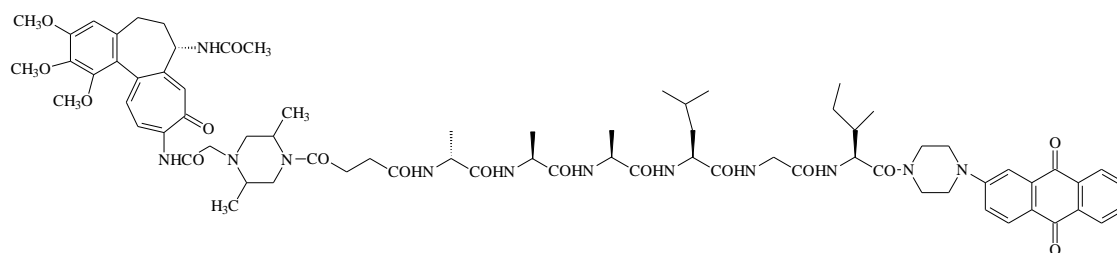
YD9-DMPIP-SUCC-ᴅ-Ala-Ala-Ala-Leu-Gly-Ile-PIP-AQ (YD 34) **(27)**
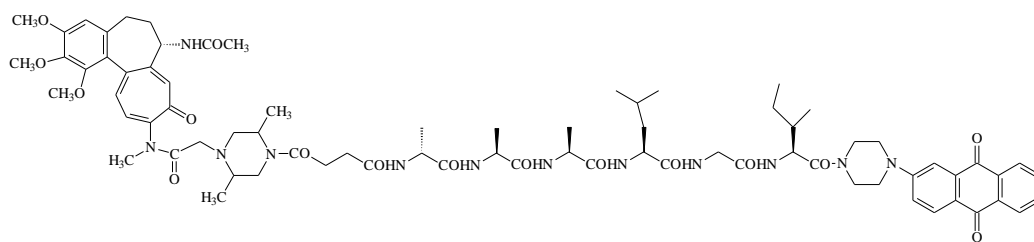
YD36-DMPIP-SUCC-D-Ala-Ala-Ala-Leu-Gly-Ile-PIP-AQ (YD 42) **(29)**
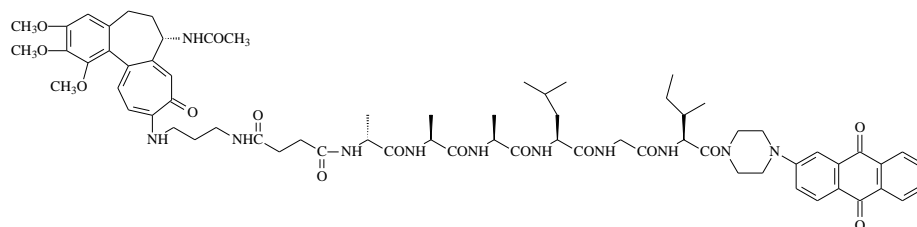
MB1-SUCC-D-Ala-Ala-Ala-Leu-Gly-Ile-PIP-AQ (YD 58) **(31)**
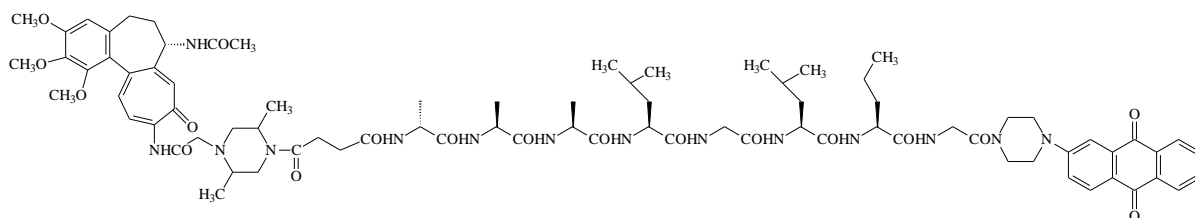
YD9-DMPIP-SUCC-D-Ala-Ala-Ala-Leu-Gly-Leu-Nva-Gly-PIP-AQ (YD 18) **(32)**
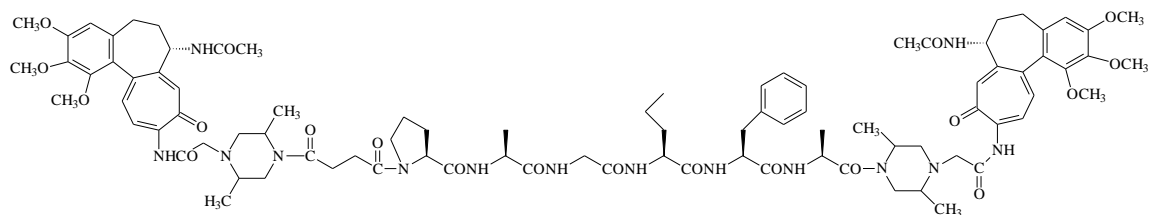
YD9-DMPIP-SUCC-Pro-Ala-Gly-Nva-Phe-Ala-DMPIP-YD9 (YD 55) **(3)**
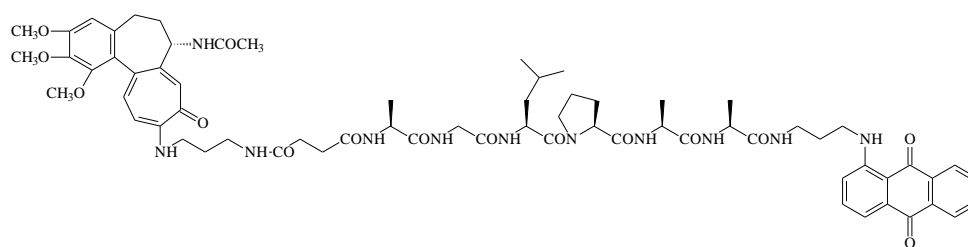
MB1-SUCC-Ala-Gly-Leu-Pro-Ala-Ala-APA-AQ (YD 63) **(34)**
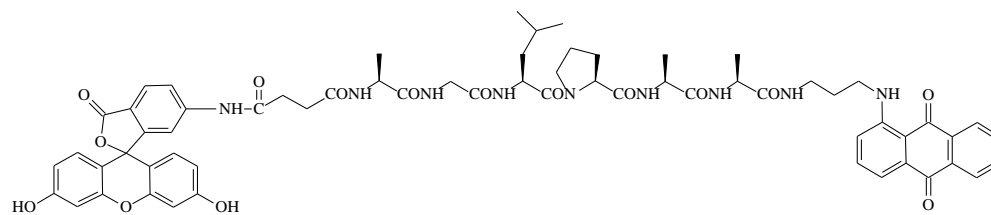
AF-SUCC-Ala-Gly-Leu-Pro-Ala-Ala-APA-AQ (YD 64) **(35)**
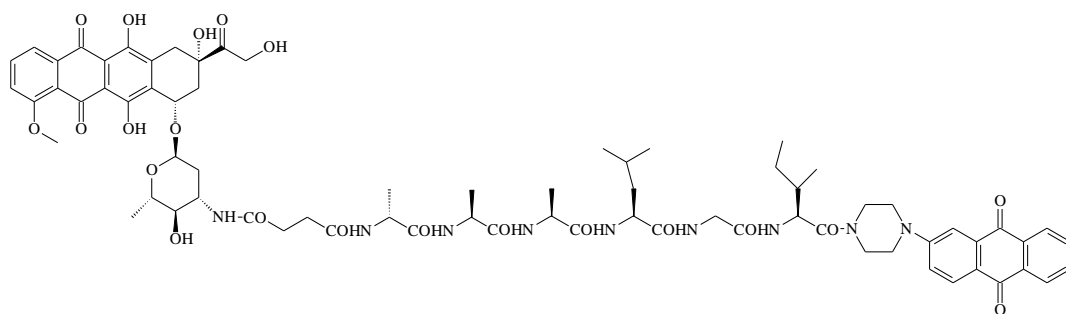
Epi-SUCC-D-Ala-Ala-Ala-Leu-Gly-Ile-PIP-AQ (YD 35) (**36**)
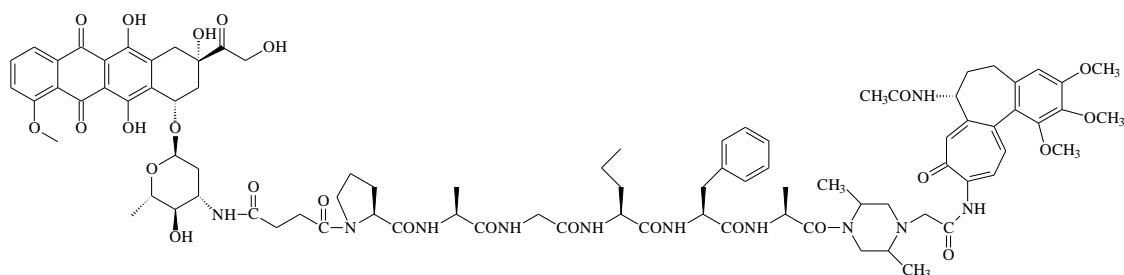
Epi-SUCC-Pro-Ala-Gly-Nva-Phe-Ala-DMPIP-YD9 (YD 61) (**4**)
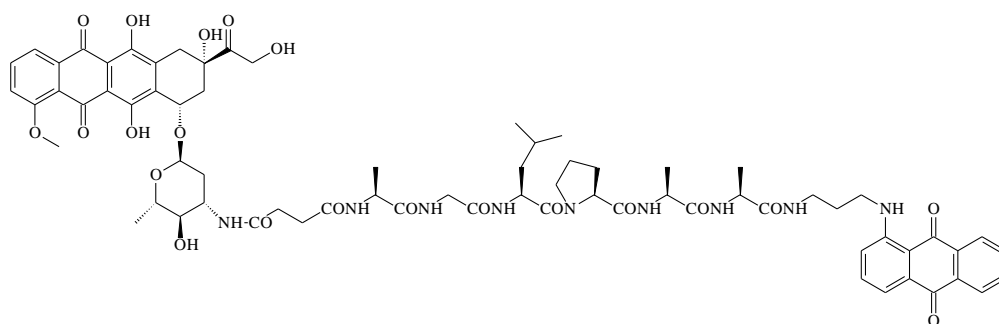
Epi-SUCC-Ala-Gly-Leu-Pro-Ala-Ala-APA-AQ (YD 67) (**21**)
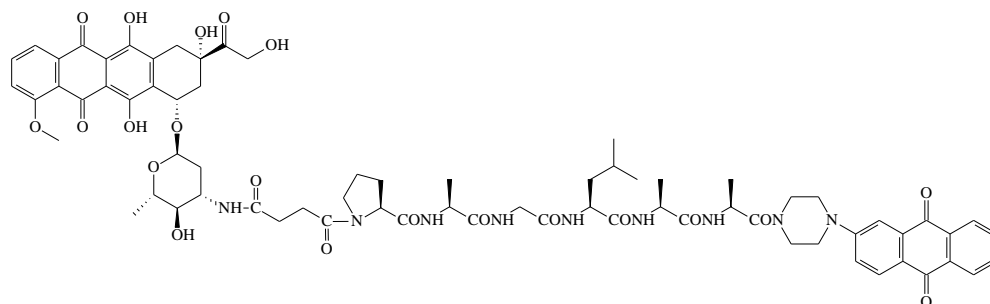
Epi-SUCC-Pro-Ala-Gly-Leu-Ala-Ala-PIP-AQ (YD 75) (**39**)

FITC-Ala-Nva-Gly-Leu-Pro-Aib-(oxypiperidine)-AQ (YD 17) (**43**)

81
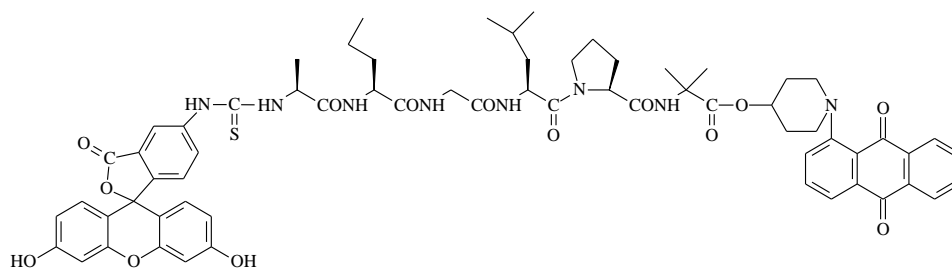
1.5.5 Miscellaneous compounds including prodrug intermediates
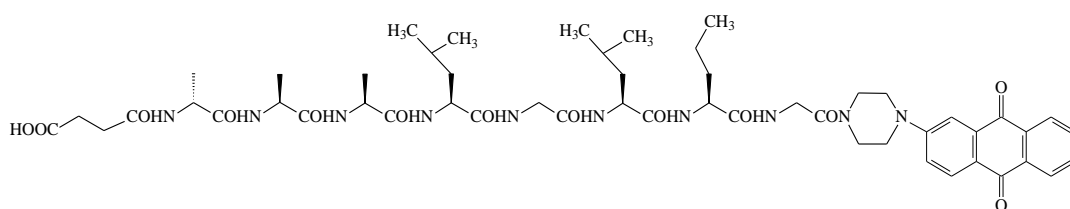
SUCC-D-Ala-Ala-Ala-Leu-Gly-Leu-Nva-Gly-PIP-AQ (YD 12) **(33)**
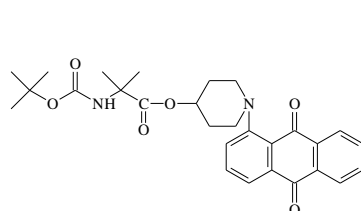
Boc-Aib-(oxypiperidine)-AQ
(YD 13) **(45)**
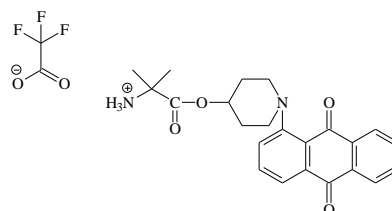
Aib-(oxypiperidine)-AQ [TFA] (YD 14)
(46)
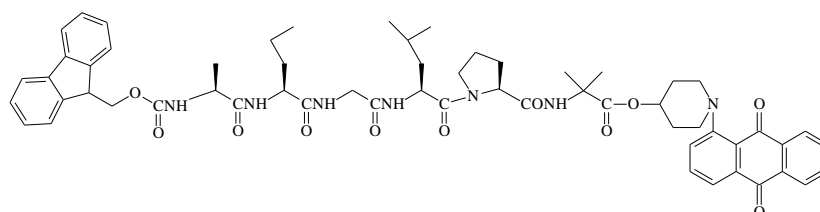
Fmoc-Ala-Nva-Gly-Leu-Pro-Aib-(oxypiperidine)-AQ (YD 15) **(48)**
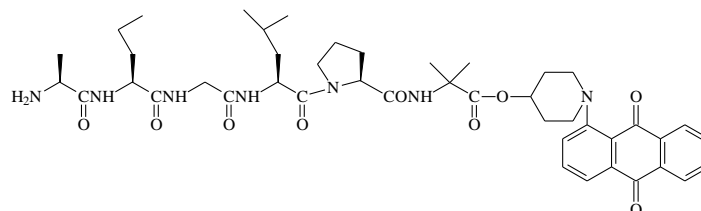
Ala-Nva-Gly-Leu-Pro-Aib-(oxypiperidine)-AQ (YD 16) **(49)**
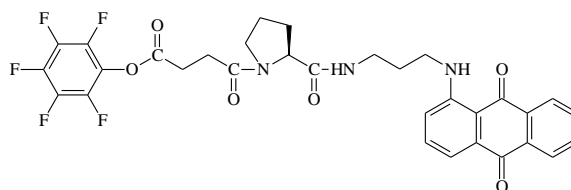
PFPO-SUCC-Pro-APA-AQ (YD 19) **(24)**
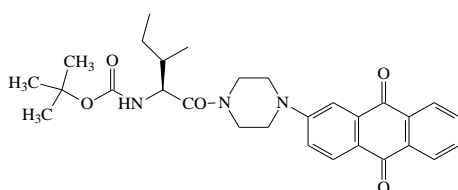
NU:UB 234 Boc **(55)**
Boc-Ile-PIP-AQ
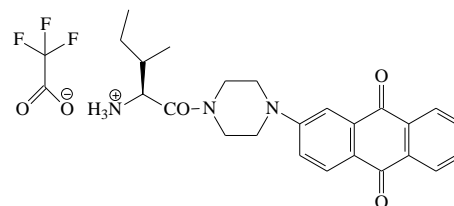
NU:UB 234 **(19)**
Ile-PIP-AQ [TFA]
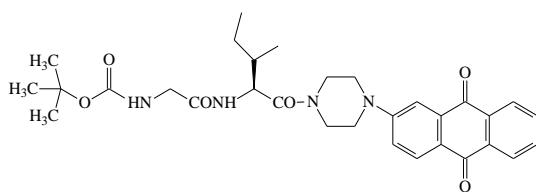
NU:UB 359 Boc **(56)**
Boc-Gly-Ile-PIP-AQ
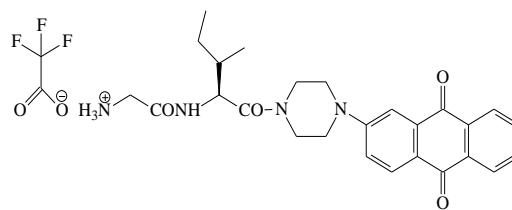
NU:UB 359 **(73)**
Gly-Ile-PIP-AQ [TFA]
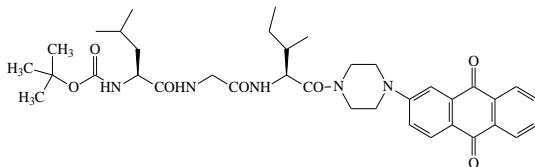
NU:UB 360 Boc **(57)**
Boc-Leu-Gly-Ile-PIP-AQ
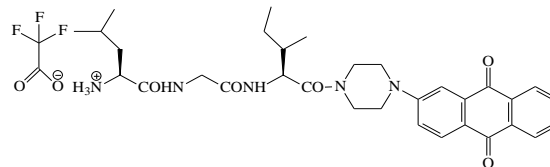
NU:UB 360 **(74)**
Leu-Gly-Ile-PIP-AQ [TFA]
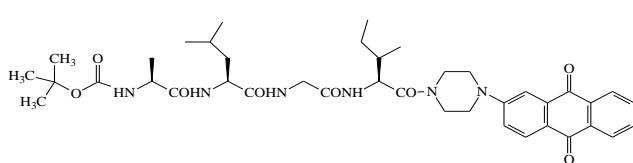
NU:UB 361 Boc **(58)**
Boc-Ala-Leu-Gly-Ile-PIP-AQ
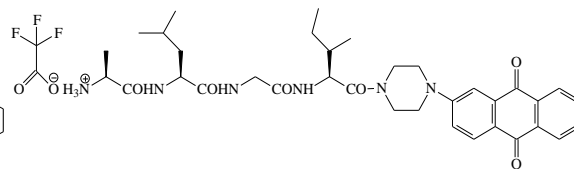
NU:UB 361 **(75)**
Ala-Leu-Gly-Ile-PIP-AQ [TFA]
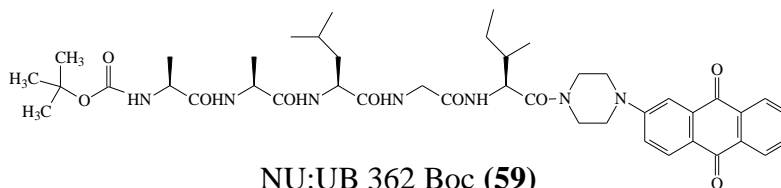
NU:UB 362 Boc **(59)**
Boc-Ala-Ala-Leu-Gly-Ile-PIP-AQ
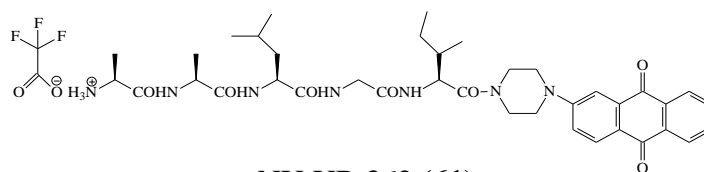
NU:UB 362 **(61)**
Ala-Ala-Leu-Gly-Ile-PIP-AQ [TFA]
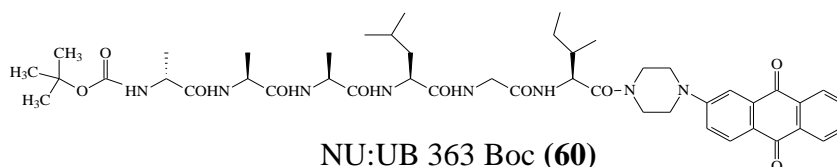
NU:UB 363 Boc **(60)**
Boc-D-Ala-Ala-Ala-Leu-Gly-Ile-PIP-AQ
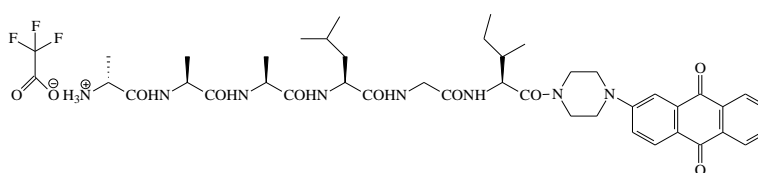
NU:UB 363 **(30)**
D-Ala-Ala-Ala-Leu-Gly-Ile-PIP-AQ [TFA]

83
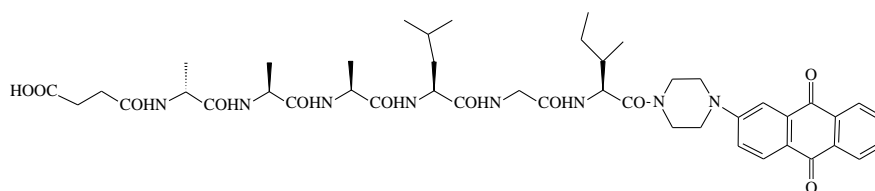
SUCC-ᴅ-Ala-Ala-Ala-Leu-Gly-Ile-PIP-AQ (YD 30) **(28)**
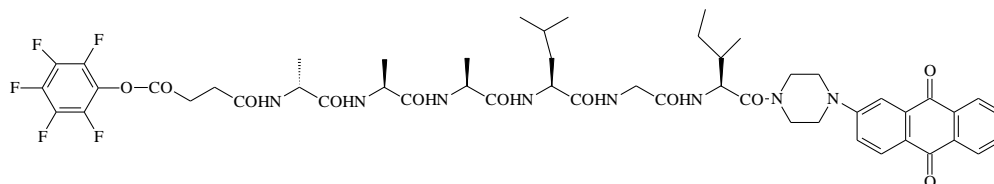
PFPO-SUCC-ᴅ-Ala-Ala-Ala-Leu-Gly-Ile-PIP-AQ (YD 32) **(37)**
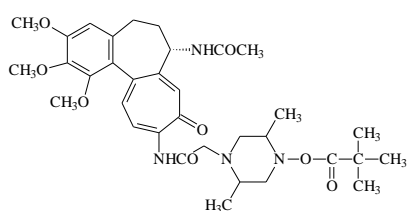
YD9-DMPIP-Boc (YD 31) **(11)**
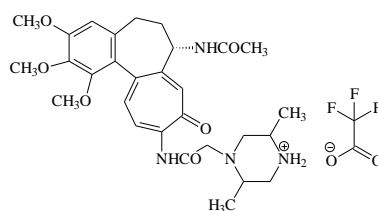
YD9-DMPIP [TFA] (YD 33) **(12)**
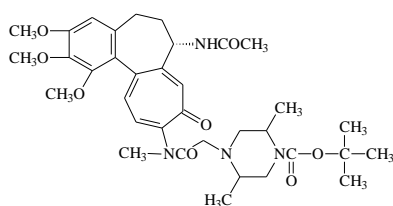
YD36-DMPIP-Boc (YD 40) **(15)**
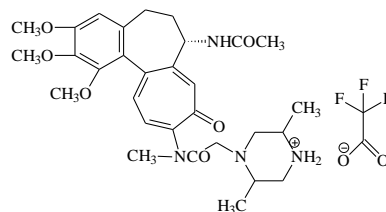
YD36-DMPIP [TFA] (YD 41) **(16)**
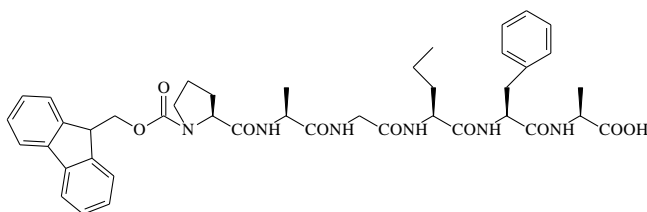
Fmoc-Pro-Ala-gly-Nva-Phe-Ala-OH (YD 43) **(52)**
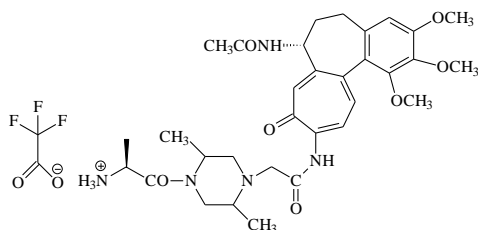
Ala-DMPIP-YD9 [TFA]
(YD 48) **(65)**

Phe-Ala-DMPIP-YD9 [TFA]
(YD 49) **(66)**

84
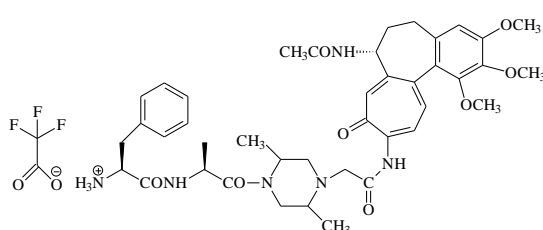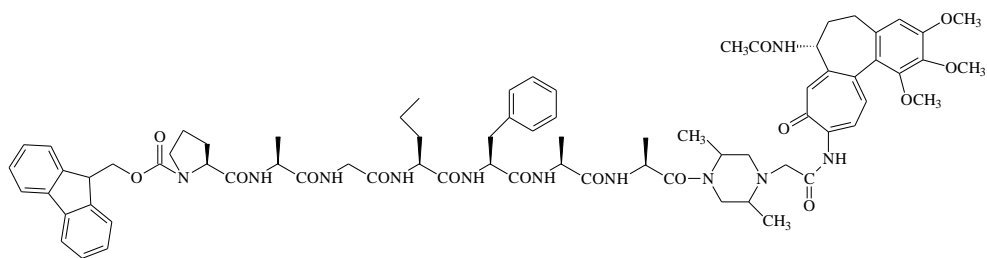
Fmoc-Pro-Ala-Gly-Nva-Phe-Ala-Ala-DMPIP-YD9 (YD 50) **(69)**
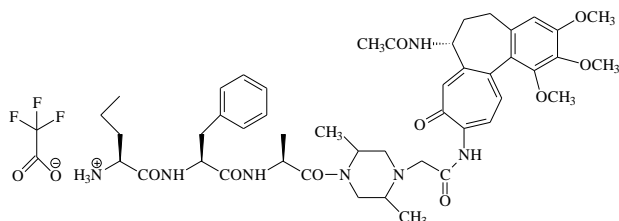
Nva-Phe-Ala-DMPIP-YD9 [TFA] (YD 51) **(67)**
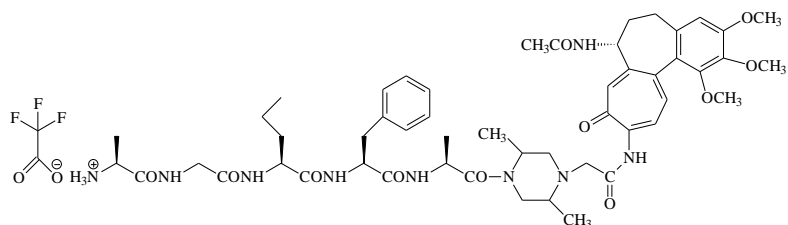
Ala-Gly-Nva-Phe-Ala-DMPIP-YD9 [TFA] (YD 52) **(68)**
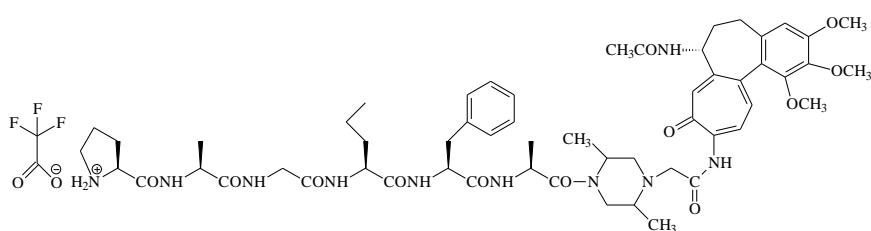
Pro-Ala-Gly-Nva-Phe-Ala-DMPIP-YD9 [TFA] (YD 53) **(64)**
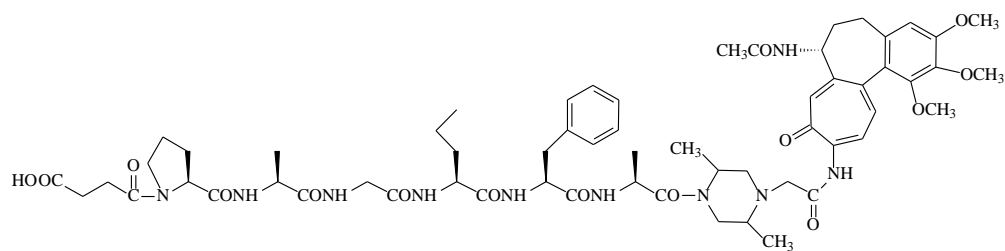
SUCC-Pro-Ala-Gly-Nva-Phe-Ala-DMPIP-YD9 (YD 54) **(18)**
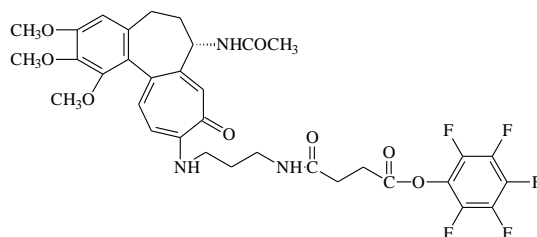
MB1-SUCC-OPFP (YD 57) **(26)**
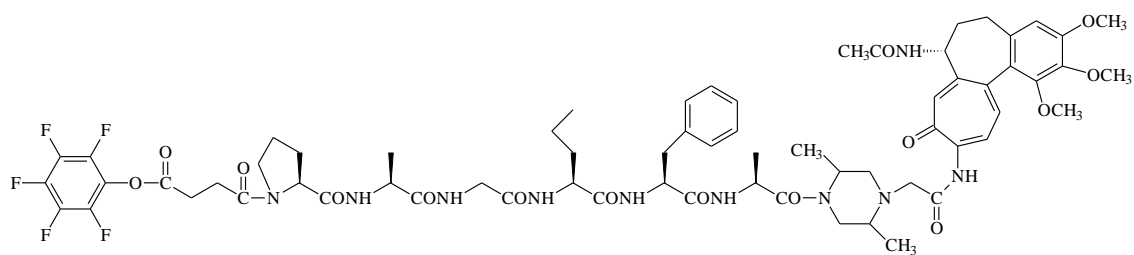
PFPO-SUCC-Pro-Ala-Gly-Nva-Phe-Ala-DMPIP-YD9 (YD 60) **(38)**
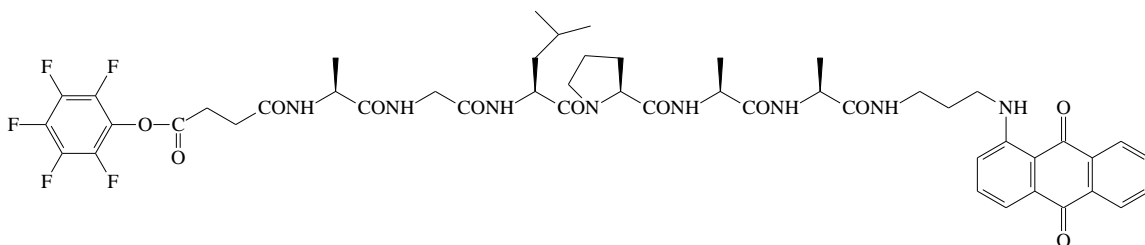
PFPO-SUCC-Ala-Gly-Leu-Pro-Ala-Ala-APA-AQ (YD 62) **(23)**
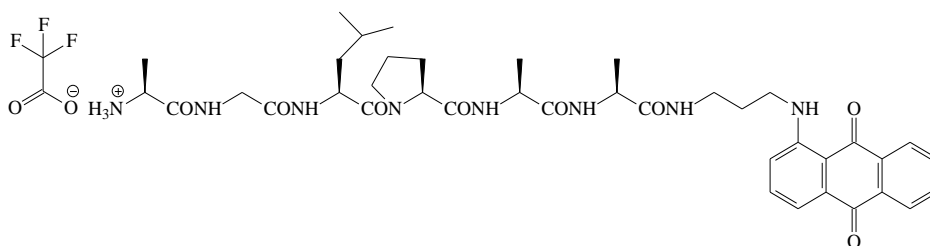
Ala-Gly-Leu-Pro-Ala-Ala-APA-AQ [TFA] C5 **(71)**
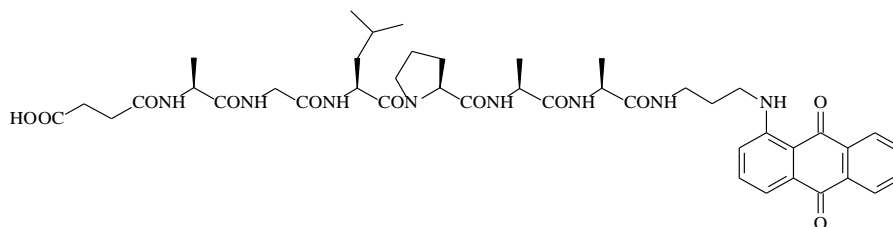
SUCC-Ala-Gly-Leu-Pro-Ala-Ala-APA-AQ C6 **(70)**
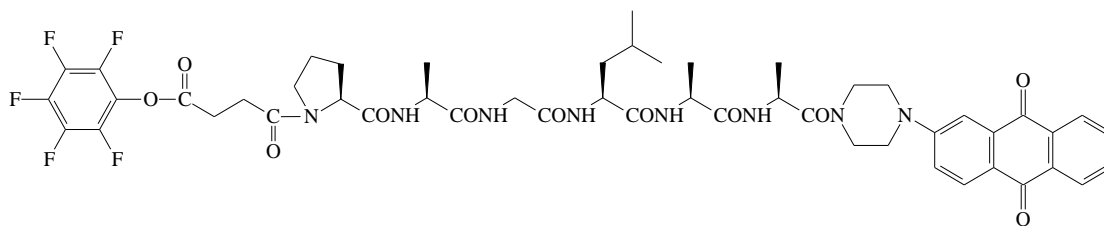
PFPO-SUCC-Pro-Ala-Gly-Leu-Ala-Ala-PIP-AQ (YD 74) **(42)**

1.6   <u>EXPERIMENTAL</u>

1.6.1   <u>General Techniques</u>

1.6.1.1   <u>Chromatography</u>

1.6.1.2   <u>TLC</u>

Kieselgel 60 F_{254} pre-loaded aluminium sheets (Merck company product) were used for thin layer chromatography (TLC). Most compounds synthesised absorb in the visible region, additional visualisation where required, was by short-wave U.V. light. Additionally, colour tests were occasionally used where bromocresol green showed a bright yellow spot against dark blue background as a positive test for a carboxylic acid and ninhydrin showed the presence of a primary amine as a blue spot.

1.6.1.3   <u>Thick Layer TLC</u>

Thick-layer chromatography plates were prepared by mixing silica gel 60 PF_{254} (100g) with water (300mL), after stirring well, the slurry was applied evenly to a depth of 1mm on 20cm×20cm glass plates. The TLC plates were dried in an oven at 60°C for 24h. Then TLC plates were stored in a cool and dark place.

The crude compound was dissolved in a small amount of chloroform or methanol before loading onto thick TLC plates, which were eluted using a suitable solvent system. The band containing the major compound was collected from the plate, eluted from the silica with chloroform and methanol, and then evaporated to dryness.

1.6.1.4   <u>Fine silica gel column chromatography</u>

Kieselgel 60 F_{254} silica gel was used in silica gel column chromatography. A small pump was applied on the top of the glass column to supply air pressure in the column when necessary.

1.6.1.5   <u>Nuclear Magnetic Resonance</u>

NMR spectra were recored on either a Bruker AC300 or a Bruker AC400 NMR Spectrometer (at 300MHz or 400MHz for 1H; 75MHz for 13C) in d6-DMSO or CDCl$_3$.

1.6.1.6   <u>Mass spectrometry</u>

High resolution electrospray mass spectra were recored on Thermofisher LTQ Orbitrap XL.

Low resolution nano-electrospray mass spectra were recored on Waters ZQ4000.

1.6.2   <u>General Synthetic Chemistry</u>

1.6.2.1   <u>Method A: General method for the synthesis of succinate compounds</u>

The amine component (1 equivalent), succinic anhydride (3 equivalents) were dissolved in DMF. DIPEA (1 equivalent) was added into the reaction solution. After 12h, a mini extraction was carried out and the progress of the reaction was checked by TLC. The reaction solution was evaporated to dryness, and then extracted with water. Litmus blue test paper was applied to check whether excess succinic acid was washed out or not. Also, bromocresol green could be applied to check if there was a bright yellow spot (succinic acid) against a blue background on the TLC plate. If necessary, further purification was carried out by silica gel column chromatography. Fractions containing the major product were combined, filtered and evaporated to dryness.

1.6.2.2   <u>Method B: General method for the deprotection of *N*-tertiarybutoxycarbonyl (^{t}Boc) protected compounds</u>

The ^{t}Boc protected compound (0.5g) was dissolved in trifluoroacetic acid (7mL) at RT. After 30min, the progress of this reaction was checked by TLC. After the reaction was complete, trifluoroacetic acid was then evaporated and the residual solid was re-

evaporated with methanol (3×5mL), where necessary. Diethyl ether (50mL) was added to give a precipitate of the deprotected compound at 4 °C. The *N*-terminal trifluoroacetate salt was filtered off and dried *in vacuo*.

1.6.2.3 Method C: General method for coupling an *N*-α-protected amino acid/ peptide with free carboxyl terminus to an amine component using in-situ coupling reagents

The amine component (1equivalent), *N*-α-protected amino acid with free carboxyl terminus (1.1 equivalents), HOBt (1.1 equivalents), TBTU or PyBOP (1.1 equivalents) were all dissolved in DMF, and then *N,N*-diisopropylethylamine (3.2 equivalents) was added into this reaction mixture, which was stirred for 2-8h at RT. The progress of the reaction was checked by TLC. The compound was partitioned between chloroform and water (1:2, 150mL), dried (MgSO₄), filtered, and evaporated to a very low volume before applying onto a silica gel chromatography column. Fractions from the chromatography column containing the major product were combined, filtered and evaporated to dryness.

1.6.2.4 Method D: General method for the deprotection of *N*-α-fluorenylmethoxycarbonyl (Fmoc) protected compounds

The Fmoc protected compound (0.15g) was dissolved in a solution of 20% (v/v) piperidine in DMF (4mL) and stirred for 15-30 min. Once the reaction was finished (checking by TLC), the mixture was partitioned between chloroform and water (1:2, 150mL), and washed with water (3×50mL), dried (MgSO₄), filtered and evaporated to a low volume before applying onto a silica gel chromatography column. Fractions containing the major product were combined, filtered and evaporated to dryness.

1.6.2.5   Method E: General method for forming a pentafluorophenolate ester

N,*N*'-dicyclohexylcarbodiimide (1.1 equivalents), 4-dimethylaminopyridine (1.1 equivalenta) and pentafluorophenol (1.1 equivalents) were added into a stirred solution of the succinate compound (1 equivalent) [from method A] in dichloromethane (or chloroform). On completeion, the precipitated dicyclohexylurea was filtered off and the compound was used without further purification.

1.6.2.6   Method F: solid phase peptide synthesis (SPPS)

1.6.2.6.1   Swelling

In order to enlarge the surface area of resin to a maximum, resins need to be swelled well first. Resins were weighed and transferred to a SPPS reaction vessel. Dry dichloromethane (~10mL/g of resin) was added and the SPPS vessel was put onto an orbital shaker and kept shaking for one hour. Then dichloromethane was drained off and resins were washed with DMF (3× ~10mL/g of resin).

1.6.2.6.2   Coupling

Fmoc protected amino acid (1 equivalent), TBTU (1.9 equivalents) and HOBt (1.9 equivalents) were dissolved in DMF (~20mL/g of resins), and then DIPEA (4 equivalents) was added into this solution. The mixture was split into two portions and each portion was added into an SPPS reaction vessel separately and kept shaking for 30min. Then the solution was drained off and the resin were washed with DMF (3× ~10mL/g of resin).

1.6.2.6.3   Deprotection

A solution of 20% (v/v) piperidine in DMF was added into the SPPS reaction vessel (3×~10mL/g resin) and the vessel was kept shaking for 15 min, and then the solution was drained away and the resin was washed with DMF (3× ~10mL/g of resin).

1.6.2.6.4 **Kaiser Test**

After each coupling and deprotection, a Kaiser test was carried out to make sure each step was complet. Three solutions need to be prepared for Kaiser test: ninhydrin (1g) was dissolved in ethanol (20mL) and kept in the dark; liquified phenol (16g) was dissolved in ethanol (4mL) and kept in the dark; aqueous solution of potassium cyanide (0.001M, 400μl) was added into pyridine (19.6mL).

After coupling or deprotection and washing with DMF three times, a few beads were transferred from SPPS vessel to a micro tube and one drop of each of the three Kaiser test solutions were added, and then the micro tube was heated at ~80°C for 3-5min. The result should be positive (for NH_2): beads should be dark blue or purple; negative (no NH_2): beads should be clear or pale yellow.

1.6.2.6.5 **Cleavage**

A solution of 1-5% trifluoroacetic acid (TFA) in dichloromethane (~10mL/g of resin) was added into the SPPS vessel and kept shaking for 2min. Then the solution was drained. Resin was washed with the 1-5% TFA solution up to 10 times, the progress was checked by TLC (dichloromethane: methanol 6:1). Then resin was washed with dichloromethane (×3), methanol (×3), dichloromethane (×3). All filtrates were combined and evaporated to a very low volume, and then diethyl ether was added to precipitate the peptide. The solid peptide was filtered and dried *in vacuo*.

1.6.3 **'Warheads' (active agents)**

1.6.3.1 **Synthesis of colchiceinamide (YD 9) (6)**

Ammonia (5mL) was added into a stirred solution of colchicine (**5**) (1g, 2.5mmol) in DMF (5mL). The reaction mixture was stirred at RT and kept in the dark for 3 days.

TLC (chloroform: methanol 7:1); R_f 0.50 (yellow) product. The reaction mixture was evaporated to dryness to give yellow solid compound. Yield (0.997g). The purity of YD 9 (**6**) was confirmed by its homogeneous character on TLC and by its ^{1}H-NMR spectrum.

^{1}H-NMR spectrum (d6-DMSO, 200 MHz) δ: 1.80 (3H, s, NHCOC$\underline{H}_3$); 1.85-2.20 (4H, m, C_5-C$\underline{H}_2$, C_6-C$\underline{H}_2$); 3.42 (3H, s, C_1-OC$\underline{H}_3$); 3.72 (3H, s, C_3-OC$\underline{H}_3$); 3.77 (3H, s, C_2-OC$\underline{H}_3$); 4.31 (1H, m, C_7-C$\underline{H}$); 6.69 (1H, s, C_4-C$\underline{H}$); 6.84 (1H, d, C_{11}-C$\underline{H}$); 7.03 (1H, d, C_{12}-C$\underline{H}$); 7.08 (1H, s, C_8-C$\underline{H}$); 8.53 (1H, d, N$\underline{H}$COCH$_3$).

1.6.3.2 Synthesis of *N*-methylcolchiceinamide (YD 36) (7)

Colchicine (**5**) (1g, 0.0025mol) was dissolved in methylamine (8mL) and stirred for 15min at RT. The precipitated solid was filtered and washed with ice-cold water, dried *in vacuo*. TLC (dichloromethane: ethyl acetate: methanol 7:2:1); R_f 0.54 (yellow) product (homogeneous on TLC). Yield (0.735g, 74%).

^{1}H-NMR spectrum (CDCl$_3$, 200 MHz) δ: 1.80-1.98 (4H,s+m, NHCOC$\underline{H}_3$ + C_6-C$\underline{H}$); 2.10-2.46 (3H, m, C_5-C$\underline{H}_2$ + C_6-C$\underline{H}$); 3.03 (3H, d, NHC$\underline{H}_3$); 3.56 (3H, s, C_1-OC$\underline{H}_3$); 3.83 (3H, s, C_3-OC$\underline{H}_3$); 3.88 (3H, s, C_2-OC$\underline{H}_3$); 4.62 (1H, m, C_7-C$\underline{H}$); 6.48 (1H, s, C_4-C$\underline{H}$); 6.52 (1H, d, C_{11}-C$\underline{H}$); 7.18 (1H, q, N$\underline{H}$CH$_3$); 7.37 (1H, s, C_8-C$\underline{H}$); 7.44 (1H, d, C_{12}-C$\underline{H}$); 7.95 (1H, d, N$\underline{H}$COCH$_3$).

1.6.3.3 Synthesis of 10-(3-aminopropyl)amino-10-demethoxycolchicine (MB1) (8)

Colchicine (**5**) (0.5g, 1.25mmol) was mixed with 1,3-diaminopropane (5mL). The solution was stirred at RT for 3h. TLC (dichloromethane: methanol 5:1); R_f 0.30 (yellow) product. The reaction mixture was transferred to an evaporating basin to evaporate in the fume cupboard. Then the dried mixture was re-dissolved in dichloromethane and filtered to remove the white imputity, the yellow pure (chromatographically homogeneous) MB1 (**8**) dichloromethane solution was partitioned

between dichloromethane and water (1:2, 150mL), dried ($MgSO_4$), filtered and evaporated to dryness.

Yield (0.5g, 90%).

^{1}H-NMR spectrum (d$_6$-DMSO, 300 MHz) δ: 1.70 (2H, t, -(CH$_2$)$_3$NH$_2$); 1.85 (3H, s, NHCOCH$_3$); 1.95-2.20 (4H, m, C$_5$-CH$_2$, C$_6$-CH$_2$); 3.40 (6H, s, -(CH$_2$)$_3$NH$_2$); 3.45 (3H, s, C$_1$-OCH$_3$); 3.74 (3H, s, C$_3$-OCH$_3$); 3.81 (3H, s, C$_2$-OCH$_3$); 4.34 (1H, m, C$_7$-CH); 6.65 (1H, d, C$_{11}$-CH); 6.82 (1H, s, C$_4$-CH); 7.07 (1H, s, C$_8$-CH); 7.18 (1H, d, C$_{12}$-CH); 7.78 (1H, t, C$_{10}$-NH); 8.53 (1H, d, NHCOCH$_3$).

1.6.4 'Warheads'-spacer/ linker compounds

1.6.4.1 Synthesis of *N*-chloroacetylcolchiceinamide (YD 10) (9)

Colchiceinamide (**5**) (0.4g, 1mmol) was dissolved in DMF (6mL). Sodium bicarbonate (0.84g, 10mmol) was added and the suspension was stirred over an ice bath for 10min, then to the solution chloroacetyl chloride (96.6μL, 1.2mmol) was added. The mixture was allowed to rise to RT and left for 24h to react. A mini extraction was carried out and the progress of the reaction was checked by TLC (chloroform: methanol 9:1); R_f 0.28 (yellow) product. The whole reaction solution was then added drop-wise to excess water. The precipitate was filtered and dried.

Yield (0.22g, 46%). Compound YD 10 (**9**) was chromatographically homogeneous (single spot on TLC).

^{1}H-NMR spectrum (d$_6$-DMSO, 200 MHz) δ: 1.90 (3H, s, NHCOCH$_3$); 2.05-2.45 (4H, m, C$_5$-CH$_2$, C$_6$-CH$_2$); 3.55 (3H, s, C$_1$-OCH$_3$); 3.75 (3H, s, C$_3$-OCH$_3$); 3.85 (3H, s, C$_2$-OCH$_3$); 4.15 (2H, s, CH$_2$Cl); 4.60 (1H, m, C$_7$-CH); 6.45 (1H, s, C$_4$-CH); 6.70 (1H, d, C$_7$-NHCOCH$_3$); 7.35 (1H, d, C$_{12}$-CH); 7.50 (1H, s, C$_8$-CH); 8.85 (1H, d, C$_{11}$-CH); 10.30 (1H, s, C$_{10}$-NHCO).

1.6.4.2 Synthesis of YD9-DMPIP (YD 11) (10)

N-chloroacetyl colchiceinamide YD 10 **(9)** (0.22g, 0.48mmol) was dissolved in DMF (4mL). Trans-2,5-dimethyl-piperazine (0.27g, 2.37mmol) was dissolved in DMF (6mL), separately, stirred well, to which the solution of *N*-chloroacetyl colchiceinamide **(9)** was added drop wise. Overnight, a mini extraction was carried out and the progress of the reaction was checked by TLC (chloroform: methanol 5:1); R_f 0.30 (yellow) product. The reaction solution was partitioned between chloroform and water (1:5, 60mL), dried ($MgSO_4$), filtered and evaporated to dryness. YD 11 **(10)** was deemed sufficiently pure for use without further purification.

Yield (0.22g, 85%).

1.6.4.3 Synthesis of YD9-DMPIP-Boc (YD 31) (11)

Colchiceinamide dimethylpiperazine-spacer compound YD 11 **(10)** (0.9g, 0.0017mol) was dissolved in dried methanol (5mL) at $0^{o}C$ and stirred. Di-*t*-butyl-dicarbonate (0.73g, 0.0033mol) was dissolved in dried methanol (5mL), separately, and then the mixture was added drop wise into cooled, stirred solution of YD 11 **(10)**. TLC (dichloromethane: ethyl acetate: methanol 16:4:1); R_f 0.56 (yellow) product. The solution was evaporated a very low volume and then re-dissolved in chloroform before applying onto a silica gel chromatography column (2.2cm×15cm), and eluted with dichloromethane: ethyl acetate: methanol (16:4:1). Fractions containing the major product were combined, filtered and evaporated to dryness.

1.6.4.4 Synthesis of YD9-DMPIP [TFA] (YD 33) (12)

N-*t*Boc protected YD 31 **(11)** was treated with TFA (4mL) and left reacting at RT for 30min [following method B]. TLC (chloroform: methanol 7:1); R_f 0.35 (yellow) product.

Yield (0.69g, 62.2%).

1.6.4.5   Synthesis of *N*-chloroacetylmethylcolchiceinamide (YD 38) (13)

YD 36 **(7)** (0.3g, 0.75mmol) was dissolved in THF (4mL). Sodium bicarbonate was added (0.63g, 7.54mmol) and the suspension was stirred over an ice bath for 10min. Chloroacetyl chloride (0.073mL, 0.9mmol) was added. This reaction mixture was allowed to rise to RT. Four hours later, the progress of this reaction was checked by TLC (dichloromethane: ethyl acetate: methanol 7:2:1); R_f 0.66 (yellow) product. The excess sodium bicarbonate was filtered off. The reaction solution was partitioned between chloroform and water (1:2, 150mL), dried ($MgSO_4$), filtered, and evaporated (no heat) until nearly dry, then diethyl ether was added to give a precipitate of the yellow compound which was filtered and dried *in vacuo*.

Yield (0.32g, 89%).

1.6.4.6   Synthesis of YD36-DMPIP (YD 39) (14)

N-chloroacetylmethylcolchiceinamide (YD 38) **(13)** (0.3g, 0.63mmol) was dissolved in THF/DMSO (10:1, 8mL total volume). Trans-2,5-dimethyl-piperazine (0.43g, 3.8mmol) was dissolved in a solution (5mL) of (THF/DMSO 10:1), to which the solution of YD 38 **(13)** was added drop wise, with stirring. One and half days later, the progress of this reaction was checked by TLC (dichloromethane: ethyl acetate: methanol 7:2:1); R_f 0.05 (yellow) product. The reaction solution was filtered and THF was evaporated. The compound in DMSO was partitioned between dichloromethane and water (1:2, 60mL), the organic layer was dried ($MgSO_4$), filtered, and evaporated until nearly dry, and then diethyl ether was to precipitate the compound which was filtered and dried *in vacuo*.

Yield (0.234g, 67%).

1.6.4.7   Synthesis of YD36-DMPIP-Boc (YD 40) (15)

YD36-DMPIP (YD 39) **(14)** (0.2g, 0.36mmol) was dissolved in dried methanol (2mL) at 0°C and stirred. Di-*t*-butyl-dicarbonate (0.16g, 0.72mmol) was dissolved in dried

methanol (2mL) and was slowly added drop wise to a cooled, stirred YD 39 **(14)** solution. Three hours later, a mini extraction was carried out and checked by TLC (dichloromethane: methanol 12:1); R_f 0.4 (yellow) product. The reaction solution was evaporated then re-dissolved in chloroform before appling to a silica gel chromatography column (2.2cm×15cm), eluted with chloroform: methanol (15:1). Fractions containing the major product were combined, filtered, and evaporated to dryness.

1.6.4.8   Synthesis of YD36-DMPIP [TFA] (YD 41) (16)

TFA (3mL) was added to the *N-^{t}*Boc protected compound YD 40 **(15)** and left for 45min at RT [following method B]. TLC (chloroform: methanol 7:1); R_f 0.29 (yellow) product. The purity of YD 41 **(16)** was confirmed by its homogeneous character on TLC and by its mass spectrum.

Yield (0.147g, 61%).

ESMS(+) m/z: 553.4 (96%) (M+H)$^+$; ESMS(-) m/z: 113.0 (100%) trifluoroacetate anion.

1.6.4.9   Synthesis of MB1-SUCC (YD 56) (17)

MB1 **(8)** (0.1g, 0.23mmol) and succinic anhydride (0.068g, 0.68mmol) were dissolved in DMF (2mL). DIPEA (0.04mL, 0.23mmol) was added into this reaction mixture [following method A]. TLC (dichloromethane: methanol 5:1) R_f 0.59 (yellow) product. Compound was put on silica gel chromatography column (2.2cm×15cm) twice, each time eluted with dichloromethane: methanol (5:1), to remove extra succinic acid. Then it was left to evaporate to dryness.

1.6.5   Model compounds (Model prodrugs)

1.6.5.1   Synthesis of Epi-SUCC-Pro-APA-AQ (YD 20) (20)

Epirubicin hydrochloride **(2)** (0.056g, 0.096mmol) and anthraquinone spacer pentafluorophenyl ester YD 19 **(24)** (0.064g, 0.1mmol) were dissolved in DMF (15mL),

followed by adding DIPEA (0.016mL, 0.094mmol) into this stirred reaction solution. A mini extraction was carried out and the progress of this reaction was checked by TLC (butanol: acetic acid: water 4:5:1); R_f 0.75 (red) product. The compound was partitioned between dichloromethane and water (1:2, 210mL), dried (MgSO4), filtered and evaporated to dryness before it was applied onto a silica gel chromatography column (2.2cm×15cm), eluted with dichloromethane (then increasing gradient to dichloromethane: methanol 19:1 → 9:1). Fractions containing the major product were combined, filtered and evaporated to dryness. Purity of the final compound was checked by TLC (dichloromethane: methanol 9:1); R_f 0.72 (red) product.

Yield (0.0491g, 51%). Mp: 174-176°C.

ESMS(-) m/z: 1001.3449 (35%) (M-H)$^-$; ESMS(+) m/z: 1025.3418 (100%) (M+Na)$^+$.

1.6.5.2   Synthesis of Epi-SUCC-MB1 (YD 59) (25)

MB1-SUCC-OPFP (YD 57) **(26)** (0.032g, 0.0450mmol) and epirubicin hydrochloride (0.017g, 0.029mmol) were dissolved in DMF (3mL). DIPEA (0.005mL, 0.029mmol) was added into this reaction mixture. A mini extraction was carried out and the progress of this reaction was checked by TLC (dichloromethane: methanol 7:1); R_f 0.20 (red) product. The compound was evaporated to dryness before it was applied onto thick TLC plates, eluted with dichloromethane: methanol (7:1). The red bands containing the major product were combined, washed with dichloromethane and methanol, filtered and evaporated to dryness. TLC (dichloromethane: methanol 7:1); R_f 0.20 (red) product. The purity of Epi-SUCC-MB1 (YD 59) **(25)** was confirmed by its homogeneous character on TLC and by its high resolution mass spectrum.

Yield (0.005g, 16%).

ESMS(+) m/z: 1067.4127 (15%) (M+H)$^+$.

1.6.6   Target prodrugs

1.6.6.1   Synthesis of YD9-DMPIP-SUCC-ᴅ-Ala-Ala-Ala-Leu-Gly-Ile-PIP-AQ (YD 34) (27): a twin prodrug of active agents NU:UB 234 (19) and the colchiceinamide derivative (YD33) (12)

The anthraquinone spacer oligopeptide succinate compound YD 30 (**28**) (0.02g, 0.0225mmol), trifluoroacetate salt YD 33 (**12**) (0.0162g, 0.025mmol), PyBOP (0.013g, 0.025mmol) and HOBt (0.0038g, 0.025mmol) were dissolved in DMF (2mL). Followed by adding DIPEA (0.0125mL, 0.072mmol) into this reaction solution [following method C] and reacted for 2h. The progress of this reaction was checked by TLC (dichloromethane: ethyl acetate: methanol 4:1:1); R_f 0.65 (orange) product (homogeneous on TLC).

Yield (0.029g, 91%).

ESMS(+) m/z: 1431.7 (5%) (M+Na)$^+$.

1.6.6.2   Synthesis of YD36-DMPIP-SUCC-ᴅ-Ala-Ala-Ala-Leu-Gly-Ile-PIP-AQ (YD 42) (29): a twin prodrug of active agents NU:UB 234 (19) and the *N*-methylcolchiceinamide derivative (YD41) (16)

The anthraquinone spacer oligopeptide succinate compound YD 30 (**28**) (0.01g, 0.0113mmol), trifluoroacetate salt YD 41 (**16**) (0.0083g, 0.0125mmol), TBTU (0.0040g, 0.0125mmol) and HOBt (0.0019g, 0.0124mmol) were dissolved in DMF (2mL). DIPEA (0.0063mL, 0.0362mmol) was added into this reaction solution afterwards [following method C]. The progress of this reaction was checked by TLC (dichloromethane: ethyl acetate: methanol 5:2:1); R_f 0.15 (orange) product. The DMF was evaporated to dryness in the fume cupboard and the compound was re-dissolved in chloroform before applying onto a thick TLC plate which was eluted with dichloromethane: ethyl acetate: methanol

(5:2:1). The second orange band from the thick TLC plate was collected. Final product was washed off from silica gel using methanol, and evaporated to dryness. The purity of (YD 42) **(29)** was confirmed by its homogeneous character on TLC and by its high resolution mass spectrum.

Yield (0.009g, 56%).

ESMS(+) m/z: 1423.7272 (84%) (M+H)$^+$.

1.6.6.3 <u>Synthesis of MB1-SUCC-ᴅ-Ala-Ala-Ala-Leu-Gly-Ile-PIP-AQ (YD 58) (31): a twin prodrug of active agents NU:UB 234 (19) and the colchicine derivative (MB1) (8)</u>

The first attempt was unsuccessful, so YD 58 **(31)** was synthesised by reacting MB1 **(8)** (0.016g, 0.037mmol) with NU:UB 363 **(30)** succinate compound YD 30 **(28)** (0.03g, 0.034mmol), TBTU (0.0119g, 0.037mmol) and HOBt (0.0057g, 0.037mmol) were dissolved in DMF (2mL). Then DIPEA (0.0188mL, 0.108mmol) was added into this reaction mixture. Two hours later, the progress of this reaction was checked on TLC plate. TLC (dichloromethane: methanol 7:1); R_f 0.45 (orange) product. After evaporating DMF, YD 58 **(31)** was purified by applying onto a thick –layer TLC plate, eluted with dichloromethane: methanol (7:1). A dark orange band corresponding to the new product was collected, washed with dichloromethane and methanol and dried to afford YD 58 **(31)**. The purity of YD 58 **(31)** was confirmed by its homogeneous character on TLC and by its high resolution mass spectrum.

Yield (0.04g, 91%). Mp: 183-185°C.

ESMS(+) m/z (z=2): 656.8336 (53%)[(M+2H)/2]$^{2+}$; m/z: 1312.6671 (3%)(M+H)$^+$, 1334.6471 (5%)(M+Na)$^+$.

1.6.6.4 Synthesis of YD9-DMPIP-SUCC-ᴅ-Ala-Ala-Ala-Leu-Gly-Leu-Nva-Gly-PIP-AQ (YD 18) (32): a twin prodrug of active agents NU:UB 347 and the *N*-colchiceinamide derivative (YD11) (10)

Colchiceinamide dimethylpiperazine-spacer compound YD 11 (**10**) (0.027g, 0.05mmol), succinate compound YD 12 (**33**) (0.0534g, 0.05mmol), TBTU (0.0164g, 0.05mmol), and HOBt (0.0078g, 0.05mmol) were dissolved in DMF (12mL), followed by adding DIPEA (0.027mL, 0.15mmol) into this reaction mixture. The reaction solution was stirred for 3 hours. The coupling reaction was carried out by following method C. The progress of this reaction was checked by TLC (butanol: acetic acid: water 4:5:1); R_f 0.77 (orange) product. The product was purified by a silica gel chromatography column (2.2cm×15.5cm) eluted with chloroform: methanol (19:1). Fractions containing the major product were combined and evaporated to a low volume before applying onto two thick-layer chromatography plates (20cm×20cm, 1mm thick silica gel layer), eluted with (butanol: acetic acid: water 4:5:1, 150mL). The darker orange bands were collected and washed with methanol. The compound solution was evaporated to a very low volume. Diethyl ether (100mL) was added to help to precipitate YD 18 (**32**) from solution (overnight at 4°C) and collected.

Yield (0.019g, 24.4%). Mp: 204-206ºC.

ESMS(+) m/z: 1588.0 (100%)(M+Na)⁺.

1.6.6.5 Synthesis of YD9-DMPIP-SUCC-Pro-Ala-Gly-Nva-Phe-Ala-DMPIP-YD9 (YD 55) (3): an identical twin prodrug of the *N*-colchiceinamide derivative (YD11) (10)

YD 33 (**12**) (0.015g, 0.023mmol), YD 54 (**18**) (0.025g, 0.02mmol), TBTU (0.0075g, 0.023mmol) and HOBt (0.0036g, 0.024mmol) were dissolved in DMF (1.5mL). DIPEA

(0.011mL, 0.064mmol) was added into this reaction mixture afterwards [following method C]. It was left to react overnight. TLC (dichloromethane: methanol 7:1) showed R_f 0.55 (pale yellow) product. The product was purified by thick-layer chromatography, eluted with dichloromethane: methanol (7:1). The upper yellow band was collected and the product was recovered by washing with methanol, then evaporated to dryness. Yield (0.021g, 58%).

ESMS(+) m/z: 1701.8528 (4%) (M+H)$^+$.

1.6.6.6 Synthesis of MB1-SUCC-Ala-Gly-Leu-Pro-Ala-Ala-APA-AQ (YD 63) (34): a twin prodrug of Ala-APA-AQ and colchiceinamide derivative (MB1) (8)

YD 62 (23) (0.05g, 0.049mmol) and MB1 (8) (0.0215g, 0.049mmol) were dissolved in DMF (5mL). DIPEA (0.0017mL, 0.039mmol) was then added. Two days later, the progress of this reaction was checked by TLC (chloroform: methanol 6:1); R_f 0.32 (purple) product. The reaction solution was evaporated to near dryness, and then re-dissolved in chloroform before applying onto a thick-layer chromatography plate, which was eluted with chloroform: methanol 6:1. The lower purple band from the plate was collected and washed with chloroform and methanol, and then it was filtered and evaporated to dryness. The purity of YD 63 (34) was confirmed by its homogeneous character on TLC and by its high resolution mass spectrum.
Yield (0.019g, 31%).

ESMS(+) m/z: 642.8182 (100%)[(M+2H)/2]$^{2+}$.

1.6.6.7 Synthesis of AF-SUCC-Ala-Gly-Leu-Pro-Ala-Ala-APA-AQ (YD 64) (35): a FRET probe of 6-aminofluorescein (22) and its quencher APA-AQ (72)

YD 62 (23) (0.09g, 0.088mmol) and 6-aminofluorescein (22) (0.031g, 0.088mmol) were dissolved in DMF (5mL). DIPEA (0.015mL, 0.088mmol) was then added. Two days

later, the progress of this reaction was checked on TLC (chloroform: ethyl acetate: methanol 5:2:1); a new product spot was detected. R_f 0.08 (brown) product. The reaction mixture was evaporated to near dryness, and then re-dissolved in methanol before applying onto two thick-layer chromatography plates, eluted with chloroform: ethyl acetate: methanol (5:2:1). The brown bands were collected from both plates combined, and re-chromatographed on fresh plates, eluted with chloroform: methanol (6:1). The brown bands were collected, washed with methanol, filtered and evaporated to dryness. The title compound was isolated in solid form (homogeneous on TLC) with the aid of diethyl ether.

Yield (0.0095g, 9%).

ESMS(+) m/z: 1212.4 (7%) (M+Na)$^+$, 1228.4 (8%) (M+K)$^+$.

1.6.6.8   Synthesis of Epi-SUCC-D-Ala-Ala-Ala-Leu-Gly-Ile-PIP-AQ (YD 35) (36): a twin prodrug of active agents NU:UB 234 (19) and epirubicin (2)

Pentafluorophenyl ester YD 32 **(37)** (0.08g, 0.076mmol) and epirubicin hydrochloride (0.04g, 0.069mmol) were dissolved in DMF (8mL). DIPEA (0.012mL, 0.069mmol) was then added; with overnight stirring. A mini extraction of the reaction solution was carried out and the progress of this reaction was checked by TLC (dichloromethane: ethyl acetate: methanol 7:2:1); R_f 0.17 (orange) product. The reaction mixture was partitioned between dichloromethane and water (1:2, 360mL), dried (MgSO$_4$), filtered and evaporated to a very low volume before applying onto a silica gel chromatography column (3.2cm×18cm), eluted with dichloromethane: methanol (12:1, increasing gradient 12:1 → 9:1). Fractions containing the major product were combined and evaporated to a low volume again, then applied onto two thick-layer chromatography plates eluted with dichloromethane: methanol (9:1). The lower orange band from each

plate were collected and washed with methanol and dichloromethane, and evaporated to dryness to afford the title compound (homogeneous on TLC).

Yield (0.091g, 84.6%). Mp: 195-197°C.

ESMS(+) m/z: 1431.6349 (55%) $(M+NH_4)^+$.

1.6.6.9 Synthesis of Epi-SUCC-Pro-Ala-Gly-Nva-Phe-Ala-DMPIP-YD9 (YD 61) (4): a twin prodrug of active agents the *N*-colchiceinamide derivative (YD11) (10) and epirubicin (2)

Epirubicin hydrochloride (0.01g, 0.0172mmol) and dried YD 60 (**38**) were dissolved in DMF (3mL), and then DIPEA was added. Two hours later, the reaction was complete, on TLC (dichloromethane: methanol 6:1); R_f 0.38 (orange) product. The reaction solution was concentrated and applied in dichloromethane to a thick-layer plate which was eluted with dichloromethane: methanol 6:1. The dark red band was collected and extracted with dichloromethane and methanol, and then evaporated to dryness to afford the title compound (homogeneous on TLC).

Yield (0.0218g, 74.2%).

ESMS(+) m/z: 1706.7479 (20%) $(M+H)^+$.

1.6.6.10 Synthesis of Epi-SUCC-Ala-Gly-Leu-Pro-Ala-Ala-APA-AQ (YD 67) (21): a twin prodrug of active agents Ala-APA-AQ (72) and epirubicin (2)

YD 62 (**23**) (0.045g, 0.044mmol) and epirubicin hydrochloride (0.025g, 0.044mmol) were mixed together and both dissolved in DMF (4mL) under basic conditions by using DIPEA (0.0076mL, 0.044mmol). After overnight reaction at RT, the progress of this reaction was checked by TLC (chloroform: methanol 6:1), R_f 0.35 (red) product. The whole reaction solution was transferred into an evaporating basin to evaporate till totally dry. Then, the solid compound was re-dissolved in a small amount of chloroform and

methanol before it was loaded onto a thick-layer chromatography plate, which was eluted with chloroform: methanol (6:1). The second red band from bottom was collected, washed with methanol, filtered and evaporated. Diethyl ether (15mL) was applied to precipitate pure (chromatographically homogeneous on TLC) YD 67 **(21)** which was dried *in vacuo*.

Yield (0.0112g, 18.5%). Mp: 175-177°C.

ESMS(+) m/z: 1386.5755 (100%) (M+H)$^+$.

1.6.6.11 Synthesis of Epi-SUCC-Pro-Ala-Gly-Leu-Ala-Ala-PIP-AQ (YD 75) (39): a twin prodrug of active agents Ala-PIP-AQ and epirubicin (2)

Dual prodrug YD 75 **(39)** was synthesised by reacting epirubicin hydrochloride (0.029g, 0.0505mmol) with pentafluorophenyl ester YD 74 **(42)** (0.0524g, 0.0505mmol), followed by adding DIPEA (0.0088mL, 0.0506mmol). After overnight reaction, the progress of this reaction was checked on TLC (dichloromethane: methanol 9:1) R$_f$ 0.32 (orange). However, there was still some unreacted epirubicin hydrochloride on TLC, so an additional equivalent of DIPEA was added and upon completion, the product was purified by thick-layer chromatography, eluted with dichloromethane: methanol 9:1. The middle dark red band was collected, washed with dichloromethane and methanol, filtered and evaporated to dryness to afford the title compound.

Yield (0.0432g, 61.3%).

ESMS(+) m/z: 1415.6036 (100%) (M+NH$_4$)$^+$.

1.6.6.12 Synthesis FITC-Ala-Nva-Gly-Leu-Pro-Aib-(oxypiperidine)-AQ (YD 17) (43): a FRET probe of FITC and its quencher 1-(4-hydroxypiperidyl) anthraquinone (44)

Anthraquinone oligopeptide conjugate YD 16 **(49)** (0.09g, 0.11mmol) and fluorescein isothiocyanate (0.047g, 0.12mmol) were dissolved in DMF (5mL), followed by adding

DIPEA (0.057mL, 0.33mmol). The mixture was kept stirring for 4h. A mini extraction was carried out and the progress of the reaction was checked by TLC (chloroform: methanol 4:1) R_f 0.6 (yellow) product. The mixture was partitioned between chloroform and water (1:2, 240mL), dried (MgSO$_4$), filtered and evaporated to a low volume before applying onto a silica gel chromatography column (2.2cm×17cm), eluted with chloroform: methanol (19:1). The fractions containing major product were combined and evaporated to dryness.

Yield (0.034g. 26%). Mp: 184-186°C.

ESMS(-) m/z: 1217.7 (100%) (M-H)$^-$.

1.6.7   Miscellaneous compounds including prodrug intermediates

1.6.7.1   Synthesis of SUCC-D-Ala-Ala-Ala-Leu-Gly-Leu-Nva-Gly-PIP-AQ (YD 12) (33)

NU:UB 349 (50) (0.09g, 0.084mmol) and succinic anhydride (0.01g, 0.1mmol) were dissolved in DMF (2mL). DIPEA (0.029mL, 0.17mmol) was added into this reaction mixture [following method A]. TLC showed a new product (chloroform: methanol 3:2) R_f 0.89 (orange). Due to poor aqueous solubility of succinate compound YD 12 (33) it was separated and transferred into three 2mL eppendorfs. Distilled water was added into each eppendorf and filled up to 2mL levels. The eppendorfs were then kept shaking for one hour, then centrifuged and the water layer was checked by litmus blue test paper. Succinate compound YD 12 (33) was further washed with distilled water until there was no colour change on litmus blue test paper. The title compound was air-dried at RT.

Yield (0.063g, 72%).

ESMS(-) m/z: 1043.5 (100%)(M-H)$^-$.

1.6.7.2   Synthesis of Boc-Aib-(oxypiperidine)-AQ (YD 13) (45)

N,N'-Dicyclohexylcarbodiimide   (DCC)   (0.74g,   3.59mmol)   and   4-dimethylaminopyridine (DMAP) (0.02g, 0.163mmol) were added to a cooled, stirred

105

solution of 1-(4-hydroxypiperidyl)anthraquinone **(44)** (1g, 3.26mmol) and Boc-Aib (0.73g, 3.59mmol) in chloroform (40mL). The precipitated dicyclohexylurea (DCU) was filtered off and the solution was partitioned between chloroform and water (1:1, 100mL), washed with saturated sodium bicarbonate solution (2×50mL) and water (2×50mL), dried (MgSO$_4$), filtered and evaporated to dryness. The residual solid was dissolved in toluene, applied onto a silica gel chromatography column (2.2cm×16cm), and eluted with toluene: ethyl acetate (4:1). Fractions containing the major product were combined, evaporated, and then ethyl acetate was added. The whole mixture was cooled (4°C overnight) and filtered to remove any remaining DCU. The product was isolated by evaporation to dryness. TLC (toluene: ethyl acetate 4:1); R$_f$ 0.27 (purple) product; homogeneous on TLC.

Yield (0.41g, 26%).

1.6.7.3   Synthesis of Aib-(oxypiperidine)-AQ [TFA] (YD 14) (46)

The ^{t}Boc protected compound YD13 **(45)** (0.35g, 0.71mmol) was deprotected by using trifluoroacetic acid [following method B]. The progress of this deprotection was checked by TLC (butanol: acetic acid: water 14:5:1); R$_f$ 0.50 (purple) product; homogeneous on TLC.

Yield (0.24g, 67%).

1.6.7.4   Synthesis of Fmoc-Ala-Nva-Gly-Leu-Pro-Aib-(oxypiperidine)-AQ (YD 15) (48)

N-terminal trifluoroacetate salt YD 14 **(46)** (0.136g, 0.27mmol), *N*-Fmoc-Ala-Nva-Gly-Leu-Pro-OH **(47)** (0.2g, 0.295mmol), TBTU (0.095g, 0.296mmol), and HOBt (0.045g, 0.295mmol) were dissolved in DMF (9mL) and stirred well, then DIPEA (0.15mL, 0.863mmol) was added. The coupling reaction was carried out by following method C. A silica gel chromatography column (2.2cm×15.5cm) was used for purification, eluted

with chloroform: methanol (9:1). The purity of the final compound was confirmed by its homogeneous character on TLC (butanol: acetic acid: water 14:5:1); R_f 0.8 (purple) single product spot.

Yield (0.22g, 77.5%).

1.6.7.5   Synthesis of Ala-Nva-Gly-Leu-Pro-Aib-(oxypiperidine)-AQ (YD 16) (49)

Fmoc protected YD 15 **(48)** (0.15g, 0.143mmol) was dissolved in 20% (v/v) piperidine in DMF solution (3.75mL) and kept stirring for 10min. This deprotection reaction was carried out by following method D. The progress of this deprotection was checked by TLC (chloroform: methanol 9:1); R_f 0.1 (purple) product. A silica gel column (2.2cm×16cm) was for flash chromatography, eluted with chloroform: methanol (19:1, increasing gradient 19:1 → 5:1 → 3:1 → 3:2).

Yield (0.1027g, 87%). Compound YD 16 **(49)** was used for subsequent reaction without further purification.

1.6.7.6   Synthesis of PFPO-SUCC-Pro-APA-AQ (YD 19) (24)

N,N'-dicyclohexylcarbodiimide DCC (0.025g, 0.123mmol), 4-dimethylaminopyridine DMAP (0.015g, 0.123mmol) and pentafluorophenol (0.0225g, 0.122mmol) were added into a stirred solution of NU:UB 354 **(51)** (0.05g, 0.11mmol) in dichloromethane (20mL). The reaction was carried out by following method E for overnight. The progress of this reaction was checked by TLC (dichloromethane: methanol 9:1) showed a major product; R_f 0.94 (purple). A silica gel chromatography column (2.2cm×15.5cm) was used for purification with chloroform: methanol (19:1 increasing gradient 19:1 → 9:1). Fractions containing the major product were combined, filtered and evaporated to dryness.

Yield (0.065g, 91%).

1.6.7.7   Synthesis of Ile-PIP-AQ [TFA] (NU:UB 234) (19)

Impure *N-*^{*t*}Boc protected NU:UB 234 **(55)** was deprotected by treating with TFA [following method B] for 30min. TLC (dichloromethane: methanol 9:1); R_f 0.34 (orange) product; homogeneous on TLC.

1.6.7.8   Synthesis of Boc-Gly-Ile-PIP-AQ (NU:UB 359 Boc) (56)

NU:UB 234 **(19)** (1.2g, 0.0023mol) and Boc-Gly-OSu (0.69g, 0.0025mol) were dissolved in DMF (15mL) with stirring, this followed by adding DIPEA (0.804mL, 0.0046mol) [following method C] and reacted for 6h. A mini extraction was carried out and the progress of this reaction was checked by TLC (dichloromethane: methanol 9:1); R_f 0.74 (orange) product. During purification, the compound was loaded onto a silica gel column (3.2cm×20cm) and eluted with chloroform: methanol (15:1).

1.6.7.9   Synthesis of Gly-Ile-PIP-AQ [TFA] (NU:UB 359) (73)

N-^{*t*}Boc-protected NU:UB 359 **(56)** was treated with TFA (10mL) [following method B] for 35min. TLC (dichloromethane: methanol 9:1); R_f 0.64 (orange) product; homogeneous on TLC.

1.6.7.10   Synthesis of Boc-Leu-Gly-Ile-PIP-AQ (NU:UB 360 Boc) (57)

DIPEA (0.905mL, 0.0052mol) was added into a well stirred solution of NU:UB 359 **(73)** (1.5g, 0.0026mol) and Boc-Leu-OSu (0.94g, 0.0029mol) in DMF (20mL) [following method C]. Three hours later, TLC showed formation of the product (dichloromethane: methanol 9:1); R_f 0.86 (orange) product. For purification, the compound was loaded onto a silica gel column (3.2cm×18cm) and eluted by chloroform: methanol (15:1).

1.6.7.11   Synthesis of Leu-Gly-Ile-PIP-AQ [TFA] (NU:UB 360) (74)

N-^{t}Boc-protected NU:UB 360 **(57)** was treated with TFA (10mL) [following method B] for 50min. TLC (dichloromethane: methanol 9:1); R_f 0.625 (orange) product; homogeneous on TLC.

1.6.7.12   Synthesis of Boc-Ala-Leu-Gly-Ile-PIP-AQ (NU:UB 361 Boc) (58)

Trifluoroacetate salt NU:UB 360 **(74)** (1.8g, 0.0026mol) and Boc-Ala-OSu (0.822g, 0.0029mol) were dissolved in DMF (10mL). DIPEA (0.908mL, 0.0052mol) was added into this well stirred reaction solution [following method C] and reacted for 2h. The progress of this reaction was checked by TLC (dichloromethane: methanol 9:1); R_f 0.625 (orange) product. The product was obtained in a chromatographically pure form from a silica gel column (3.2cm×23cm) and eluted by chloroform: methanol (10:1).

1.6.7.13   Synthesis of Ala-Leu-Gly-Ile-PIP-AQ [TFA] (NU:UB 361) (75)

N-^{t}Boc-protected NU:UB 361 **(58)** was treated with TFA (12mL) [following method B] for 40min. TLC (dichloromethane: methanol 9:1); R_f 0.44 (orange) product; homogeneous on TLC.

1.6.7.14   Synthesis of Boc-Ala-Ala-Leu-Gly-Ile-PIP-AQ (NU:UB 362 Boc) (59)

Trifluoroacetate salt NU:UB 361 **(75)** (1.8g, 0.0024mol) and Boc-Ala-OSu (0.75g, 0.0026mol) were dissolved in DMF (15mL), followed by adding DIPEA (0.824mL, 0.0047mol) into the well stirred reaction solution [following method C] and reacted for 1.5h. The reaction was monitored by TLC (dichloromethane: methanol 9:1); R_f 0.62 (orange) product. The chromatographically pure product was isolated by silica gel column chromatography (3.2cm×22cm) eluted with chloroform: methanol (12:1).

1.6.7.15 Synthesis of Ala-Ala-Leu-Gly-Ile-PIP-AQ [TFA] (NU:UB 362) (61)

N-^{t}Boc-protected NU:UB 362 **(59)** was treated with TFA (4.5mL) [following method B] for 40min. TLC (dichloromethane: methanol 9:1); R_f 0.38 (orange) product; homogeneous on TLC.

1.6.7.16 Synthesis of Boc-D-Ala-Ala-Ala-Leu-Gly-Ile-PIP-AQ (NU:UB 363 Boc) (60)

Trifluoroacetate salt NU:UB 362 **(61)** (1.5g, 0.0018mol) and Boc-D-Ala-OSu (0.57g, 0.0020mol) were dissolved in DMF (10mL). DIPEA (0.628mL, 0.0036mol) was added into this stirred well reaction solution [following method C]. After 2h, TLC showed (dichloromethane: methanol 7:1); R_f 0.64 (orange) product. Chromatography on a silica gel column (3.2cm×19cm) eluted with chloroform: methanol (10:1) afforded chromatographically pure product.

1.6.7.17 Synthesis of D-Ala-Ala-Ala-Leu-Gly-Ile-PIP-AQ [TFA] (NU:UB 363) (30)

N-^{t}Boc-protected NU:UB 363 **(60)** was treated with TFA (15mL) [following method B] for 40min. TLC (dichloromethane: methanol 7:1); R_f 0.3 (orange) product; homogeneous on TLC.

Yield (1.55g).

ESMS(+) m/z: 789.4277 (100%) (M+H)$^+$; ESMS(-) m/z: 113.0 (100%) trifluoroacetate anion.

1.6.7.18 Synthesis of SUCC-D-Ala-Ala-Ala-Leu-Gly-Ile-PIP-AQ (YD 30) (28)

Trifluoroacetate salt NU:UB 363 **(30)** (0.5g, 0.55mmol) and succinic anhydride (0.17g, 1.663mmol) were dissolved in DMF (5mL) followed by adding DIPEA (0.0964mL, 0.5545mmol [following method A]. The reaction was left for 2 days. A mini extraction was carried out and the progress of this reaction was checked by TLC (butanol: acetic

acid: water 4:5:1); R$_f$ 0.88 (orange) product. Because YD 30 did not dissolve in water, washing with water was continued until no more succinic anhydride was detected, and then the chromatographically pure product (homogeneous on TLC) was dried *in vacuo*.

Yield: (0.38g, 77%).

1.6.7.19   Synthesis of PFPO-SUCC-D-Ala-Ala-Ala-Leu-Gly-Ile-PIP-AQ (YD 32) (37)

The anthraquinone spacer oligopeptide succinate compound YD 30 **(28)** (0.1g, 0.1127mmol) was suspended in chloroform (55mL), then N,N'-dicyclohexylcarbodiimide (0.026g, 0.126mmol), 4-dimethylaminopyridine (0.015g, 0.123mmol) and pentafluorophenol (0.023g, 0.125mmol) were added into this well-stirred reaction solution [following method E]. TLC (dichloromethane: ethyl acetate: methanol 7:2:1) indictaed a new product spot; R$_f$ 0.46 (orange) product.

1.6.7.20   Synthesis of Fmoc-Pro-Ala-Gly-Nva-Phe-Ala-OH (YD 43) (52)

Alanine pre-loaded resin with a 2-chlorotrityl linker (0.5g, 0.31mmol/g) was swollen in dichloromethane (5mL) for 1h. Coupling and deprotection cycles were carried on as follows:

1st cycle: *N*-Fmoc-L-phenylalanine (0.12g, 2 equivalents), TBTU (0.095g, 1.9 equivalents), and HOBt (0.037g, 1.9 equivalents) were dissolved in DMF (10mL), and then DIPEA (0.11mL, 4 equivalents) was added into this solution [following SPPS coupling and deprotection methods].

2nd cycle: *N*-Fmoc-L-norvaline (0.105g, 2 equivalents), TBTU (0.095g, 1.9 equivalents), and HOBt (0.037g, 1.9 equivalents) were dissolved in DMF (10mL), and then DIPEA (0.1078mL, 4 equivalents) was added into this solution [following SPPS coupling and deprotection methods].

3rd cycle: *N*-Fmoc-L-glycine (0.092g, 2 equivalents), TBTU (0.095g, 1.9 equivalents), and HOBt (0.037g, 1.9 equivalents) were dissolved in DMF (10mL), and then DIPEA (0.1078mL, 4 equivalents) was added into this solution [following SPPS coupling and deprotection methods].

4th cycle: *N*-Fmoc-L-alanine (0.0965g, 2 equivalents), TBTU (0.095g, 1.9 equivalents), and HOBt (0.037g, 1.9 equivalents) were dissolved in DMF (10mL), and then DIPEA (0.1078mL, 4 equivalents) was added into this solution [following SPPS coupling and deprotection methods].

5th cycle: *N*-Fmoc-L-proline (0.1046g, 2 equivalents), TBTU (0.0945g, 1.9 equivalents), and HOBt (0.0368g, 1.9 equivalents) were dissolved in DMF (10mL), and then DIPEA (0.1078mL, 4 equivalents) was added into this solution [following SPPS coupling and deprotection methods].

After coupling five *N*-Fmoc-protected amino acids onto pre-loaded resins in sequence, the hexapeptide was cleaved off from the resin [following SPPS cleavage method].

Yield: (0.115g).

ESMS(+) m/z: 783.3711 (39%) $(M+H)^+$, 800.3979 (100%) $(M+NH_4)^+$.

1.6.7.21   Synthesis of Ala-DMPIP-YD9 [TFA] (YD 48) (65)

N-*t*Boc protected alanine colchiceinamide spacer conjugate was treated with TFA (5mL) for 30min [following method B]. TLC (dichloromethane: ethyl acetate: methanol 6:2:1); R_f 0.125 (pale yellow) product; homogeneous on TLC.

Yield (0.55g, 83%).

1.6.7.22   Synthesis of Phe-Ala-DMPIP-YD9 [TFA] (YD 49) (66)

YD 48 (**65**) (0.g, 0.575mmol) and Boc-Phe-OSu (0.313g, 0.86mmol) were dissolved in DMF (4mL). DIPEA (0.22mL, 1.27mmol) was added into this well-stirred reaction

112

solution [following method C] for 48h. The product was purified on a silica gel chromatography column (2.2cm×15cm) eluted with dichloromethane: ethyl acetate: methanol (6:2:1). TLC (dichloromethane: ethyl acetate: methanol 6:2:1); R_f 0.62 (pale yellow) product. Then the product was treated with TFA (5mL) for 45min [following method B]. TLC (dichloromethane: ethyl acetate: methanol 6:2:1); R_f 0.44 (pale yellow) product; homogeneous on TLC.

Yield (0.46g, 93%).

1.6.7.23   Synthesis of Fmoc-Pro-Ala-Gly-Nva-Phe-Ala-Ala-DMPIP-YD9 (YD 50) (69)

Ala-DMPIP-YD9 [TFA] (YD 48) **(65)** (0.097g, 0.133mmol), Fmoc-Pro-Ala-Gly-Nva-Phe-Ala-OH YD 43 **(52)** (0.0951g, 0.122mmol), PyBOP (0.0696g, 0.1338mmol) and HOBt (0.0205g, 0.1340mmol) were dissolved in DMF (2mL), followed by adding DIPEA (0.0677mL, 0.3894mmol). Compound YD 50 **(69)** was used for subsequent reaction without further purification.

ESMS(+) m/z: 1374.6753 (50%) $(M+H)^+$.

1.6.7.24   Synthesis of Nva-Phe-Ala-DMPIP-YD9 [TFA] (YD 51) (67)

Phe-Ala-DMPIP-YD9 [TFA] (YD 49) **(66)** (0.45g, 0.52mmol), Boc-Nva-OH (0.124g, 0.57mmol), PyBOP (0.3g, 0.57mmol), and HOBt (0.087g, 0.57mmol) were dissolved in DMF (4mL). DIPEA (0.29mL, 0.0017mol) was added into this well-stirred reaction solution [following method C]. Following overnight reaction and silica gel column (2.2cm×17cm) chromatography, eluted by dichloromethane: ethyl acetate: methanol (6:2:1) the product was obtained in a chromatographically pure form. TLC (dichloromethane: ethyl acetate: methanol 6:2:1); R_f 0.48 (pale yellow) product. Chromatographically pure product was treated with TFA (5mL) for 45min [following

method B]. TLC (dichloromethane: ethyl acetate: methanol 6:2:1); R_f 0.32 (pale yellow) product; homogeneous on TLC.

Yield (0.41g, 82%).

1.6.7.25   <u>Synthesis of Ala-Gly-Nva-Phe-Ala-DMPIP-YD9 [TFA] (YD 52) (68)</u>

Nva-Phe-Ala-DMPIP-YD9 [TFA] (YD 51) **(67)** (0.4g, 0.413mmol) and Boc-Ala-Gly-OSu (0.212g, 0.62mmol) were dissolved in DMF (3mL). DIPEA (0.16mL, 0.91mmol) was added [following method C]. Overnight reaction and silica gel column chromatography (2.2cm×15cm) in dichloromethane: ethyl acetate: methanol (6:2:1) afforded the product. TLC (dichloromethane: ethyl acetate: methanol 6:2:1); R_f 0.47 (pale yellow) product. N-^{t}Boc-protected product was treated with TFA (3mL) for 45min [following method B]. TLC (dichloromethane: ethyl acetate: methanol 6:2:1); R_f 0.08 (pale yellow) product; homogeneous on TLC.

Yield (0.32g, 70%).

1.6.7.26   <u>Synthesis of Pro-Ala-Gly-Nva-Phe-Ala-DMPIP-YD9 [TFA] (YD 53) (64)</u>

Ala-Gly-Nva-Phe-Ala-DMPIP-YD9 [TFA] (YD 52) **(68)** (0.3g, 0.27mmol), Boc-Pro-OH (0.088g, 0.41mmol), PyBOP (0.213g, 0.41mmol), HOBt (0.063g, 0.41mmol) were dissolved in DMF (2mL). DIPEA (0.17mL, 0.96mmol) was added with stirring [following method C]. The reaction was maintained overnight. Silica gel column (2.2cm×17cm) chromatography afforded the product, eluting with dichloromethane: ethyl acetate: methanol (6:2:1). TLC (dichloromethane: ethyl acetate: methanol 6:2:1); R_f 0.46 (pale yellow) product. N-^{t}Boc-protected YD 53 **(70)** was treated with TFA (3mL) for 45min [following method B]. TLC (dichloromethane: ethyl acetate: methanol 6:2:1); R_f 0.07 (pale yellow) product; homogeneous on TLC.

Yield (0.27g, 83%).

ESMS(+) m/z: 1081.5708 (100%) (M+H)$^+$.

1.6.7.27   Synthesis of SUCC-Pro-Ala-Gly-Nva-Phe-Ala-DMPIP-YD9 (YD 54) (18)

Pro-Ala-Gly-Nva-Phe-Ala-DMPIP-YD9 [TFA] (YD 53) **(64)** (0.1g, 0.084mmol) and succinic anhydride (0.025g, 0.25mmol) were dissolved in DMF (2mL), then DIPEA (0.015mL, 0.084mmol) was added [following method A]. TLC (dichloromethane: methanol 6:1) R_f 0.45 (pale yellow) product.

Yield (0.033g, 34%).

1.6.7.28   Synthesis of MB1-SUCC-OPFP (YD 57) (26)

MB1-SUCC (YD 56) **(17)** (0.135g, 0.25mmol) was dissolved in dichloromethane (20mL) first, and then DCC (0.057g, 0.27mmol) was added into this well-stirred solution. DMAP (0.034g, 0.27mmol) and OPFP (0.051g, 0.27mmol) were added into this reaction solution [following method E].

1.6.7.29   Synthesis of PFPO-SUCC-Pro-Ala-Gly-Nva-Phe-Ala-DMPIP-YD9 (YD 60) (YD 60) (38)

SUCC-Pro-Ala-Gly-Nva-Phe-Ala-DMPIP-YD9 (YD 54) **(18)** (0.04g, 0.035mmol) and DCC (0.0079g, 0.038mmol) were dissolved in dichloromethane first, and then pentafluorophenol (0.007g, 0.038mmol) and DMAP (0.0047g, 0.039mmol) were added into this reaction mixture [following method E]. Four hours later, the progress of this reaction was checked on TLC (dichloromethane: ethyl acetate: methanol 5:1:1); R_f 0.49 (yellow) product. White solid DCU was filtered off and the solution was evaporated to dryness. The residue was used without further purification.

1.6.7.30   Synthesis of PFPO-SUCC-Ala-Gly-Leu-Pro-Ala-Ala-APA-AQ (YD 62) (23)

C6 **(70)** (0.150g, 0.17mmol) and DCC (0.04g, 0.19mmol) were dissolved in chloroform and kept at 0°C first, and then DMAP (0.023g, 0.19mmol) and pentafluorophenol (0.035g, 0.19mmol) were added into this reaction mixture [following method E]. After 48h, the progress of this reaction was checked on TLC (chloroform: methanol 4:1); R_f 0.37 (purple) product. The reaction mixture was partitioned between chloroform and water (1:3, 120mL), washed with saturated sodium bicarbonate solution (50mL) and water (50mL), dried (Na_2SO_4), filtered and evaporated to dryness. Addition of diethyl ether (30mL) gave a precipitate of YD 62 **(23)**. This OPFP compound was filtered off and dried *in vacuo*.

Yield (0.145g, 81%).

1.6.7.31   Synthesis of PFPO-SUCC-Pro-Ala-Gly-Leu-Ala-Ala-PIP-AQ (YD 74) (42)

SUCC-Pro-Ala-Gly-Leu-Ala-Ala-PIP-AQ (HZ 15) **(41)** (0.1g, 0.115mmol) and DCC (0.026g, 0.126mmol) were dissolved in dichloromethane and kept at 4°C for five minutes, and then pentafluorophenol (0.0232g, 0.126mmol) and DMAP (0.0154g, 0.126mmol) were added [following method E]. The progress of this reaction was monitored by TLC (dichloromethane: methanol 9:1), R_f 0.52 (orange) product. DCU was filtered off from the reaction solution, and then the whole reaction mixture was evaporated to a solid residue which was used without further purification.

1.7 <u>REFERENCES</u>

Andreu, J. M. and Timasheff, S. N. (1982) Conformational states of tubulin liganded tocolchicine, tropolone methyl ether, and podophyllotoxin. *Biochemistry*. **21**(25), 6465-76.

Atlas, D., Levit, S., Schechter, I. and Berger, A. (1970) On the active site of elastase: Partial mapping by means of specific peptide substrates. *FEBS Lett*. **11** (4), 281-283.

Avila, J. (1990) Microtubule dynamics. *FASEB J*. **4**(15), 3284-90.

Bagshawe, K. D. (1987) Antibody directed enzymes revive anti-cancer prodrugs concept. *Br. J. Cancer*. **56** (5), 531-532.

Bagshawe, K. D. (1994) Antibody-directed enzyme prodrug therapy (Adept). *J. Controlled Release*. **28**, 187-193.

Balalaie, S., Mahdidoust, M. and Eshaghi-Najafabadi, R. (2008) 2-(1-*H*-Benzotriazole-1-yl)-1,1,3,3-Tetramethyluronium Tetrafluoro Borate (TBTU) as an Efficient Coupling Reagent for the Esterification of Carboxylic acids with Alcohols and Phenols at Room Temperature. *Chin. J. Chem.* **26**, 1141-1144.

Bergers, G., Brekken, R., McMahon, G., Vu, T. H., Itoh, T., Tamaki, K., Tanzawa, K., Thorpe, P., Itohara, S., Werb, Z. and Hanahan, D. (2000) Matrix metalloproteinase-9 triggers the angiogenic switch during carcinogenesis. *Nat. Cell Biol*. **2** (10), 737-744.

Bhattacharyya, B. and Wolff, J. (1974) Promotion of fluorescence upon binding of colchicine to tubulin. *Proc. Natl. Acad. Sci. USA*. **71**(7), 2627-31.

Birkedal-Hansen, H. (1995) Proteolytic remodelling of extracellular matrix. *Curr. Opin. Cell Biol.* **7**(5), 728-735.

Birkedal-Hansen, H., Moore, W. G. I., Bodden, M. K., Windsor, L. J., Birkedal-Hansen, B., DeCarlo, A., and Engler, J. A. (1993) Matrix metalloproteinases: A review. *Crit. Rev. Oral Biol. Med*. **42**, 197-250.

Brooks, P. C., Silletti, S., von Schalscha, T. L., Friedlander, M. and Cheresh, D. A. (1998) Disruption of angiogenesis by PEX, a noncatalytic metalloproteinase fragment with integrin binding activity. *Cell*. **92** (3), 391-400.

Butler, G. S., Butler, M. J., Atkinson, S. J., Will, H., Tamura, T., Westrum, S. S. V., Crabbe, T., Clements, J., d'Ortho, M. and Murphy, G. (1998) The TIMP2 membrane type 1 metalloproteinase 'receptor' regulates the concentration and efficient activation of progelatinase A. *J. Biol. Chem.* **273**(2), 871-880.

Cao, Y. (2001) Endogenous angiogenesis inhibitors and their therapeutic implications. *Int. J. Biochem. Cell Biol*. **33**, 357-69.

Cerquaglia, C., Diaco, M., Nucera, G., La Regina, M., Montalto, M. and Manna, R. (2005) Pharmacological and clinical basis of treatment of Familial Mediterranean Fever (FMF) with colchicine or analogues: an update. *Curr. Drug Targets Inflamm. Allergy*. **4**(1), 117-24.

Chau, I., Rigg, A. and Cunningham, D. (2003) Matrix metalloproteinase inhibitors--an emphasis on gastrointestinal malignancies. *Crit. Rev. Oncol/Hematol*. **45**, 151-176.

Chen, E. I., Kridel, S. J., Howard, E. W., Li, W., Godzik, A. and Smith, J. W. (2002) A unique substrate recognition profile for matrix metalloproteinase-2. *J. Biol. Chem.* **277**(6), 4485-4491.

Chen, E. I., Li, W., Godzik, A., Howard, E. W. and Smith, J. W. (2003) A residue in the S2 subsite controls substrate selectivity of matrix metalloproteinase-2 and matrix metalloproteinase-9. *J. Biol. Chem.* **278**(19), 17158-17163.

Chung, L., Dinakarpandian, D., Yoshida, N., Lauer-Fields, J. L., Fields, G. B., Visse, R. and Nagase, H. (2004) Collagenase unwinds triple-helical collagen prior to peptide bond hydrolysis. *EMBO J*. **23**(15), 3020-3030.

Clark, I. M., Swingler, T. E., Sampieri, C. L. and Edwards, D. R. (2008) The regulation of matrix metalloproteinases and their inhibitors. *Int. J. Biochem. Cell Biol.* **40**, 1362-1378.

Combeau, C., Provost. J., Lancelin, F., Tournoux, Y., Prod'homme, F., Herman, F., Lavelle, F., Leboul, J. and Vuilhorgne, M. (2000) RPR112378 and RPR115781: two representatives of a new family of microtubule assembly inhibitors. *Mol. Pharmacol.* **57**(3), 553-63.

Cunningham, L. A., Wetzel, M. and Rosenberg, G. A. (2005) Multiple roles for MMPs and TIMPs in cerebral ischemia. *Glia*. **50**(4), 329-339.

Curran, S. and Murray, G. I. (2000) Matrix metalloproteinases: molecular aspects of their roles in tumour invasion and metastasis. *Eur. J. Cancer*. **36**, 1621-1630.

Davis, P. J. (1981) Microbial Transformations of *N*-Methylcolchiceinamide. *Antimicrob. Agents Chemother.* **19**(3), 465-469.

DeClerck, Y. A. (2000) Interactions between tumour cells and stromal cells and proteolytic modification of the extracellular matrix by metalloproteinases in cancer. *Eur. J. Cancer*. **36**, 1258-1268.

Drummond, A. H., Beckett, P., Brown, P. D., Boone, E. A., Davidson, A. H., Galloway, W. A., Gearing, A. J. H., Huxley, P., Laber, D., McCourt, M., Whittaker, M., Wood, L. M. and Wright, A. (1999) Preclinical and Clinical Studies of MMP Inhibitors in Cancer. *Ann. N.Y. Acad. Sci.* **878**(1), 228-235.

Dufour, A. and Overall, C. M. (2013) Missing the target: matrix metalloproteinase antitargets in inflammation and cancer. *Trends. Pharmacol. Sci*. **34**(4), 233-42.

Duncan, R., Sat-Klopsch, Y. N., Burger, A. M., Bibby, M. C., Fiebig, H. H. and Sausville, E. A. (2013) Validation of tumour models for use in anticancer nanomedicine evaluation: the EPR effect and cathepsin B-mediated drug release rate. *Cancer Chemother. Pharmacol*. **72**(2), 417-27.

English, W. R., Holtz, B., Vogt, G., Knäuper, V. and Murphy, G. (2001) Characterization of the role of the "MT-loop": an eight-amino acid insertion specific to progelatinase A (MMP2) activating membrane-type matrix metalloproteinases. *J. Biol. Chem.* **276**(45), 42018-42026.

Farrell, K. W. and Wilson, L. (1980) Proposed mechanism for colchicine poisoning of microtubules reassembled in vitro from Strongylocentrotus purpuratus sperm tail outer doublet tubulin. *Biochemistry*. **19**(13), 3048-54.

Friedman, M. (2004) Applications of the ninhydrin Reaction for Analysis of Amino Acids, Peptides, and Proteins to Agricultural and Biomedical Sciences. *J. Agric. Food Chem.* **52**(3), 385-406.

Giavazzi, R. and Taraboletti, G. (2001) Preclinical development of metalloproteasis inhibitors in cancer therapy. *Crit. Rev. Oncol/Hematol*. **37**, 53-60.

Gross, J. and Lapiere, C. M. (1962) Collagenolytic activity in amphibian tissues: a tissue culture assay. *Proc. Natl. Acad. Sci. USA*. **48**, 1014-1022.

Guan, J., Zhu, X. K., Tachibana, Y., Bastow, K. F., Brossi, A., Hamel, E. and Lee, K. H. (1998) Antitumor agents. Part 186: Synthesis and biological evaluation of demethylcolchiceinamide analogues as cytotoxic DNA topoisomerase II inhibitors. *Bioorg. Med. Chem.* **6**(11), 2127-31.

Hadler-Olsen, E., Winberg, J. O. and Uhlin-Hansen, L. (2013) Matrix metalloproteinases in cancer: their value as diagnostic and prognostic markers and therapeutic targets. *Tumour Biol*. **34**(4), 2041-51.

Haiko, J., Suomalainen, M., Ojala, T., Lähteenmäki, K. and Korhonen, T. K. (2009) Invited review: Breaking barriers--attack on innate immune defences by omptin surface proteases of enterobacterial pathogens. *Innate. Immunity*. **15**(2), 67-80.

Hamano, Y., Zeisberg, M., Sugimoto, H., Lively, J. C., Maeshima, Y., Yang, C., Hynes, R. O., Werb, Z., Sudhakar, A. and Kalluri, R. (2003) Physiological levels of tumstatin, a fragment of collagen IV alpha3 chain, are generated by MMP-9 proteolysis and suppress angiogenesis via alphaV beta3 integrin. *Cancer Cell.* **3**(6)**,** 589-601.

Han, H. K. and Amidon, G. L. (2000) Targeted prodrug design to optimize drug delivery. *AAPS Pharmsci*. **2**(1), 48-58.

Hartwell, J. L., Nadkarni, M. V. and Leiter, J. (1952) *N*-Substituted Colchiceinamides. *J. Am. Chem. Soc*. 74(12), 3180-3181.

Hastie, S. B. (1989) Spectroscopic and kinetic features of allocolchicine binding to tubulin. *Biochemistry*. **28**(19), 7753-60.

Hidalgo, M. and Eckhardt, S. G. (2001) Development of Matrix Metalloproteinase Inhibitors in Cancer Therapy. *J. Natl. Cancer Inst*. **93**, 178-193.

Hobbs, S. K., Monsky, W. L., Yuan, F., Roberts, W. G., Griffith, L., Torchilin, V. P. and Jain, R. K. (1998) Regulation of transport pathways in tumor vessels: role of tumor type and microenvironment. *Proc. Natl. Acad. Sci. USA*. **95**, 4607-4312.

Imai, K., Hiramatsu, A., Fukushima, D., Pierschbacher, M. D. and Okada, Y. (1997) Degradation of decorin by matrix metalloproteinases: identification of the cleavage sites, kinetic analyses and transforming growth factor-β1 release. *Biochem. J.* **322**, 809-814.

Jain, P., Saravanan, C. and Singh, S. K. (2013) Sulphonamides: Deserving class as MMP inhibitors? *Eur. J. Med. Chem.* **60**, 89-100.

Jain, R. K. (1999) Transport of molecules, particles, and cells in solid tumors. *Annu. Rev. Biomed. Eng.* **1**, 241.

Jang, S. H., Wientjes, M. G., Lu, D. and Au, J. L. (2003) Drug delivery and transport to solid tumors. *Pharm. Res.* **20**(9), 1337-50.

Jordan, M. A. and Wilson, L. (1998) Microtubules and actin filaments: dynamic targets for cancer chemotherapy. *Curr. Opin. Cell Biol*. **10**(1), 123-30.

Juillerat-Jeanneret, L. and Schmitt, F. (2007) Chemical modification of therapeutic drugs or drug vector systems to achieve targeted therapy: looking for the grail. *Med. Res. Rev*. **27**(4), 574-590.

Kim, Y. M., Jang, J. W., Lee, O. H., Yeon, J., Choi, E. Y., Kim, K. W., Lee, S. T. and Kwon, Y. G. (2000) Endostatin inhibits endothelial and tumour cellular invasion by blocking the activation and catalytic activity of matrix metalloproteinase 2. *Cancer Res*. **60**, 5410-3.

Klein, G., Vellenga, E., Fraaije, M. W., Kamps, W. A. and de Bont, E. S. J. M. (2004) The possible role of matrix metalloproteinase (MMP)-2 and MMP-9 in cancer, e.g. acute leukemia. *Crit. Rev. Oncol/hematol*. **50**, 87-100.

Knäuper, V., Will, H., López-Otin, C., Smith, B., Atkinson, S. J., Stanton, H., Hembry, R. M. and Murphy, G. (1996) Cellular mechanisms for human procollagenase-3 (MMP-13) activation. Evidence that MT1-MMP (MMP-14) and gelatinase a (MMP-2) are able to generate active enzyme. *J. Biol. Chem.* **271**(29), 17124-17131.

Kolodziej, S. J., Wagenknecht, T., Strickland, D. K. and Stoops J. K. (2002) The three-dimensional structure of the human alpha 2-macroglobulin dimer reveals its structural organization in the tetrameric native and chymotrypsin alpha 2-macroglobulin complexes. *J. Biol. Chem.* **277**, 28031-7.

Koop, E. A. and Voest, E. E. (2002) Tumor vasculature as a target. In: Baguley, B. C. and Kerr, D. J. editors. (2002) *Anticancer Drug Development*. 123-136.

Kratz, F., Ryppa, C., Müller, I. and Warnecke, A. (2008) Prodrug strategies in anticancer chemotherapy. *ChemMedChem*. **3**, 20-53.

Kridel, S. J., Chen, E., Kotra, L. P., Howard, E. W., Mobashery, S. and Smith, J. W. (2001) Substrate hydrolysis by matrix metalloproteinase-9. *J. Biol. Chem.* **276**(23), 20572-20578.

Lee, R. M. and Gewirtz, D. A. (2008) Colchicine site inhibitors of microtubule interity as vascular disrupting agents. *Drug Dev. Res.* **69**, 352-358.

Lehti, K., Valtanen, H., Wickström, S., Lohi, J. and Keski-Oja, J. (2000) Regulation of membrane-type-1 matrix metalloproteinase activity by its cytoplasmic domain. *J. Biol. Chem.* **275**, 150006-15013.

Liu, D., Nakano, J., Ishikawa, S., Yokomise, H., Ueno, M., Kadota, K., Urushihara, M. and Huang, C. L. (2007) Overexpression of matrix metalloproteinase-7 (MMP-7) correlates with tumor proliferation, and a poor prognosis in non-small cell lung cancer. *Lung Cancer.* **58**, 384-391.

Liu, Y. E., Wang, M., Greene, J., Su, J., Ulrich, S., Li, H., Sheng, S., Alexander, P., Sang, Q. A. and Shi, Y. E. (1997) Preparation and characterization of recombinant tissue inhibitor of metalloproteinase (TIMP-4). *J. Biol. Chem.* **272**, 20479-20483.

Lu, Y., Yang, J. and Sega, E. (2006) Issues related to targeted delivery of proteins and peptides. *AAPS J.* **8**(3), 466-478.

Maeda, H., Greish, K. and Fang, J. (2006) The EPR Effect and Polymeric Drugs: A Paradigm Shift for Cancer Chemotherapy in the 21st Century. *Adv. Polym. Sci.* **193**,103-121.

Mahato, R., Tai, W. and Cheng, K. (2011) Prodrugs for improving tumor targetability and efficiency. *Adv. Drug Deliv. Rev.* **63**(8), 659-70.

Marchenko, N. D., Marchenko, G. N., Weinreb, R. N., Lindsey, J. D., Kyshtoobayeva, A., Crawford, H. C. and Strongin, A. Y. (2004) Beta-catenin regulates the gene of MMP-26, a novel metalloproteinase expressed both in carcinomas and normal epithelial cells. *Int. J. Biochem. Cell Biol.* **36(5)**, 942-956.

Margolis, R. L. and Wilson, L. (1977) Addition of colchicine--tubulin complex to microtubule ends: the mechanism of substoichiometric colchicine poisoning. *Proc. Natl. Acad. Sci. USA.* **74**(8), 3466-70.

Massova, I., Fridman, R. and Mobashery, S. (1997) Structural insights into the catalytic domains of human matrix metalloprotease-2 and human matrix metalloprotease-9: implications for substrate specificities. *J. Mol. Model.* **3**, 17-30.

Matsumura, Y. and Maeda, H. (1986) A new concept for macromolecular therapeutics in cancer chemotherapy: mechanism of tumoritropic accumulation of proteins and the antitumor agent smancs. *Cancer Research.* **46**, 6387-6392.

McCawley, L. J. and Matrisian, L. M. (2000) Matrix metalloproteinases: multifunctional contributors to tumour progression. *Molecular Medicine Today.* **6**, 149-156.

McGeehan, M., Bickett, D. M., Green, M., Kassel, D., Wiseman, J. S. and Berman, J. (1994) Characterization of the Peptide Substrate Specificities of Interstitial Collagenase and 92-kDa Gelatinase. *J. Biol. Chem.* **269**(52), 32814-32820.

Medrano, F. J., Andreu, J. M., Gorbunoff, M. J. and Timasheff, S. N. (1989) Roles of colchicine rings B and C in the binding process to tubulin. *Biochemistry*. **28**(13), 5589-99.

Mincher, D. J., Turnbull, A. and Kay, G. G. (Inventors) (2003) Anthracene derivatives as anti-cancer agents. World Patent WO0144190 A1 [Publication Date: 21-06-2001].

Montalbetti, C. A. G. N. and Falque, V. (2005) Amide bond formation and peptide coupling. *Tetrahedron*. **61**, 10827-10852.

Mori, M., Massaro, A., Calderone, V., Fragai, M., Luchinat, C. and Mordini, A. (2013) Discovery of a New Class of Potent MMP Inhibitors by Structure-Based Optimization of the Arylsulfonamide Scaffold. *ACS Med. Chem. Lett.* **4**, 565-569.

Moses, M. A. (1997) The regulation of neovascularization of matrix metalloproteinases and their inhibitors. *Stem Cells*. **15**, 180-189.

Muller, G. and Poittevin, A. (1966) *Desacetylamino-N-methyl colchiceinamide*. US Patent 3,249,638.

Murphy, G. and Nagase, H. (2008) Progress in matrix metalloproteinase research. *Molecular Aspects of Medicine.* **29**, 290-308.

Murphy, G., Segain, J. P., O'Shea, M., Cockett, M., Ioannou, C., Lefebure, O., Chambon, P. and Basset, P. (1993) The 28-kDa *N*-terminal domain of mouse stromelysin-3 has the general properties of a weak metalloproteinase. *J. Biol. Chem.* **268 (21)**, 15435-15441.

Nagase, H., Visse, R. and Murphy, Gillian. (2006) Structure and function of matrix metalloproteinases and TIMPs. *Cardiovascular Research*. **69**, 562-573.

Nagase, H. and Woessner J. F. (1999) Matrix metalloproteinases. *J. Biol. Chem*. **274**, 21491-4.

Newby, A. C. (2012) Matrix metalloproteinase inhibition therapy for vascular diseases. *Vascul. Pharmacol.* **56**, 232-44.

Noguchi, Y., Wu, J., Duncan, R., Strohalm, J., Ulbrich, K., Akaike, T. and Maeda, H. (1998) Early phase tumour accumulation of macromolecules: a great difference in clearance rate between tumour and normal tissues. *Jpn. J. Cancer Res*. **89**, 307-314.

Oriuchi, N., Watanabe, N., Kanda, H., Hashimoto, M., Sugiyama, S., Takenoshita, S., Imai, K., Ueda, R. and Endo, K. (1998) Antibody-dependent difference in biodistribution of monoclonal antibodies in animal models and humans. *Cancer Immunol. Immunother*. **46**, 311-317.

Patrick, G. L. (2009) *An Introduction to Medicinal Chemistry*. New York: Oxford University Press Inc.

Pei, D. and Weiss, S. J. (1995) Furin-dependent intracellular activation of the human stromelysin-3 zymogen. *Nature*. **375**(6528), 244-247.

Ramu, P., Lobo, L. A., Kukkonen, M., Bjur, E., Suomalainen, M. Raukola, H., Miettinen, M., Julkunen, I., Holst, O., Rhen, M., Korhonen, T. K. and Lähteenmäki, K. (2008) Activation of pro-matrix metalloproteinase-9 and degradation of gelatine by the surface protease PgtE of Salmonella enteric serovar Typhimurium. *Int. J. Med. Microbiol.* **298**, 263-278.

Ramu, P., Tanskanen, R., Holmberg, M., Lahteenmaki, K., Korhonen, T. K. and Meri, S. (2007) The surface protease PgtE of Salmonella enteric affects complement activity by proteolytically cleaving C3b, C4b and C5. *FEBS Lett.* **581**, 1716-1720.

Raspaglio, G., Ferlini, C., Mozzetti, S., Prislei, S., Gallo, D., Das, N. and Scambia, G. (2005) Thiocolchicine dimers: a novel class of topoisomerase-I inhibitors. *Biochem. Pharmacol.* **69**(1), 113-21.

Satchi, R., Connors, T. A. and Duncan, R. (2001) PDEPT: polymer-directed enzyme prodrug therapy 1. HPMA copolymer-cathepsin B and PK1 as a model combination. *Br. J. Cancer.* **85**(7), 1070-1076.

Senter, P. D., Saulnier, M. G., Schreiber, G. J., Hirschberg, D. L., Brown, J. P., Hellstrom, I. and Hellstrom, K. E. (1988) Anti-tumour effects of antibody-alkaline phosphatise conjugates in combination with etoposide phosphate. *Proc. Natl. Acad. Sci. USA.* **85**, 4842-4846.

Stetler-Stevenson, W. G. (1996) Matrix metalloproteinases and tumour invasion: from correlation and causality to the clinic. *Semin. Cancer Biol.* **7**, 147-154.

Stetler-Stevenson, W. G. (1999) Matrix metalloproteinases in angiogenesis: a moving target for therapeutic intervention. *J. Clin. Invest.* **103**(9), 1237-1241.

Sudhakar A., Sugimoto H. and Yang C. (2003) Human tumstatin and human endostatin exhibit distinct antiangiogenic activities mediated by alpha v beta 3 and alpha 5 beta 1 integrins. *Proc. Natl. Acad. Sci. USA.* **100**, 4766-71.

Tallant, C., Marrero, A. and Gomis-Rüth, F. X. (2010) Matrix metalloproteinases: Fold and function of their catalytic domains. *Biochimica et Biophysica Acta.* **1803**, 20-28.

Uppuluri, S., Knipling, L., Sackett, D. L. and Wolff, J. (1993) Localization of the colchicine-binding site of tubulin. *Proc. Natl. Acad. Sci. USA.* **90**(24), 11598-602.

Vacca, A., Ria, R., Semeraro, F., Merchionne, F., Coluccia, M., Boccarelli, A., Scavelli, C., Nico, B., Gernone, A., Battelli, F., Tabilio, A., Guidolin, Diego., Petrucci, M. T., Ribatti, D. and Dammacco, F. (2003) Endothelial cells in the bone marrow of patients with multiple myeloma. *Blood.* **102**(9), 3340-3348.

Vacca, A., Ribatti, D., Presta, M., Minischetti, M., Iurlaro, M., Ria, R., Albini, A., Bussolino, F. and Dammacco, F. (1999) Bone marrow neovascularization, plasma cell angiogenic potential, and matrix metalloproteinase-2 secretion parallel progression of human multiple myeloma. *Blood.* **93**, 3064-73.

Van Valckenborgh, E., Asosingh, K., Riet, I. V., Camp. B. V. and Vanderkerken, K. (2004) Matrix metalloproteinases in multiple myeloma. *Cancer Therapy.* **2**, 29-38.

Van Valckenborgh, E., Mincher, D., Salvo, A. D., Riet, I. V., Young, L., Camp, B. V. and Vanderkerken, K. (2005) Targeting an MMP-9-activated prodrug to multiple myeloma-diseased bone marrow: a proof of principle in the 5T33MM mouse model. *Leukemia*. **19**, 1628-1633.

Van Wart, H. E. and Birkedal-Hansen, H. (1990) The cysteine switch: a principle of regulation of metalloproteinase activity with potential applicability to the entire matrix metalloproteinase gene family. *Proc. Natl. Acad. Sci. USA*. **87**, 5578-82.

Vargová, V., Pytliak, M. and Mechírová, V. (2012) Matrix metalloproteinases. *EXS*. **103**, 1-33.

Venturoli, D. and Rippe, B. (2005) Ficoll and dextran vs. globular proteins as probes for testing glomerular permselectivity: effects of molecular size, shape, charge, and deformability. *Am. J. Physiol*. **288**, F605-613.

Verma, R. P. and Hansch, C. (2007) Matrix metalloproteinases (MMPs): Chemical-biological functions and (Q)SARs. *Bioorg. Med. Chem.* **15**, 2223-2268.

Vihinen, P. and Kähäri, V. M. (2002) Matrix metalloproteinases in cancer: prognostic markers and therapeutic targets. *Int. J. Cancer.* **99**(2), 157-66.

Windridge, G. C. and Jorgensen, E. C. (1971) 1-Hydroxybenzotriazole as a Racemization-Suppressing reagent for the Incorporation of *im*-Benzyl-L-histidine into Peptides. *J. Am. Chem. Soc*. **17**, 6318-6319

Woessner, J. F. JR. (1991) Matrix metalloproteinases and their inhibitors in connective tissue remodeling. *FASEB J*. **5**, 2145-2154.

Young, L. (2006) Novel anticancer agents and oligopeptide drug conjugates: Biochemistry of topoisomerase inhibition and MMP-activation. PhD, Edinburgh Napier University.

Yu, W. H. and Woessner, J. F., Jr. (2000) Heparan sulfate proteoglycans as extracellular docking molecules for matrilysin (Matrix Metalloproteinase 7). *J. Biol. Chem*. **275**, 4183-4191.

Yuan, F., Dellian, M., Fukumura, D., Leunig, M., Berk, D. A., Torchilin, V. P. and Jain, R. K. (1995) Vascular permeability in a human tumour xenograft: molecular size dependence and cutoff size. *Cancer Research*. **55**, 3752-3756.

Zetter, B. R. (1998) Angiogenesis and tumor metastasis. *Annu. Rev. Med*. **49**, 407-424.

Zucker, S., Cao. J. and Molloy. C. J. (2002) Role of matrix metalloproteinases and plasminogen activators in cancer invasion and metastasis: therapeutic strategies. **In**: Baguley, B. C and Kerr, D. J. (eds). (2002) *Anticancer Drug Development*. Orlando: Harcourt Inc., 91-122.

Zucker, S., Hymowitz, M., Conner, C., Zarrabi, H. M., Hurewtz, A. N., Matristian, L., Boyd, D., Nicholson, G. and Montana, S. (1999) Measurement of matrix metalloproteinases (MMPs) and tissue inhibitors of metalloproteinases (TIMPs) in blood and tissues. *Ann. N.Y. Acad. Sci*. **878**, 212-227.

Contents

Chapter II. Legumain-Targeted Prodrug and Molecular Probe Design

2.1 INTRODUCTION

2.1.1 Legumain

Legumain, also called asparaginyl endopeptidase (AEP), was named by Kembhavi *et al*., who isolated and characterised this endopeptidase from moth bean (*Vigna aconitifolia*) (Kembhavi *et al*., 1993). Legumain is well conserved in plants, parasites and mammals. In plants, legumain is known as vacuolar processing enzyme (VPE) which is associated with maturation/activation of different vacuolar proteins (Shimada *et al.*, 2003). Acidic conditions are required to activate legumain and studies have shown that legumain, the only known AEP, has a restricted specificity cleavage site at the carboxyl end of asparagine, which is absolutely required at the P1 position of a substrate sequence (Kembhavi *et al*., 1993; Chen *et al*., 2000; Clerin *et al*., 2008). Mammalian legumain, which has been discovered and studied in the past two decades, is a lysosomal protease that belongs to the C13 family of cysteine endopeptidases (Chen *et al*., 1997; Chen *et al*., 2000). The first mammalian legumain was purified from pig kidney by Chen *et al.* (1997) and it has been proved that it exists in various mammalian tissues, for example, kidney, spleen, liver, placenta and testis. Among these organs, kidney and placenta have higher specific activity of legumain. Mammalian legumain has also been shown to require acidic conditions (pH 3-6) for activation, and it specifically hydrolyses asparaginyl bonds. The enzymic activity of mammalian legumain can be inhibited by both human cystatin C and

chicken egg-white cystatin (Chen *et al.,* 1998). In normal tissues, legumain can be found intracellularly in endosome and lysosome systems and is associated with intracellular protein degradation. In kidney, legumain is mainly expressed in proximal tubules and it acts as an intracellular lysosomal protein (Yamane *et al.*, 2002; Wu *et al.,* 2006; Liu, 2008).

2.1.2 Prolegumain activation

N-terminal propeptide (Val^{18}-Asp^{25})

C-terminal prodomain (Asp^{324}-Tyr^{433})

N-terminal

C-terminal

Signal peptide (Met^1-Ala^{17})

Legumain domain (Gly^{26}-Asn^{323})
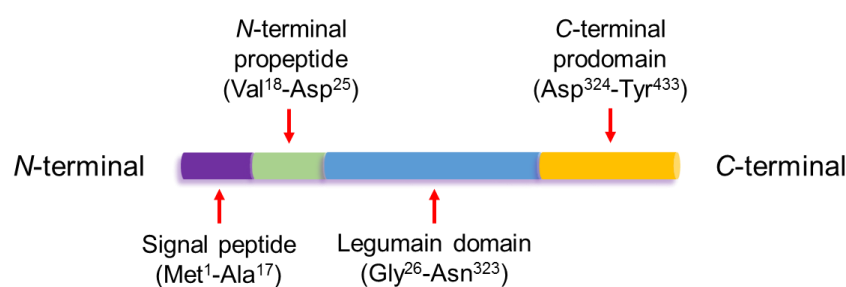
Figure 2.1. The structure of prolegumain domains

Prolegumain [**Figure 2.1**] consists of a signal peptide (Met^1-Ala^{17}) which can be cleaved during secretion, an *N*-terminal propeptide (Val^{18}-Asp^{25}), the legumain domain (Gly^{26}-Asn^{323}) and a *C*-terminal prodomain (Asp^{324}-Tyr^{433}) (Chen *et al.*, 1997). Chen and colleagues pointed out that after C13 cells were extracted with pH 7.2 lysis buffer, legumain maintains as an inactive pro-form which has a mass of 56 kDa in the lysate. If the lysate was incubated at 30°C for 3 hours at pH 5.8, the pro-form of legumain would be converted into the 47 kDa intermediate form which is also inactive, whereas if the lysate was incubated at pH 4.5 for 4 hours, both inactive forms of legumain 56 kDa and 47 kDa can be converted into the 46 kDa active form of legumain which reveals an increased enzyme activity by 15-fold. The authors also claimed that because the *N*-terminal peptide showed the same sequence in all 56, 47 and 46 kDa legumain forms,

126

activation of prolegumain was required by single cleavage after Asn^{323} from the *C*-terminal of inactive forms of legumain (Chen *et al.,* 2000). However, 3 years later, Li and colleagues pointed out that there is an 8 residue difference at the *N*-terminal between the 47 and 46 kDa forms. Also, the subsequent cleavage after Asp^{25} from the *N*-terminal peptide can only happen when the pH is lower than 5.0 and it is the key activating cleavage to convert the 47 kDa intermediate form into the 46 kDa active form (Li *et al.,* 2003). However, Dall and Brandstetter proved that the *N*-terminal propeptide Val^{18}-Asp^{25} does not inhibit enzymatic activity and upon lowering the pH from 5.0 to 4.5, the Gly^{26}-Asn^{323} form (widely accepted as the active form of legumain) only reached 50% of the highest activity for legumain that was incubated at pH 4.0 at 37°C (Dall and Brandstetter, 2012). Further autocleavage of the 46 kDa active form by other lysosomal peptidases at pH 4.5 would generate a mature active form of 36 kDa legumain, which shows similar activity to the 46 kDa form. Even though legumain is insensitive to the cysteine protease inhibitor E-64, this conversion of 46 kDa protease to the 36 kDa form can be inhibited by E-64 and leupeptin (Chen *et al.,* 2000). Dall and Brandstetter also confirmed that at 37°C, at pH 4.0 a further autocatalytic cleavage happened at the sites of Asp^{303} or Asp^{309} from the *C*-terminus which would release the maximal activity of legumain both *in vitro* and *in vivo* (Dall and Brandstetter, 2012).

2.1.3   Dependence of legumain activity upon temperature and substrates

It has been shown that by using the same buffer system, at 25°C, pig legumain maximal activity was found at pH 6.4; and at 30°C, the maximal activity was occurred at pH 5.8 and no enzymatic activity survived at pH 6.0 during two hours incubation. Hence, it suggested that at higher pH values of 6.0 or above, legumain activity was strongly

dependent on temperature (Chen *et al.*, 1997). Dall and Brandstetter also showed that at 37ºC, at pH 5.5, legumain activity favours substrates with Asn at the P1 position and at pH 4.0, it favours substrates with Asp (aspartic acid) at the P1 position (although this is unlikely to be a therapeutically relevant pH). Thus, legumain activity is substrate-dependent as well (Dall and Brandstetter, 2012).

2.1.4 <u>Legumain expression and tumours</u>

It has been shown that legumain can encourage cell migration, and overexpressed legumain is associated with enhanced tissue invasion and metastasis. Recent studies have found that legumain is highly expressed on the surface of tumour associated macrophages (TAMs) and tumour angiogenic endothelial cells, where it is co-localised with integrins (Murthy *et al.,* 2005). The presence of legumain can be found in the majority of tumours, notably breast, ovarian, colon and prostate tumours; and also in a few central nervous system neoplasms (Liu *et al.,* 2003; Liu, 2008). Nevertheless, legumain expression is very limited in normal tissues from which tumours are generated due to legumain's requirement for acidic conditions to be functionally active, which can be provided in the tumour microenvironment. Hence, if any legumain escaped from the tumour microenvironment, it would stay inactive as it would be quickly inactivated by neutral (or slightly alkaline) pH conditions in plasma and normal tissues (Liu, 2008).

Liu proved that $\alpha_v\beta_3$ integrin [(a vitronectin receptor that can interact with vitronectin, fibronectin and MMP2, therefore, it associates with cell migration, tumour invasion and angiogenesis (Felding-Habermann and Cheresh, 1993; Hermann *et al.,* 1999)] not only helps legumain to locate onto invasive cell surfaces, but also it is a very important co-

factor for legumain that would regulate legumain enzymatic activity and its dependence on acidic conditions. The higher concentration of $\alpha_v\beta_3$ integrin protein, the more enzymatic activity of legumain had been noted. Legumain amidolytic activity can be increased up to almost 100-fold when legumain binds with $\alpha_v\beta_3$ integrin. Also, the complex of legumain: $\alpha_v\beta_3$ integrin can still be active at around pH 7; a condition, in which legumain would be inactivated. The expressions of legumain and $\alpha_v\beta_3$ integrin were both very limited under normal conditions in cell culture, however, when they were under hypoxia, dramatically increased levels of legumain and $\alpha_v\beta_3$ integrin had been observed on the cell surface. Complexes of legumain and a few integrin subtypes, for instance β_1, $\alpha_v\beta_3$ and $\alpha_5\beta_1$, were highly expressed in human breast and pancreatic tumours, also the complex of legumain and integrin is very important in invasive tumour growth and is crucial for angiogenesis (Liu, 2008). Wu *et al.,* proved that legumain can be found extracellularly in the tumour microenvironment as well and it has connections with both extracellular matrix and cell surfaces (Wu *et al.,* 2006). This finding is particularly relevant to this research project.

Very recently, Wang *et al.,* had confirmed that in ovarian cancer, the legumain level was found five-fold higher when compared with those in normal ovarian tissues. The authors also pointed out that cancer cell proliferation and apoptosis cannot be affected by overexpressed legumain in ovarian tumours, however, *in vitro* it had been noticed that cancer cell migratory and invasive activities had been enhanced. Hence they suggested this could be due to the regulation of extracellular matrix remodelling by legumain (Wang *et al.*, 2012).

2.1.5   Activation of pro-MMP2 by legumain

Cells that can overexpress legumain show increased invasive and migratory abilities (Liu *et al.*, 2003). These abilities may be due to the activation of MMP2, which plays an important role in extracellular matrix degradation, and also the activation of MMP2 requires cleavage of an asparaginyl bond in the inactive proform of MMP2, which is a universal cleavage 'hot spot' for legumain. Both Chen and Liu had proved that legumain is capable of converting MMP2 72 kDa inactive form into its 62 kDa active form. When the concentration of legumain was doubled during incubation, more 62 kDa active form was formed. No enhanced MMP2 activity was shown when legumain was absent. This activation can be inhibited by cystatin, a legumain inhibitor, but unaffected by E-64 (a broad-spectrum cysteine peptidase(s) inhibitor, which has no inhibitory action on legumain) (Chen *et al.,* 1997) or 1,10-phenanthroline (an inhibitor of metallopeptidases) or phenylmethanesulphonyl fluoride (PMSF, a serine protease inhibitor). These observations provided good evidence that the activation of pro-MMP2 was carried out by legumain. However, on the other hand and interestingly, very little or no pro-MMP9 was converted to its active form during incubation with legumain in despite of being a very functionally similar (to MMP2) gelatinase overexpressed in tumours (Chen *et al.*, 2001; Liu *et al.*, 2003).

2.1.6   Legumain-activated prodrugs

LEG-3 (*N*-succinyl-β-alanyl-L-alanyl-L-asparaginyl-L-leucyl-doxorubicin) **(1)** [**Figure 2.2**], a cell-impermeable doxorubicin prodrug was designed to be activated by legumain exclusively in the low pH of the tumour microenvironment (Wu *et al*., 2006).
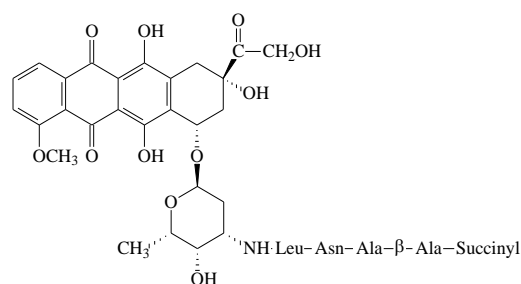
Figure 2.2. LEG-3 (1)

LEG-3 (**1**) was almost noncytotoxic to control cells that do not express legumain, but it showed very high cytotoxicity to cells that were transfected with legumain cDNA and hence can express legumain on the cell surface. When added into cell cultures, LEG-3 (**1**) did not enter cells and showed a lack of cytotoxicity, whereas doxorubicin (the active drug) entered cells very quickly. However, when added into legumain expressing cells in culture, LEG-3 (**1**) was degraded to doxorubicin which can be found in cells. This indicated that LEG-3 (**1**) was activated extracellularly. Prodrug LEG-3 (**1**) activation can be inhibited by the legumain inhibitor cystatin. In cytotoxicity study, when legumain-expressing cells were treated with LEG-3 (**1**) and cystatin together, a significant cell survival rate was observed. *In vivo* toxicity studies showed LEG-3 (**1**) had a significantly higher maximum tolerable dose (MTD) and greater LD_{50} than doxorubicin. When HT1080 fibrosarcoma, a fast-growing tumour and a common sensitive model used in doxorubicin therapy, was treated with LEG-3 (**1**), the prodrug showed significant tumouricidal activity. However, when MDA-PCa-2b prostate carcinoma, a doxorubicin resistant tumour, was treated with LEG-3 (**1**), the prodrug still showed positive results and efficiently prolonged the life span of MDA-PCa-2b tumour bearing mice (Wu *et al.*, 2006). However, most succinates can breakdown on average with half-lives of around 2h.

131

The better aspect about succinates is that because they will be negatively charged carboxylates at pH 7.2, they should not penetrate cells. If succinates are designed to be activated extracellularly, then this designing strategy could be an advantage. Nevertheless, succinates are not good capping groups because they introduce an unhindered (non-bulky) group at the *N*-terminus that still has a very accessible amide bond – which may be susceptible to cleavage by other endoproteases (capping with a fluorophore like fluorescein is unlikely to suffer this fate due to its bulk). Trouet *et al.*, reported that after incubating in blood for just one hour, 99% of 'uncapped' substrate *N*-L-alanyl-L-leucyl-L-alanyl-L-leucyl-doxorubicin would be degraded by blood peptidases, however, *N*-β-alanyl-L-leucyl-L-alanyl-L-leucyl-doxorubicin is relatively insensitive to blood peptidases (Trouet *et al.*, 2001). This may be because β-alanine is not an alpha amino acid; hence, it should be less recognisable to proteases. This is the same idea as introducing a D-amino acid for the same reason that it works to some extent, but tends to slow rather than abolish degradation. It is true that the succinate prodrug LEG-3 **(1)**, like all carboxylates will be negatively charged at physical pH and therefore not get into cells (ensuring extracellular activation), but the downside is that LEG-3 **(1)** can be degraded in blood easily in a very short time before it can reach its target site. In other words, the suspicion is that much of the antitumour activity may well have been due to premature release of doxorubicin via decomposition.

Stern and co-workers synthesised a novel legumain cleavable prodrug carbobenzyloxy-Ala-Ala-Asn-ethylenediamine-etoposide **(2)** [**Figure 2.3**].
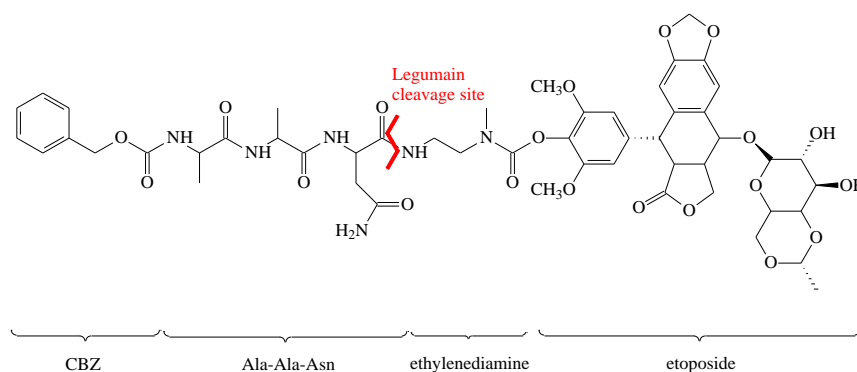
Figure 2.3. Chemical structure of carbobenzyloxy-Ala-Ala-Asn-ethylenediamine-etoposide (2)

The authors claimed that after being cleaved by legumain, this etoposide prodrug (**2**) would release active agent. However, from the HPLC analysis data it showed that after incubating with rh-legumain for 24h, this etoposide prodrug (**2**) did not release the active agent etoposide, instead it was (an inactive) ethylenediamine-etoposide conjugate. Ethylenediamine, an amide-linked spacer in this prodrug, cannot be liberated from active agent etoposide. This explains why they could not find the expected IC_{50} value when this prodrug was incubated with 293 HEK-Leg cells (human embryonic kidney cells stably transfected to overexpress legumain), even though this prodrug can be 100% cleaved with 3h incubation (Stern *et al.,* 2009).

In the examples above, an unstable *N*-terminus capping group [LEG-3 (**1**)] and inability to release active agent from spacer after cleavage by legumain [etoposide prodrug (**2**)] highlight two major problems in legumain anti-cancer prodrug(s) development. In order to design a better legumain prodrug, the novel prodrug has to be stable in blood while being delivered to its target site and has to be able to release active agent after cleavage by legumain. Hence, in this research project, a capping group was applied to ensure the

stability of the prodrug (by conferring resistance to *N*-terminal degradation by aminopeptidases) and no spacer was applied between peptide and active agent to overcome those problems that have been found in previous studies.

2.1.7 <u>Weakness of current biomarkers for ovarian and breast cancer</u>

Antigen CA125, a widely studied serum biomarker for ovarian cancer, has been shown to have poor sensitivity and specificity for early stage detection (Sengoku *et al.,* 1994; van Haaften-Day *et al.,* 2001) and may lead to misdiagnosis. Anderson and co-workers pointed out that the concentrations of CA125, human epididymis protein 4 (HE4) and mesothelin (three potential ovarian cancer biomarkers) started to rise 3 years before patients were diagnosed, however, the concentrations for all three biomarkers cannot be detected until the final year before most patients were diagnosed with advanced-stage cancer (Anderson *et al.,* 2010). Among the first identified tumour antigens, carcinoembryonic antigen (CEA) has been shown to be of limited clinical value for breast cancer detection due to lack of diagnostic sensitivity and specificity (Cheung *et al.,* 2000; Wang *et al*., 2012). However, due to being overexpressed by the majority of tumour cells and its specific cleavage site at the carboxyl end of asparagine, legumain can be a promising biomarker for detection with novel fluorogenic probes (in addition to being a target of anti-cancer prodrug therapy).

2.2 <u>AIM</u>

The principal aim of this project is to design sensitive chemical probes and fluorimetric procedures for use in the diagnosis and prognosis of breast (and other forms of) cancer by exploiting the proteolytic action of legumain. The novel probes are fluorogenic – i.e. latently fluorescent until activated by the cancer biomarker. The extent of fluorescence release should correlate with patient biomarker levels and an aggressive cancer phenotype.
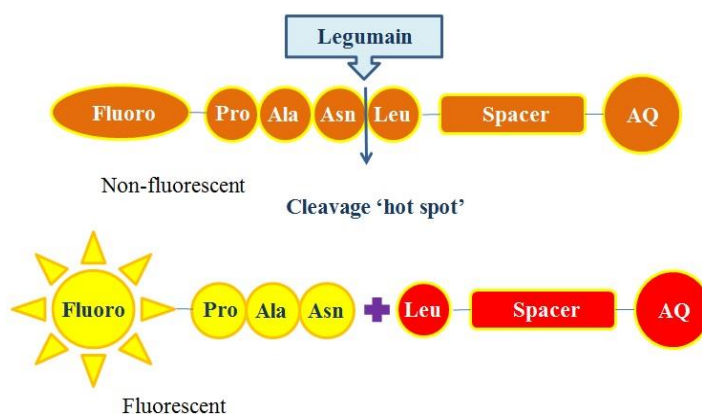
Figure 2.4. Biomarker probe design for TL11 (3)

In **Figure 2.4** is shown a tetrapeptide substrate sequence designed for cleavage by legumain, the figure shows that fluorescence of the fluoro group, a fluorescein-based moiety silenced by 'dark quencher' anthraquinone AQ, will be released once the fluorogenic probe is cleaved by legumain strictly on the *C*-terminal side of asparagine. The concept exploits the principle of FRET (fluorescence resonance energy transfer) and which in this project takes advantage of exceptionally good overlap between the absorption spectrum of the aminoanthraquinone quencher (acceptor) and the emission spectrum of the fluorescein-based fluorophore (donor) [**Figure 2.5**].

135
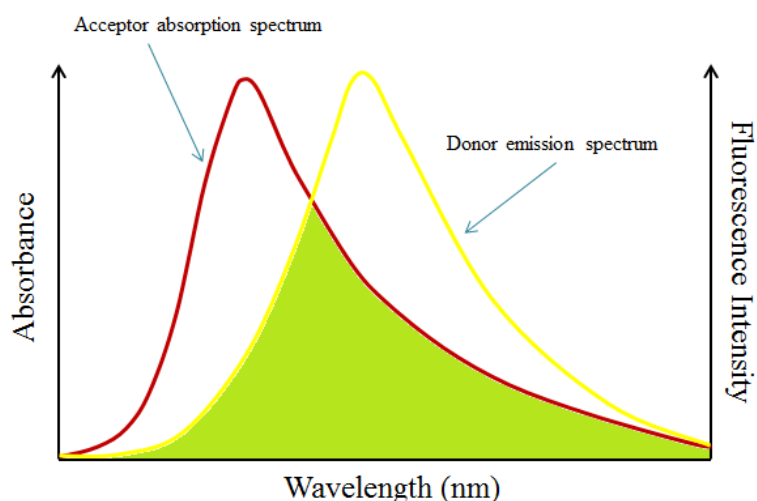
Figure 2.5. <u>F</u>luorescence <u>R</u>esonance <u>E</u>nergy <u>T</u>ransfer

FRET involves a process of transferring energy from one chromophore to the other by intermolecular non-radiative dipole-dipole interaction and it is very sensitive to the centre-to-centre separation distance which is from 10Å to 100Å (Clegg, 1995).
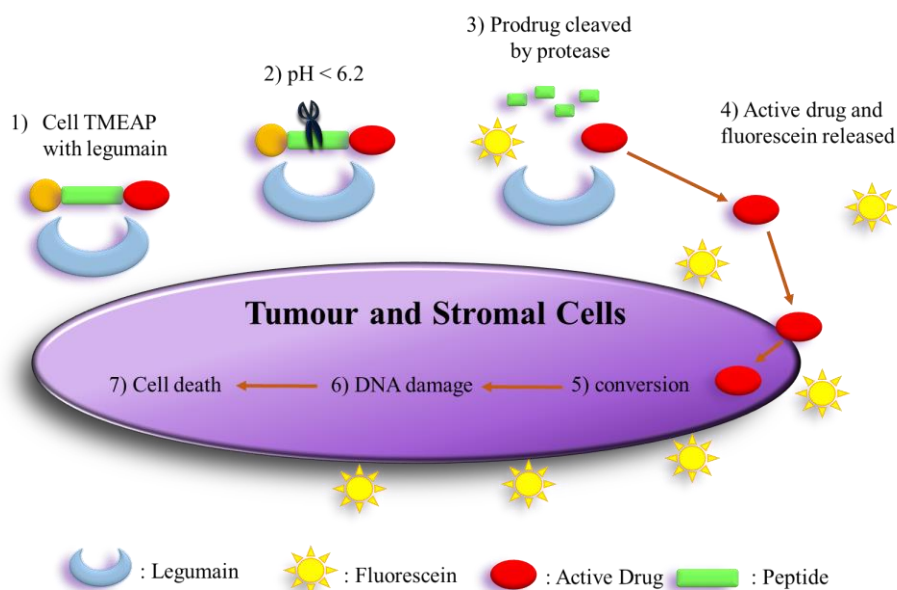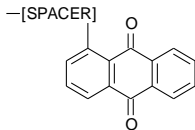
Figure 2.6. Mechanism of Cell-Impermeable Tumour Microenvironment Activated Prodrug (TMEAP) activation in the tumour microenvironment (Adapted from Liu, 2008).

Figure 2.6 shows the concept of the intended activation mechanism (cell-impermeable tumour microenvironment activated prodrug or TMEAP) in the protease-rich tumour microenvironment. Prodrugs or probes made in this project are designed to target

136

legumain which can be found on the surface of tumour cells and tumour associated macrophages, in addition to the lysosomes. In the tumour microenvironment, the conditions are both acidic and hypoxic, under which legumain can be activated in order to cleave peptides at the carboxyl end of asparagine. With the follow-on help of aminopeptidase and carboxypeptidase actions which can further hydrolyse the peptide bond of an amino acid residue at the amino-terminal end and carboxy-terminal end respectively. A fluorescein residue and active drug would then be released. A fluorescein label would be helpful to indicate the presence of overexpressed protease biomarkers of tumours cells in tumour diagnosis. On the other hand, release of active drug would afford entry into tumour cells, for example, if it were a DNA-targeting agent, cause DNA damage and eventually kill tumour cells or it would enter tumour associated macrophages and finally cause cell death. Given that growth factors, such as VEGF, which are secreted by tumour associated macrophages (TAMs), reduced TAMs would lead to a dramatically decreased number of tumour growth factors which support tumour cell immortalisation (Liu, 2008).

2.3 <u>RESULTS AND DISCUSSION</u>

This section describes the design, synthesis and preliminary biological evaluation of a series of novel peptide fluorogenic substrates of legumain. An overview of the library of compounds is shown in **Table 2.1**. The fluorophore in these compounds was variously fluorescein isothiocyanate isomer I (FITC) **(4)** or 5(6)-carboxyfluorescein (FAM) **(5)** [**Figure 2.7**] and the acceptor molecule was an aminoanthraquinone derivative with a spacer group consisting of a short hydrophobic chain or a more hydrophilic PEG-like structure.

CODE	Fluorophore	P_3	P_2	P_1	P_1'	P_2'	SPACER	TEMPLATE
FF **(6)**	FITC	**ala**	**ala**	**asn**	**leu**		-HN-(CH$_2$)$_3$-NH-	
MK8 **(7)**	FITC	**ala**	**ala**	**asn**	**ala**		-HN-(CH$_2$)$_3$-NH-	
TL11 **(3)**	FAM	**pro**	**ala**	**asn**	**leu**		-HN-(CH$_2$)$_2$-O-(CH$_2$)$_2$-O-(CH$_2$)$_2$-NH-	
AD17 **(8)**	FAM	**pro**	**gly**	**asn**	**leu**		-HN-(CH$_2$)$_2$-O-(CH$_2$)$_2$-O-(CH$_2$)$_2$-NH-	
AD20 **(9)**	FAM	**pro**	**ser**	**asn**	**leu**		-HN-(CH$_2$)$_2$-O-(CH$_2$)$_2$-O-(CH$_2$)$_2$-NH-	
VG **(10)**	FAM	**pro**	**thr**	**asn**	**leu**		-HN-(CH$_2$)$_2$-O-(CH$_2$)$_2$-O-(CH$_2$)$_2$-NH-	
PN11 **(11)**	FAM		**ala**	**asn**	**leu**	**ala**	-HN-(CH$_2$)$_2$-O-(CH$_2$)$_2$-O-(CH$_2$)$_2$-NH-	

Table 2.1. Library of legumain substrates.

FITC **(4)**   5(6)-Carboxyfluorescein **(5)**
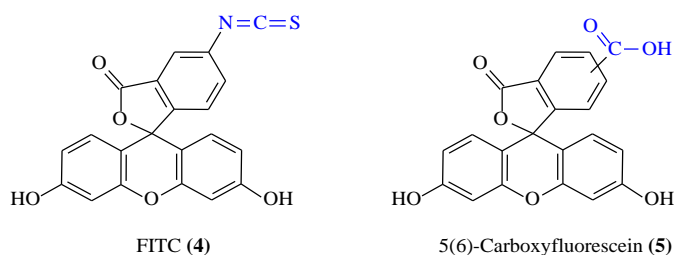
Figure 2.7. Chemical structures of FITC (4) and 5(6)-carboxyfluorescein (5)

The reasons why 5(6)-FAM **(5)** and PEG-spacer were chosen for later legumain probe design and syntheses are:

1) By using both 5(6)-FAM **(5)** and PEG-spacer can improve probes solubility during synthesis when compared with FITC labelled probes FF and MK8;

138

2) Unlike the thiocyanate group in FITC **(4)**, 5(6)-FAM **(5)** has a carboxylic acid group which can easily form an amide bond with the other amine, hence, this makes 5(6)-FAM **(5)** more biocompatible than FITC **(4)**;

3) 5(6)-FAM **(5)** can be used not only in solution phase peptide synthesis, but in solid phase peptide synthesis as well. However, FITC **(4)** is restricted for being used for solid phase peptide synthesis; because the FITC labelled peptides can undergo a cyclisation during cleavage stage [**Figure 2.8**] (Edman, 1956; Jullian *et al.*, 2009).
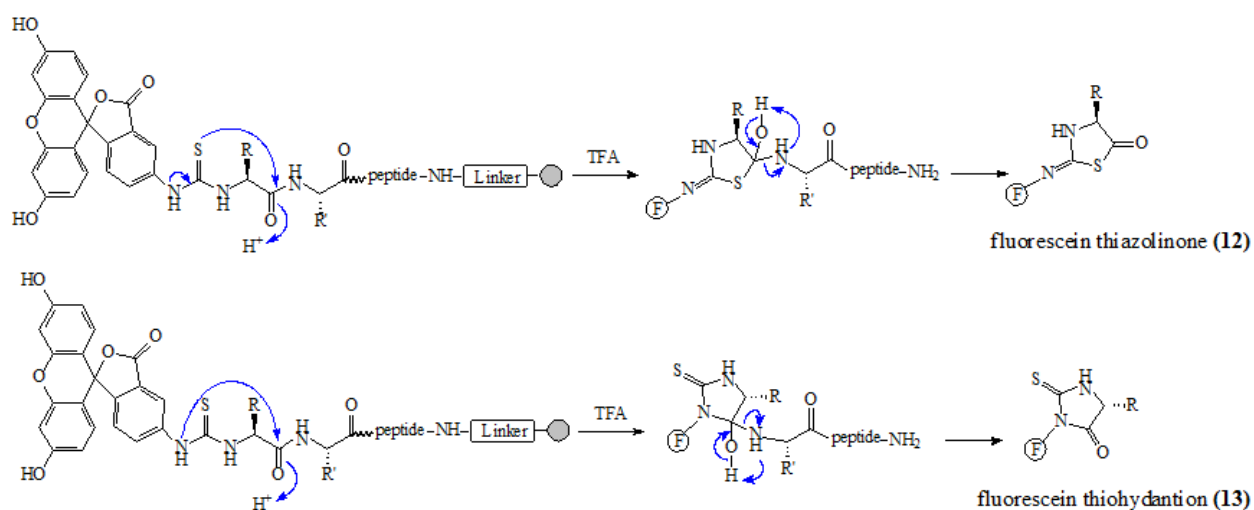
Figure 2.8. FITC (4) cyclisation during SPPS cleavage stage to form fluorescein thiazolinone (12) and fluorescein thiohydantion (13).

2.3.1 Design of legumain fluorogenic probe TL11 (3)

There is a lack of sensitive methods for legumain detection in biological matrices, and in order to meet this need, a novel FRET (Fluorescence Resonance Energy Transfer) technology was designed in this project. The chemical synthesis of a novel legumain substrate fluorogenic probe (TL11) **(3)** was performed by using solution phase peptide

chemistry and fluorophore/quencher conjugation. 5(6)-Carboxyfluorescein **(5)** was used

to label the *N*-terminus of a tetrapeptide legumain substrate: Pro-Ala-Asn-Leu, and the

C-terminus was occupied by an aminoanthraquinone 'dark' or 'black hole' quencher

group. Spectrofluorimetry was used to demonstrate quenching of the fluorogenic probe

and to determine fluorescence release upon incubation with human recombinant legumain.
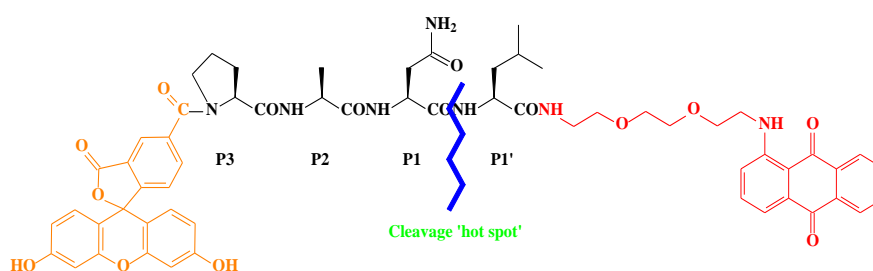
Figure 2.9. Structure of TL11 (3) and its cleavage 'hot spot'

The fluorogenic probe TL11 **(3)** [**Figure 2.9**] contains 5(6)-carboxyfluorescein **(5)**

(replacing an *N*-FITC group **(4)** in a prototype) at the *N*-terminus of the tetrapeptide and

a dark ('black-hole') anthraquinone-spacer quencher group at the carboxyl terminus. The

critical asparagine residue was put into the P1 position, and a P3 proline was introduced

to make an effective fit into the active site of legumain; this decision was based on an

observation of a note in the literature which indicated proline was favourable in the P3

position of an activity-based probe (Sexton *et al.*, 2007). The latter class of probe is not

fluorogenic, but carries a label and is designed to bind to and inhibit the enzyme.

Nevertheless, given that it is important for both inhibitors and substrates to make a good

fit into the active site of the enzyme, it was decided to introduce this feature (P3 Pro) into

the substrate TL11 **(3)**. The tetrapeptide was designed with the sequence: Pro-Ala-Asn↓-

Leu that contains a cleavage 'hot spot' at the carboxyl end of asparagine (indicated by the

arrow).

The complete synthesis of TL11 (**3**) is shown in the abbreviated form in **Scheme 2.1**
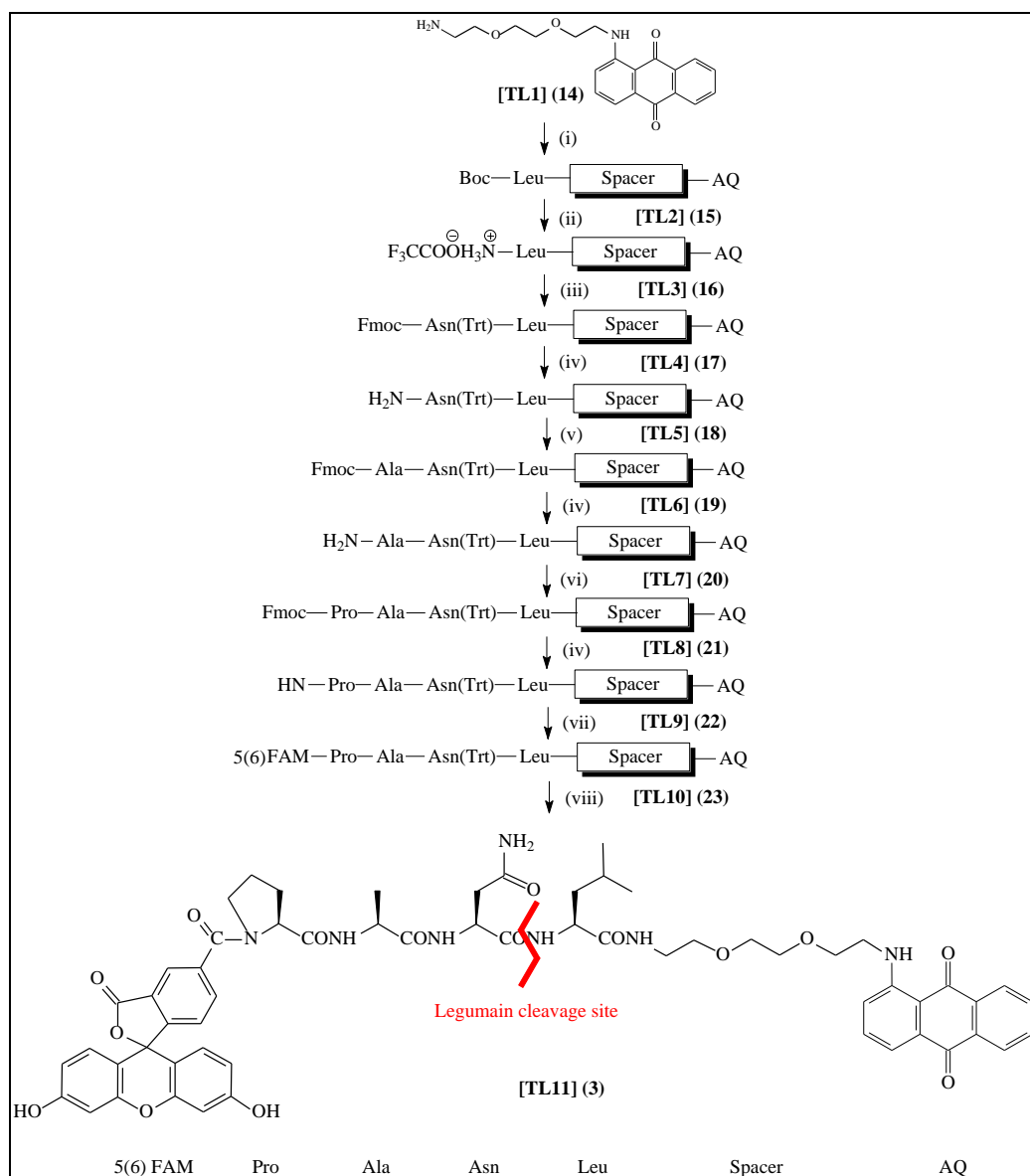
Reagents and conditions: (i) Boc-Leu-OSu, DIPEA, DMF, RT, 2.5h. (ii) TFA, RT, 30min. (iii) Fmoc-Asn(Trt)-OH, TBTU, HOBt, DIPEA, DMF, RT, 3h. (iv) 20% piperidine in DMF, RT, 30min. (v) Fmoc-Ala-OH, TBTU, HOBt, DIPEA, DMF, RT, 3h. (vi) Fmoc-Pro-OH, TBTU, HOBt, DIPEA, DMF, RT, 3h. (vii) 5(6)-FAM, TBTU, HOBt, DIPEA, DMF, 24h. (viii) TFA, RT, 4h.

Scheme 2.1. Synthesis of legumain fluorogenic probe TL11 (3)

The following sub-sections describe in detail some of the key steps leading to probe TL11 (**3**).

2.3.1.1 Synthesis of [PEG Spacer]-AQ [TL1] (14)
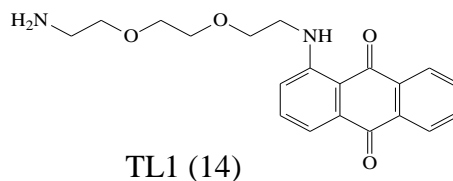
Figure 2.10. Chemical structure of [PEG Spacer]-AQ TL1 (14)

This [PEG Spacer]-anthraquinone compound, TL1 **(14)** [**Figure 2.10**], was synthesised by mixing 1-chloroanthraquinone with 2-[2-(2-aminoethoxy)ethoxy]ethan-1-amine in DMSO, and then the reaction mixture was heated over a water bath for 4 hours. It had been noticed that within 5 minutes, the yellow compound 1-chloroanthraquinone was changed to a typical dark red colour. The process of this reaction was monitored by TLC, and once it was finished, the whole reaction mixture was poured into water slowly in order to let the [PEG Spacer]-anthraquinone compound TL1 **(14)** precipitate from solution. Usually, the spacer compound was used without further purification or could be purified easily by column chromatography in a mixture of chloroform and methanol. The TL1 TFA salt ^{1}H NMR spectrum showed a 2-proton multiplet signal at 3.00ppm and a 2-proton multiplet signal at 3.20ppm which were assigned to C$\underline{H}_2$NH$_2$ and OC$\underline{H}_2$CH$_2$NH$_2$ respectively. Signals for the 4-proton multiplet found between 3.60 and 3.70ppm were assigned to OC$\underline{H}_2$C$\underline{H}_2$O. Signals for the methylene protons next to the anthraquinone amino group can be found between 3.70 and 3.80ppm. Two double doublet signals at 7.30 and 7.40ppm were assigned to the H-2 and H-4 protons respectively. Signals for H-5 and H-8 protons can be found between 8.10 and 8.20ppm. The anthraquinone amino group proton gave a triplet at 9.75ppm.

142

2.3.1.2   Synthesis of H-Leu-[PEG Spacer]-AQ trifluoroacetate salt [TL3] (16)
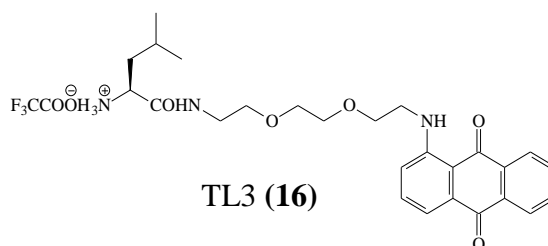
TL3 (**16**)

Figure 2.11. Chemical structure of H-Leu-[PEG Spacer]-AQ trifluoroacetate salt TL3 (16)

This H-Leu-[PEG Spacer]-anthraquinone trifluoroacetate salt, TL3 (**16**) [**Figure 2.11**], was synthesised by coupling Boc-Leu-OSu onto the free amino group of [PEG Spacer]-anthraquinone TL1 (**14**) [**Figure 2.10**] to form an *N*-*t*Boc group protected Boc-Leu-[PEG Spacer]-anthraquinone conjugate TL2 (**15**), which was purified by silica gel chromatography, and then followed by treating TL2 (**15**) with trifluoroacetic acid to remove the Boc protecting group to form the trifluoroacetate salt TL3 (**16**) [**Scheme 2.1**].

The structure of TL2 (**15**) was determined by its ^{1}H NMR spectrum which showed, for example, a 6-proton double doublet at 0.90ppm that was assigned to two methyl groups protons in leucine. Two signals for a 1-proton singlet and an 8-proton singlet at 1.45ppm confirming the prescence of the *t*Boc group (as observed for several Boc group signals in other examples of amino acid anthraquinone conjugates from this laboratory, in contrast to a 9-proton singlet). A multiplet signal at 4.15ppm was assigned to the proton at the α-carbon. The doublet signal of the amide proton next to the α-carbon was found at 5.0ppm. A triplet signal at 9.90ppm was given to anthraquinone amino proton, together with full assignment of all other proton signals.

The structure of TL3 (**16**) was confirmed by its ^{1}H NMR spectrum which showed, for example, a triplet signal of 6 protons at 0.85ppm was assigned to the methyl protons at the two δ carbons in the leucine side-chain. A multiplet signal for the 3-proton at the β and γ carbons in leucine can be found between 1.45 and 1.65ppm. The ethylene group in between two oxygens in the spacer gave a 4-proton multiplet between 3.55 and 3.65ppm. Two triplet signals at 8.55 and 9.75ppm were assigned to the amide proton and the amino proton on the anthraquinone, respectively, together with full assignment of all other proton signals (apart from the terminal amino protons in the leucine residue which were unresolved, presumably due to proton exchange).

2.3.1.3   Synthesis of H-Asn(Trt)-Leu-[PEG Spacer]-AQ [TL5] (18)
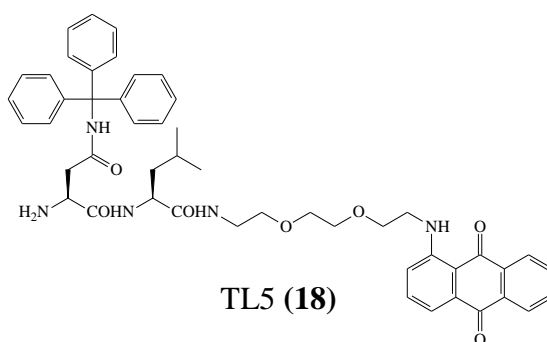
TL5 (**18**)

Figure 2.12. Chemical structure of H-Asn(Trt)-Leu-[PEG Spacer]-AQ TL5 (18)

To assemble an H-Asn(Trt)-Leu dipeptide conjugate TL5 (**18**), Fmoc-Asn(Trt)-OH was coupled onto trifluoroacetate salt TL3 (**16**) [**Figure 2.11**] by following normal amino acid coupling procedure (TBTU, HOBt, DIPEA) to give an *N*-Fmoc protected dipeptide spacer-anthraquinone compound TL4 (**17**), which was purified by silica gel chromatography. After purification, the Fmoc protecting group was removed from TL4 (**17**) to give the final product dipeptide spacer-anthraquinone TL5 (**18**), as shown in **Figure 2.12** [**Scheme 2.1**].

144

2.3.1.4 Rationale for the side-chain *N*-protection of asparagine

Free primary amide in the side chain of asparagine would undergo a side reaction during reaction [**Scheme 2.2**]. Furthermore, unprotected side chain asparagine has very poor solubility; hence, it may slow down coupling rates.
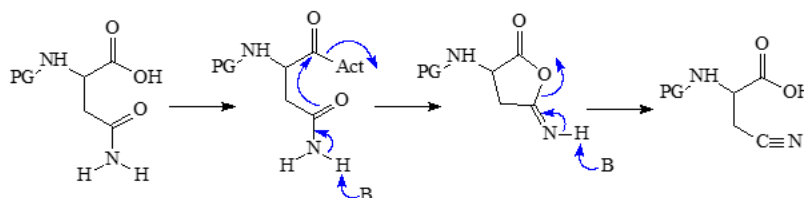
Scheme 2.2. **Dehydration of asparagine**

This dehydration of asparagines would change the primary amide structure in the side chain to a nitrile group; hence it would not be asparagine in the final peptide sequence, and would be unproductive in this project as legumain can only recognise and cleave at the carboxyl end of asparagine. So, *N*-trityl protection was applied during this coupling stage. The primary amide was protected by the trityl (Trt) group in the side chain because it was very stable during normal peptide coupling synthesis and Fmoc removal basic conditions. Trityl protecting groups can be removed by treating with 95% TFA in dichloromethane for typically 1 to 3h and the by-product triphenylmethanol can be simply filtered off from the TFA solution.

2.3.1.5 Synthesis of H-Ala-Asn(Trt)-Leu-[PEG Spacer]-AQ [TL7] (20)
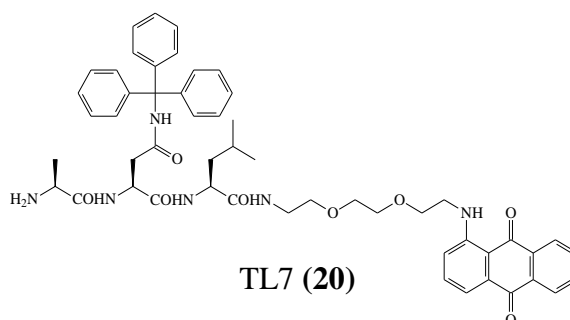
TL7 **(20)**

Figure 2.13. Chemical structure of H-Ala-Asn(Trt)-Leu-[PEG Spacer]-AQ TL7 (20)

Tripeptide spacer-anthraquinone conjugate, TL7 **(20)** [**Figure 2.13**], was synthesised by coupling Fmoc-Ala-OH onto the free amine end of dipeptide spacer-anthraquinone conjugate TL5 **(18)** [**Figure 2.12**] by following normal amino acid coupling procedures, and then the Fmoc protected compound TL6 **(19)** was purified by silica gel chromatography. After purification, the Fmoc protecting group was removed from the amine end of TL6 **(19)** to give the final product TL7 **(20)** [**Scheme 2.1**].

2.3.1.6 **Synthesis of H-Pro-Ala-Asn(Trt)-Leu-[PEG Spacer]-AQ [TL9] (22)**

Figure 2.14. Chemical structure of H-Pro-Ala-Asn(Trt)-Leu-[PEG Spacer]-AQ TL9 (22)

This H-Pro-Ala-Asn(Trt)-Leu-[PEG Spacer]-anthraquinone TL9 **(22)** [**Figure 2.14**] was synthesised by coupling tripeptide spacer-anthraquinone compound TL7 **(20)** [**Figure 2.13**] with Fmoc-Pro-OH following normal amino acid coupling procedure to form an Fmoc group protected tetrapeptide spacer-anthraquinone conjugate TL8 **(21)**, which was then treated with 20% piperidine in DMF for 30min to remove the Fmoc protecting group from the protected tetrapeptide spacer-anthraquinone conjugate. The crude product TL9 **(22)** was washed with water to remove extra piperidine and DMF mixture and then purified by loading onto a silica gel chromatography column which was eluted with dichloromethane: ethyl acetate: methanol (7:2:1) [**Scheme 2.1**].

2.3.1.7   Synthesis of 5(6)-FAM-Pro-Ala-Asn(Trt)-Leu-[PEG Spacer]-AQ [TL10] (23)

TL10 **(23)**

Figure 2.15. Chemical structure of 5(6)-FAM-Pro-Ala-Asn(Trt)-Leu-[PEG Spacer]-AQ TL10 (23)

This trityl protected 5(6)-FAM-labelled tetrapeptide spacer-anthraquinone product TL10

(23) [**Figure 2.15**] was synthesised by mixing TL9 **(22)** [**Figure 2.14**] and 5(6)-

carboxyfluorescein **(5)** together in DMF, along with coupling reagents TBTU, HOBt and

base DIPEA. This reaction was covered with foil and kept in the dark at room temperature

for 24 hours. Once the reaction was completed (confirmed by TLC), the reaction mixture

was extracted between chloroform and water, and then purified by silica gel

chromatography running with a solvent mixture of chloroform: ethyl acetate: methanol

(5:2:1) [**Scheme 2.1**].

2.3.1.8   Synthesis of 5(6)-FAM-Pro-Ala-Asn-Leu-[PEG Spacer]-AQ probe [TL11] (3)

TL11 **(3)**

Figure 2.16. Chemical structure of 5(6)-FAM-Pro-Ala-Asn-Leu-[PEG Spacer]-AQ probe TL11 (3)

In order to synthesise the final legumain fluorogenic probe TL11 **(3)** [**Figure 2.16**], the

N protecting group triphenylmethyl (trityl) has to be removed from the asparagine side

chain. So, TL10 **(23)** [**Figure 2.15**] was treated with trifluoroacetic acid for four hours.

The progress of this reaction was checked by TLC. Once the reaction was finished, the reaction mixture was evaporated to dryness and this crude product was purified by loading onto a silica gel chromatography column which was eluted with dichloromethane: ethyl acetate: methanol (5:2:1).

2.3.1.9   Mass Spectral Characterisation of TL11 (3)

The pure (chromatographically homogeneous) target FRET substrate TL11 (**3**) was analysed by nanoelectrospray ionisation in the negative mode. It was found that negative ion mode was preferred to positive ion mode for TL11 (**3**), probably due to the case with which an ion could be generated from the phenolic OH group in the fluorescein structure.
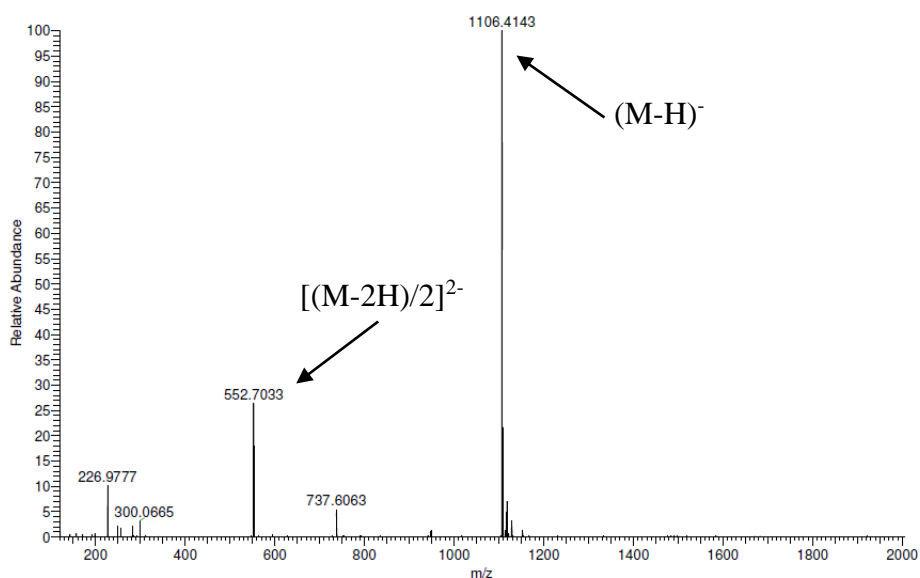
Figure 2.17. Mass Spectrum of TL11 (3)

The structure of TL11 (**3**) was confirmed by its nanoelectrospray negative ionisation mass spectrum which had a peak at m/z 1106.4143 for the species (M-H)$^-$, at m/z 552.7033 for the doubly charged ion [(M-2H)/2]$^{2-}$ and also there was good agreement between the

theoretical isotope model and the observed data which proved probe TL11 **(3)** had the correct structure [**Figure 2.17**].

2.3.2 Design of legumain fluorogenic probes AD17 (8), AD20 (9), VG (10) and PN11 (11)

Based on the success of designing and synthesising legumain probe TL11 **(3),** four further probes were designed and synthesised by altering one or two amino acids in the substrate peptide sequence, whereas the fluorophore and spacer-AQ were kept constant in all four probes' chemical structures [**Scheme 2.3**].
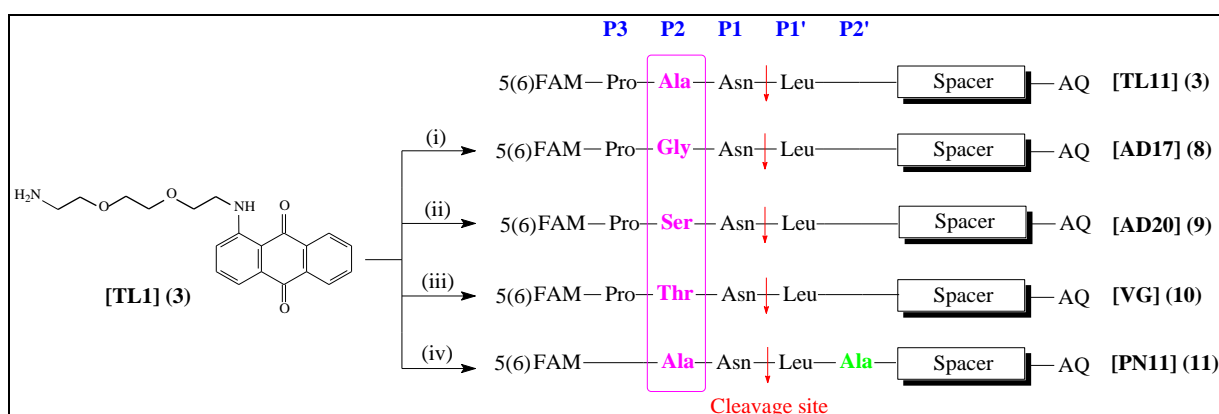
Scheme 2.3 General synthesis for legumain fluorogenic probes AD17 (8), AD20 (9), VG (10) and PN11 (11).

Notes; Reagents and conditions: Syntheses for four legumain fluorogenic probes were very similar to the synthesis of TL11 **(3)**. The only differences were:

(i)   Fmoc-Pro-Gly-OH, TBTU, DIPEA, DMF, RT, 1h. Thus substituting Gly for Ala at the P2 position of TL11 **(3)**.

(ii)   Fmoc-Ser('Bu)-OSu, DIPEA, DMF, RT, 1h. Thus substituting Ser for Ala at the P2 position of TL11 **(3)**. It should be noted that the side-chain primary OH group of serine required O-'Bu protection during peptide synthesis and protection was removed by TFA treatment in parallel with removal of the Asn trityl protecting group.

(iii)   Fmoc-Thr('Bu)-OH, HOBt, TBTU, DIPEA, DMF, RT, 1h. Thus substituting Thr for Ala at the P2 position of TL11 **(3)**. It should be noted that the side-chain secondary OH group of threonine required O-'Bu protection during peptide synthesis and protection was removed by TFA treatment in parallel with removal of the Asn trityl protecting group.

149

(iv)   Fmoc-Ala-OH, HOBt, TBTU, DIPEA, DMF, RT, 2h. Alanine substitution was used twice in the whole procedure, to introduce initially a P2 ´Ala and later a P2 Ala residue. With respect to TL11 (**3**), the sequence: Ala-Asn-Ala was preserved but proline was deleted at the *N*-terminus and Ala was added to the *C*-terminus.

2.3.2.1   <u>Rationale for selection of amino acids in positions of the legumain peptide substrate library</u>

The most conserved feature of the probe library was the leucine residue joined to the anthraquinone quencher template, connecting it to the carboxylic acid group of the Asn residue, thus at the amino end of the scissile bond marked for legumain cleavage.

In part, the choice of leucine was based upon published work on the known simple prodrug of doxorubicin, known as leucyl-doxorubicin (a leucyl conjugate of the amino group of the sugar moiety in the drug doxorubicin).

Many studies have shown that prodrug *N*-L-leucyl-doxorubicin (Leu-Dox) is relatively stable in serum (Trouet *et al.,* 1982) and only 25% of this prodrug can be converted into free doxorubicin in heart, muscle and liver tissues in mice (de Jong *et al.,* 1992). Hence, Leu-Dox shows lower cardiotoxicity when compared with free doxorubicin. Nevertheless, prodrug Leu-Dox can be selectively converted to doxorubicin in tumours; Huang and Oliff suggested that this conversion may be performed by the cathepsin family of proteases (Huang and Oliff, 2001). Based on previous studies about Leu-Dox and also for future work (intended here) to introduce Leu-Dox or Leu-Epi into legumain probes, leucine was chosen for the P1' positions in TL11 (**3**), AD17 (**8**), AD20 (**9**), VG (**10**) and PN11 (**11**) probes. Legumain can only cleave at the carboxyl end of asparagine, hence, in

all legumain probes, asparagine was chosen for the P1 position. Sexton and colleagues suggested that the P3 position is favoured by proline in legumain activity-based (i.e. inhibitor-based) probes (Sexton *et al.*, 2007), so proline was chosen at the P3 position in TL11 **(3)**, AD17 **(8)**, AD20 **(9)** and VG **(10)** probes. The only uncertain site in legumain substrate peptides is the P2 position. According to the *MEROPS* database (Rawlings, Barrett and Bateman, 2012), among currently reported legumain active probes, 10 of them had threonine at the P2 position, 6 of them had serine, 5 had alanine and 4 had glycine. Apart from threonine, the other 19 common amino acids have similar probability for being at the P2 position. Serine has a similar structure to threonine, they both have one hydroxyl group in the side chain, but one is primary hydroxyl group and the other is a secondary hydroxyl, respectively. Alanine and glycine are similar and both small amino acids when compared with others. Thus, alanine, glycine, serine and threonine were chosen for P2 position in TL11 **(3)**, AD17 **(8)**, AD20 **(9)** and VG **(10)** probes individually, based on their size and/or functional group similarities and on their frequency of representation in the sequences of published legumain substrates.

Currently, in this project most legumain active substrate probes were designed containing tetrapeptides spanning the P3 to P1' positions which is in common with some simple sequences reported in the literature, including the commercially available coumarin-labelled fluorogenic probe (Mathieu *et al.*, 2002). There is no report describing if an extra amino acid is introduced at the P2' position or if one amino acid is missing at P2, it would lead to any significant legumain cleavage activity changes when this kind of probe is

incubated with activated legumain. Hence, in PN11 **(11)**, one additional substituent residue, alanine was introduced at the P2' position and proline was removed at the P3 position when compared with the tetrapeptide starting sequence in TL11 **(3)**.
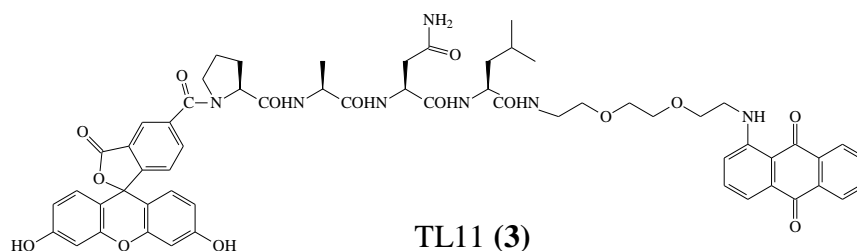
2.3.2.2 Synthesis of 5(6)-FAM-Pro-Gly-Asn-Leu-[PEG Spacer]-AQ probe [AD17] (8)
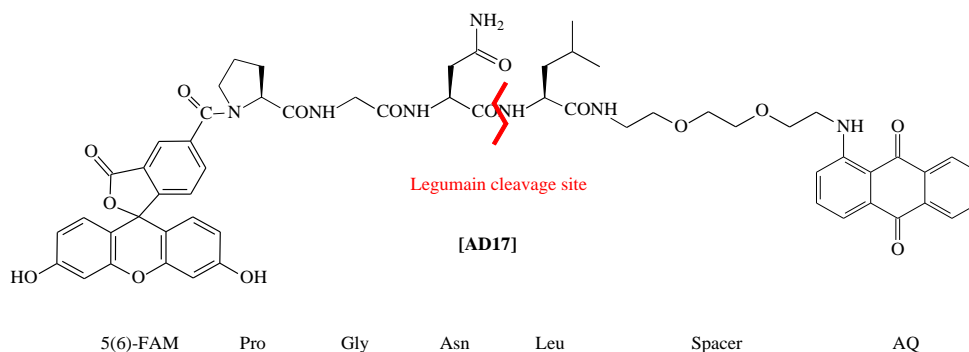
Figure 2.18. Chemical structure of 5(6)-FAM-Pro-Gly-Asn-Leu-[PEG Spacer]-AQ probe AD17 (8)

The whole synthesis procedure of legumain probe AD17 **(8)** was very similar to the synthesis of probe TL11 **(3)**. The only difference was that the dipeptide Fmoc-Pro-Gly-OH was applied during the synthesis of AD17 **(8)** to simultaneously insert the amino acids in the P3-P2 positions, but its coupling method was still the same as the one applied during the synthesis of TL11 **(3)** (reagents and conditions summarised in outline in **Scheme 2.3** above and in detail in **Scheme 2.1**, earlier).

2.3.2.2.1 Mass Spectral Characterisation of AD17 (8)

AD17 **(8)** was characterised by using nanoelectrospray ionisation in the positive mode.
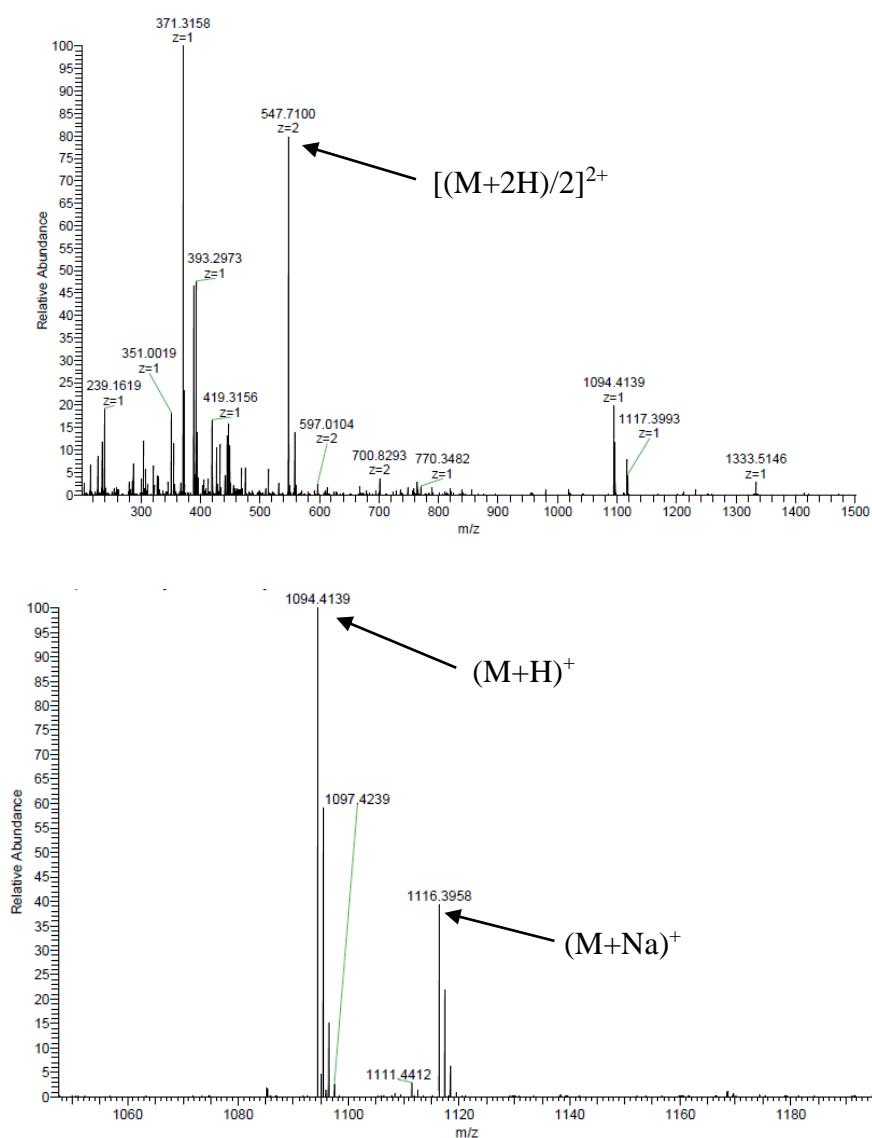
Figure 2.19. Mass Spectrum of AD17 (8)

The structure of AD17 **(8)** was confirmed by its nanoelectrospray positive ionisation mass

spectrum, in which it had a doubly-charged signal at m/z 547.7100 (z=2) for the species

$[(M+2H)/2]^{2+}$, a signal at m/z 1094.4139 which indicated the species $(M+H)^+$, a signal at

m/z 1116.3958 for the species $(M+Na)^+$, and also the observed data matched the

theoretical isotope pattern which proved that probe AD17 **(8)** had the correct structure

[**Figure 2.19**].

2.3.2.3 <u>Synthesis of 5(6)-FAM-Pro-Ser-Asn-Leu-[PEG Spacer]-AQ probe</u>
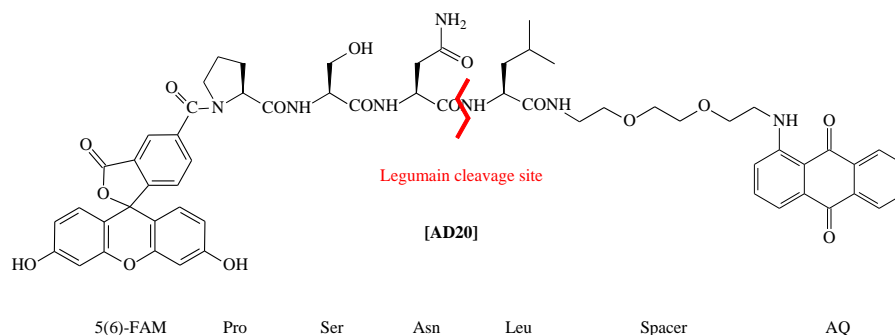
<u>[AD20] (9)</u>

Figure 2.20. Chemical structure of 5(6)-FAM-Pro-Ser-Asn-Leu-[PEG Spacer]-AQ probe AD20 (9)

The only difference between probes TL11 **(3)** and AD20 **(9)** is that during the synthesis, alanine at the P2 position in TL11 **(3)** was replaced by serine. Due to the presence of an alcohol group side chain in serine, during the synthesis, Fmoc-Ser(*t*Bu)-OSu was applied to prevent dehydration side reaction. This O-*tert*-butyl side chain protection group in serine was removed by TFA at the very last stage, i.e. during the trityl deprotection from asparagine.

2.3.2.3.1 <u>Mass Spectral Characterisation of AD20 (9)</u>

As for the prototype probe TL11 **(3)**, nanoelectrospray ionisation (ESI) was used for AD20 **(9)**. However, the conjugate gave a satisfactory result in the positive ion mode upon first analysis and so, negative ion mode was not used.
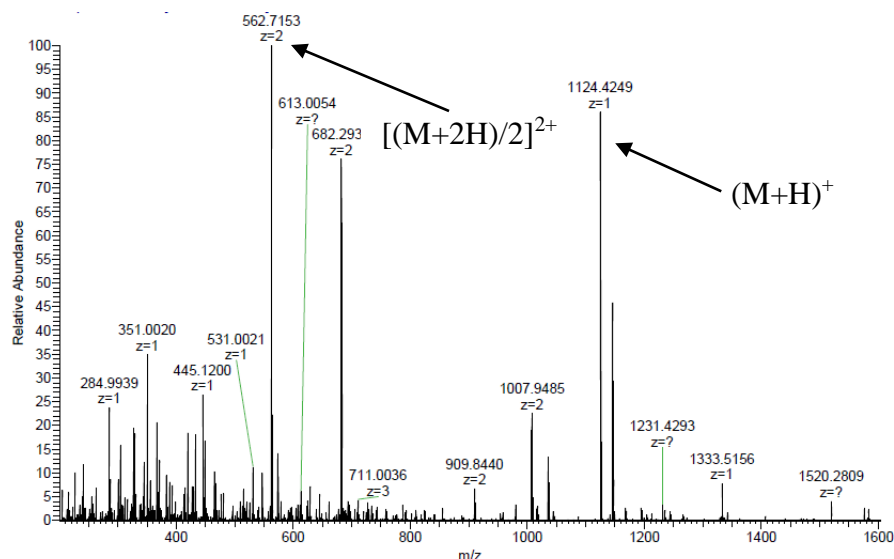
Figure 2.21. Mass Spectrum of AD20 (9)

The structure of AD20 **(9)** was confirmed by its nanoelectrospray positive ionisation mass spectrum, in which it showed a signal at m/z 1124.4249 for the species $(M+H)^+$ and a doubly-charged signal at m/z 562.7153 (z=2) for the species $[(M+2H)/2]^{2+}$, and also the observed data matched the theoretical isotope pattern which proved that probe AD20 **(9)** had the correct structure [**Figure 2.21**].

2.3.2.4 Synthesis of 5(6)-FAM-Pro-Thr-Asn-Leu-[PEG Spacer]-AQ probe [VG] (10)
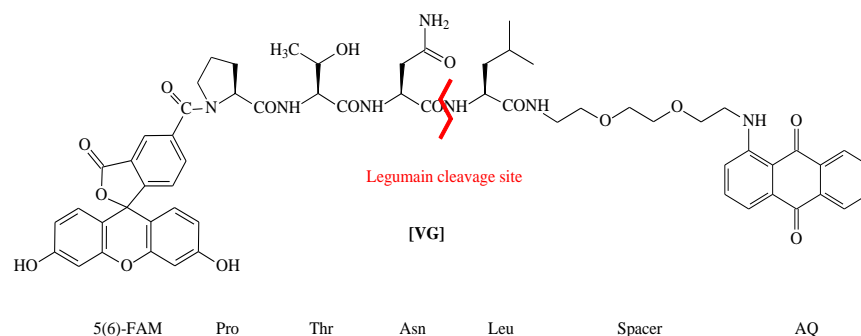
Figure 2.22. Chemical structure of 5(6)-FAM-Pro-Thr-Asn-Leu-[PEG Spacer]-AQ probe VG (10)

The synthesis of VG **(10)** was similar to the synthesis of TL11 **(3)** as well. The only difference is that alanine at the P2 position in probe TL11 **(3)** was replaced with threonine. As for serine, in threonine, there is a (secondary) alcohol group in the side chain. In order

155

to prevent side reaction, the -OH group was protected by *O-tert*-butyl protection group during synthesis, which was removed by TFA at the end of the synthesis at the same time when the trityl group was removed from the asparagine.

2.3.2.4.1 <u>Mass Spectral Characterisation of VG (10)</u>

The threonine containing substrate VG **(10)** was successfully characterised also by using nanoelectrospay positive ionisation mass spectrometry.
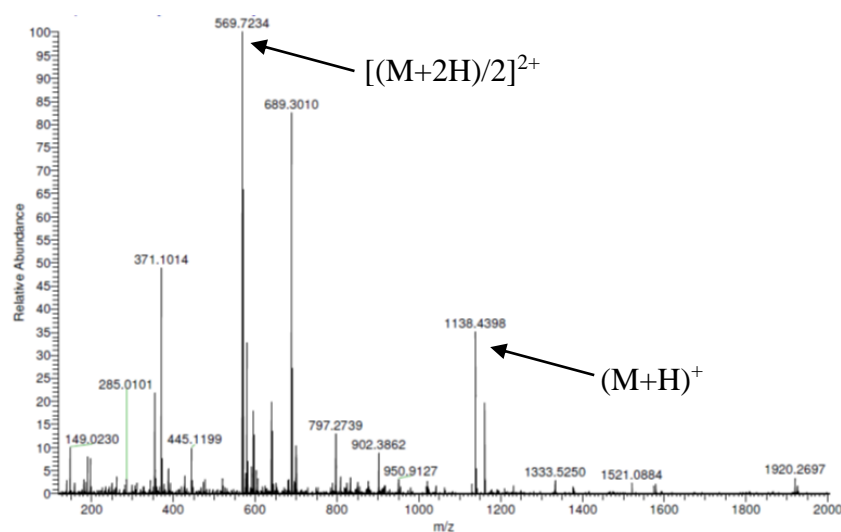
Figure 2.23. Mass Spectrum of probe VG (10)

In the probe VG **(10)** nanoelectrospray positive ionisation mass spectrum, there were a signal at m/z 1138.4398 which indicated the species $(M+H)^+$ and a doubly-charged signal at m/z 569.7234 (z=2) for the species $[(M+2H)/2]^{2+}$, also there was a good match between the theoretical isotope model and the observed data which proved probe VG **(10)** had the correct structure [**Figure 2.23**].

2.3.2.5   Synthesis of 5(6)-FAM-Ala-Asn-Leu-Ala-[PEG Spacer]-AQ probe [PN11] (11)
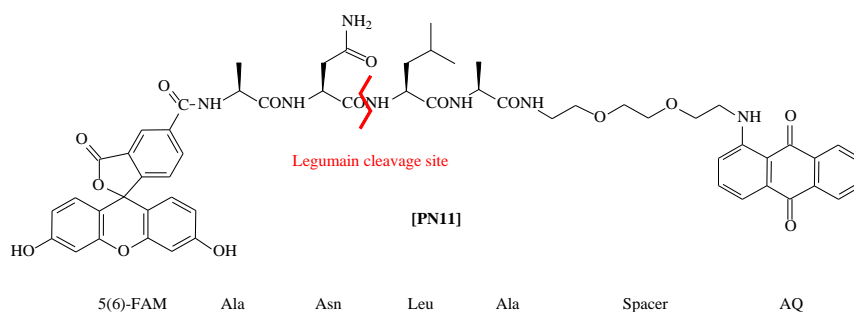
Figure 2.24. Chemical structure of 5(6)-FAM-Ala-Asn-Leu-Ala-[PEG Spacer]-AQ probe PN11 (11)

The differences between probes TL11 **(3)** and PN11 **(11)** are 1) in PN11 **(11)**, there is an extra alanine at the P2' position in its substrate peptide; 2) proline is missing from PN11 **(11)** substrate peptide sequence when compared with TL11 **(3)**. The reason for designing this substrate peptide sequence is in order to see whether one extra amino acid at the P2' position and one amino acid missing at the P3 position would lead to any kind of significant alteration (positive or negative) in cleavage sensitivity during incubation with activated legumain.

2.3.2.5.1   Mass Spectral Characterisation of PN11 (11)

Probe PN11 **(11)** was successfully characterised by using nanoelectrospray negative ionisation mass spectrometry.
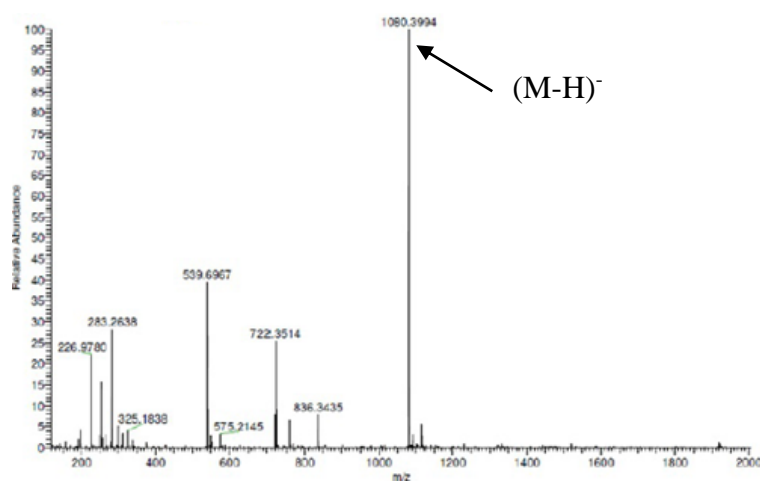
Figure 2.25. Mass Spectrum of PN11 (11)

157

In this negative ionisation mass spectrum, there was a signal at m/z 1080.3934 for the species (M-H)$^-$ which confirmed a molecular mass of 1081.

2.3.3 Design of legumain fluorogenic probes FF (6) and MK8 (7)

Before design and syntheses of 5(6)-FAM-labelled legumain fluorogenic probes [**Table 2.1**], two FITC-labelled legumain fluorogenic probes FF **(6)** and MK8 **(7)** [**Table 2.1**] were designed as model compounds in order to discover a better synthesis method for this series of legumain fluorogenic probes, and also to establish whether or not these probes can be successfully cleaved by activated legumain at the carboxyl end of asparagine.

Based on the successful synthesis of FITC-labelled MMP9 fluorogenic probe EV1-FITC (Van Valckenborgh *et al.,* 2005), fluorescein isothiocyanate (FITC) **(4)** and propyl spacer were chosen as fluorophore and spacer for both probes FF **(6)** and MK8 **(7)** to target activated legumain.
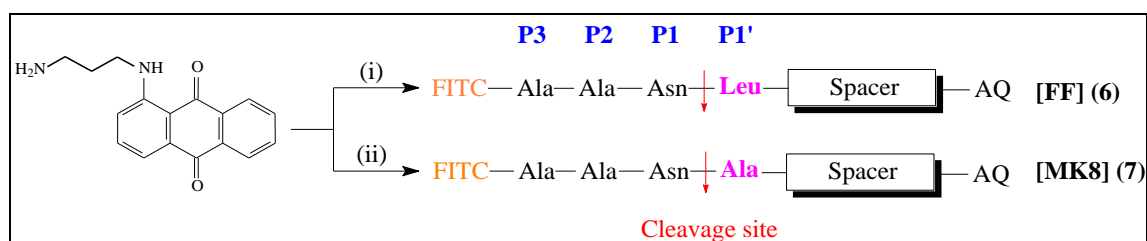
Scheme 2.4 General synthesis for FITC-labelled legumain fluorogenic probes FF (6) and MK8 (7)

Notes; Reagents and conditions: Syntheses for FITC labelled legumain fluorogenic probes FF **(6)** and MK8 **(7)** were very similar with only one difference at the P1' position:
(i)   Boc-Leu-OSu, DIPEA, DMF, RT, 1h. Hence Leu at the P1' position of MK8 **(7)**
(ii)   Boc-Ala-OH, TBTU, HOBt, DIPEA, DMF, RT, 2h. Hence Ala at the P1' position of FF **(6)**.

2.3.3.1 Rationale for selection of amino acids in positions of the legumain peptide substrate library

Based on the success of synthesis of FITC-labelled MMP9 fluorogenic probes FITC (**4**) had been chosen as fluorophore for both probes FF (**6**) and MK8 (**7**). In the legumain commercial substrate, benzyloxycarbonyl-Ala-Ala-Asn-7-amido-4-methylcoumarin (Z-AAN-AMC) (**24**) [**Figure 2.26**] two alanines occupied the P3 and P2 positions (R&D systems, 2012), so they were chosen at the same positions here in both of the experimental probes FF (**6**) and MK8 (**7**).
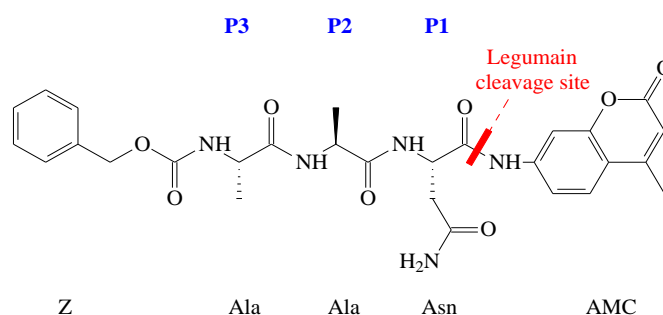
Figure 2.26. Chemical structure of legumain commercial substrate Z-AAN-AMC (24)

Due to the fact that legumain can only cleave at the carboxyl end of asparagine, asparagine was incorporated at the P1 position in both FF (**6**) and MK8 (**7**) probes. The only difference in the peptide sequence between probes FF (**6**) and MK8 (**7**) is at the P1' position: leucine was chosen for probe FF (**6**), (the same reason as described in **section 2.3.2.1**), while alanine was chosen for probe MK8 (**7**). FITC can perform a cyclisation under strong acid conditions, including with TFA [**Figure 2.8**], so the trityl protecting group on the side chain of asparagine had to be removed before the FITC coupling stage in the syntheses of both probes FF (**6**) and MK8 (**7**). This is different from the syntheses of 5(6)-FAM labelled probes, in which, the trityl group on the side chain of asparagine

was removed after the coupling of 5(6)-FAM onto tetrapeptide-[PEG Spacer]-AQ conjugate.

2.3.3.2 Synthesis of FITC-Ala-Ala-Asn-Leu-[Propyl Spacer]-AQ probe [FF] (6)
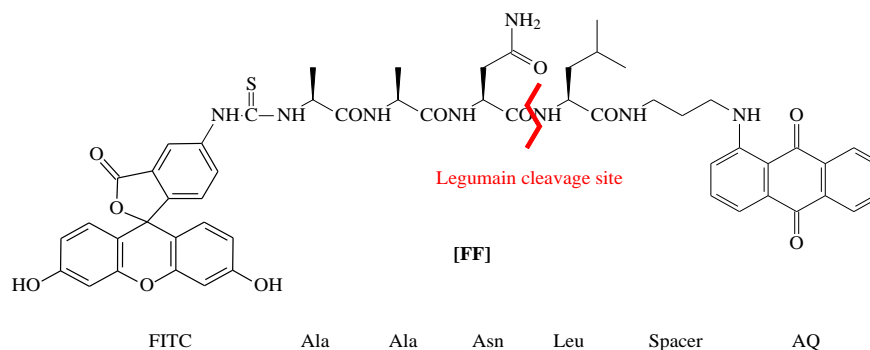
Figure 2.27. Chemical structure of legumain probe FF (6)

Because FITC **(4)** was known to have restricted use in solid phase peptide synthesis (side reactions and complex and difficult to purify reaction products), so the tetrapeptide-[Propyl Spacer]-AQ conjugate was synthesised by solution phase methods. Also, in order to avoid cyclisation happening for the thio-urea derived from FITC-labelled peptides, the trityl protecting group was removed from asparagine before the coupling of FITC onto tetrapeptide-[Propyl Spacer]-AQ conjugate.

2.3.3.2.1 Mass Spectral Characterisation of FF (6)

Both nanoelectrospray ionisation in positive and negative modes had been applied for probe FF **(6)** characterisation.
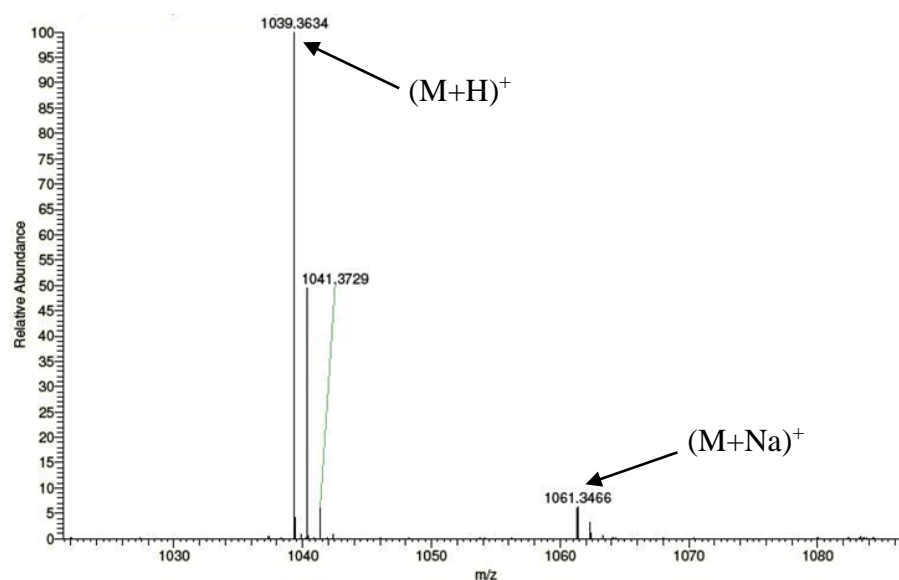
Figure 2.28. Nanoelectrospray positive ionisation mass spectrum of probe FF (6)

In the probe FF **(6)** nanoelectrospray positive ionisation mass spectrum [**Figure 2.28**], signals at m/z 1039.3634 indicated the species $(M+H)^+$, and at m/z 1061.3466 indicated the species $(M+Na)^+$ both suggested a molecular weight of 1038 Da for the probe FF **(6)**.
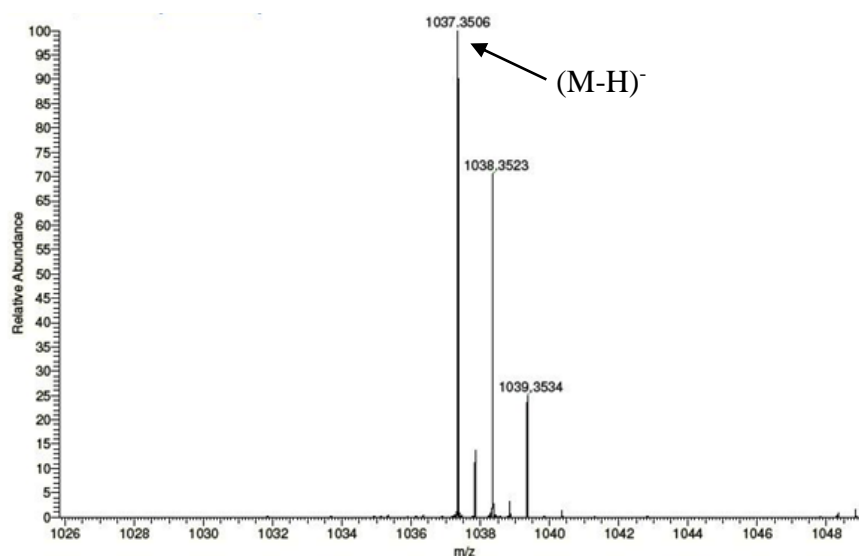
Figure 2.29. Nanoelectrospray negative ionisation mass spectrum of probe FF (6)

In the probe FF **(6)** the nanoelectrospray negative ionisation mass spectrum [**Figure 2.29**], signal at m/z 1037.3506 indicated the species $(M-H)^-$.

Hence, both positive and negative mass spectra confirmed the correct structure of probe FF **(6)**.

2.3.3.3   Synthesis of FITC-Ala-Ala-Asn-Ala-[Propyl Spacer]-AQ probe [MK8] (7)
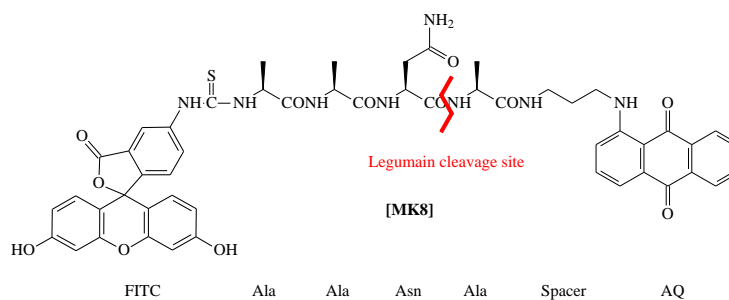
Figure 2.30. Chemical structure of legumain probe MK8 (7)

The synthesis of probe MK8 (**7**) was similar to the synthesis of probe FF (**6**) and the trityl

protecting group was removed before the FITC coupling stage as well. The only

difference between these two FITC labelled probes is that leucine at the P1' position in

probe FF (**6**) was replaced with alanine.

2.3.3.3.1   Mass Spectral Characterisation of MK8 (7)

This FITC-labelled probe MK8 (**7**) was successfully characterised by nanoelectrospay

negative ionisation mass spectrometry.
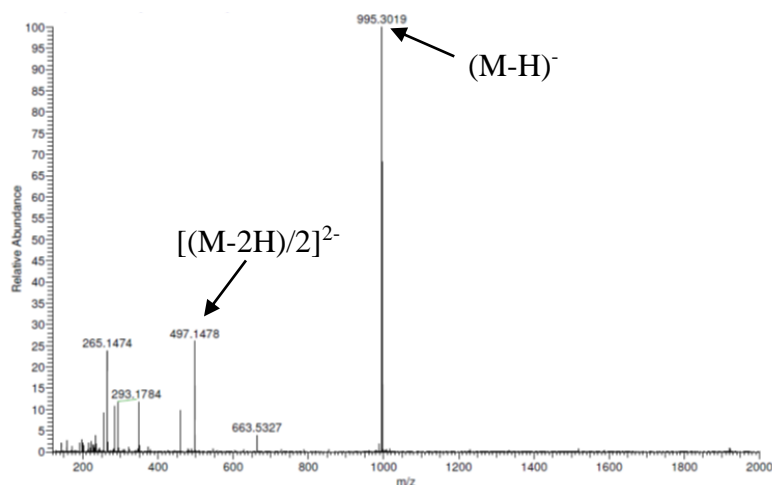
Figure 2.31. Mass spectrum of probe MK8 (7)

A signal at m/z 995.3019 in the nanoelectrospray negative mass spectrum [**Figure 2.31**]

corresponded to the expected molecular mass and a signal at m/z 497.1478 indicated the

species $[(M-2H)/2]^{2-}$. And also, there was good correlation between the observed data and the theoretical isotope model for $(M-H)^-$. Hence, it can be confirmed that probe MK8 **(7)** has the correct target structure.

During the syntheses of FITC-labelled probes FF **(6)** and MK8 **(7)**, it had been noticed that both compounds had poor solubility and were difficult to purify to remove unreacted FITC **(4)**. Hence, later both fluorophore and spacer had been changed to 5(6)-FAM **(5)** and the anthraquinone-PEG-spacer to improve compounds' solubility, and also this permitted the trityl group to stay on to protect the side chain of asparagine till the last synthesis step, hence, to improve syntheses yields.

2.3.4 Legumain probes activity study

Before any *in vitro* tests were carried out for TL11 **(3)**, a FRET study and fluorescence spectroscopy assay (see sections **2.3.4.1** and **2.3.4.2**) for probe TL11 **(3)** was applied to demonstrate that the anthraquinone-spacer part does indeed quench fluorescence from fluorophore 5(6)-carboxyfluorescein **(5)** very well. This would rule out the possibility that any fluorescence observed in further *in vitro* tests was not due to background fluorescence from probe TL11 **(3)**. Then, a fluorimetric assay (section **2.3.4.3**) was developed, so that the rh-legumain incubations determined whether or not the probes TL11 **(3)**, VG **(10)** and PN11 **(11)** [**Table 2.2**] are activated. Legumain enzyme kinetics assays were applied for three different probes TL11 **(3)**, VG **(10)** and PN11 **(11)** [**Table 2.2**] to determine which substrate binds to legumain better than others (section **2.3.4.4**).
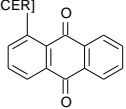
CODE	Fluorophore	P_3	P_2	P_1	P_1'	P_2'	SPACER	TEMPLATE
TL11 (3)	FAM	pro	ala	asn	leu		-HN-(CH$_2$)$_2$-O-(CH$_2$)$_2$-O-(CH$_2$)$_2$-NH-	
VG (10)	FAM	pro	thr	asn	leu		-HN-(CH$_2$)$_2$-O-(CH$_2$)$_2$-O-(CH$_2$)$_2$-NH-	
PN11 (11)	FAM		ala	asn	leu	ala	-HN-(CH$_2$)$_2$-O-(CH$_2$)$_2$-O-(CH$_2$)$_2$-NH-	

Table 2.2. Library structures of probes TL11 (3), VG (10) and PN11 (11).

Preliminary cytotoxicity and proliferation assays were applied to determine whether the probe TL11 (**3**) or its cleavage product were cytotoxic (section **2.3.4.5**).

2.3.4.1 FRET study between fluorophore 5(6)-FAM (5) and its quencher TFA-Leu-Spacer-AQ [TL3] (16)
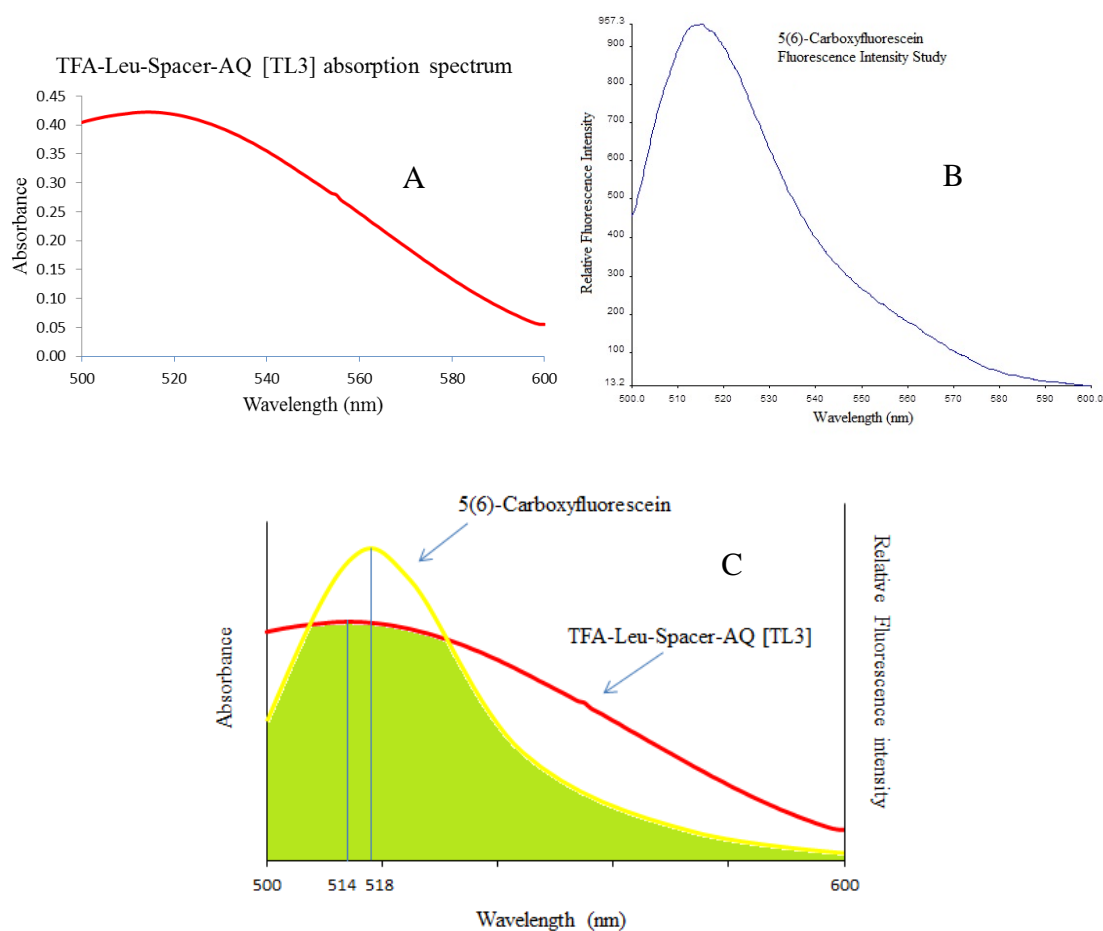
Figure 2.32. A, TFA-Leu-Spacer-AQ [TL3] (16) (50 μM in legumain assay buffer, pH 5.0) absorption spectrum; B, 5(6)-FAM (5) (0.5 μM in legumain assay buffer, pH 5.0) fluorescence intensity spectrum, λ_{ex} 492nm; C, FRET concept diagram (simulation) for TL3 (16) and 5(6)-FAM (5)

The FRET study for TL11 (**3**) probe fluorophore and its quencher component was applied to find out whether the absorption spectrum of TFA-Leu-Spacer-AQ quencher [TL3 (**16**) (acceptor)] would overlap well with the emission spectrum of 5(6)-carboxyfluorescein (**5**) (donor).

From the UV-Vis absorption spectrum of TFA Leu-Spacer-AQ compound TL3 (**16**) (50 μM) [**Figure 2.32 A**], it showed that the wavelength at maximum absorbance was 514nm, and in the fluorescence emission spectrum of 5(6)-carboxyfluorescein (**5**) (0.5 μM) [**Figure 2.32 B**], the wavelength at maximum fluorescence intensity was 518nm. According to these two overlapped absorbance and fluorescence spectra, it could easily be predicted that in theory, TL3 (**16**) can perfectly quench the fluorescence released from 5(6)-carboxyfluorescein (**5**) [**Figure 2.32 C**], hence there should be no or very little fluorescence detected from probe TL11 (**3**).

In order to evaluate legumain substrates that have been designed and synthesised in this lab, during their enzyme kinetics studies, they were compared with the legumain commercial substrate benzyloxycarbonyl-Ala-Ala-Asn-7-amido-4-methylcoumarin (Z-AAN-AMC) (**24**) [**Figure 2.26**] (Stern *et al.*, 2009; R&D systems, 2012). Unlike legumain substrates made in this project which have 5(6)-carboxyfluorescein (**5**) or FITC (**4**) as fluorophore, the fluorophore in this commercial substrate Z-AAN-AMC (**24**) is 7-amino-4-methylcoumarin (AMC) which requires measurement at excitation $\lambda = 360$nm and emission $\lambda = 460$nm (Stern *et al.*, 2009). Also this commercial fluorimetric probe is not a FRET model like all fluorimetric probes designed and synthesised in this project, the silencing of fluorescence from Z-AAN-AMC (**24**) is due to the amide bond formation between the amino group of 7-amino-4-methylcoumarin (AMC) when capped with a

peptide, not because the absorption spectrum of the Z-group can overlap the emission spectrum of AMC. More result details are shown in legumain substrates fluorimetric assay and enzyme kinetics assay sections.

2.3.4.2 <u>Fluorescence Spectroscopy Assay</u>

The ability of the anthraquinone chromophore to quench the fluorescence emission of the fluorophore in the probe TL11 **(3)** was determined by fluorescence spectroscopy.

In **Figure 2.33**, data from fluorophore quenching studies showed that the relative fluorescence intensity of the fluorogenic probe TL11 **(3)** was nearly 70 fold lower than the fluorophore 5(6)-carboxyfluorescein **(5)**, even when the concentration of TL11 **(3)** was 10 times higher than 5(6)-carboxyfluorescein **(5)** during the test.
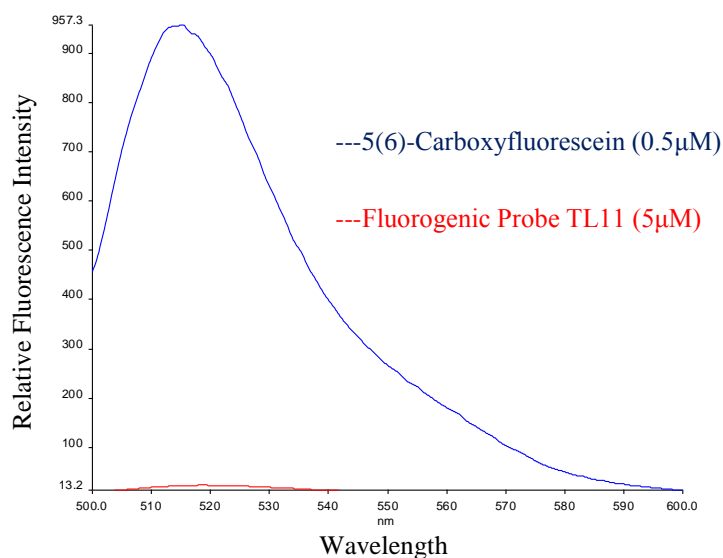
Figure 2.33. Comparison of relative fluorescence intensities of 5(6)-carboxyfluorescein (5) (0.5 μM) and fluorogenic probe TL11 (3) (5 μM) in legumain assay buffer, pH 5.0, λ_{ex} 492nm.

The data in **Figure 2.33** indicates that there is efficient quenching of fluorescein fluorescence by the anthraquinone 'dark quencher'.

2.3.4.3 Fluorimetric Assay

The ability of activated rh-legumain to cleave the probe at the designed cleavage site, the carboxyl end of asparagine, in order to release a fluorescent fluorescein-labelled peptide fragment during incubation, was determined by fluorimetric assay.

2.3.4.3.1 TL11 (3) Fluorimetric Assay

TL11 **(3)** (10 μM) was incubated with legumain (40ng) at 37°C. Fluorescence was released from TL11 **(3)** immediately when TL11 **(3)** was mixed with legumain. During the first 20 minutes incubation, the relative fluorescence intensity maintained a consistent rate increase. Then, the graph of fluorescence intensity over time levelled-out and the relative fluorescence intensity reached maximum after 100 minutes incubation [**Figure 2.34**].
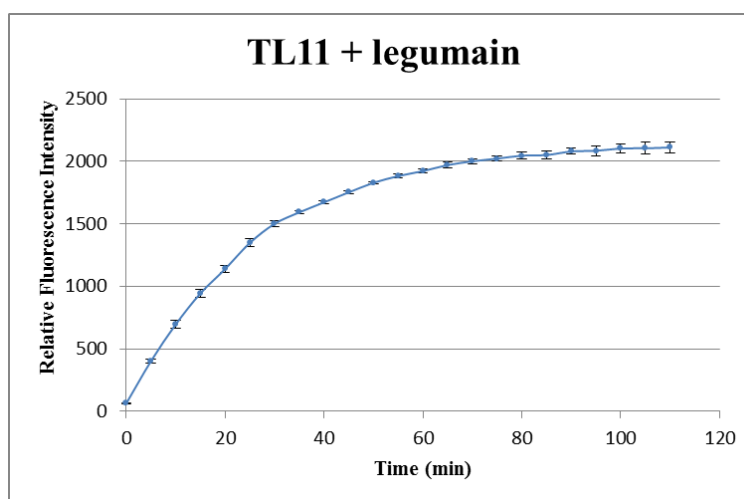
Figure 2.34. Relative fluorescence intensity release with time during the incubation of fluorogenic probe (TL11 (3), 10 μM) with recombinant human legumain (40ng) in legumain assay buffer, pH 5.0, λ_{ex} 492nm, λ_{em} 520nm (Mean values ± SD from triplicates from one experiment are presented)

After fluorimetric assay, the TL11 **(3)** legumain incubation solution was extracted with chloroform. On a TLC plate, the chloroform extract showed a red spot for the free base of the H-Leu-[PEG Spacer]-AQ compound **(25)** [**Figure 2.35**]. The result showed the extract had an R_f value identical to an authentic sample (available as an intermediate in TL11 **(3)** synthesis), confirming legumain had cleaved the tetrapeptide of TL11 **(3)** selectively at the carboxyl side of asparagine successfully.

H-Leu-[PEG Spacer]-AQ **(25)**
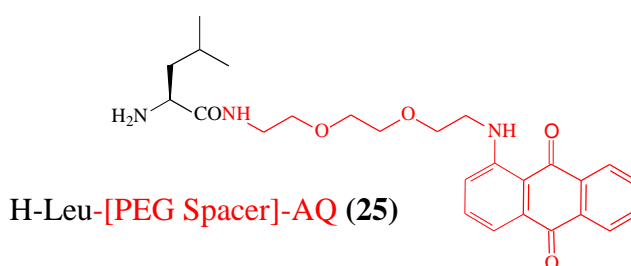
Figure 2.35. Residue isolated post-cleavage: H-Leu-[PEG Spacer]-AQ (25)

After cleavage by legumain, TL11 **(3)** was separated into two parts: fluorescently-labelled tripeptide, 5(6)-FAM-Pro-Ala-Asn-OH **(26)** and H-Leu-[PEG Spacer]-AQ **(25),** the anthraquinone-leucine conjugate. A synthesised sample of authentic 5(6)-FAM-Pro-Ala-Asn-OH residue **(26)**, the first-formed fluorophore, released when the fluorogenic substrate is cleaved was subjected to fluorimetric assay so that a standard curve could be generated. In *in vivo* incubations or experiments with cell lysates, the first-formed fluorescent tripeptide might be further degraded but here, the use of recombinant legumain may be expected to stop at the initial cleavage product.

2.3.4.3.2   5(6)-FAM-Pro-Ala-Asn-OH (26) Fluorimetric Assay

5(6)-FAM-Pro-Ala-Asn-OH

$y = 2864.6x + 237.99$
$R^2 = 0.9995$
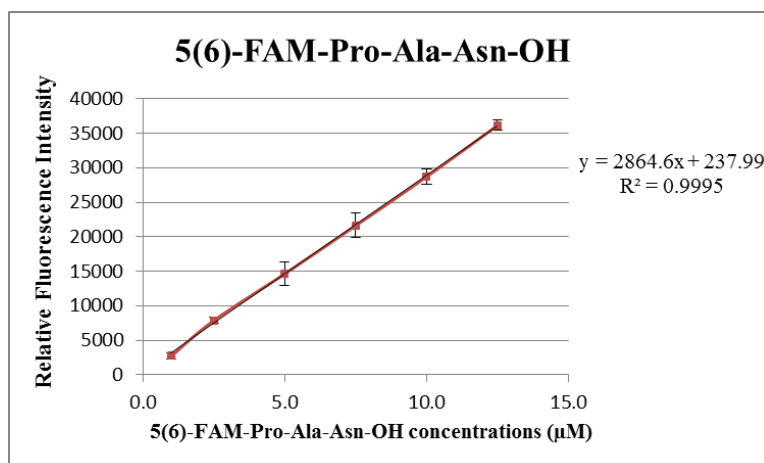
Figure 2.36. Mean variation of fluorescence emission with concentration of the fluorophore 5(6)-FAM-Pro-Ala-Asn-OH (26) (1 to 12.5 μM) in legumain assay buffer, pH 5.0, λ_{ex} 492nm, λ_{em} 520nm (n=3)

The fluorimetric assay for this fluorophore 5(6)-FAM-Pro-Ala-Asn-OH **(26)** (1 to 12.5 μM) was conducted for 110 minutes. As time passed by, each average relative fluorescence intensity from different fluorophore concentrations decreased slightly. This may due to fluorophore 5(6)-FAM-Pro-Ala-Asn-OH **(26)** might have come out of solution and adhered onto the wall of each well or (more probably) after a period of time a photobleaching effect of this fluorophore residue took place.

2.3.4.3.3   Z-AAN-AMC (24) Fluorimetric Assay

In order to compare the TL11 **(3)** fluorimetric assay result, the legumain commercial substrate Z-AAN-AMC **(24)** (10 μM) was incubated with legumain (40ng) at 37°C for 110 minutes during its fluorimetric assay [**Figure 2.37**] which was under the same conditions as TL11 **(3)** but the wavelengths for excitation and emission were reset as 355nm and 460nm, respectively.
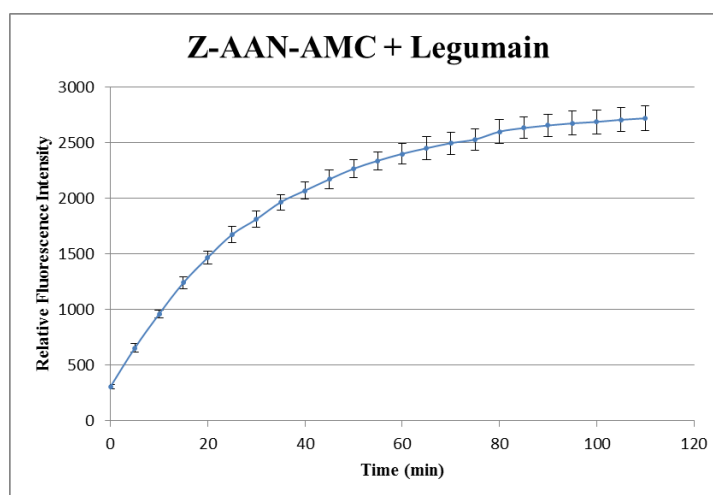
Figure 2.37. Relative fluorescence intensity release with time from the incubation of legumain commercial substrate Z-AAN-AMC (24) (10 μM) with recombinant human legumain (40ng) in legumain assay buffer, pH 5.0, λ_{ex} 355nm, λ_{em} 460nm (Mean values ± SD from triplicates from one experiment are presented)

When compared, both graphs from TL11 (**3**) [**Figure 2.34**] and (above) Z-AAN-AMC (**24**) fluorimetric assays, looked quite similar to each other, but the same concentration of Z-AAN-AMC (**24**) (10 μM) gave higher fluorescence intensity than TL11 (**3**) after the same period of incubation with legumain. However, when comparing the fluorescence intensities from wells which only contained assay buffer and substrate alone, it had been noticed that after subtracting the fluorescence intensity from assay buffer, commercial substrate Z-AAN-AMC (**24**) released more background fluorescence than TL11 (**3**).

2.3.4.3.4 AD17 (8) Fluorimetric Assay

Legumain probe AD17 (**8**) was incubated with rh-legumain at 37°C for 110min during its fluorimetric assay [**Figure 2.38**] which was under the same conditions as for TL11 (**3**).
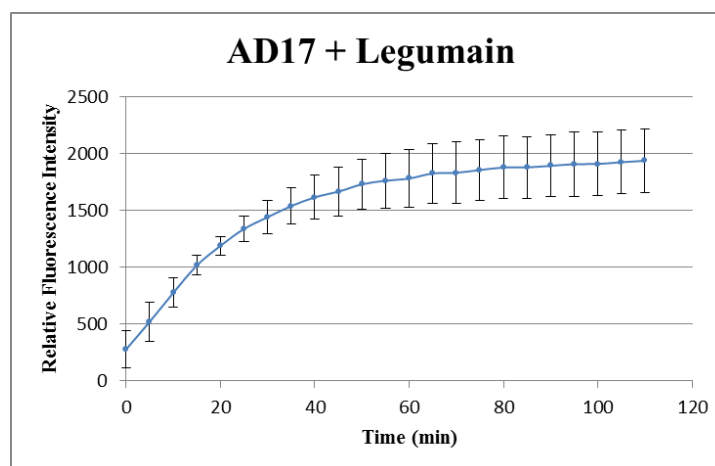
Figure 2.38. Relative fluorescence intensity release with time from the incubation of legumain probe AD17 (8) (10 μM) with recombinant human legumain (40ng) in legumain assay buffer, pH 5.0, λ_{ex} 492nm, λ_{em} 520nm (Mean values ± SD from triplicates from one experiment are presented)

Fluorimetric assay indicated that probe AD17 **(8)** can be successfully cleaved by activated legumain as had been expected. From **Figure 2.38**, it showed that after one hour incubation with activated legumain, the increase of fluorescence intensity started to slow down and almost reached the maximum after 100min.

2.3.4.3.5 AD20 (9) Fluorimetric Assay

Under the same conditions as TL11 **(3),** legumain probe AD20 **(9)** was incubated with legumain at 37°C for 110 minutes during its fluorimetric assay [**Figure 2.39**].

Figure 2.39. Relative fluorescence intensity release with time from the incubation of legumain probe AD20 (9) (10 μM) with recombinant human legumain (40ng) in legumain assay buffer, pH 5.0, λ_{ex} 492nm, λ_{em} 520nm (Mean values ± SD from triplicates from one experiment are presented)

AD20 **(9)** fluorimetric assay showed similar results to TL11 **(3);** this indicated that AD20 **(9)** can also be cleaved by activated legumain to release fluorescence. However, it had been noticed that when compared with TL11 **(3)** [**Figure 2.34**], the maximum fluorescence that had been released from AD20 **(9)** incubation with activated legumain was 3000 RFU, which was almost 700 RFU higher than the one from TL11 **(3)** fluorimetric assay result when assayed simultaneously. Also, when comparing both graphs' slopes during the first 10 minutes, the slope from AD20 **(9)** incubation is 1.3-fold greater than the slope from TL11 **(3)** incubation. This may suggest that replacing alanine with serine at the P2 position would improve the rate of conversion to its fluorescent product by the same amount of activated legumain under the same conditions.

2.3.4.3.6 VG (10) Fluorimetric Assay

Legumain probe VG **(10)** was incubated with legumain at 37°C for 110 minutes during its fluorimetric assay [**Figure 2.40**] which was under the same conditions as TL11 **(3)**.
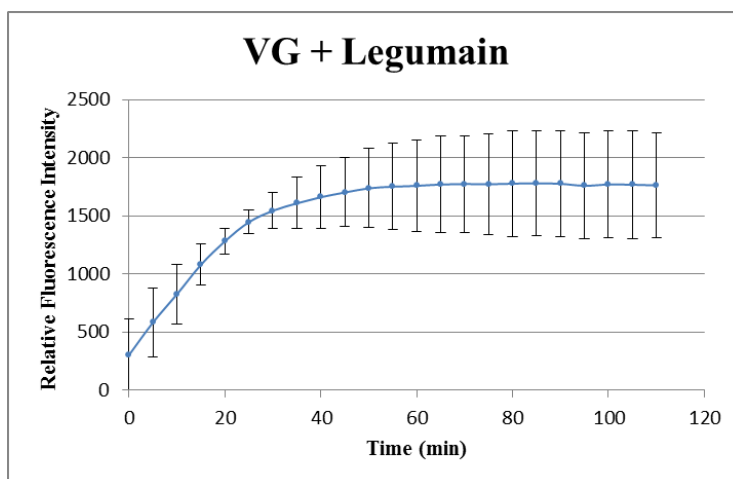
Figure 2.40. Relative fluorescence intensity release with time from the incubation of legumain probe VG (10) (10 μM) with recombinant human legumain (40ng) in legumain assay buffer, pH 5.0, λ_{ex} 492nm, λ_{em} 520nm (Mean values ± SD from triplicates from one experiment are presented)

VG **(10)** fluorimetric assay result was very similar to AD17 **(8)**. From **Figure 2.40**, it can be clearly noticed that after 30 minutes incubation with activated legumain, the increase of fluorescence intensity released from VG **(10)** started to slow down very quickly and reached its maximum around 1750 RFU after 50 minutes incubation. When compared with TL11 **(3)** the maximum fluorescence intensity released from VG **(10)** was 350 RFU lower than the one released from TL11 **(3)** fluorimetric assay result when assayed simultaneously. It was noted that the release of fluorescence from VG (10) was linear over 20 minutes, which could make it a suitable probe.

2.3.4.3.7 PN11 (11) Fluorimetric Assay

Under the same conditions as TL11 **(3)** fluorimetric assay, legumain probe PN11 **(11)** was incubated with legumain at 37°C for 110min during its fluorimetric assay [**Figure 2.41**].
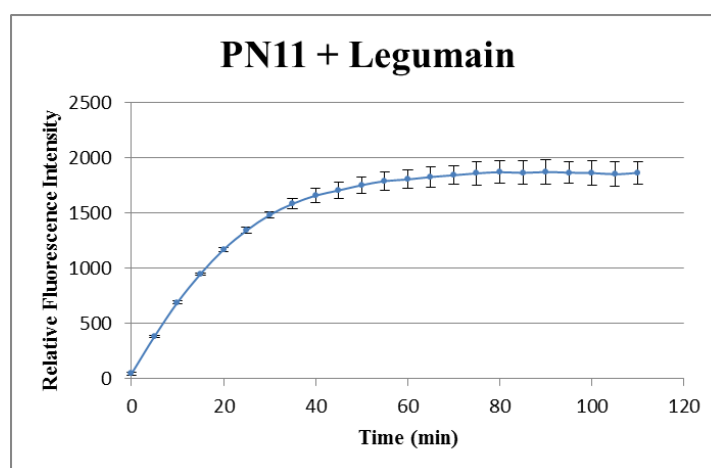
Figure 2.41. Relative fluorescence intensity release with time from the incubation of legumain probe PN11 (11) (10 μM) with recombinant human legumain (40ng) in legumain assay buffer, pH 5.0, λ_{ex} 492nm, λ_{em} 520nm (Mean values ± SD from triplicates from one experiment are presented)

Result from PN11 (**11**) fluorimetric assay showed that this rationally designed probe with one extra alanine at the P2' position and a 'missing' P3 position in the tetrapeptide can still be successfully cleaved by activated legumain. When comparing both graphs from probes PN11 (**11**) and TL11 (**3**) during the first 10 minutes incubation, they both showed quite similar slopes.

After comparing the slopes for all 5(6)-FAM labelled probes (TL11 (**3**), AD17 (**8**), AD20 (**9**), VG (**10**) and PN11 (**11**)) during the first 10 minutes incubation with legumain, it suggests a slight preference for the P2 position in the legumain substrates is Ser>Ala>Thr≥Gly.

2.3.4.3.8   FF (6) Fluorimetric Assay

By applying the same method as TL11 (**3**) fluorimetric assay, legumain probe FF (**6**) was incubated with legumain at 37°C for 120 minutes during its fluorimetric assay [**Figure 2.42**].
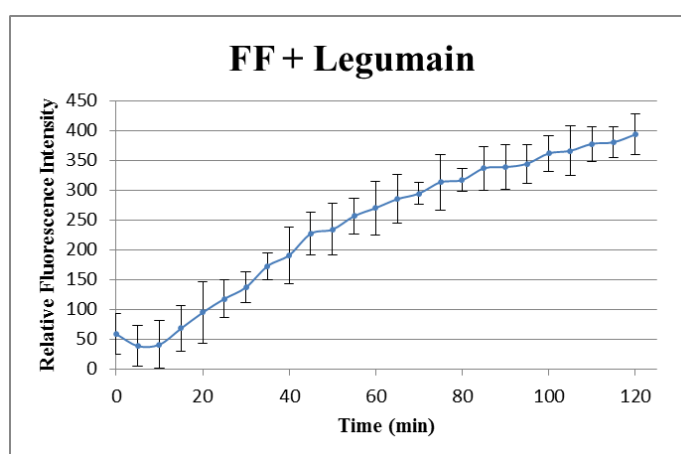
Figure 2.42. Relative fluorescence intensity release with time from the incubation of legumain probe FF (6) (10 μM) with recombinant human legumain (40ng) in legumain assay buffer, pH 5.0, λ_{ex} 492nm, λ_{em} 520nm (Mean values ± SD from triplicates from one experiment are presented)

Result from FF (**6**) fluorimetric assay showed that the cleavage rate of FF (**6**) did not reach its maximum but showed a sign of slowing down after 2h incubation with activated legumain. And also, the fluorescence released from probe FF (**6**) during this 2h incubation was low.

2.3.4.3.9   MK8 (7) Fluorimetric Assay

Probe MK8 (**7**) was incubated with activated legumain at 37°C for 120 minutes during its fluorimetric assay [**Figure 2.43**] by applying the same method used for probe TL11 (**3**).
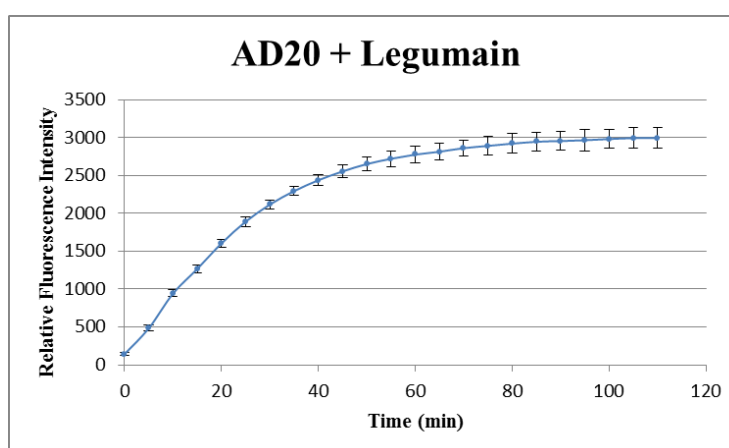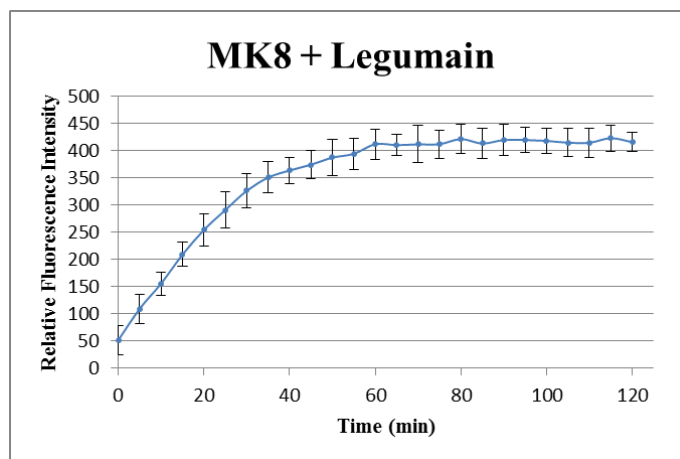

Figure 2.43. Relative fluorescence intensity release with time from the incubation of legumain probe MK8 (7) (10 μM) with recombinant human legumain (40ng) in legumain assay buffer, pH 5.0, λ_{ex} 492nm, λ_{em} 520nm (Mean values ± SD from triplicates from one experiment are presented)

The graph in **Figure 2.43** is very similar to the one for TL11 (**3**) fluorimetric assay; however, it showed much less fluorescence intensity. MK8 (**7**) fluorimetric assay indicated that after 30 minutes incubation with activated legumain, the cleavage rate of MK8 (**7**) had slowed down significantly, and after one hour incubation, the cleavage rate reached its maximum.

2.3.4.4   TL11 (3), PN11 (11) and VG (10) probes Enzyme Kinetics Assay

In order to find out which substrate peptide among TL11 **(3)**, PN11 **(11)**, VG **(10)** these three probes and legumain commercial substrate Z-AAN-AMC **(24)** can be cleaved faster by activated legumain and also which one has the higher binding affinity to legumain, an enzyme kinetics assay was carried out for probes TL11 **(3)**, PN11 **(11)** and VG **(10)**. The Michaelis-Menten equation $\upsilon=V_{max}[S]/(K_m+[S])$, proposed by Michaelis and Menten and further improved by Briggs and Haldane (Johnson and Goody, 2011), is very important to enzyme kinetics. The equation has two constants: V_{max}, the maximum velocity that an enzyme could achieve; and Michaelis-Menten constant K_m which can indicate the binding strength of the enzyme to its substrate. From enzyme kinetics studies of these three probes, it would reveal which substrate can be converted into product by legumain faster than others and which one has higher binding affinity onto legumain.

2.3.4.4.1   TL11 (3) Enzyme Kinetics Assay

TL11 **(3)** and legumain were incubated at $37^{\circ}C$ and emission spectra were recorded every 2 minutes on a FluoStar Omega multi-mode Microplate Reader using carboxyfluorescein excitation and emission analytical wavelengths of 485nm and 520nm, respectively. Relative fluorescence intensities in triplicate wells D3~F9 were adjusted by subtracting relative fluorescence intensities from corresponding TL11 **(3)** concentration in wells A3~C9 (**see section 2.7.5.1**) (any background fluorescence). According to the equation y = 2864.6x + 237.99 which was obtained by plotting fluorescence intensity versus various concentrations of 5(6)-FAM-Pro-Ala-Asn-OH (the cleavage product from the incubation

of TL11 (**3**) with legumain) in **Figure 2.36**, relative fluorescence intensities were converted to its corresponding 5(6)-FAM-Pro-Ala-Asn-OH (**26**) concentration, which is also equal to the concentration of TL11 (**3**) that had been cleaved by legumain. Although the fluorophore cleavage products from PN11 (**11**) and VG (**10**) were 5(6)-FAM-Ala-Asn-OH and 5(6)-FAM-Pro-Thr-Asn-OH, respectively, structurally different from 5(6)-FAM-Pro-Ala-Asn-OH (**26**), equation y = 2864.6x + 237.99 from **Figure 2.36** was still applied for both PN11 (**11**) and VG (**10**) enzyme kinetics assays. Therefore the relationship between fluorescence intensity and concentration is an approximation for PN11 (**11**) and VG (**10**). This approximation was deemed valid since the composition of the substrates was unlikely to have significant effects on the intensity of fluorescence from fluorescein labels, particularly in the early time points. Clearly, to afford comparisons with greater accuracy, authentic samples of each unique FAM-tripeptide would be required by synthesis. SigmaPlot 12 software was applied to analyse final data and plot a non-linear regression curve [**Figure 2.44**]. V_{max} and K_m were calculated by the enzyme kinetics tool in SigmaPlot 12.
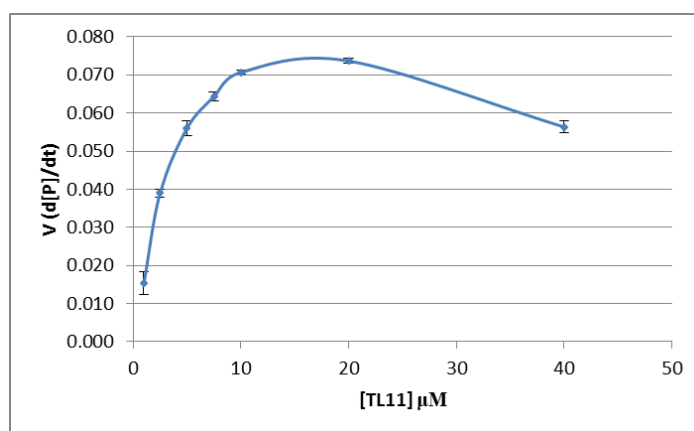
Figure 2.44. Non-linear regression curve of TL11 (3) reaction rates against various concentrations of TL11 (3) in legumain assay buffer, pH 5.0, λ_{ex} 492nm, λ_{em} 520nm (n=3)

Parameters of TL11 **(3)** enzyme kinetics assay:

	Value	± Std. Error	95% Conf. Interval
V_{max}	7.206×10^{-2} (μM/min)	3.879×10^{-3}	6.384×10^{-2} to 8.028×10^{-2}
K_m	1.4749 (μM)	0.4682	0.4822 to 2.4675

Table 2.3. Parameters from TL11 (3) enzyme kinetics assay

According to the recombinant human legumain/asparaginyl endopeptidase protocal (R&D systems, 2012), compound specific activity of legumain can be calculated by using following equation:

$$\textbf{Specific Activity (pmol/min/μg)} = \frac{\textbf{\textit{Vmax}} \, (\mu \, \textbf{M/min}) \times \textbf{V} \, (\mu \textbf{L})}{\textbf{amount of enzyme} \, (\mu \textbf{g})}$$

So, TL11 **(3)** specific activity of recombinant human legumain was 180.15 (pmol/min/μg).

2.3.4.4.2 PN11 (11) Enzyme Kinetics assay

Most literature reports, whenever discussing legumain substrates, despite different peptide sequences, they all have a few views in common: 1) asparagine is always at the P1 position due to the specific cleavage site of legumain; 2) peptide sequences in different legumain substrates always contain four amino acids from the P3 to P1' positions. So, is it necessary to place one amino acid at the P3 position or will it still have the same enzyme activity with one amino acid that fits the P2' position? With these questions in mind, the other legumain substrate PN11 **(11)** [**Figure 2.45**] was designed and synthesised.
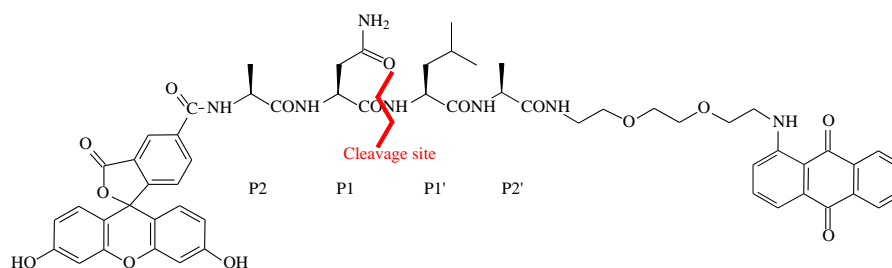
Figure 2.45. Chemical structure of PN11 (11)

PN11 (**11**) enzyme kinetics was carried out using the same method as TL11 (**3**). PN11

(**11**) enzyme kinetics study result is shown in **Figure 2.46**.
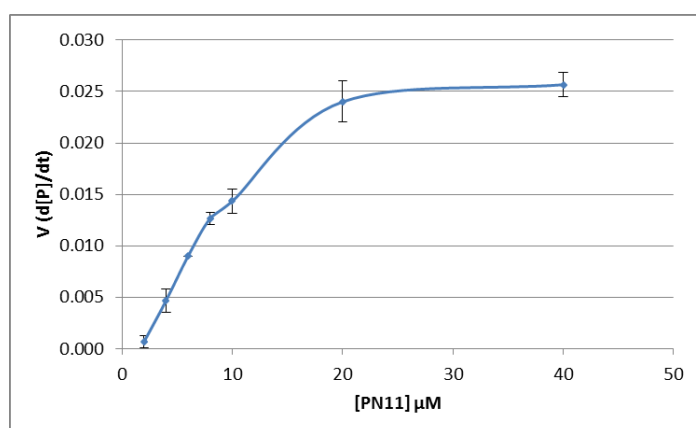
Figure 2.46. Non-linear regression curve of PN11 (11) reaction rates against various concentrations of PN11 (11) in legumain assay buffer, pH 5.0, λ_{ex} 492nm, λ_{em} 520nm (n=3)

Parameters of PN11 (**11**) enzyme kinetics assay:

	Value	$\pm$ Std. Error	95% Conf. Interval
V_{max}	4.092×10^{-2} (μM/min)	4.080×10^{-3}	3.238×10^{-2} to 4.946×10^{-2}
K_m	19.4982 (μM)	3.7909	11.5635 to 27.4328

Table 2.4. Parameters from PN11 (11) enzyme kinetics assay

PN11 (**11**) specific activity of recombinant human legumain can be calculated by using

the specific activity equation as shown earlier. Hence, PN11 (**11**) specific activity of

recombinant human legumain was determined as 102.3 (pmol/min/μg).

179

Wu *et al.* pointed out that although LEG-3 **(1)**, succinyl-β-Ala-Ala-Asn-Leu-Dox [**Figure 2.2**], has been proved to be a highly efficient legumain-activated prodrug, whereas its similar compound LEG-4 **(27)**, succinyl-Ala-Asn-Leu-Dox [**Figure 2.47**] which is one alanine shorter, was ineffective. An *In vivo* study showed that after incubating with leguamin, LEG-4 **(27)** was not cleaved by legumain and hence it showed no antitumour activity at all (Wu *et al.*, 2006).

Figure 2.47. Chemical structure of LEG-4 (27)

Both PN11 **(11)** and LEG-4 **(27)** lack P3 position substituents in their peptide sequences, but PN11 **(11)** has one extra alanine at the P2' position while LEG-4 **(27)** does not, so this gives PN11 **(11)** four amino acids in its peptide to fit in the P2, P1, P1' and P2' positions compared with LEG-4 **(27)** with three amino acids in its peptide from the P2 position to the P1' position. Further studies showed that after incubating with legumain, PN11 **(11)** can be cleaved by this asparagine endopeptidase while LEG-4 **(27)** stays inactive. This may indicate that the P3 and the P2' positions in the legumain substrate do not necessarily require occupation by amino acids, as long as asparagine is at the P1 position and the whole peptide has at least four amino acids, then this substrate should be able to be cleaved by legumain.

2.3.4.4.3   VG (10) Enzyme Kinetics assay

Based on the success of probe TL11 (**3**), a new probe was designed with slightly modified substrate peptide sequence. According to the *MEROPS* database website (Rawlings, Barrett and Bateman, 2012), the most popular amino acid at the P2 position is threonine. In order to find out whether threonine at the P2 position can improve substrate specific activity or not, in VG (**10**) [**Figure 2.48**], the sequence was kept the same as TL11 (**3**); just simply replaced alanine with threonine at the P2 position.
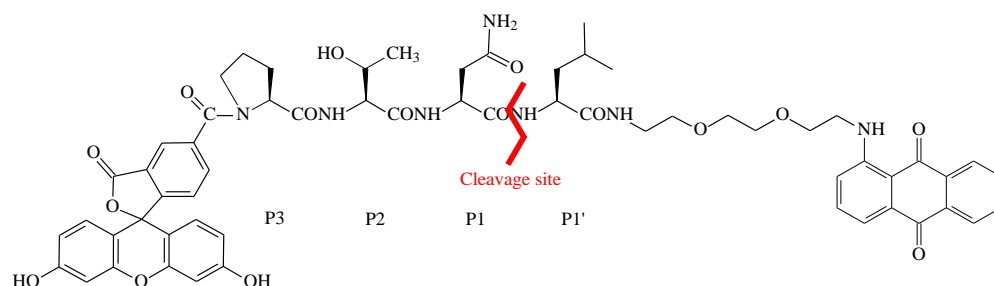
Figure 2.48. Chemical structure of VG (10)

VG (**10**) enzyme kinetics assay followed the same protocol as TL11 (**3**) enzyme kinetics assay; the result is shown in **Figure 2.49**.
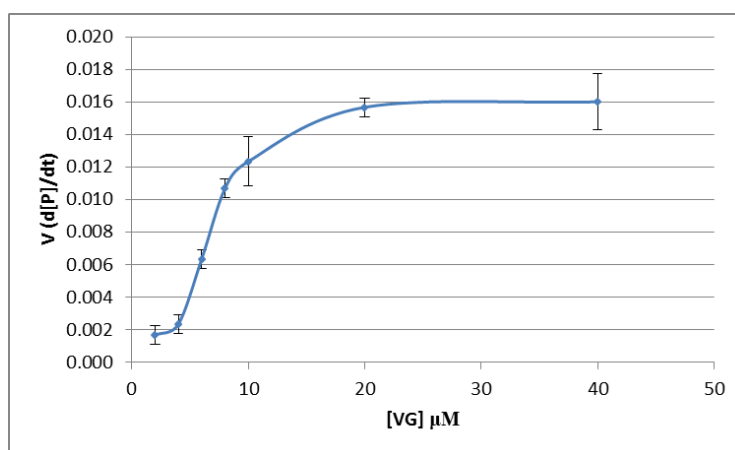
Figure 2.49. Non-linear regression curve of VG (10) reaction rates against various concentrations of VG (10) in legumain assay buffer, pH 5.0, λ_{ex} 492nm, λ_{em} 520nm (n=3)

Parameters of VG (**10**) enzyme kinetics assay:

	Value	± Std. Error	95% Conf. Interval
V_{max}	2.138×10^{-2} (µM/min)	1.955×10^{-3}	1.724×10^{-2} to 2.553×10^{-2}
K_m	10.7329 (µM)	2.6160	5.1872 to 16.2786

Table 2.5. Parameters from VG (10) enzyme kinetics assay

The specific activity equation was used to calculate VG **(10)** specific activity of recombinant human legumain. Hence, VG **(10)** specific activity of recombinant human legumain is 53.45 (pmol/min/µg).

	P3	P2	P1	P1'	P2'	V_{max}(µM/min)	K_m(µM)	Specific Activity (pmol/min/µg)
TL11 **(3)**	Pro	Ala	Asn	Leu		0.072	1.47	180
PN11 **(11)**		Ala	Asn	Leu	Ala	0.041	19.50	102
VG **(10)**	Pro	Thr	Asn	Leu		0.021	10.73	53

Table 2.6. Structure and enzyme kinetics assay parameters of TL11 (3), PN11 (11) and VG (10)

Enzyme kinetics assay revealed that TL11 **(3)** was the best legumain substrate when compared with PN11 **(11)** and VG **(10)**, due to TL11 **(3)** specific activity of legumain (180pmol/min/µg) was almost 1.8 times greater than PN11 **(11)** which had a specific activity value of 102 (pmol/min/µg) and approximately 3.4-fold greater than VG **(10)** (53pmol/min/µg). TL11 **(3)** and PN11 **(11)** are very alike legumain substrates; both have 5(6)-carboxyfluorescein **(5)** as fluorophore and the same AQ-spacer. However, PN11 **(11)** does not have an amino acid that is placed at the P3 position in the peptide sequence whereas TL11 **(3)** has proline fitted in the same position, and also PN11 **(11)** has an extra alanine at the P2' position which is absent in TL11 **(3)**. This could indicate that having

182

proline at the P3 position of a legumain substrate, can increases specific activity by almost 2-fold. The only difference between TL11 (**3**) and VG (**10**) is the amino acid at the P2 position. From the enzyme kinetics assay, it indicated that alanine at the P2 position can improve legumain substrate specific activity by more than 3-fold when compared with threonine at the P2 position.

In enzyme kinetics assay, V_{max} indicates the rate that a substrate can be converted into product(s) once bound to the enzyme. Hence from data in **Table 2.6**, it shows that TL11 (**3**) can be cleaved by legumain to release fluorescence 1.8-fold faster than substrate PN11 (**11**) and > 3-fold than VG (**10**). This may suggest a preference for the P2 position: Ala>Thr in substrates. K_m is the concentration of substrate at which ½ V_{max} is achieved and it represents the concentration of substrate at which half of the enzyme active sites have been filled with substrate. Hence, K_m indicates how effectively the enzyme would bind with substrate. So, in order to bind with the same amount of enzyme, the concentrations of substrate PN11 (**11**) and VG (**10**) were almost 13 fold and 7 fold higher than the concentration that was needed for TL11 (**3**) respectively.

When one compares V_{max} for substrate PN11 (**11**) and VG (**10**), it was shown that PN11 (**11**) can be converted into products by legumain almost twice as fast than VG (**10**), however, the K_m value for both substrates indicated that PN11's (**11**) legumain affinity is only about 50% of VG (**10**) legumain affinity.

According to the R&D systems recombinant human legumain/asparaginyl endopeptidase protocol, the specific activity for commercial (fluorogenic, but non-FRET) substrate, Z-AAN-AMC (**24**) is greater than 250 (pmol/min/µg) (R&D systems, 2012). So, from

Table 2.6, the data shows that none of those substrates synthesised in this laboratory have better specific activity for recombinant human legumain, than commercial substrate Z-AAN-AMC **(24)**. However, Mathieu and colleagues reported that K_m value for Z-AAN-AMC **(24)** binding with recombinant human legumain is 80 ± 6 µM, while in **Table 2.6** it clearly shows that all K_m values for those three substrates designed and synthesised are much smaller than 80 ± 6 µM (Mathieu *et al.*, 2002). This could suggest that all three substrates designed and synthesised in this laboratory, especially TL11 **(3)**, have much higher affinity with recombinant human legumain than Z-AAN-AMC **(24)**. Hence, adding Leu at the P1' position in substrate can improve substrate's affinity for legumain. The commercial substrate is unsuitable for working in biological matrixes (cells; tissues) because the matrix infers with the spectral properties of the fluorogenic probe. A major advantage of the FRET-based probes here is that methods for studying fluorescein fluorescence from biological matrixes is well established in molecular biology.

2.3.4.5 TL3 (16) and TL11 (3) Cytotoxicity and Proliferation Assays

In cytotoxicity and proliferation assays, several methods can be used to check the number of viable cells. The most reliable and direct method is treating the sample cells with a vital dye, for instance, trypan blue followed by using a hemocytometer and microscope to count the remaining viable cells at the end of an assay. Due to it is quite time consuming, it is not suitable for a large number of samples (Riss and Moravec, 1996). Luminescence and colorimetric based assays would allow viable cells counting directly by using ELISA plate reader or a microtiter plate reader (Weyermann *et al.*, 2005).
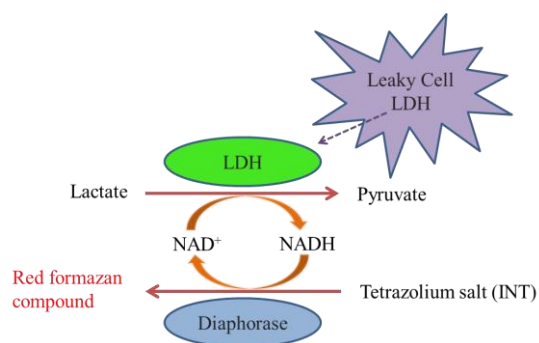
Scheme 2.5. LDH Assay

Quantitative lactate dehydrogenase (LDH), shown in **scheme 2.5**, a stable cytosolic enzyme that can be released during cell lysis, was measured in the LDH assay. In culture supernatants, released LDH was measured with a half an hour coupled enzymatic assay, which involves two steps. First, the released LDH from lysed cells catalyse conversion of lactate to pyruvate, from which NAD^+ is reduced to NADH. Then, diaphorase, a catalyst transfers H (hydride) from NADH to a tetrazolium salt 2-(4-iodophenyl)-3-(4-nitrophenyl)-5-phenyltetrazolium chloride (INT), which results a red formazan compound. The amount of red formazan product that had been generated could be used to indicate the number of lysed cells.
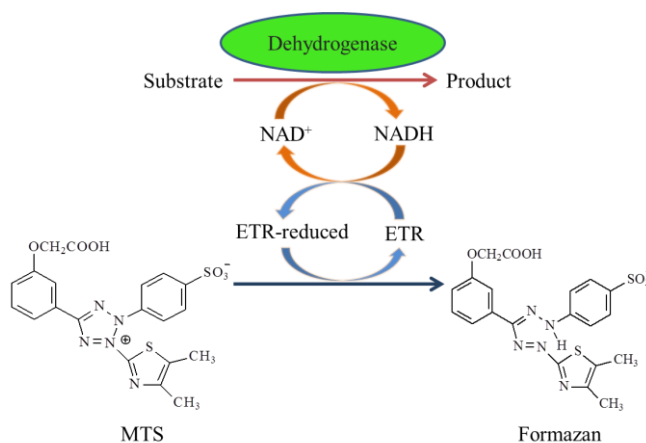
Scheme 2.6. MTS assay

The MTS assay is a colorimetric method that is applied to determine the amount of viable cells in chemosensitivity or proliferation assays. During cellular metabolism [**Scheme**

185

2.6], NAD$^+$ would be reduced by dehydrogenase enzymes to NADH, which can donate electrons to an electron transfer reagent (ETR) phenazine methosulfate (PMS). Reduced ETR then can reduce tetrazolium compound [3-(4,5-dimethylthiazol-2-yl)-5-(3-carboxymethoxyphenyl)-2-(4-sulfophenyl)-2H-tetrazolium, inner salt (MTS), into a deeply coloured formazan product which is soluble in tissue culture medium (Riss and Moravec, 1996).

The toxicity of probes TL11 (**3**) and TL3 (**16**), the product from TL11 (**3**) after cleavage by legumain, were tested in both cytotoxicity and proliferation assays.
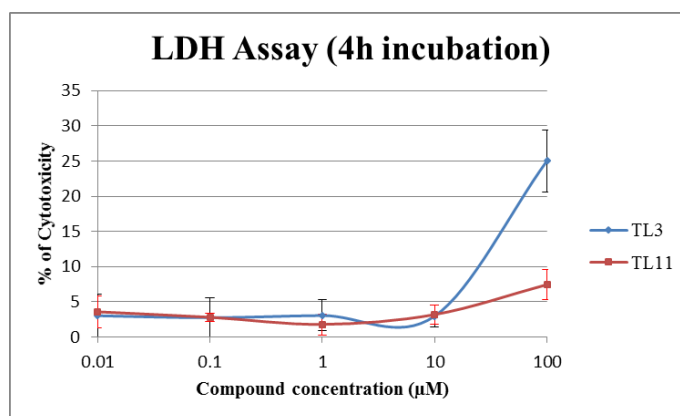
Figure 2.50. TL3 (16) and TL11 (3) LDH Assay (measured at 492nm, n=3)

From **Figure 2.50**, the data illustrated that during an LDH cytotoxicity assay, after 4h incubation with MCF-7 breast cancer cells, both TL3 (**16**) and TL11 (**3**) acted quite similarly. Lower concentrations (0.01~10 μM) of both compounds showed very low cytotoxicity to MCF-7 breast cancer cells, however, at high concentration of 100 μM, TL3 (**16**) revealed over 8 fold cytotoxicity when compared with lower concentrations, and the cytotoxicity of TL11 (**3**) at 100 μM was approximately 2-fold greater than at the lower test concentrations; neither compound showing a significant cytotoxic effect. This result indicated that both TL3 (**16**) and TL11 (**3**) had low cytotoxic activity at lower

concentrations till they reached a higher concentration at $100\,\mu M$. This value would normally be regarded as a poorly cytotoxic compound; this is important for the compounds to act as probes of the biomarker legumain.
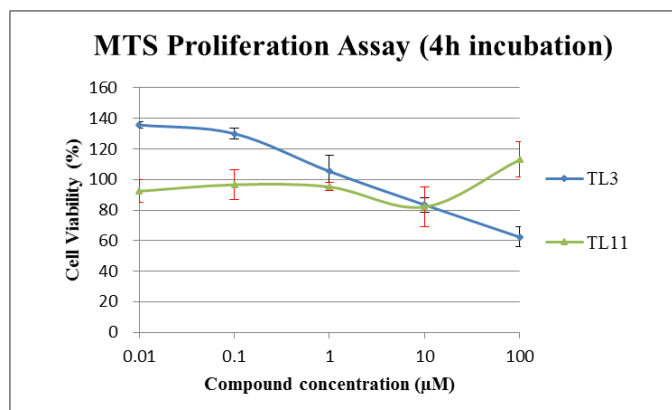
Figure 2.51. TL3 (16) and TL11 (3) MTS Cell Proliferation Assay (measured at 492nm, n=3)

From data in **Figure 2.51** it was shown that after 4h incubation with TL3 (**16**), MCF-7 breast cancer cells revealed similar viabilities. With increasing TL3 (**16**) concentration, results showed decreasing cell viabilities; however the rate of cell viability inhibition was not very significant until the anthraquinone leucine conjugate TL3 (**16**) concentration had been increased up to 10 and $100\,\mu M$. On the other hand, during the (legumain) probe TL11 (**3**) MTS assay, no inhibition of MCF-7 cell growth was observed from 4h incubation.

2.3.5 New approach to design and synthesis of legumain probes

Fluorescence intensity assay showed that almost no background fluorescence was released from TL11 (**3**). This may have been due to TL11 (**3**) being very pure (chromatographically homogeneous); that it had no 5(6)-carboxyfluorescein (**5**) present at all. Also, it proved that fluorescence from the fluorophore 5(6)-carboxyfluorescein can be quenched efficiently by the aminoanthraquinone, the 'dark quencher'. This newly

designed substrate of biomarker legumain, TL11 (**3**) was very sensitive when treated with legumain which confirmed that the enzyme can successfully cleave at the *C*-terminal side of asparagine on the tetrapeptide chain of TL11 (**3**). After cleavage, the fluorophore is no longer be attached to the 'dark quencher' anthraquinone; hence fluorescence can be released and detected. Cytotoxicity and proliferation assays showed that TL11 (**3**) had low cytotoxic activities on MCF-7 cells until higher concentrations were used (and then only above the concentration that the probe has been determined to be effective; $10\,\mu M$). All of these showed that probe TL11 (**3**) has the potential for use in the diagnosis and prognosis of breast cancer by targeting legumain.

2.3.5.0   Design of epirubicin labelled legumain prodrug/probes

As epirubicin has already been proved and applied as an efficient clinical anti-cancer in the treatment of breast cancer and its chemical structure has a coloured anthraquinone chromophore which makes it a potential 'dark quencher' for 5(6)-carboxyfluorescein (**5**) or other fluoro groups. Thus, it would perhaps be possible to synthesise a new probe based on the success of TL11 (**3**) that can have a fluorophore at one end, a similar or the same tetrapeptide chain in the middle as a linker which contained asparagine at the P1 position, and clinically proven epirubicin at the other end. In theory, when this ideal probe is delivered into the tumour environment which contains overexpressed legumain, this probe would be cleaved at the carboxyl end of asparagine by legumain to deliver the active drug. Without connection to the 'dark quencher' epirubicin, fluorescence can be released from the fluorophore again to indicate on the one hand, the presence of tumour cells expressing legumain (a diagnostic role); and on the other hand, epirubicin can work

as the clinically-effective anti-cancer agent to target tumour cells (hence constituting a combined theranostic probe/prodrug).

It has been learned that the stage of coupling epirubicin is very crucial, in that it would be better to couple epirubicin onto any other compounds at the very last stage in any prodrug synthesis. From previous experiences gained during coupling epirubicin (explained in part in Chapter one of this thesis), it was shown that the widely used coupling reagents HOBt and TBTU could cause complex reaction mixtures in the coupling stage and would not help epirubicin to form the final product. In order to avoid using coupling reagents, it would be better and easier to couple epirubicin onto an activated ester compound which would ideally be OPFP or OSu esters, so only a base at most e.g. DIPEA, would be required during coupling the peptide to the amino group of the sugar in epirubicin; no other reagents would be necessary.

Unprotected side chain asparagine can undergo a dehydration reaction, during which the free primary amide in the side chain would form a nitrile (cyanide) group, hence the structure of asparagine will be altered and legumain can no longer recognise its cleavage site in the peptide chain. Some studies suggested that DCC (Kashelikar and Ressler, 1964; Paul and Kende, 1964), a typical reagent that has been used for making an OPFP ester; or using TBTU alone while coupling free side chain asparagine can cause the dehydration in the free side chain. So, in order to make an OPFP ester compound, the primary amide on the side chain of asparagine might have to stay in the protected form. Once the OPFP ester compound has been synthesised, then the trityl protecting group on the side chain of asparagine can be removed by treating with neat TFA, however, there is a chance that the

OPFP ester bond might not survive under neat TFA strong acid condition, unless trace

water is strictly excluded. So, one 'mini test reaction' was carried out to see whether the

OPFP ester bond would be stable in such conditions or not.
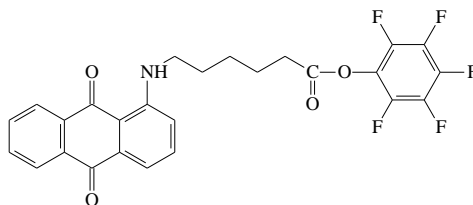
Figure 2.52. **Pentafluorophenyl 6-[(1-anthraquinone)amino]hexanoate (28)**

Pentafluorophenyl 6-[(1-anthraquinone)amino]hexanoate **(28)** [**Figure 2.52**] was chosen

as a model compound for this mini test reaction. It was treated with neat TFA for one

hour, and then it was compared with this OPFP compound without TFA treatment. On

the TLC plate, no differences between this AQ-spacer-OPFP compound before or after

TFA treatment were observed. A further investigation was carried on as well, after TFA

treatment, pentafluorophenyl 6-[(1-anthraquinone)amino]hexanoate **(28)** was reacted

with an available anthraquinone-pentapeptide conjugate, NU:UB 363 **(29)** which has an

amine group at the end of its structure, and then the product was compared with the

product from reaction of this OPFP-spacer-AQ compound without treatment of TFA

reacted with NU:UB 363 **(29)**. TLC results showed both products from these two

reactions were the same, but the reaction products were not completely clean. This

indicated that the OPFP ester bond might survive in neat TFA strong acid condition and

after treatment, the OPFP ester compound could still be functional for further reaction.

Based on this investigation, OPFP succinate Asn-Leu-[PEG Spacer]-AQ ester [YD93]

(30) was synthesised and hopefully it could react with another component that has a free

amino end after this OPFP ester had been treated with neat TFA to remove trityl protecting group on the side chain of asparagine.

In **Scheme 2.7**, it is outlined that initially in the synthesis of Epi-succinyl-dipeptide spacer-anthraquinone compound YD98 **(31)**, it was designed to couple epirubicin with OPFP ester. However, a small-scale reaction ('mini test') showed that OPFP ester YD93 **(30)** was not reactive, so succinyl-dipeptide spacer-anthraquinone compound YD91 **(32)** was deprotected by removing trityl protecting group from asparagine side chain, and then followed by converting it into an OSu ester YD97 **(33)**, which later on was shown to couple with epirubicin successfully, confirmed by its mass spectrum.
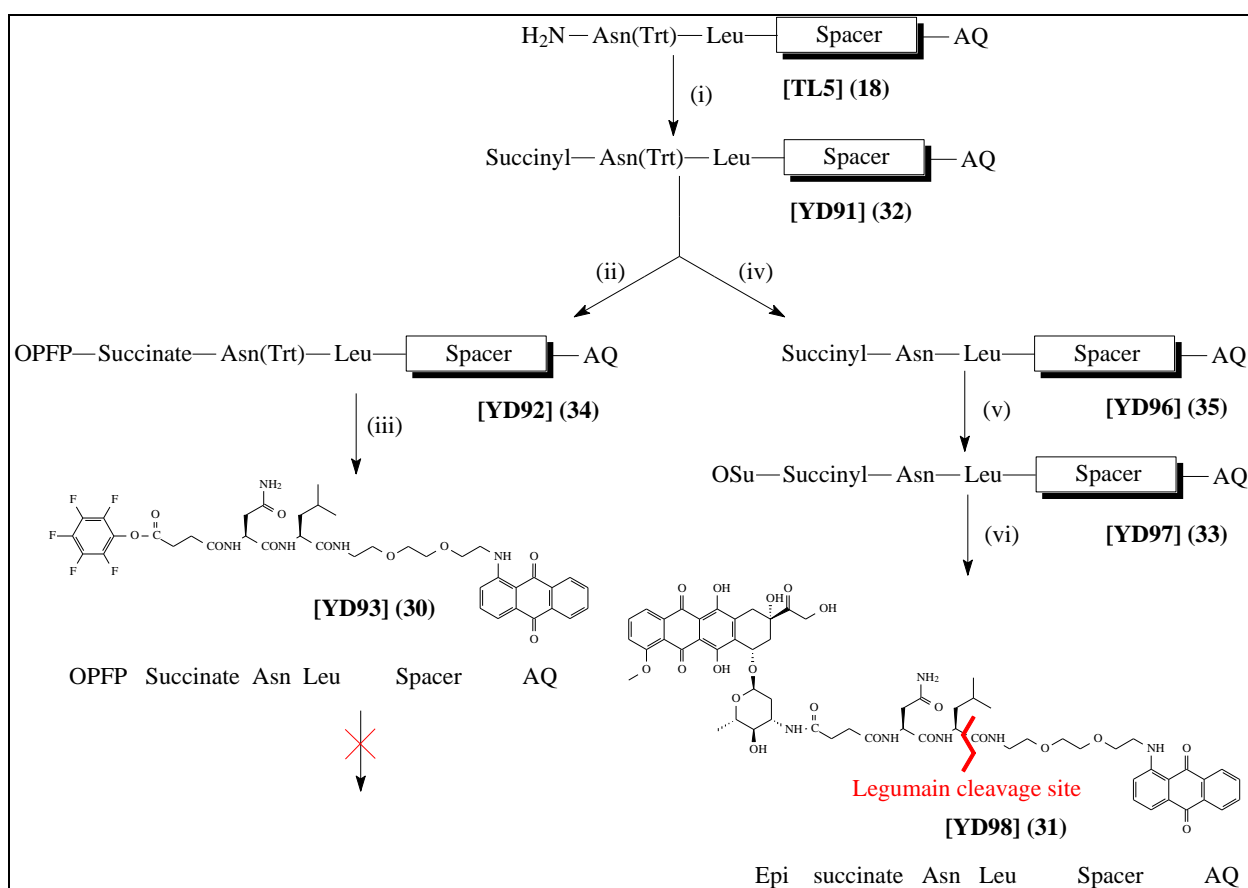
Reagents and conditions: (i) succinic anhydride, DMF, DIPEA, RT, overnight. (ii) DCC, OPFP, DMAP, CH$_2$Cl$_2$, RT, 3h. (iii) TFA, RT, 1h. (iv) TFA, RT, 40min. (v) TSTU, DMAP, DMF, RT, 30min. (vi) Epirubicin hydrochloride, DMF, DIPEA, RT, 1h.

Scheme 2.7. New approach to synthesis of legumain-activated potential clinical prodrug YD98 (31)

191

2.3.5.1 Synthesis of succinate Asn(Trt)-Leu-[PEG Spacer]-AQ [YD 91] (32)
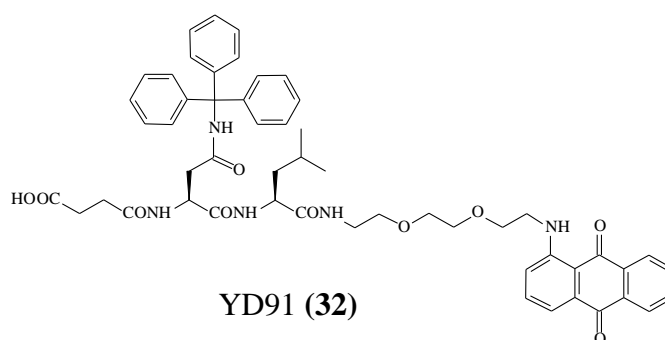
Figure 2.53. Chemical structure of succinate Asn(Trt)-Leu-[PEG Spacer]-AQ YD91 (32)

Succinate Asn(Trt)-Leu-[PEG Spacer]-anthraquinone YD91 **(32)** [**Figure 2.53**] was synthesised by treating Fmoc-Asn(Trt)-Leu-[PEG Spacer]-anthraquinone TL4 **(17)** with 20% piperidine in DMF to remove the Fmoc protecting group from asparagine, then Asn(Trt)-Leu-[PEG Spacer]-anthraquinone TL5 **(18)** was reacted with succinic anhydride in DMF followed by adding DIPEA as base in this reaction [**Scheme 2.7**]. Overnight, after confirmation on TLC plates that this reaction had completed, YD91 **(32)** reaction solution was then added drop wise into a saturated solution of sodium hydrogen sulphate. A dark red precipitate was formed immediately which was then filtered and washed with water, and dried.

2.3.5.2 Synthesis of OPFP succinate Asn-Leu-[PEG Spacer]-AQ ester [YD 93] (30)
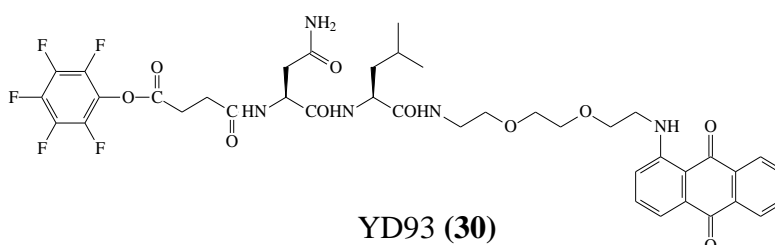
Figure 2.54. Chemical structure of OPFP succinate Asn-Leu-[PEG Spacer]-AQ ester YD93 (30)

Succinate Asn(Trt)-Leu-[PEG Spacer]-anthraquinone YD91 **(32)** [**Figure 2.53**] was reacted with pentafluorophenol in dichloromethane, by using DCC as coupling reagent and DMAP as base in this reaction to form the OPFP succinate Asn(Trt)-Leu-[PEG Spacer]-anthraquinone ester YD92 **(34)**. When the reaction was confirmed by TLC, crystals of DCU were filtered off and the reaction solution was evaporated to dry without any purification. Then this OPFP ester was treated with neat TFA for one hour at room temperature, the progress of this reaction was monitored on TLC plate. When it was finished, TFA was evaporated and the sticky product was treated with diethyl ether to help it to precipitate [**Scheme 2.7**].

Once this OPFP succinate Asn-Leu-[PEG Spacer]-anthraquinone ester YD93 **(30)** [**Figure 2.54**] was dried and collected, it was then reacted with 10-demothoxy-10-(3-aminopropyl)aminocolchicine in DMF, followed by adding DIPEA as base. However, on TLC, it was shown that this reaction did not happen at all because there was no new product spot that was expected to form; only starting material was found on TLC. This may suggest that the OPFP ester did not survive in neat TFA treatment for further reaction.

Instead of treating ester compound in neat TFA conditions while removing trityl protecting group on the side chain of asparagine, the trityl protecting group was removed first, then attempts were made to convert this compound containing unprotected asparagine into an ester. As the study had shown that unprotected asparagine would not survive in the reaction when DCC was present, during synthesis of the OPFP ester, TSTU was applied to convert this succinate Asn-Leu-[PEG Spacer]-anthraquinone to an OSu ester.

2.3.5.3   Synthesis of OSu succinate Asn-Leu-[PEG Spacer]-AQ ester [YD97] (33)
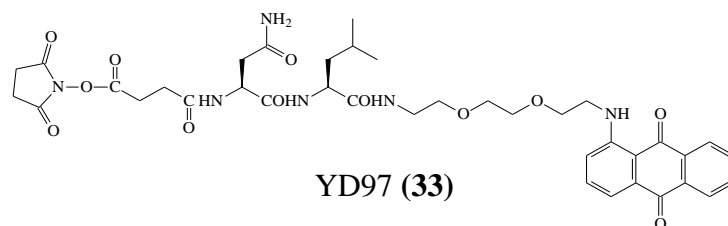
YD97 (33)

Figure 2.55. Chemical structure of OSu succinate Asn-Leu-[PEG Spacer]-AQ ester YD97 (33)

The OSu succinate Asn-Leu-[PEG Spacer]-anthraquinone ester YD97 **(33)** [**Figure 2.55**]

was synthesised by removing the trityl protecting group from YD91 **(32)** [**Figure 2.53**]

in the treatment with neat TFA. Then, the dried dark red product was mixed with TSTU

and DMAP in DMF to form the final OSu ester YD97 **(33)** [**Scheme 2.7**].

2.3.5.4   Synthesis of epirubicin succinate Asn-Leu-[PEG Spacer]-AQ [YD98] (31)
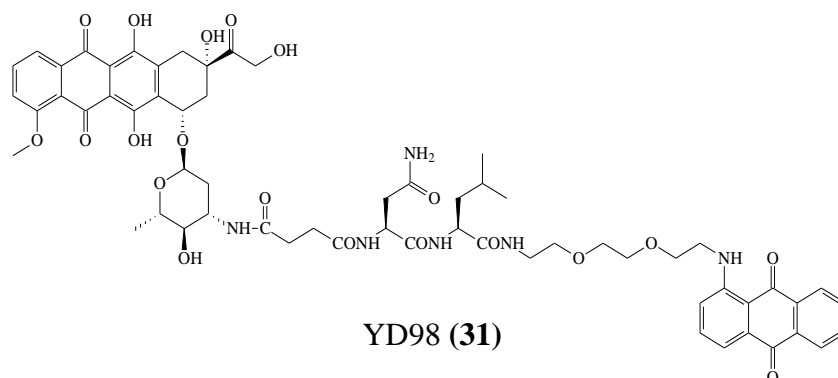
YD98 (31)

Figure 2.56. Chemical structure of Epi-succiniyl-dipeptide spacer-AQ compound YD98 (31)

This model compound epirubicin succinate Asn-Leu-[PEG Spacer]-anthraquinone YD98

(31) [**Figure 2.56**] was synthesised by mixing OSu ester YD97 **(33)** [**Figure 2.55**] with

epirubicin hydrochloride in DMF, followed by adding DIPEA into this reaction mixture.

The progress of this reaction was monitored by TLC. When it was completed, YD98 **(31)**

was purified by applying onto a thick layer silica gel preparative chromatography plate

[**Scheme 2.7**].

Monitoring the preparative plate of YD98 **(31)**, there was only one clear new dark red spot which was formed from this reaction, and also, the mass spectrum [**Figure 2.57**] confirmed this epirubicin succinate Asn-Leu-[PEG Spacer]-anthraquinone YD98 **(31)** structure was correct. The ES(+) mass spectrum displayed a signal at m/z 1207.4707 corresponding to (M+H)$^+$, which confirmed the YD98 **(31)** molecular mass of 1206. Hence, the method of using TSTU to convert the carboxylic acid end of a compound into an OSu ester is an alternative way to couple with epirubicin successfully in a short period time without forming many major by-products.

2.3.5.5   Mass Spectral Characterisation of YD98 (31)

This model compound epirubicin succinate Asn-Leu-[PEG Spacer]-anthraquinone [YD98] **(31)** was characterised by using nanoelectrospay positive ionisation mass spectrometry.
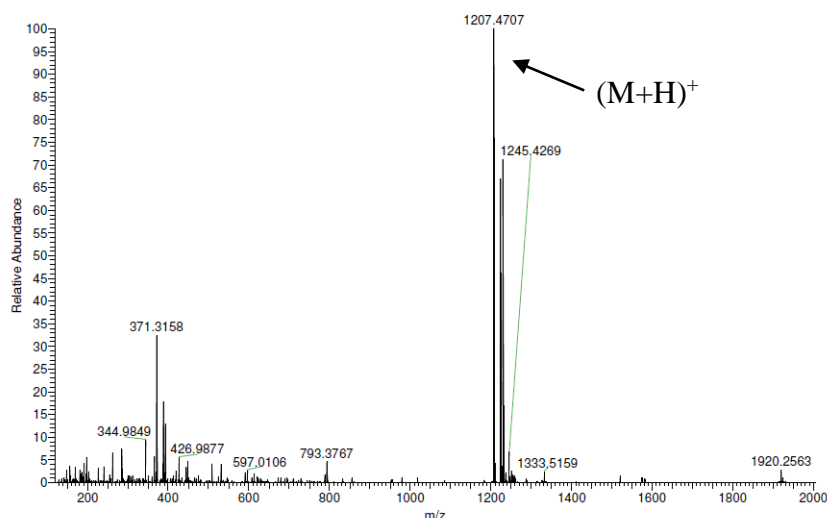
Figure 2.57. Mass Spectrum of YD98 (31)

In the model compound YD98 **(31)** positive ionisation mass spectrum, there was a signal at m/z 1207.4707 (100%) corresponding to (M+H)$^+$, also the theoretical isotope model

matched the observed data which proved the model compound YD98 **(31)** had the correct structure.

Because this model compound reaction having worked very well, carboxyfluorescein-tetra peptide-epirubicin compound YD101 **(36)** [**Figure 2.58**] synthesis was attempted, based on the same synthetic method of making model compound epirubicin succinate Asn-Leu-[PEG Spacer]-anthraquinone YD98 **(31)**.
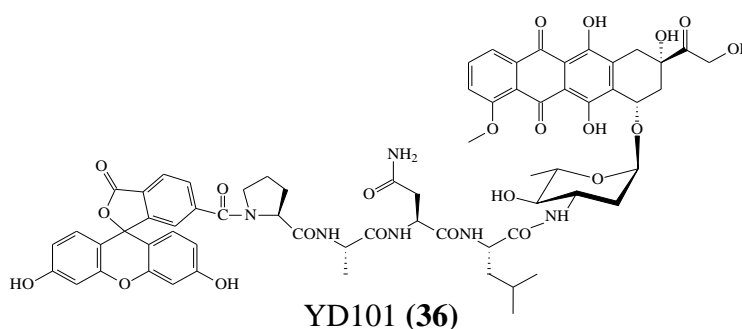
YD101 **(36)**

Figure 2.58. Chemical structure of 5(6)-FAM-Pro-Ala-Asn-Leu-epirubicin [YD101] (36)

In the previous experience gained in this lab, it was not easily feasible to attach 5(6)-carboxyfluorescein **(5)** onto a peptide by using SPPS methods, however, if 5(6)-carboxyfluorescein **(5)** was joined with an amino acid (here, proline) first, then this conjugate would be able to couple onto a peptide by using the SPPS method.
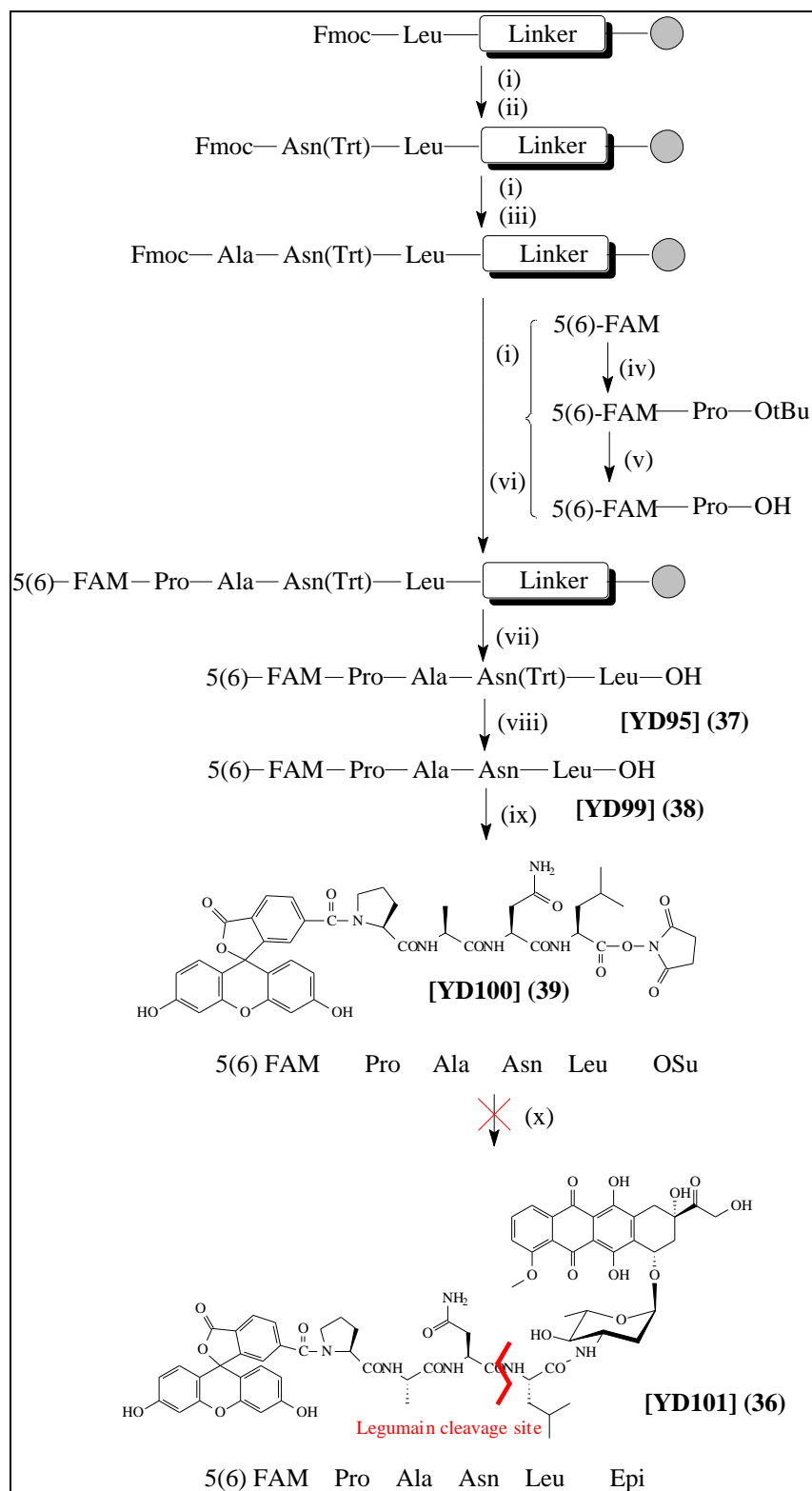
Reagents and conditions: (i) 20% piperidine in DMF, RT, 30min. (ii) Fmoc-Asn(Trt)-OH, PyBOP, DMF, DIPEA, RT, 1h. (iii) Fmoc-Ala-OH, PyBOP, DMF, DIPEA, RT, 1h. (iv) H-Pro-OtBu·HCl, DMF, DIPEA, RT, 2h. (v) TFA, RT, 3h. (vi) 5(6)-FAM-Pro-OH **(53)**, PyBOP, DMF, DIPEA, RT, 2h. (vii) 0.5%~2.5% TFA, RT, 2 days. (viii) TFA, RT, 1.5h. (ix) TSTU, DMAP, DMF, RT, 1.5h. (x) epirubicin hydrochloride, DMF, DIPEA, RT, 1h.

Scheme 2.8. Attempted synthesis of legumain fluorogenic probe/ potential clinical prodrug YD101 (36)

2.3.5.6   Synthesis of 5(6)-FAM-Pro-Ala-Asn(Trt)-Leu-OH [YD95] (37)
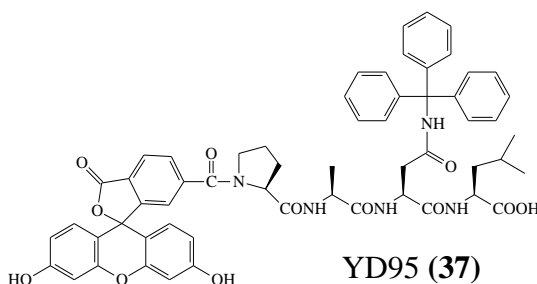
YD95 **(37)**

Figure 2.59. Chemical structure of 5(6)-FAM-tetrapeptide-OH compound YD95 (37)

The tripeptide Ala-Asn-Leu-OH was synthesised by using an SPPS method. Because

unprotected asparagine may undergo a dehydration reaction on the side chain through the

SPPS process and normal coupling reactions, Fmoc-Asn(Trt)-OH was applied during this

tripeptide synthesis. Because common SPPS resins, such as Wang resins, require high

concentration of TFA at the very last stage to cleave off the peptide from resins, and in

order to keep the trityl protection group on the side chain of asparagine through the

cleavage stage during the SPPS process, NovaSyn®TGT resins **(40)** [**Figure 2.60**] were

applied.
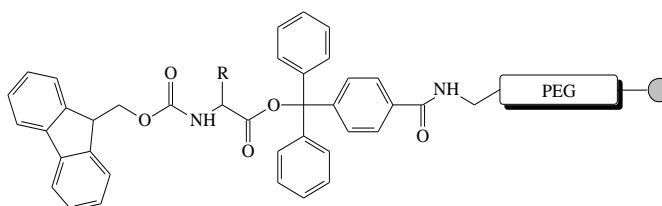
Figure 2.60. NovaSyn®TGT resins (40)

Peptides attached to NovaSyn®TGT resins **(40)** can be cleaved off by treatment with 0.5%

TFA in dichloromethane to give protected peptide compounds without harming sensitive

side chain protecting groups. However, the downside of NovaSyn®TGT resins **(40)** is that

normally the first amino acid loading on this kind of resins is quite low, around 0.1-

0.3mmol/g. On appositive note, due to low loading on NovaSyn®TGT resins **(40)**, amino acids or peptides could 'spread out' on the surface of each resin bead easily and give more space for the in-coming amino acids to attach efficiently, and this could make peptide synthesis on this kind of resin easier when compared with high loading resins.

Once the yellow fluo-protected, 5(6)-FAM-Pro-OH **(41)** had coupled onto Ala-Asn(Trt)-Leu-OH tripeptide, the typical colour test reagents would not be suitable for the detection of un-reacted tripeptide. This is because the red colour test reagent [pentafluorophenyl-6-((1-anthraquinone)amino)hexanoate] **(28)**, an OPFP ester, could react with two phenol groups on 5(6)-carboxyfluorescein **(5)** and then show red colour on the resin beads to give a false indication that this coupling has not completed yet. Given the trityl protecting group on the side chain of asparagine is UV active under UV light, which will show a dark spot, the completion of this final 5(6)-FAM-Pro-OH **(41)** coupling onto peptide-resin was monitored by taking a few beads from the SPPS reaction vessel, treating them with 0.5% TFA in dichloromethane to cleave everything off from the resin beads, spotting the solution onto a TLC plate and checking under UV light to see if there was any dark UV active spot that had no fluorescence at all on the bottom of the TLC plate. The dark UV active spot with no fluorescence indicated uncoupled tripeptide Ala-Asn(Trt)-Leu-OH, so if the coupling of 5(6)-FAM-Pro-OH **(41)** onto NovaSyn®TGT resins **(40)** containing tripeptide Ala-Asn(Trt)-Leu-OH had completed, there should be only one yellow fluorescent spot appearing on the TLC plate under UV light without any trace of dark spot on the bottom. When the coupling reaction was completed, yellow resin beads were then first treated with 0.5% TFA in dichloromethane every 20 minutes, however, a few hours later, fractions from the SPPS vessel still showed spots with very strong yellow

fluorescence, so the percentage of TFA in dichloromethane was then increased up to 2.5%.

After almost two days of TFA treatment to cleave 5(6)-FAM-Pro-Ala-Asn(Trt)-Leu-OH

YD99 **(38)** off from NovaSyn®TGT resins **(40)**, the resin beads were still yellow, however,

the fractions from SPPS vessel showed a very week yellow colour. Then all fractions

were combined and evaporated to dryness [**Scheme 2.8**].

2.3.5.7   Synthesis of 5(6)-FAM-Pro-Ala-Asn-Leu-OSu ester [YD100] (39)
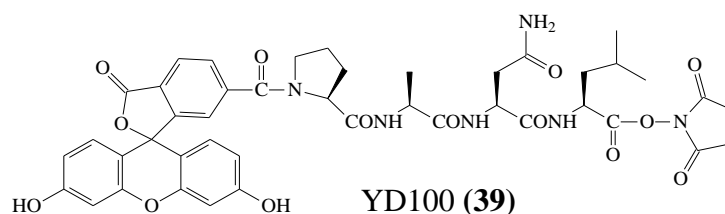
YD100 **(39)**

Figure 2.61. Chemical structure of 5(6)-FAM-tetrapeptide-OSu ester YD100 (39)

After cleavage from resin beads and evaporation to dryness, 5(6)-FAM-tetrapeptide YD

95 **(37)** [**Figure 2.59**] was then treated with neat TFA to remove the side chain trityl

protecting group on asparagine. The structure of this free side chain tetrapeptide, 5(6)-

FAM-Pro-Ala-Asn-Leu-OH YD99 **(38)** was confirmed by it ES(-) mass spectrum which

displayed a signal at m/z 770.2667 for the fragment (M-H)⁻ [**Figure 2.62**].
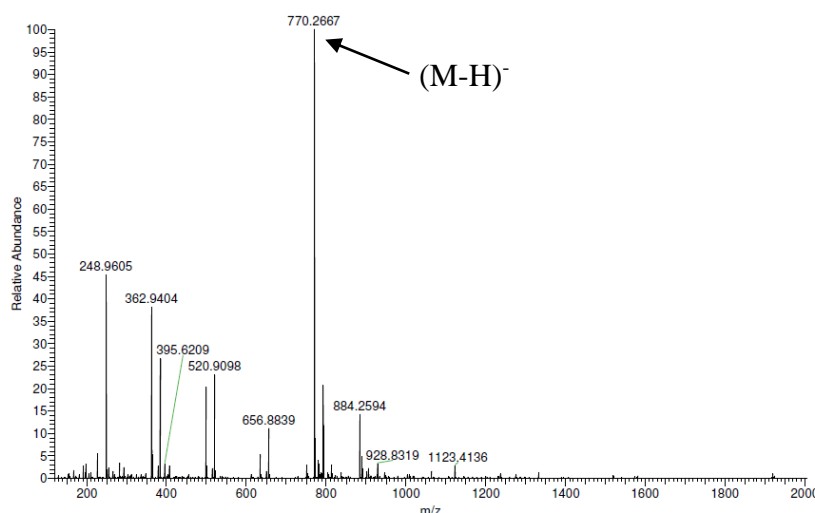
Figure 2.62. Mass Spectrum of free side chain 5(6)-FAM-Pro-Ala-Asn-Leu-OH YD99 (38)

This deprotected conjugate was then reacted with TSTU in DMF by using DMAP as base

in this reaction, based on the successful synthesis of the OSu succinate Asn-Leu-[PEG

Spacer]-anthraquinone ester YD97 **(33)**, to synthesise 5(6)-FAM-tetrapeptide-OSu ester

YD100 **(39)** [**Figure 2.61**], [**Scheme 2.8**].

2.3.5.8   Attempted synthesis of 5(6)-FAM-Pro-Ala-Asn-Leu-epirubicin [YD101] (36)
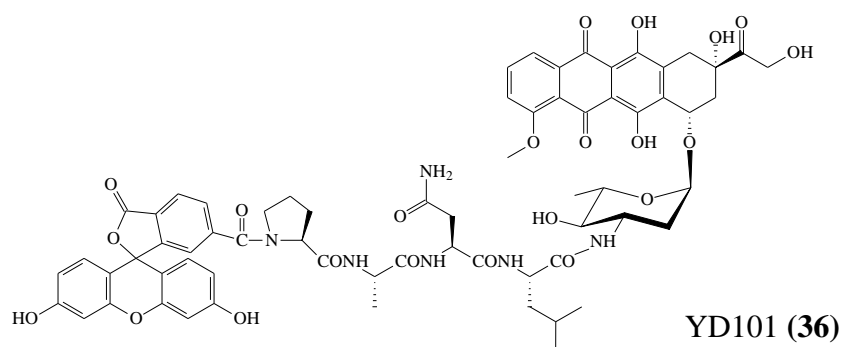
YD101 **(36)**

Figure 2.63. Chemical structure of 5(6)-FAM-Pro-Ala-Asn-Leu-epirubicin YD101 (36)

5(6)-FAM-Pro-Ala-Asn-Leu-OSu YD100 **(39)** [**Figure 2.61**] was mixed with epirubicin

hydrochloride in DMF, followed by adding DIPEA as base into this reaction [**Scheme

2.8**]. One hour later, the progress of this reaction was checked on TLC, which showed a

few new spots and among those new spots, there was a very strong orange spot which

suggested that it could be the target compound. This assumed orange 'correct' compound

was purified by thick layer chromatography. However, this chromatographically pure

orange compound from thick TLC plate was later on proved not to be the correct

compound as had been expected. When it was incubated with legumain, there was no sign

of fluorescence that released; when it was treated with proteinase K, fluorescence

intensity was barely increased. From the UV-Vis spectrum, it indicated that a fluorescein-

based fluorophore was not a part of the structure of this orange compound isolated.

2.3.5.9   Synthesis of Boc-Asn-[Propyl Spacer]-anthraquinone: investigation into suitable methods for coupling side-chain unprotected asparagine

A previous attempt to couple side chain unprotected Boc-Asparagine-OH to the propyl spacer-anthraquinone compound resulted in formation of the dehydration product [AT26] **(42)** [**Figure 2.64**]. The reaction conditions were: Boc-Asn-OH, DCC, pentafluorophenol in ethyl acetate to give the OPFP active ester which was then reacted with the AQ-propyl spacer in DMF to give the dehydration product, AT26 **(42)** [Note: The asparagine conjugate was successfully synthesised by use of Fmoc-Asn(Trt)-OH] (Turnbull, 2003).
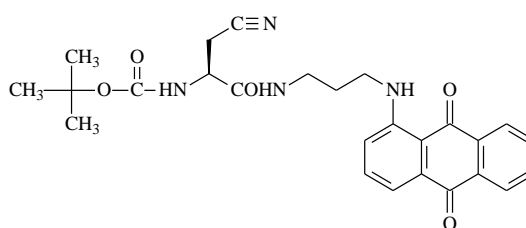
Figure 2.64. **Dehydration product AT26 (42)**

Merck synthesis notes report that it is possible to incorporate asparagine without side chain protection and that formation of the undesirable dehydration product (nitrile) can be minimised by addition of HOBt to the coupling reaction (this side reaction occurs with many different coupling agents i.e. PyBOP, HBTU, carbodiimides).

Although coupling of epirubicin to anthraquinone-peptides containing side-chain unprotected asparagine was achieved using TSTU, this method has proved to be problematic with carboxyfluorescein derivatives, hence, the need to investigate the use of alternative peptide coupling methods. Previously, we have successfully coupled epirubicin to *N*-protected peptides using standard TBTU, HOBt, DIPEA methods

(DiSalvo, 2004). The epirubicin-peptide conjugates were obtained in reasonable yield (30-50%) and we have also shown that standard TBTU, HOBt, DIPEA coupling methods are compatible with carboxyfluorescein.
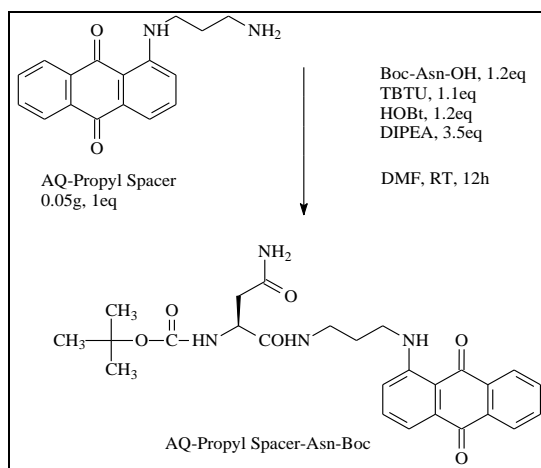
Scheme 2.9. Synthesis of Boc-Asn-[Propyl Spacer]-anthraquinone

After 12 hours, there was little evidence on TLC of any product formation; additional reagents were added and DIPEA was added from a newly opened bottle, TLC (chloroform: methanol, 9:1) showed formation of a major new product with very little formation of the dehydration product [AT26] **(42)**. The product was purified by solvent extraction and column chromatography. The column (2.2cm×12cm) was prepared using chloroform and eluted using gradient elution with chloroform and ethyl acetate by increasing ratio from 9:1 to 4:1, additional methanol was added to increase solvent polarity.

2.3.5.10   Synthesis   of   5(6)-FAM-β-Ala-Pro-Ala-Gly-Nva-Pro-Asn-[Propyl Spacer]-AQ [YD103] (43)
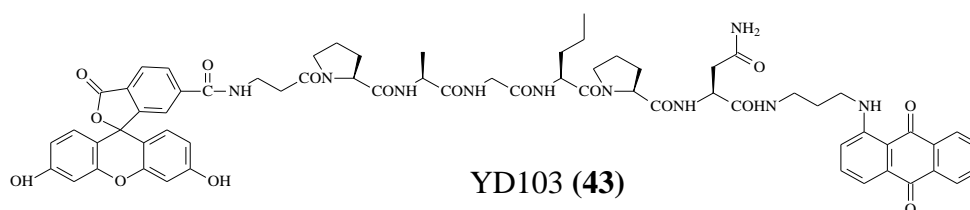
YD103 **(43)**

Figure 2.65. Chemical structure of 5(6)-FAM-heptapeptide-spacer-AQ YD103 (43)

Boc—Asn—OH   Propyl Spacer AQ

(i)

Boc—Asn—[Spacer]—AQ

(ii)

NH₂

Legumain cleavage site

[YD103] (43)

5(6) FAM   β–Ala   Pro   Ala   Gly   Nva   Pro   Asn   Spacer   AQ
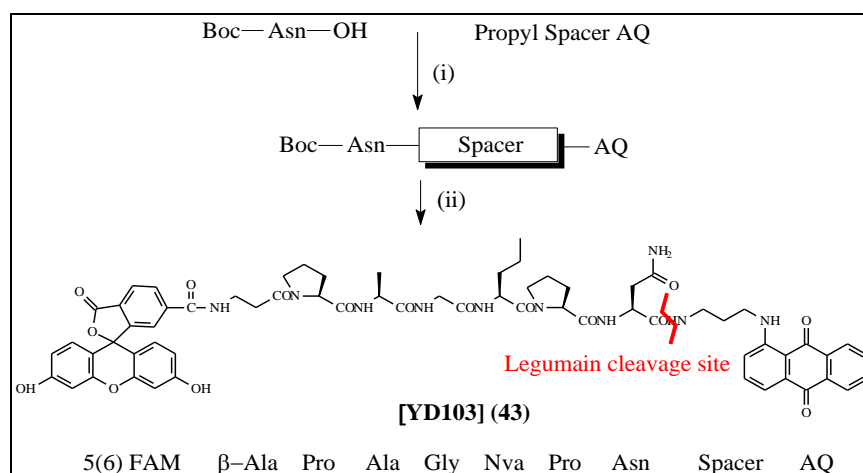
Reagents and conditions: (i) TBTU, HOBt, DIPEA, DMF, RT, 12h. (ii) 5(6)-FAM-β-Ala-Pro-Ala-Gly-Nva-Pro-OH, TBTU, HOBt, DIPEA, DMF, RT, 1h.

Scheme 2.10. Synthesis of 5(6)-FAM-heptapeptide-spacer-AQ YD103 (43)

There are two motivations to synthesise this fluoro-peptide-propyl spacer-AQ compound YD103 **(43)**. First, it was designed to prove that a fluorophore peptide conjugate can couple onto an unprotected asparagine compound by using standard TBTU, HOBt, DIPEA coupling methods; second, in most papers, the authors mentioned that legumain has the specific cleavage spot at the carboxyl end of asparagine (Chen *et al.*, 1998; Chen *et al.*, 2000; Stern *et al.*, 2009) and there was always an extra amino acid at the P1' position (usually Leucine) (Liu *et al.*, 2003), however, they did not discuss if the presence of extra amino acid at the P1' position or the peptide chain has more than four amino acids is necessary or crucial during legumain cleavage.

Asn-[Propyl Spacer]-AQ TFA salt was dissolved in DMF and treated with DIPEA first, to convert this TFA salt to a free base compound, then it was mixed with 5(6)-FAM-β-Ala-Pro-Ala-Gly-Nva-Pro-OH. This reaction was kept at room temperature for 1h. The final compound was extracted with chloroform and water, and purified by loading onto a thick layer chromatography plate.

2.3.5.10.1   Mass Spectral Characterisation of YD103 (43)

5(6)-FAM-heptapeptide-spacer-AQ YD103 **(43)** was analysed by nanoelectrospray

ionisation in both negative and positive modes. It was shown that negative ion mode was

preferred to positive ion mode for YD103 **(43)**.
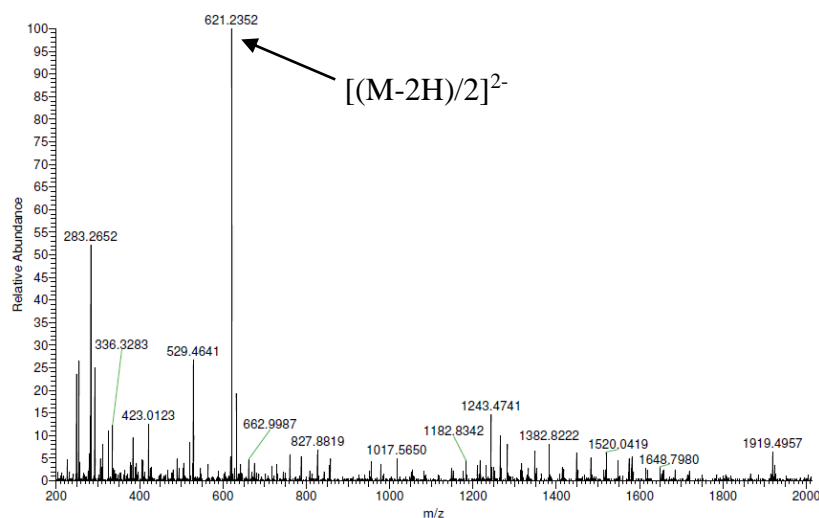
Figure 2.66. Nanoelectrospray Negative Ionisation Mass Spectrum of YD103 (43)
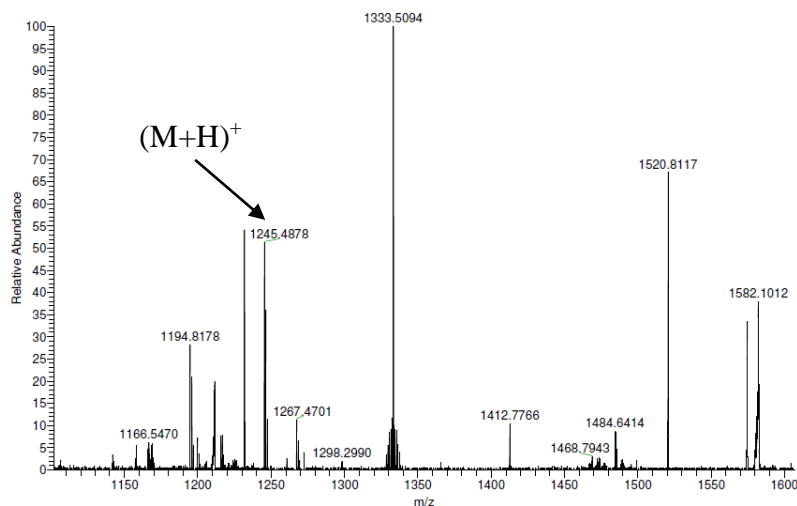
Figure 2.67. Nanoelectrospray Positive Ionisation Mass Spectrum of YD103 (43)

In the nanoelectrospray negative ionisation mass spectrum [**Figure 2.66**], a strong

doubly-charged signal at m/z 621.2352 (100%) which indicated $[(M-2H)/2]^{2-}$ had been

detected; whereas in the nanoelectrospray positive ionisation mass spectrum [**Figure

2.67**], a signal $(M+H)^+$ corresponding to the singly-charged ion at m/z 1245.4878 was

205

also found. So, both of these two mass spectra proved YD103 **(43)** was the correct target structure.

2.3.5.10.2 <u>YD103 (43) Fluorimetric Assay</u>

The ability of YD103 **(43)** that it can be cleaved by activated legumain at the carboxyl end of asparagine in order to release fluorescence was determined by fluorimetric assay.

During fluorimetric assay, after incubating with activated legumain at 37°C, YD103 **(43)** showed similar result [**Figure 2.68**] to TL11 **(3)** fluorimetric assay. In the first 20 minutes, the graph was quite linear; and after 55 minutes, the increase of fluorescence intensity was very low and the graph started to reach a plateau. This indicated that YD103 **(43)** can be cleaved by legumain at the carboxyl end of asparagine. The results from YD103 **(43)** fluorimetric assay showed that even though there was no amino acid at the P1' position on the substrate and there were up to seven amino acids in the substrate peptide chain, legumain can still cleave at the *C*-end of asparagine.
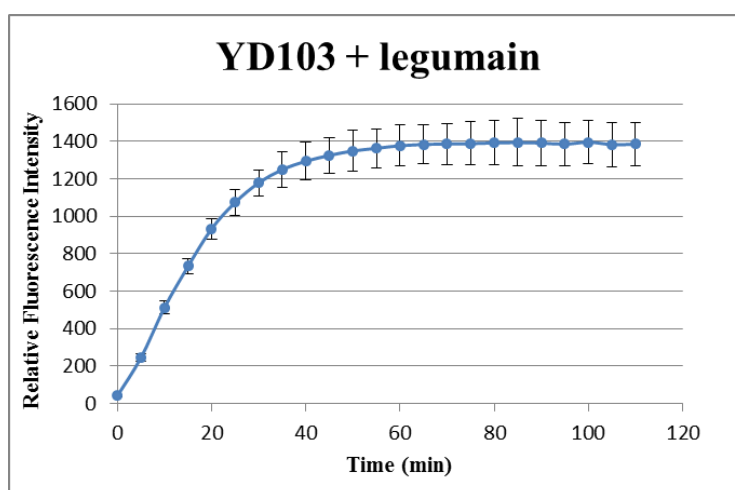
Figure 2.68. **Relative fluorescence intensity release with time from the incubation of legumain probe (YD103) (43) (10 μM) with recombinant human legumain (40ng) in legumain assay buffer, pH 5.0, λex 492nm, λem 520nm (Mean values ± SD from triplicates from one experiment are presented).**

After fluorimetric assay, additional YD103 **(43)** was mixed and incubated with additional legumain at 37°C overnight. The next day, this mixture was extracted (partitioned) between chloroform and water. The chloroform layer was kept and checked by TLC, along with an authentic sample of [Propyl Spacer]-AQ compound. (chloroform:methanol 9:1) $R_f = 0.14$; Red. On the TLC plate, it was shown that the extracted compound from the chloroform layer was the same as [Propyl Spacer]-AQ compound, in further confirmation of the position of the legumain 'cleavage hotspot'.
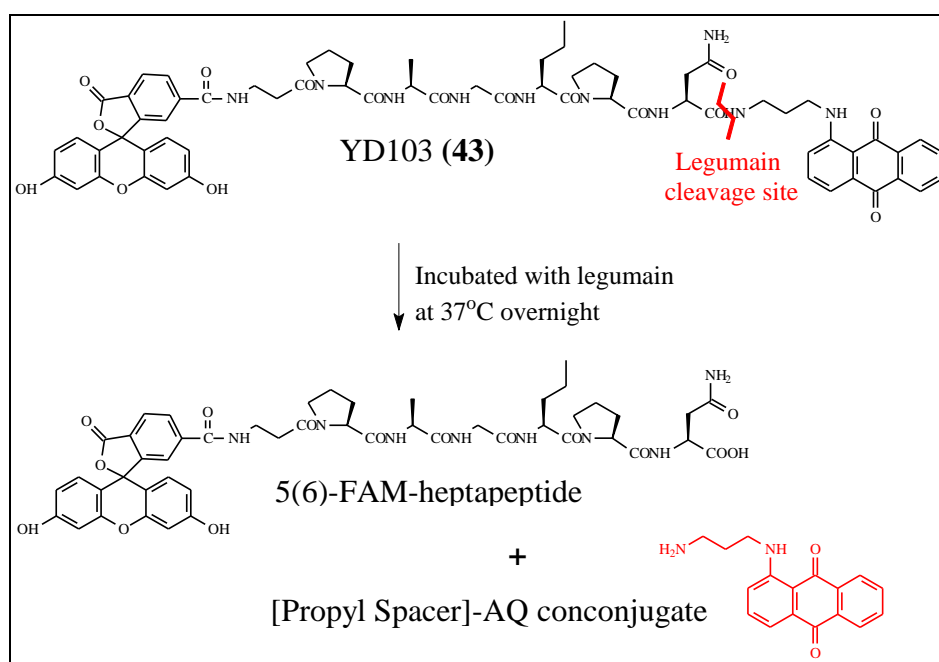
Scheme 2.11. **Cleavage of YD103 (43) at the carboxyl end of asparagine by legumain.**

This confirmed that after cleavage by legumain, YD103 **(43)** generated the two anticipated compounds, 5(6)-FAM-heptapeptide and [Propyl Spacer]-AQ conjugate [**Scheme 2.11**].

2.4 <u>CONCLUSION</u>

Legumain is overexpressed by tumour cells and can only be activated in acidic conditions, such as the tumour microenvironment, also it requires highly specific substrate, and all of these features suggest that legumain could be a perfect potential target for anti-cancer prodrug development and a unique sensitive tumour biomarker for early stage detection. Motivated by evidence in recent studies that legumain is an attractive target, the fluorogenic probe TL11 (**3**) was designed as a substrate for the potential breast cancer biomarker legumain, which specifically cleaves peptides at the carboxyl side of asparagine. In the intact fluorogenic conjugate, fluorescence from 5(6)-carboxyfluorescein (**5**) was quenched by the anthraquinone residue [**Figure 2.35**]. The fluorophore quenching study showed that probe TL11 (**3**) had almost no fluorescence, which indicated that it is a good FRET probe for fluorimetric assay. After cleavage by legumain at the cleavage 'hot spot' Asn↓-Leu, fluorescence from 5(6)-carboxyfluorescein (**5**) can be released and detected again [**Figure 2.34**]. Fluorimetric assay showed rapid fluorescence release and the relative fluorescence intensity released from probe TL11 (**3**) reached maximum in less than 2 hours. Importantly, fluorescence release with time was linear across the first 10 minutes.

An amino acid at the P3 position in a legumain substrate is not necessarily compulsory for a good fit into the active site; however, legumain enzyme kinetics assay for probe TL11 (**3**), VG (**10**) and PN11 (**11**) indicated that having proline fits in the P3 position of legumain substrate will enhance binding affinity between legumain and its substrate.

208

Fluorimetric assay for probes TL11 (**3**), AD17 (**8**), AD20 (**9**) and VG (**10**), concluded that the favoured choice for the P2 position in a substrate tetrapeptide is Ser>Ala>Thr≥Gly. Also YD103 (**43**) fluorimetric assay revealed the P1' position is not essential to afford a substrate as well. Thus, a legumain substrate with a peptide sequence that ends at the P1-asparagine carboxyl side can still be recognised and cleaved off by legumain as long as it contains at least four amino acids.

Results from fluorimetric assay showed that all 5(6)-FAM labelled probes performed much better than FITC labelled probes during the same period of incubation with activated legumain. Maximum fluorescence intensity released from 5(6)-FAM labelled probes (at $10\,\mu$M concentration) were between 2000 to 3000RFI, however, from FITC labelled probes were in the order of 400RFI. It had been noticed that even though two different fluorophores had been chosen for these two kinds of probes, the fluorescence intensity released from the same concentration of comparator fluorophores, 5(6)-FAM (**5**) and FITC (**4**) under the same conditions were very similar. Hence, results from 5(6)-FAM labelled probes and FITC (**4**) labelled probes were comparable. When comparing fluorimetric assay results between TL11 (**3**), FF (**6**) and MK8 (**7**) probes, the large fluorescence intensity released from TL11 (**3**) may suggest that having proline at the P3 position in the substrate peptide can greatly improve the cleavage rate between substrate and activated legumain, in common with the observations by Sexton and colleagues (Sexton *et al.*, 2007).

During attempts to find an alternative way of synthesising fluoro-tetrapeptide-epirubicin YD101 **(36)**, the success of making epirubicin succinate Asn-Leu-[PEG Spacer]-AQ YD98 **(31)** illustrated a new approach to couple epirubicin with an OSu ester instead of a OPFP ester. The synthesis of an OSu ester which can use DMF as solvent and does not require DCC, was superior to using OPFP esters. However, the failure to make the fluoro-tetrapeptide-epirubicin YD101 **(36)** remains unresolved.

2.5   <u>FUTURE WORK</u>

The future work can focus on cloning/*in vitro* metabolism studies (HPLC methods) using recombinant enzymes (i.e. legumain) and tissue homogenates with a series of prodrugs that are based on fluorogenic probe TL11 **(3)** containing anticancer agents to optimise delivery, activation and release of the active agent(s).

2.6 **STRUCTURE LIBRARY**
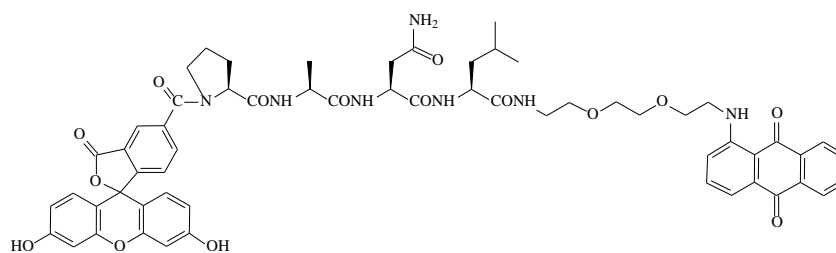
5(6)-FAM-Pro-Ala-Asn-Leu-[PEG Spacer]-AQ [TL11] **(3)**

1-{2-[2-(2-(*N*-5(6)-carboxyfluoresceinylcarbonyl-L-prolyl-L-alanyl-L-asparaginyl-L-leucylamino)ethoxy)ethoxy]ethylamino}anthracene-9,10-dione
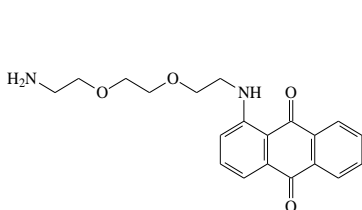
[PEG Spacer]-AQ [TL1] **(14)**

1-{2-[2-(2-aminoethoxy)ethoxy]ethylamino}anthracene-9,10-dione
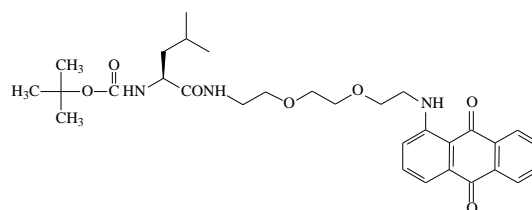
Boc-Leu-[PEG Spacer]-AQ [TL2] **(15)**

1-{2-[2-(2-(*N*-tertiarybutoxycarbonyl-L-leucylamino)ethoxy)ethoxy]ethylamino}anthracene-9,10-dione
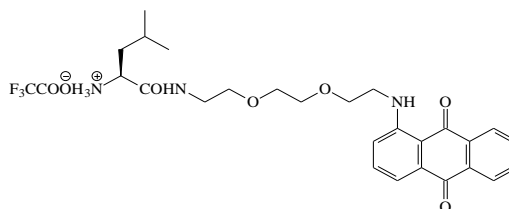
H-Leu-[PEG Spacer]-AQ trifluoroacetate salt [TL3] **(16)**

1-{2-[2-(2-(L-leucylamino)ethoxy)ethoxy]ethylamino}anthracene-9,10-dione trifluoroacetate
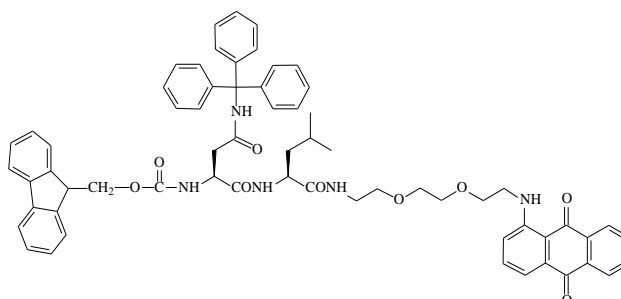
Fmoc-Asn(Trt)-Leu-[PEG Spacer]-AQ [TL4] **(17)**

1-{2-[2-(2-(*N*α-(9-fluorenylmethoxycarbonyl)-*N*γ-trityl-L-aspaginyl-L-leucylamino)ethoxy)ethoxy]ethylamino}anthracene-9,10-dione
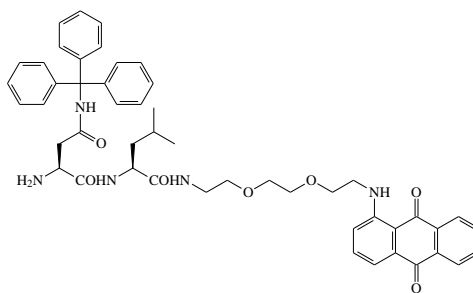
H-Asn(Trt)-Leu-[PEG Spacer]-AQ [TL5] **(18)**

1-{2-[2-(2-(*N*γ-trityl-ʟ-aspaginyl-ʟ-leucylamino)ethoxy)ethoxy]ethylamino}anthracene-9,10-dione
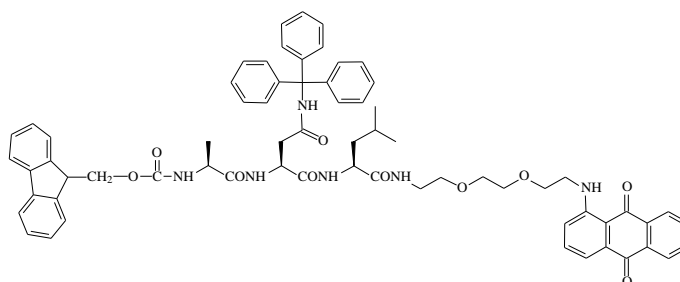
Fmoc-Ala-Asn(Trt)-Leu-[PEG Spacer]-AQ [TL6] **(19)**

1-{2-[2-(2-(*N*α-(9-fluorenylmethoxycarbonyl)-ʟ-alanyl-*N*γ-trityl-ʟ-aspaginyl-ʟ-leucylamino)ethoxy)ethoxy]ethylamino}anthracene-9,10-dione

H-Ala-Asn(Trt)-Leu-[PEG Spacer]-AQ [TL7] **(20)**

1-{2-[2-(2-(ʟ-alanyl-*N*γ-trityl-ʟ-aspaginyl-ʟ-leucylamino)ethoxy)ethoxy]ethylamino}anthracene-9,10-dione

Fmoc-Pro-Ala-Asn(Trt)-Leu-[PEG Spacer]-AQ [TL8] **(21)**

1-{2-[2-(2-(*N*α-(9-fluorenylmethoxycarbonyl)-ʟ-prolyl-ʟ-alanyl-*N*γ-trityl-ʟ-aspaginyl-ʟ-leucylamino)ethoxy)ethoxy]ethylamino}anthracene-9,10-dione
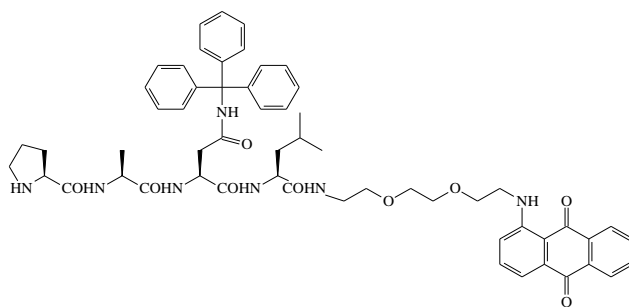
H-Pro-Ala-Asn(Trt)-Leu-[PEG Spacer]-AQ [TL9] **(22)**

1-{2-[2-(2-(L-prolyl-L-alanyl-*N*γ-trityl-L-aspaginyl-L-leucylamino)ethoxy)ethoxy]ethylamino}anthracene-9,10-dione
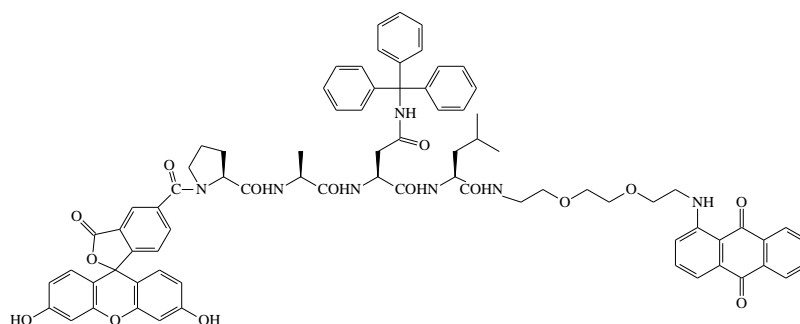
5(6)-FAM-Pro-Ala-Asn(Trt)-Leu-[PEG Spacer]-AQ [TL10] **(23)**

1-{2-[2-(2-(*N*-5(6)-carboxyfluoresceinylcarbonyl-L-prolyl-L-alanyl-*N*γ-trityl-L-asparaginyl-L-leucylamino)ethoxy)ethoxy]ethylamino}anthracene-9,10-dione
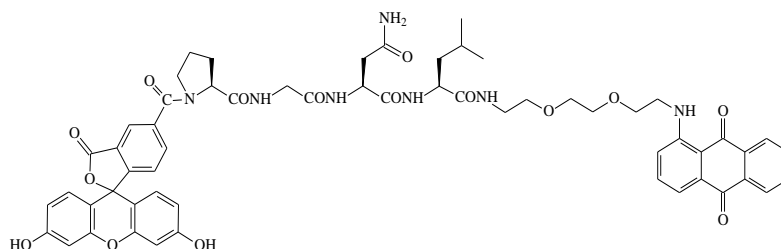
5(6)-FAM-Pro-Gly-Asn-Leu-[PEG Spacer]-AQ [AD17] **(8)**

1-{2-[2-(2-(*N*-5(6)-carboxyfluoresceinylcarbonyl-L-prolyl-glycyl-L-asparaginyl-L-leucylamino)ethoxy)ethoxy]ethylamino}anthracene-9,10-dione
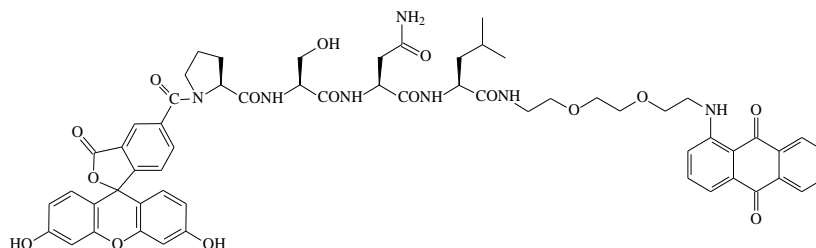
5(6)-FAM-Pro-Ser-Asn-Leu-[PEG Spacer]-AQ [AD20] **(9)**

1-{2-[2-(2-(*N*-5(6)-carboxyfluoresceinylcarbonyl-L-prolyl-L-seryl-L-asparaginyl-L-leucylamino)ethoxy)ethoxy]ethylamino}anthracene-9,10-dione
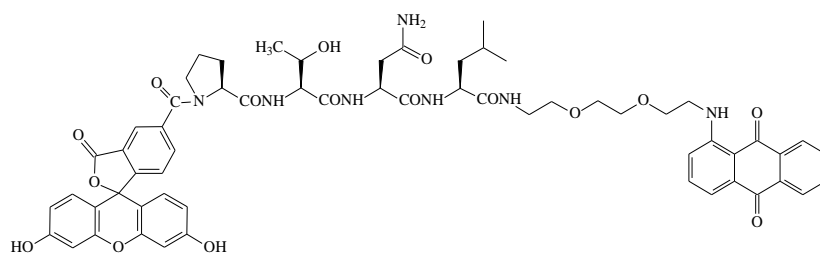
5(6)-FAM-Pro-Thr-Asn-Leu-[PEG Spacer]-AQ [VG] (10)

1-{2-[2-(2-(*N*-5(6)-carboxyfluoresceinylcarbonyl-L-prolyl-L-threonyl-L-asparaginyl-L-leucylamino)ethoxy)ethoxy]ethylamino}anthracene-9,10-dione
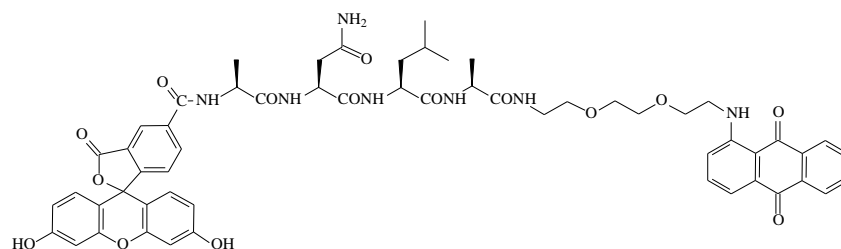
5(6)-FAM-Ala-Asn-Leu-Ala-[PEG Spacer]-AQ [PN11] (11)

1-{2-[2-(2-(*N*-5(6)-carboxyfluoresceinylcarbonyl-L-alanyl-L-asparaginyl-L-leucyl-L-alanylamino)ethoxy)ethoxy]ethylamino}anthracene-9,10-dione
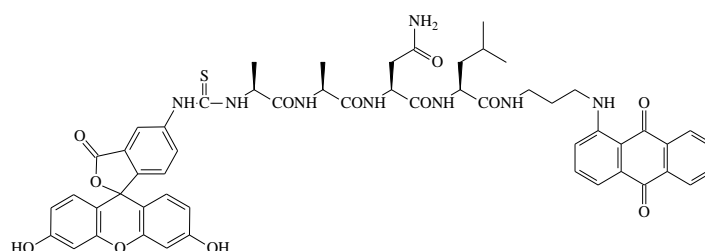
FITC-Ala-Ala-Asn-Leu-[Propyl Spacer]-AQ [FF] (6)

1-[3-(fluoresceinylthioureido-L-alanyl-L-alanyl-L-asparaginyl-L-leucylamino)propylamino]anthracene-9,10-dione
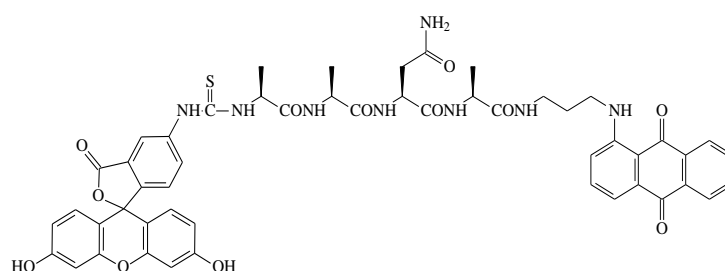
FITC-Ala-Ala-Asn-Ala-[Propyl Spacer]-AQ [MK8] (7)

1-[3-(fluoresceinylthioureido-L-alanyl-L-alanyl-L-asparaginyl-L-alanylamino)propylamino]anthracene-9,10-dione
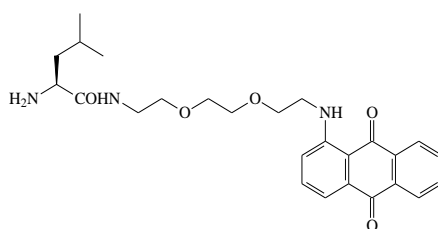
H-Leu-[Propyl Spacer]-AQ **(25)**

1-{2-[2-(2-(ʟ-leucylamino)ethoxy)ethoxy]ethylamino}anthracene-9,10-dione
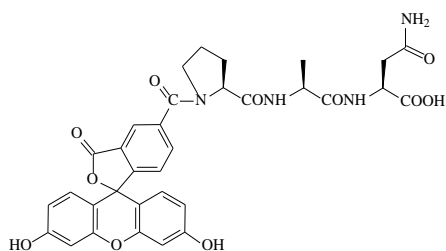
5(6)-FAM-Pro-Ala-Asn-OH **(26)**

N-[5(6)-carboxyfluoresceincarbonyl]-ʟ-prolyl-ʟ-alanyl-ʟ-asparagine
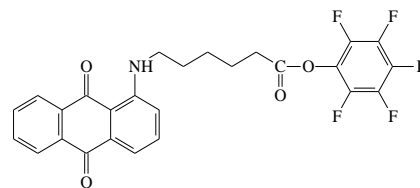
Pentafluorophenyl 6-[(9,10-dioxo-9,10-dihydroanthracen-1-yl)amino] hexanoate **(28)**
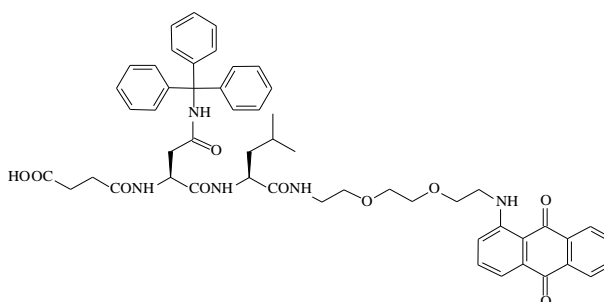
Succinate Asn(Trt)-Leu-[PEG Spacer]-AQ [YD 91] **(32)**

1-{2-[2-(2-(*N*α-succinyl-*N*γ-trityl-ʟ-asparaginyl-ʟ-leucylamino)ethoxy)ethoxy]ethylamino}anthracene-9,10-dione
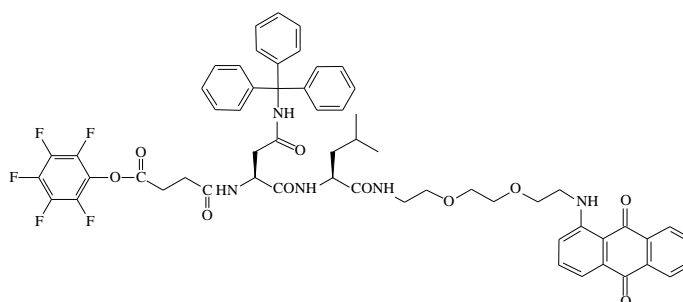
OPFP succinate Asn(Trt)-Leu-[PEG Spacer]-anthraquinone ester [YD92] **(34)**

1-{2-[2-(2-(*N*α-succinyl-*N*γ-trityl-ʟ-asparaginyl-ʟ-leucylamino)ethoxy)ethoxy]ethylamino}anthracene-9,10-dione pentafluorophenolate
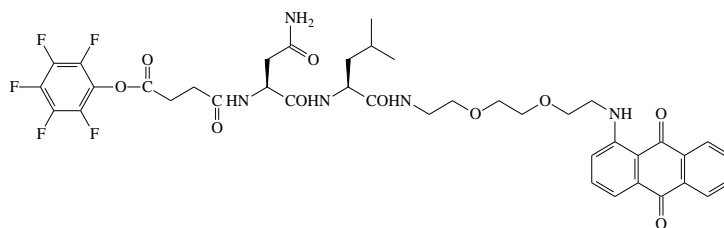
OPFP succinate Asn-Leu-[PEG Spacer]-anthraquinone ester [YD93] **(30)**

1-{2-[2-(2-(*N*α-succinyl-L-asparaginyl-L-leucylamino)ethoxy)ethoxy]ethylamino anthracene-9,10-dione}pentafluorophenolate
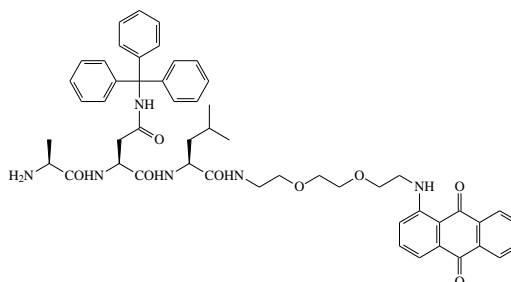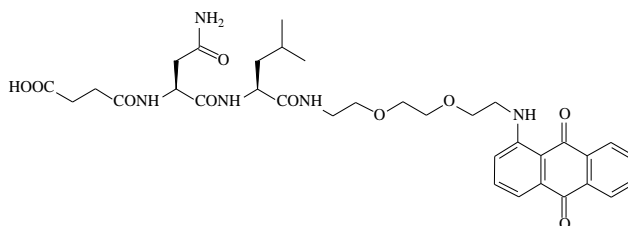

Succinate Asn-Leu-[PEG Spacer]-AQ [YD96] **(35)**

1-{2-[2-(2-(*N*α-succinyl-L-asparaginyl-L-leucylamino)ethoxy)ethoxy]ethylamino}anthracene-9,10-dione
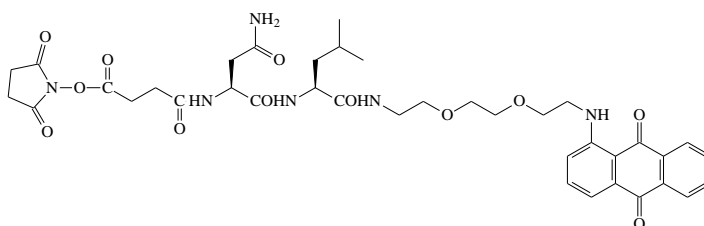
OSu succinate Asn-Leu-[PEG Spacer]-AQ ester [YD97] **(33)**

1-{2-[2-(2-(*N*α-succinyl-L-asparaginyl-L-leucylamino)ethoxy)ethoxy]ethylamino}anthracene-9,10-dione *N*-hydroxysuccinimide
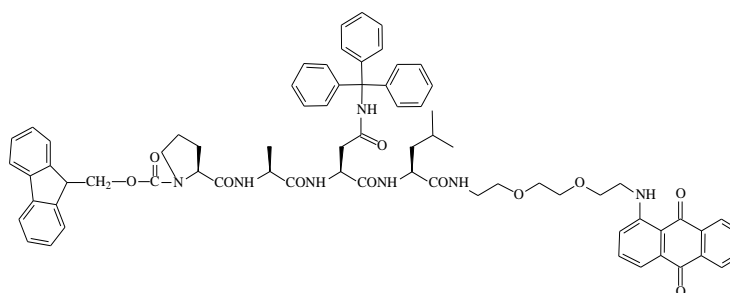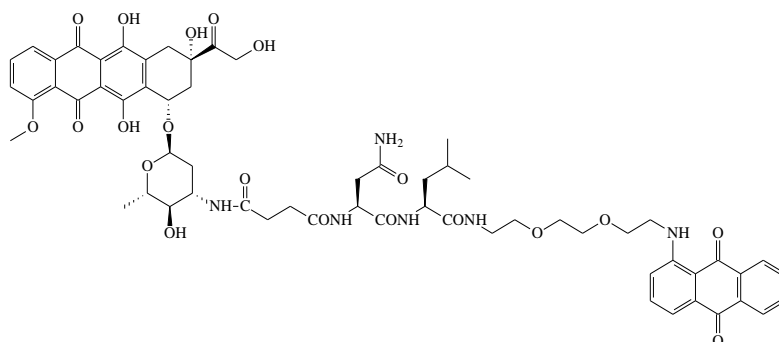

Epirubicin succinate Asn-Leu-[PEG Spacer]-AQ [YD98] **(31)**

N-Epirubicin-1-{*N*-2-[2-(2-(succinyl-L-asparaginyl-L-leucylamino)ethoxy)ethoxy]ethylamino}anthracene-9,10-dione
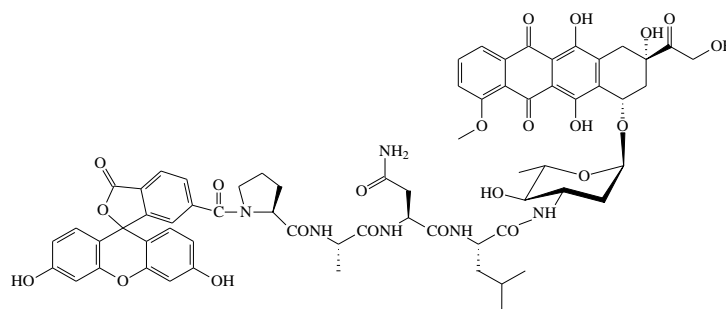
5(6)-FAM-Pro-Ala-Asn-Leu-epirubicin [YD101] **(36)**

N-[5(6)-carboxyfluorosceinylcarbonyl-L-prolyl-L-alanyl-L-asparaginyl-L-leucyl]-epirubicin
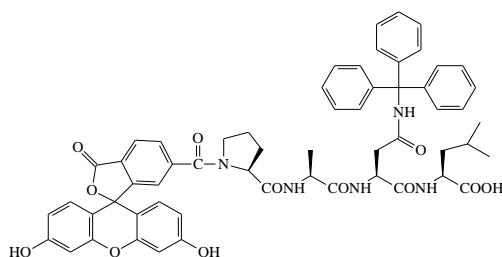
5(6)-FAM-Pro-Ala-Asn(Trt)-Leu-OH
[YD95] **(37)**

{*N*-[5(6)-carboxyfluorosceinylcarbonyl]-L-prolyl}-alanyl-*N*γ-trityl-L-asparaginyl-L-leucine
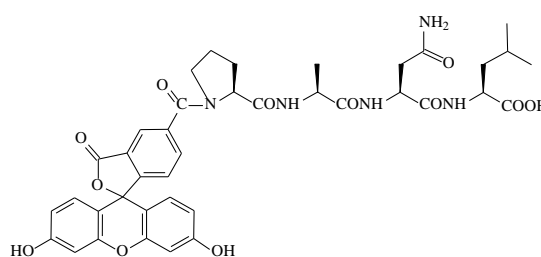
5(6)-FAM-Pro-Ala-Asn(Trt)-Leu-OH
[YD99] **(38)**

{*N*-[5(6)-carboxyfluorosceinylcarbonyl]-L-prolyl}-alanyl-L-asparaginyl-L-leucine
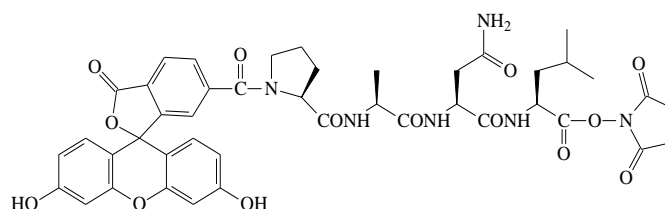
5(6)-FAM-Pro-Ala-Asn-Leu-OSu ester [YD100] **(39)**

{*N*-[5(6)-carboxyfluorosceinylcarbonyl]-L-prolyl}-L-alanyl-L-asparaginyl-L-leucine *N*-hydroxysuccinimide ester
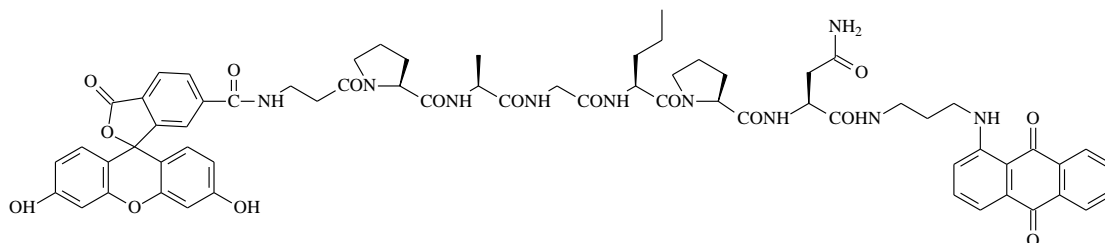
5(6)-FAM-β-Ala-Pro-Ala-Gly-Nva-Pro-Asn-[Propyl Spacer]-AQ [YD103] **(43)**

1-{3-*N*-[5(6)-carboxyfluorosceinylcarbonyl-β-alanyl-L-prolyl-L-alanyl-glycyl-L-norvalyl-L-prolyl-L-asparaginylamino]propylamino}anthracene-9,10-dione

2.7 EXPERIMENTAL

2.7.1 Chemical synthesis of legumain probes and their intermediates

General methods (grade of silica, chemical suppliers etc.) for chemical synthesis in this chapter see section **1.6.1** to **1.6.2** in Chapter I.

2.7.1.1 Synthesis of [PEG Spacer]-AQ [TL1] (14)

1-Chloroanthraquinone (3g, 0.012mol) was suspended in DMSO (5mL) and 2-[2-(2-amino-ethoxy)-ethoxy]-ethylamine (35mL, 0.24mol) was added. The mixture was heated over a water bath at 95°C for 4h. The solution was cooled and added to a large excess of water (500mL). The purple precipitated solid was filtered off, dried and used for subsequent reactions without further purification. Analytically pure samples of TL1 **(14)** were prepared by column chromatography [chloroform: ethyl acetate: methanol (80:19:1), then chloroform: methanol (9:1)]. Yield: 2g (34%). TLC [butanol: acetic acid: water (4:5:1)]: R_f 0.52 purple (product; homogeneous on TLC).

^{1}H NMR (d$_6$-DMSO 300MHz) δ: 3.00 (2H, m, C$\underline{H}_2$NH$_2$), 3.20 (2H, m, OC$\underline{H}_2$CH$_2$NH$_2$), 3.50 - 3.60 (2H, m, AQNHCH$_2$C$\underline{H}_2$O), 3.60 – 3.70 (4H, m, OC$\underline{H}_2$C$\underline{H}_2$O), 3.70 - 3.80 (2H, m, C$\underline{H}_2$NHAQ), 7.3 (1H, dd, H-2), 7.40 (1H, dd, H-4), 7.65 (1H, t, H-3), 7.75 - 7.80 (5H, m, H-6, H-7; N$\underline{H}_3^+$ unresolved), 8.10 - 8.20 (2H, m, H-5, H-8), 9.75 (1H, t, AQ-N$\underline{H}$).

^{13}C NMR spectrum (d$_6$-DMSO 75.5MHz) 38.64 (−ve, Aq-NH-$\underline{C}$H$_2$); 42.10 (−ve, $\underline{C}$H$_2$NH$_3^+$); 66.72 (−ve, Aq-NH-CH$_2$-$\underline{C}$H$_2$); 68.63 (−ve, O-$\underline{C}$H$_2$-CH$_2$NH$_3^+$); 69.62 (−ve, O-$\underline{C}$H$_2$-$\underline{C}$H$_2$-O); 112.06 (ab, $\underline{C}$F$_3$); 115.12 [+ve, aromatic (Aq) $\underline{C}$H]; 118.70 [+ve, aromatic (Aq) $\underline{C}$H]; 126.25 (+ve, aromatic $\underline{C}$H); 126.40 (+ve, aromatic $\underline{C}$H); 132.32 [ab, aromatic (Aq) $\underline{C}$-1]; 133.47

(+ve, aromatic C̲H); 134.49 (+ve, aromatic C̲H); 135.61 (+ve, aromatic C̲H); 151.27 (ab,

C̲O-TFA); 182.85 (C̲=O-quinone); 184.20 (C̲=O-quinone).

2.7.1.2   Synthesis of Boc-Leu-[PEG Spacer]-AQ [TL2] (15)

A solution of Boc-Leu-OSu (0.927g, 0.0028mol) in DMF (10mL) was added to TL1 **(14)**

(1g, 0.0021mol) in DMF (10mL), DIPEA (0.49mL, 0.0028mol) was added and the

reaction was stirred at RT for 2.5h. Chloroform (50mL) was added and the organic layer

was washed with water (2×200mL), saturated sodium bicarbonate solution (2×30mL),

water (200mL), dried (Na$_2$SO$_4$), filtered and evaporated *in vacuo* to a low volume. The

crude product was purified by silica gel column chromatography (17cm×4.5cm) eluting

with chloroform: methanol (9:1). Fractions containing major product were collected,

filtered and evaporated to dryness. Yield: 0.9g, (76%). TLC [chloroform: methanol (9:1)]:

R$_f$ 0.65 purple (product; homogeneous on TLC).

<u>^{1}H NMR (CDCl$_3$ 300MHz)</u> δ: 0.90 (6H, dd, 2×CH$_3$), 1.45 (1H, s, + 8H, s, Boc), 1.60 −

1.70 (3H, m, CH$_2$CH), 3.45 - 3.65 (6H, m, AQNHCH$_2$CH$_2$O; OCH$_2$CH$_2$NHCO), 3.65 −

3.75 (4H, m, OCH$_2$CH$_2$O), 3.85 (2H, t, CH$_2$NHAQ), 4.15 (1H, m, α-CH), 5.0 (1H, d, α-

CHNHCO), 6.75 (1H, t, CH$_2$NHCO), 7.10 (1H, dd, H-2), 7.50 − 7.65 (2H, m, H-3, H-4),

7.70 - 7.80 (2H, m, H-6, H-7), 8.20 - 8.25 (2H, m, H-5, H-8), 9.90 (1H, t, AQ-NH).

<u>^{13}C NMR spectrum (CDCl$_3$, 75.5MHz)</u> 21.95 (+ve, C̲H$_3$-leu); 22.93 (+ve, C̲H$_3$-leu); 24.71

(+ve, γ-C̲H); 28.29 [+ve, C(C̲H$_3$)$_3$]; 39.34 (−ve, Aq-NH-C̲H$_2$); 41.75 (−ve, β-C̲H$_2$-leu);

42.68 (−ve, C̲H$_2$-NHCO-leu); 53.00 (+ve, α-C̲H-leu); 69.38 (−ve, C̲H$_2$-O); 69.83 (−ve, C̲H$_2$-

O); 70.31 (−ve, C̲H$_2$-O); 70.56 (−ve, C̲H$_2$-O); 115.86 (+ve, aromatic C̲H); 117.82 (+ve,

aromatic C̲H); 126.71 [(+ve, aromatic C̲H) (AQ-6 and 7)], 132.97 (+ve, aromatic C̲H);

133.99 (+ve, aromatic $\underline{C}$H); 134.65 [ab, aromatic (Aq) $\underline{C}$-1]; 135.30 (+ve, aromatic $\underline{C}$H); 151.60 (ab, NH$\underline{C}$OO); 172.87 (ab, spacer-NH$\underline{C}$O-leu); 183.74 (ab, $\underline{C}$=O); 185.06 (ab, $\underline{C}$=O).

2.7.1.3 Synthesis of H-Leu-[PEG Spacer]-AQ trifluoroacetate salt [TL3] (16)

TL2 **(15)** (0.65g, 0.001mol) was dissolved in trifluoroacetic acid (7mL) at RT. After 0.5h the solvent was evaporated and the residual solid re-evaporated with ethanol (2mL). Addition of diethyl ether (100mL) gave a precipitate of TL3 as the *N*-terminal trifluoroacetate salt which was filtered off and dried *in vacuo*. Yield (0.54g, 84%). TLC [chloroform: methanol (9:1)]: R_f 0.36 purple (product; homogeneous on TLC).

$\underline{^1\text{H NMR (d}_6\text{-DMSO 300MHz})}$ δ: 0.85 (6H, t, 2×C$\underline{H}_3$), 1.45 – 1.65 (3H, m, C$\underline{H}_2$C$\underline{H}$), 3.25 (2H, m, C$\underline{H}_2$NHCO), 3.45 - 3.55 (4H, m, AQNHCH$_2$C$\underline{H}_2$O; OC$\underline{H}_2$CH$_2$NHCO), 3.55 – 3.65 (4H, m, OC$\underline{H}_2$C$\underline{H}_2$O), 3.65 - 3.75 (3H, m, C$\underline{H}_2$NHAQ; α-C$\underline{H}$), 7.3 (1H, dd, H-2), 7.45 (1H, dd, H-4), 7.65 (1H, t, H-3), 7.80 - 7.95 (2H, m, H-6, H-7), 8.05 - 8.20 (5H, m, H-5, H-8; N$\underline{H}_3^+$ unresolved), 8.55 (1H, t, N$\underline{H}$CO), 9.75 (1H, t, AQ-N$\underline{H}$).

$\underline{^{13}\text{C NMR spectrum (d}_6\text{-DMSO 75.5MHz})}$ 22.00 (+ve, $\underline{C}$H$_3$-leu); 22.39 (+ve, $\underline{C}$H$_3$-leu); 23.55 (+ve, γ-$\underline{C}$H-leu); 38.64 (−ve, Aq-NH-$\underline{C}$H$_2$); 40.03 (−ve, β-$\underline{C}$H$_2$-leu); 42.11 (−ve, $\underline{C}$H$_2$-NHCO-leu); 50.86 (+ve, α-$\underline{C}$H-leu); 68.69 (−ve, $\underline{C}$H$_2$-O); 68.82 (−ve, $\underline{C}$H$_2$-O); 69.56 (−ve, $\underline{C}$H$_2$-O); 69.72 (−ve, $\underline{C}$H$_2$-O); 112.06 (ab, $\underline{C}$F$_3$); 115.11 (+ve, aromatic $\underline{C}$H); 118.71 (+ve, aromatic $\underline{C}$H); 126.25 (+ve, aromatic $\underline{C}$H); 126.38 (+ve, aromatic $\underline{C}$H); 132.32 [ab, aromatic (Aq) $\underline{C}$-1]; 133.46 (+ve, aromatic $\underline{C}$H); 134.49 (+ve, aromatic $\underline{C}$H); 135.60 (+ve, aromatic $\underline{C}$H); 151.28 (ab, $\underline{C}$O-TFA); 168.97 (ab, spacer-NH$\underline{C}$O-leu); 182.85 ($\underline{C}$=O -quinone); 184.50 ($\underline{C}$=O -quinone).

2.7.1.4   Synthesis of Fmoc-Asn(Trt)-Leu-[PEG Spacer]-AQ [TL4] (17)

Fmoc-Asn(Trt)-OH (0.476g, 0.8mmol), TBTU (0.256g, 0.8mmol) and HOBt (0.12g, 0.78mmol) were dissolved in DMF (5mL), DIPEA (0.417mL, 2.4mmol) was added and reaction mixture was left at RT for 15min prior to addition to a stirred solution of TL3 **(16)** (0.5g, 0.861mmol) in DMF (5mL). After three hours, chloroform was added and the organic layer was washed with water (2×200mL), saturated sodium bicarbonate solution (2×30mL), water (200mL), dried (Na_2SO_4), filtered and evaporated *in vacuo* to a low volume. The crude product was purified by silica gel column chromatography ($17cm\times4.5cm$) eluting with chloroform: methanol (19:1). Fractions containing major product were collected, filtered and evaporated to dryness.

Yield: 0.7g (78%). TLC [chloroform: methanol (9:1)]: R_f 0.85 purple (product; homogeneous on TLC).

2.7.1.5   Synthesis of H-Asn(Trt)-Leu-[PEG Spacer]-AQ [TL5] (18)

TL4 **(17)** (0.6g, 0.57mmol) was treated with 20% piperidine in DMF for 30min. Then chloroform was added into this reaction mixture and organic layer was washed with water (2×200mL), saturated sodium bicarbonate solution (2×30mL), water (200mL), dried (Na_2SO_4), filtered and evaporated *in vacuo* to a low volume. The crude product was purified by silica gel chromatography ($7cm\times4.5cm$) which was eluted with chloroform: methanol (9:1), fractions containing major product were collected, filtered and evaporated to dryness.

Yield: 0.385g (82%). TLC [dichloromethane: methanol (9:1)]: R_f 0.53 (purple) product; homogeneous on TLC.

2.7.1.6 Synthesis of Fmoc-Ala-Asn(Trt)-Leu-[PEG Spacer]-AQ [TL6] (19)

Fmoc-Ala-OH (0.11g, 0.36mmol), TBTU (0.12g, 0.36mmol) and HOBt (0.056g, 0.36mmol) were dissolved in DMF (5mL), DIPEA (0.190mL, 1.09mmol) was added and reaction mixture was left at RT for 15min prior to addition to a s stirred solution of TL5 (18) (0.3g, 0.36mmol) in DMF (5mL) following the same procedure as described for the synthesis of TL4 (17). The crude product was purified by silica gel chromatography (10cm×4.5cm) which was eluted with dichloromethane: ethyl acetate: methanol (7:2:1), fractions containing major product were collected, filtered and evaporated to dryness.

Yield: 0.35g (86%). TLC [dichloromethane: ethyl acetate: methanol (7:2:1)]: R_f 0.74 (purple) product. Compound TL6 (19) chromatographically homogeneous (single spot on TLC).

2.7.1.7 Synthesis of H-Ala-Asn(Trt)-Leu-[PEG Spacer]-AQ [TL7] (20)

The Fmoc protecting group was removed from TL6 (19) (0.3g, 0.27mmol) using 20% piperidine in DMF following the same procedure as described for the synthesis of TL5 (18). The crude product was purified by silica gel chromatography (8cm×4.5cm) which was eluted with dichloromethane: ethyl acetate: methanol (7:2:1), fractions containing major product were collected, filtered and evaporated to dryness.

Yield: 0.21g (88%). TLC [dichloromethane: ethyl acetate: methanol (7:2:1)]: R_f 0.22 (purple) product; homogeneous on TLC.

2.7.1.8 Synthesis of Fmoc-Pro-Ala-Asn(Trt)-Leu-[PEG Spacer]-AQ [TL8] (21)

Fmoc-Pro-OH (0.0754g, 0.22mmol), TBTU (0.072g, 0.22mmol) and HOBt (0.034g, 0.22mmol) were dissolved in DMF (5mL), DIPEA (0.117mL, 0.67mmol) was added and reaction mixture was left at RT for 15min prior to addition to a stirred solution of TL7

(20) (0.2g, 0.22mmol) in DMF (5mL) following the same procedure as described for the synthesis of TL4 **(17)**.

Yield: 0.23g (85%). TLC [dichloromethane: ethyl acetate: methanol (7:2:1)]: R_f 0.63, (purple) product; homogeneous on TLC.

2.7.1.9   Synthesis of H-Pro-Ala-Asn(Trt)-Leu-[PEG Spacer]-AQ [TL9] (22)

The Fmoc protecting group in TL8 **(21)** (0.2g, 0.16mmol) was removed by using 20% piperidine in DMF for 30min following the same procedure as described for the synthesis of TL5 **(18)**. The crude product was purified by silica gel chromatography column (5cm×4.5cm) which was eluted with dichloromethane: ethyl acetate: methanol (7:2:1), fractions containing major product were collected, filtered and evaporated to dryness.

Yield: 0.13g (82%). TLC [dichloromethane: ethyl acetate: methanol (7:2:1)]: R_f 0.05 (purple) product. The purity of TL9 **(22)** was confirm by its homogeneous character on TLC.

2.7.1.10   Synthesis of 5(6)-FAM-Pro-Ala-Asn(Trt)-Leu-[PEG Spacer]-AQ [TL10] (23)

5(6)-carboxyfluorescein **(5)** (0.046g, 0.12mmol), TBTU (0.039g, 0.12mmol) and HOBt (0.0185g, 0.12mmol) were dissolved in DMF (5mL), DIPEA (0.021mL, 0.12mmol) was added and reaction mixture was left at RT for 15min prior to addition to a stirred solution of TL9 **(22)** (0.12g, 0.12mmol) in DMF (5mL) following the same procedure as described for the synthesis of TL4 **(17)**. The crude product was purified by silica gel chromatography (7cm×4.5cm) which was eluted with chloroform: ethyl acetate: methanol (5:2:1), fractions containing major product were collected, filtered and evaporated to dryness.

Yield: 0.124g (77%). TLC [chloroform: ethyl acetate: methanol (5:2:1)]: R_f 0.35 (orange) product; homogeneous on TLC.

2.7.1.11 Synthesis of 5(6)-FAM-Pro-Ala-Asn-Leu-[PEG Spacer]-AQ [TL11] (3)

TL10 **(23)** (0.1g, 0.074mmol) was treated with TFA (3mL) for 4h following the same procedure as described for the synthesis of TL3 **(16)**. The solid crude compound was purified by silica gel chromatography (10cm×4.5cm) eluting with dichloromethane: ethyl acetate: methanol (5:2:1), fractions containing major product were collected, filtered and evaporated to dryness.

Yield: 0.022g (27%). TLC [dichloromethane: ethyl acetate: methanol (5:2:1)]: R_f 0.5 (orange) product. The purity of TL11 **(3)** was confirmed by its homogeneous character on TLC and by its high resolution mass spectrum.

ESMS(-) m/z: 552.7033 (28%) $[(M-2H)/2]^{2-}$; 1106.4143 (100%) $(M-H)^-$.

2.7.1.12 Synthesis of H-Pro-Gly-Asn(Trt)-Leu-[PEG Spacer]-AQ (44)

Fmoc-Pro-Gly-OH (0.23g, 0.58mmol) and TBTU (0.18g, 0.56mmol) were dissolved in DMF (5mL), DIPEA (0.194mL, 1.12mmol) was added and reaction mixture was left at RT for 15min prior to addition to a stirred solution of TL5 **(18)** (0.4g, 0.5mmol) in DMF (5mL) following the same procedure as described for the synthesis of TL4 **(17)**. The crude yield for this red product was 0.39g (65%). TLC [dichloromethane: ethyl acetate: ethanol (4:4:1)]: R_f 0.5 (purple) product. A portion of this purple Fmoc protected product (0.15g, 0.13mmol) was treated with 20% piperidine in DMF (7mL) following the same procedure as described for the synthesis of TL5 **(18)** to remove the Fmoc protecting group. It proved

difficult to obtain the product as a dry solid, therefore the residue was used directly for subsequent reactions (*N*-labelling with fluorophores).

2.7.1.13 Synthesis of 5(6)-FAM-Pro-Gly-Asn(Trt)-Leu-[PEG Spacer]-AQ (45)

H-Pro-Gly-Asn(Trt)-Leu-[PEG Spacer]-AQ **(44)** (0.065mmol; estimated from above **2.7.1.12**) was re-dissolved in DMF (5mL). It was then mixed with a solution of 5(6)-carboxyfluorescein **(5)** (0.028g, 0.075mmol), PyBOP (0.039g, 0.075mmol) in DMF (7mL). DIPEA (0.052mL, 0.3mmol) was added into this reaction mixture afterwards following the same procedure as described for the synthesis of TL4 **(17)**.

Yield: 0.0387g (44%). TLC [chloroform: ethyl acetate: methanol (2:2:1)]: R_f 0.7 (orange) product.

2.7.1.14 Synthesis of 5(6)-FAM-Pro-Gly-Asn-Leu-[PEG Spacer]-AQ [AD17] (8)

5(6)-FAM-Pro-Gly-Asn(Trt)-Leu-[PEG Spacer]-AQ **(45)** (0.02g, 0.015mmol) was treated with TFA (5mL) at RT for 2h following the same procedure as described for the synthesis of TL3 **(16)**. The solid crude compound was purified by silica gel chromatography (10cm×4.5cm), which was eluted with chloroform: methanol (17:3), fractions containing major product were collected, filtered and evaporated to dryness.

Yield: 0.0092g (56%). TLC [chloroform: methanol (4:1)]: R_f 0.6 (orange) product. The purity of AD17 **(8)** was confirmed by its homogeneous character on TLC and by its high resolution mass spectrum.

ESMS(+): 547.7100 (80%) ($[M+2H]/2]^{2+}$; 1094.4139 (20%) $(M+H)^+$; 1116.3958 (8%) $(M+Na)^+$.

2.7.1.15 Synthesis of H-Ser(*t*Bu)-Asn(Trt)-Leu-[PEG Spacer]-AQ (46)

Fmoc-Ser(*t*Bu)-OSu (0.27g, 0.58mmol) was dissolved in DMF (5mL) with DIPEA (0.086mL, 0.495mmol) and the reaction mixture was left at RT for 15min prior to addition to a stirred solution of TL5 **(18)** (0.41g, 0.5mmol) in DMF (5mL) following the same procedure as described for the synthesis of TL4 **(17)**. The purple Fmoc protected product yielded 0.4g (68%). TLC [dichloromethane: ethyl acetate: ethanol (4:4:1)]: R_f 0.8 (purple) product. The Fmoc protected product (0.184g, 0.15mmol) was dissolved in 20% piperidine in DMF (7mL) following the same procedure as described for the synthesis of TL5 **(18)** to remove the Fmoc protecting group. TLC [dichloromethane: ethyl acetate: ethanol (4:4:1)]: R_f 0.4 (purple) product.

2.7.1.16 Synthesis of 5(6)-FAM-Pro-Ser(*t*Bu)-Asn(Trt)-Leu-[PEG Spacer]-AQ (47)

After removing Fmoc protecting group, H-Ser(*t*Bu)-Asn(Trt)-Leu-[PEG Spacer]-AQ **(46)** was dissolved in DMF (5mL) which was then added into a mixture of 5(6)-FAM-Pro-OH (0.0884g, 0.19mmol), PyBOP (0.1123g, 0.218mmol), DIPEA (0.137mL, 0.788mmol) in DMF (5mL) following the same procedure as described for the synthesis of TL4 **(17)**. TLC [dichloromethane: ethyl acetate: ethanol (4:4:1)]: R_f 0.7 (orange) product.

2.7.1.17 Synthesis of 5(6)-FAM-Pro-Ser-Asn-Leu-[PEG Spacer]-AQ [AD20] (9)

5(6)-FAM-Pro-Ser(*t*Bu)-Asn(trt)-Leu-[PEG Spacer]-AQ **(47)** was treated with TFA (5mL) at RT for 2.5h following the same procedure as described for the synthesis of TL3 **(16)**. The crude compound was purified by silica gel chromatography (12cm×4.5cm), which was eluted with chloroform: methanol (4:1), fractions containing the major product were collected, filtered and evaporated to dryness.

Yield: 0.0421g (25%). TLC [chloroform: methanol (4:1)]: R_f 0.5 (orange) product; homogeneous on TLC.

ESMS(+): 562.7153 (100%) $[(M+2H)/2]^{2+}$; 1124.4249 (86%) $(M+H)^+$.

2.7.1.18   Synthesis of H-Thr(^{t}Bu)-Asn(Trt)-Leu-[PEG Spacer]-AQ (48)

TL5 **(18)** (1.9g, 2.31mmol) was dissolved in DMF (5mL), then it was mixed with a solution of Fmoc-Thr(^{t}Bu)-OH (1.06g, 2.66mmol), HOBt (0.35g, 2.56mmol), TBTU (0.82g, 2.56mmol) in DMF (10mL) with DIPEA (1.29mL, 7.39mmol), following the same procedure as described for the synthesis of TL4 **(17)**. During purification for the Fmoc protected crude compound, chloroform: methanol (4:1) was used as the chromatography elution solvent and the silica gel column was 12cm×4.5cm. The chromatographically homogeneous Fmoc protected compound yielded 0.87g (31%), TLC [chloroform: methanol (9:1, 2mL with 3 drops of acetic acid)]: R_f 0.74 (red) product. Then 0.3g (0.25mmol) of this red product was treated with 20% piperidine in DMF (10mL) following the same procedure as described for the synthesis of TL5 **(18)** to remove Fmoc protecting group.

Yield: 0.19g (77%). TLC [chloroform: methanol (9:1)]: R_f 0.3 (red) product. Compound H-Thr(^{t}Bu)-Asn(Trt)-Leu-[PEG Spacer]-AQ **(48)** was deemed sufficiently pure for use without further purification.

2.7.1.19   Synthesis of 5(6)-FAM-Pro-Thr(^{t}Bu)-Asn(Trt)-Leu-[PEG Spacer]-AQ (49)

5(6)-FAM-Pro-OH **(41)** (0.079g, 0.17mmol), PyBOP (0.087g, 0.17mmol) were dissolved in DMF (3mL) with DIPEA (0.093mL, 0.54mmol) as base, then this solution was mixed with H-Thr(^{t}Bu)-Asn(Trt)-Leu-[PEG Spacer]-AQ **(48)** (0.18g, 0.1837mmol) in DMF (3mL) following the same procedure as described for the synthesis of TL4 **(17)**. The crude

compound was purified by silica gel chromatography (6.5cm×3.2cm) and eluted with chloroform: methanol (24:1, 100mL with 3 drops of acetic acid). Fractions containing the major product were collected, filtered and evaporated to dryness.

Yield: 0.11g (45%). TLC [chloroform: methanol (3:1, 2mL with one drop of acetic acid)]: R_f 0.43 (orange) product. Compound 5(6)-FAM-Pro-Thr(^{t}Bu)-Asn(Trt)-Leu-[PEG Spacer]-AQ (49) was deemed sufficiently pure for use without further purification.

2.7.1.20   Synthesis of 5(6)-FAM-Pro-Thr-Asn-Leu-[PEG Spacer]-AQ [VG] (10)

5(6)-FAM-Pro-Thr(^{t}Bu)-Asn(Trt)-Leu-[PEG Spacer]-AQ (49) (0.095g, 0.069mmol) was treated with TFA (5mL) at RT for 3h. The solvent was evaporated to a low volume; addition of diethyl ether gave a precipitate. The solid crude product yielded 0.06g (80%). Half of this crude product (0.030g, 0.026mmol) was purified through a silica gel chromatography column (2cm×4.5cm) which was eluted with chloroform: methanol (4:1, 50mL with one drop of acetic acid). Fractions containing main product were combined, filtered, and evaporated to dryness.

Yield: 0.002g (7%). The purity of VG (10) was confirmed by its homogeneous character on TLC and by its high resolution mass spectrum.

ESMS(+): 569.7234 (100%) $[(M+2H)/2]^{2+}$; 1138.4398 (35%) $(M+H)^+$.

2.7.1.21   Synthesis of 5(6)-FAM-Ala-Asn-Leu-Ala-[PEG Spacer]-AQ [PN11] (11)

Probe PN11 (11) was synthesised by solution phase peptide synthesis from [PEG Spacer]-AQ [TL1] (14) (1g, 2.82mmol). Four *N*-protected amino acids were applied in sequence during coupling stage: Boc-Ala-OH (0.64g, 3.38mmol), Boc-Leu-OSu (0.335g, 1.02mmol), Fmoc-Asn(Trt)-OH (0.546g, 0.92mmol) and Fmoc-Ala-OH (0.16g, 0.51mmol). HOBt and TBTU were used as coupling reagents and DIPEA was used as the

base for these coupling stages, following the same procedure as described for the synthesis of TL4 **(17)**. Boc and Fmoc protection groups were removed by following the same deprotection procedure as for the synthesis of TL3 **(16)** and TL5 **(18)**, respectively. 5(6)-FAM **(5)** (0.024g, 0.064mmol) was used for the final coupling onto the tetrapeptide spacer AQ conjugate, following the same method for synthesis of TL10 **(23)**. Trityl protection group on the side chain of asparagine was removed following the same procedure as described for the synthesis of TL11 **(3)**. The crude probe PN11 **(11)** was purified using a thick layer chromatography plate (20cm $\times$ 20cm $\times$ 0.1cm) which was eluted with dichloromethane: methanol (6:1, 70mL, with 10 drops of acetic acid). Yield (0.043g). TLC [dichloromethane: methanol (6:1, 2.8mL, with 2 drops of acetic acid)]: R_f 0.6 (orange) product. The purity of PN11 **(11)** was confirmed by its homogeneous character on TLC and by its high resolution mass spectrum.

ESMS(-) m/z: 1080.3934 (100%) (M-H)$^-$.

2.7.1.22   Synthesis of H-[Propyl Spacer]-AQ (50)

To a suspension of 1-chloroanthraquinone (3g, 0.0123mol) in DMSO (5mL), 1,3-diaminopropane (20.7mL, 0.248mmol) was added. This reaction mixture was heated over a water bath for half an hour. A large volume of water (500mL) was added to give a precipitate of crude product, which was then filtered and dried without any further purification. Yield: (3.4349 g, 98%). TLC [butanol: acetic acid: water (4:5:1)]: R_f 0.55 (red) product.

2.7.1.23   Synthesis of H-Leu-[Propyl Spacer]-AQ (51)

Boc-Leu-OSu (1.17g, 0.0036mol) was mixed with DIPEA (0.63mL, 0.0036mol) in DMF (10mL) and this mixture was left at RT for 15min before it was added into a stirred

solution of H-[Propyl Spacer]-AQ **(50)** (1g, 0.0036mol) in DMF (20mL) following the same procedure as described for the synthesis of TL4 **(17)**. This crude compound was purified by silica gel chromatography (10cm×3.2cm) which was eluted with ethyl acetate: dichloromethane (4:1). Fractions containing the major product were collected, filtered and evaporated to dryness. The Boc protected compound was treated with TFA (7mL) following the same procedure as described for the synthesis of TL3 **(16)**.

Yield: 0.7g (50%).

2.7.1.24 <u>Synthesis of H-Ala-Ala-Asn-Leu-[Propyl Spacer]-AQ (52)</u>

The tetrapeptide-[propyl Spacer]-AQ **(52)**, was prepared by solution phase peptide synthesis by step-wise addition of Fmoc-Asn(Trt)-OH (0.728g, 1.22mmol) and Boc-Ala-Ala-OH (0.288g, 1.1065mmol) following the same procedure as described for the synthesis of TL4 **(17)**. Deprotection of Fmoc, Boc and trityl groups protected compounds followed the same procedure as described for the synthesis of TL5 **(18)** and TL3 **(16)**, respectively.

2.7.1.25 <u>Synthesis of FITC-Ala-Ala-Asn-Leu-[Propyl Spacer]-AQ [FF] (6)</u>

H-Ala-Ala-Asn-Leu-[Propyl Spacer]-AQ **(52)** (0.1g, 0.154mmol) and FITC **(4)** (0.056g, 0.144mmol) were mixed in DMF (6mL), and then DIPEA (0.098mL, 0.5637mmol) was added into this reaction mixture which was kept in dark for 18h following the same procedure as described for the synthesis of TL4 **(17)**. The crude product was purified using a thick layer chromatography plate (20cm×20cm×0.1cm) eluting with chloroform: ethanol (10:3).

Yield: 6mg (4%). The purity of FF **(6)** was confirmed by its homogeneous character on TLC and by its high resolution mass spectrum.

ESMS(+) m/z: 1039.3634 (100%) (M+H)$^+$; 1061.3466 (5%) (M+Na)$^+$.

ESMS(-) m/z: 1037.3506 (100%) (M-H)$^-$.

2.7.1.26   Synthesis of FITC-Ala-Ala-Asn-Ala-[Propyl Spacer]-AQ [MK8] (7)

The FITC (4) labelled probe MK8 (7) was prepared following a similar procedure as that described for the synthesis of the other FITC (4) labelled probe FF (6) (section **2.7.1.22-25**), the only difference being that the first amino acid was Boc-Ala-OH (0.742g, 3.92mmol).

Yield: (0.0773g, 8.5%). TLC [butanol: acetic acid: water (15:4:1)]: R$_f$ 0.66 product. The purity of MK8 (7) was confirmed by its homogeneous character on TLC and by its high resolution mass spectrum.

ESMS(-) m/z: 497.1478 (27%) [(M-2H)/2]$^{2-}$; 995.3019 (100%) (M-H)$^-$.

2.7.1.27   Synthesis of succinate Asn(Trt)-Leu-[PEG Spacer]-AQ [YD 91] (32)

Succinic anhydride (0.0194g, 0.194mmol) was dissolved in DMF (3mL), followed by DIPEA (0.034mL, 0.196mmol). This mixture was added to a stirred solution of the anthraquinone-dipeptide, TL5 (18) (0.078g, 0.0947mmol) in DMF (3mL). After 12h, the reaction solution was added drop wise into a saturated solution of sodium hydrogen sulphate, and a dark red precipitate formed immediately. This dark red precipitate was then filtered and washed with water, and dried.

Yield: (0.0854g, 98%). TLC [butanol: acetic Acid: water (15:4:1)]: R$_f$ 0.95 (purple) product; homogeneous on TLC.

2.7.1.28   Synthesis of OSu succinate Asn-Leu-[PEG Spacer]-AQ ester [YD 97] (33)

The succinate Asn(Trt)-Leu-[PEG Spacer]-anthraquinone [YD 91] **(32)** (0.05g, 0.0542mmol) was treated with TFA (2mL) at RT for 40min to remove the trityl group on the side chain of asparagine. TLC [dichloromethane: methanol (8:1)]: R_f 0.27 (purple) product. The white solid (triphenylmethane) was filtered off from the TFA solution, and the product was evaporated to dryness. Succinate Asn-Leu-[PEG Spacer]-anthraquinone (YD 96) **(35)** (0.015g, 0.0221mmol) was mixed with TSTU (0.007g, 0.0232mmol) and DMAP (0.0027g, 0.0221mmol) in DMF (1mL), and the reaction was left at RT for half an hour, following the same procedure as described for the synthesis of TL4 **(17)**. The reaction mixture was partitioned between chloroform and water, the organic layer was evaporated to a very low volume and addition of diethyl ether gave a precipitate of the final product YD 97 **(33)**.

Yield: (0.0093g, 54%). TLC [dichloromethane: methanol (8:1)]: R_f 0.32 (purple) product; homogeneous on TLC.

2.7.1.29   Synthesis of epirubicin succinate Asn-Leu-[PEG Spacer]-AQ [YD 98] (31)

Epirubicin hydrochloride (0.0067g, 0.01155mmol) was dissolved in DMF (0.5mL) followed by DIPEA (0.002mL, 0.0115mmol), 10min later, it was then added into a DMF solution (0.5mL) of OSu succinate Asn-Leu-[PEG Spacer]-anthraquinone ester (YD 97) **(33)** (0.009g, 0.01156mmol). One hour later, a mini extraction was carried out and the progress of this reaction as monitored by TLC (dichloromethane: methanol 8:1) R_f 0.4 (red) product. The DMF reaction solution was evaporated to dryness and re-dissolved in a mixed solvent of dichloromethane and methanol before it was loaded onto a thick-layer

chromatography plate which was eluted with dichloromethane: methanol (8:1). The red band containing the major product was collected, washed with dichloromethane and methanol, and evaporated to dryness. The purity of YD 98 **(31)** was confirmed by its homogeneous character on TLC and by its high resolution mass spectrum.

Yield (0.0043g, 31%)

ESMS(+) m/z: 1207.4707 (100%) (M+H)$^+$.

2.7.1.30   Synthesis of 5(6)-carboxyfluorescein-Pro-OH (41)

H-Pro-OtBu·HCl (0.3g, 1.4617mmol) was dissolved in DMF (2mL), followed by treating with DIPEA (0.254mL, 1.47mmol), 10min later, it was mixed with a DMF solution (3mL) of 5(6)-carboxyfluorescein **(5)** (0.5g, 1.3287mmol) and PyBOP (0.7g, 1.3286mmol), additional DIPEA (0.46mL, 2.6574mmol) was added into this reaction solution. This reaction mixture was kept in the dark at RT for 2h following the same procedure as the synthesis of TL4 **(17)**. TLC [dichloromethane: methanol (9:1)]: R_f 0.39 (yellow) product. The crude product was purified by silica gel column chromatography (4.5cm×11cm) eluted with dichloromethane: methanol (9:1). Fractions containing the major product were collected, filtered and evaporated to dryness. Chromatographically pure, dry 5(6)-carboxyfluorescein-Pro-OtBu was treated with TFA (4mL) at RT for 3h following the same procedure as described for the synthesis of TL3 **(16)**.

Yield: (0.58g, 93%). TLC [dichloromethane: methanol (4:1)]: R_f 0.15(yellow) product. Compound 5(6)-carboxyfluorescein-Pro-OH **(41)** was deemed sufficiently pure for use without further purification.

2.7.1.31   Synthesis of 5(6)-FAM-Pro-Ala-Asn(Trt)-Leu-OH [YD 95] (37)

Fmoc-Leu-NovaSyn®TGT resin (0.68g, 0.1435mmol) was swollen in dichloromethane (5mL) for 1h. Coupling and deprotection cycles were applied by following a general SPPS synthesis procedure, which is given as follows:

1st cycle: *N*-Fmoc-Asn(Trt)-OH (0.26g, 3 equivalents), PyBOP (0.224g, 3 equivalents) were dissolved in DMF (3mL), and then DIPEA (0.15mL, 6 equivalents) was added into this solution. The mixture was split into two portions and each portion was added into an SPPS reaction vessel separately and kept shaking for 30min. Then the solution was drained out and resins were washed by DMF (3× ~10mL/g of resins). A few resin beads were taken out and a colour test was performed by using pentafluorophenyl 6-[(1-anthraquinone)amino]hexanoate **(28)** as the colour test reagent (for on-bead amine detection) in DMF with one drop of DIPEA. When the colour test showed a negative result, a solution of 20% (v/v) piperidine in DMF was added into SPPS reaction vessel (3×~10mL/g resins) and the vessel was kept shaking for 15min, and then the solution was drained away each time. Resins were then washed with DMF (3× ~10mL/g of resins) and the colour test was repeated. Positive result (resin beads turned red) indicated that deprotection had completed.

2nd cycle: *N*-Fmoc-Ala-OH (0.134g, 3 equivalents), PyBOP (0.224g, 3 equivalents) were dissolved in DMF (3mL), and then DIPEA (0.15mL, 6 equivalents) was added into this solution [following 1st cycle coupling and deproteciton methods].

3rd cycle: 5(6)-FAM-Pro-OH **(41)** (0.2036g, 3 equivalents), PyBOP (0.224g, 3 equivalents) were dissolved in DMF (3mL), and then DIPEA (0.15mL, 6 equivalents) was added into this solution [following 1st cycle coupling method].

After coupling 5(6)-FAM-Pro-OH **(41)** onto resin beads, the colour test cannot be applied to indicate the completion of the coupling procedure. Instead, a few beads were taken out of the SPPS vessel and treated with 0.5% TFA in dichloromethane and the new product monitored by TLC. Coupling of 5(6)-FAM-Pro-OH **(41)** was repeated (0.2g, 3 equivalents), and PyBOP (0.224g, 3 equivalents) in DMF (3mL), and then DIPEA (0.15mL, 6 equivalents).

TLC showed the reaction to be complete. Then the yellow resin beads were treated with portions of 0.5% TFA in dichloromethane and kept shaking for 20min each time, increasing to 2.5%, until no further product was removed from the resin. Product fractions were combined and evaporated to almost dryness and followed by treating with diethyl ether. The yellow precipitate of the title compound was then filtered off and dried *in vacuo*. Yield: 0.107g (74%)

ESMS(+) m/z: 1036.3733 (4%) (M+Na)$^+$.

2.7.1.32 Synthesis of 5(6)-FAM-β-Ala-Pro-Ala-Gly-Nva-Pro-Asn-[Propyl Spacer]-AQ [YD103] (43)

TFA Asn-[Propyl Spacer]-AQ salt (0.013g, 1.1eq) was dissolved in DMF (1mL) and treated with DIPEA (4.4 μL, 1.1eq) for 5min, then to this solution, a DMF solution (2mL) of 5(6)-FAM-β-Ala-Pro-Ala-Gly-Nva-Pro-OH (0.020g, 1eq), HOBt (0.0039g,1.1eq), TBTU (0.0081g, 1.1eq) and DIPEA (12.8 μL, 3.2eq) was added in. This reaction was kept at RT for 1h, following the same procedure as for the synthesis of TL4 **(17)**. TLC [chloroform:methanol (6:1), 2.1mL + 2 drops of TFA]: R_f 0.26 (orange) product. Chloroform:methanol 4:1 (2mL + 3 drops of TFA, $R_f = 0.54$) was determined to be a better solvent system. So YD103 was re-dissolved in a small volume of chloroform and methanol before it was chromatographed on a thick-layer plate which was eluted with

chloroform:methanol 4:1 (65mL + 96 drops of TFA) and kept in dark the whole time. The orange pure (chromatographically homogeneous) product band was collected and washed with methanol and evaporated to dryness.

Yield: 2.3mg (8%). The purity of YD103 (**43**) was confirmed by its homogeneous character on TLC and by its high resolution mass spectrum.

ESMS (-): 621 (100%) $[(M-2H)/2]^{2-}$.

ESMS (+) m/z: 1245.4878 (50%) $(M+H)^+$.

2.7.2 <u>UV-Vis Absorption Assay</u>

2.7.2.1 <u>Materials</u>

Assay buffer: 50mM MES hydrate (Sigma, M2933), 250mM NaCl, pH 5.0; Substrate: TL3, 1mg/mL stock in DMSO; Beckman DU 800 Spectrophotometer; 3mL quartz cuvette.

2.7.2.2 <u>Method</u>

UV-Vis absorption assay was applied for probe TL11 (**3**) quencher part TL3 (**16**) to determine TL3 (**16**) absorption area between wavelengths 500 to 600nm.

Assay buffer (3mL) was used as blank in TL3 (**16**) UV-Vis absorption assay. Final concentration for TL3 (**16**) in 3mL quartz cuvette was 50 μM. Wavelength scan application was selected for this assay. Scan speeds was set as 600nm/min and wavelength range was set between 500 and 600nm.

2.7.3 <u>Fluorescence Spectroscopy Assay</u>

2.7.3.1 <u>Materials</u>

Assay buffer: 50mM MES hydrate (Sigma, M2933), 250mM NaCl, pH 5.0; Substrate: Novel Fluorogenic Probe TL11 (**3**), 1mg/mL stock in DMSO; Fluorophore: 5(6)-

236

carboxyfluorescein **(5)**, 1mg/mL stock in DMSO then diluted to 100 μM in assay buffer; Perkin Elmer LS50B Luminescence Spectrometer; 3mL quartz cuvette.

2.7.3.2   Method

Fluorescence spectroscopy assay is usually applied to detect fluorescence intensity in target compounds. By using this assay, it is very straightforward and clear to compare fluorescence intensities between probe TL11 **(3)** and its fluorophore 5(6)-carboxyfluorescein **(5)**.

The excitation wavelength was set at 492nm and emission wavelength range was set between 500 and 600nm, and they were carried out at RT.

For both assays, in the final 3mL quartz cuvette, 15 μL of 100 μM 5(6)-carboxyfluorescein **(5)** was mixed with 2985 μL of assay buffer to make a final concentration 0.5μM of 5(6)-carboxyfluorescein **(5)**; and 16.6 μL of 1mg/mL TL11 **(3)** DMSO stock solution was mixed with 2983.4 μL of assay buffer to make a final concentration 5μM of TL11 **(3)**.

2.7.4   Fluorimetric Assay

2.7.4.1   TL11 (3) Fluorimetric Assay

Fluorimetric assay for probe TL11 **(3)** was applied to prove that probe TL11 **(3)** has the capability to bind with and be cleaved by activated legumain, to release fluorescence during cleavage.

2.7.4.1.1   Materials

Activation buffer: 50mM Sodium Acetate, 100mM NaCl, pH 4.0; Recombinant human legumain (R&D systems, 2199-CY-010); Assay buffer: 50mM MES hydrate (Sigma,

M2933), 250mM NaCl, pH 5.0; Substrate: Novel Fluorogenic Probe TL11 (**3**), 1mg/mL stock in DMSO; Fluorophore: 5(6)-carboxyfluorescein (**5**), 1mg/mL stock in DMSO then diluted to 100 µM in assay buffer; F16 Black Maxisorp 96 well Plate; FluoStar Omega multi-mode Microplate Reader.

2.7.4.1.2   **Method**

Stock rh-legumain (10 µg) was diluted with 100 µL activation buffer (pH 4.0) and stored at -78 ℃. Aliquots were incubated for 2h at 37ºC before dilution to 1ng/µL in assay buffer (pH 5.0).
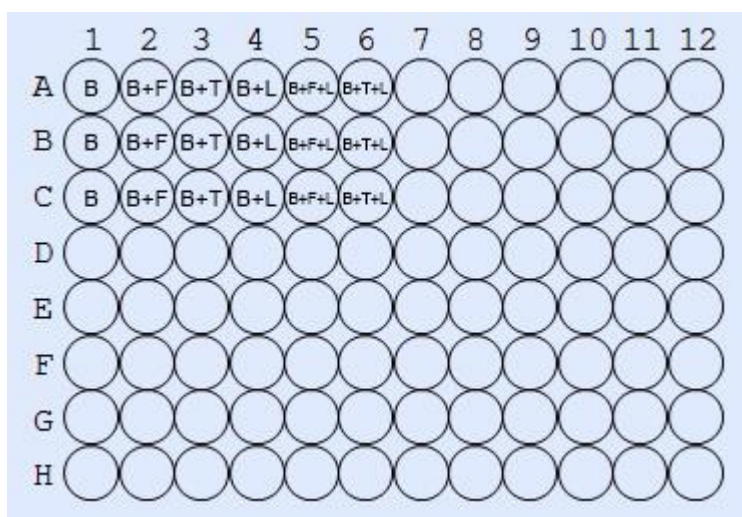
Figure 2.69. Arrangement on black 96-well plate for Fluorimetric Assay

As shown in **Figure 2.69**, in each well:

A1~C1 100 µL assay buffer (B)

A2~C2 90 µL assay buffer (B) + 10 µL 100 µM 5(6)-carboxyfluorescein (**5**) (F)

A3~C3 98.9 µL assay buffer (B) + 1.1 µL 909.1 µM fluorogenic probe TL11 (**3**) (T)

A4~C4 60 µL assay buffer (B) + 40 µL 1ng/µL Legumain stock solution (L)

A5~C5 50 µL assay buffer (B) + 10 µL 100 µM 5(6)-carboxyfluorescein (**5**) (F) + 40 µL 1ng/µL Legumain stock solution (L)

A6~C6 58.9 µL assay buffer (B) + 1.1 µL 909.1 µM fluorogenic probe TL11 (**3**) (T) + 40 µL 1ng/µL Legumain stock solution (L)

Final assay conditions per well:

- 10μM of 5(6)-carboxyfluorescein **(5)** in A2~C2 and A5~C5;

- 10μM of TL11 **(3)** in A3~C3 and A6~C6;

- 40ng of Legumain in A4~C4, A5~C5 and A6~C6.

Emission spectra were recorded at 5min intervals on a FluoStar Omega multi-mode Microplate Reader using excitation and emission analytical wavelengths of 485nm and 520nm, respectively. Gain value was set at 800 for this fluorimetric assay.

2.7.4.2   5(6)-FAM-Pro-Ala-Asn-OH (26) Fluorimetric Assay

A standard curve was prepared for 5(6)-FAM-Pro-Ala-Asn-OH **(26)** by plotting fluorescence emission against concentration for use in TL11 **(3)** fluorimetric assays.

The 5(6)-FAM-Pro-Ala-Asn-OH **(26)** 96-well plate layout is shown as follows:
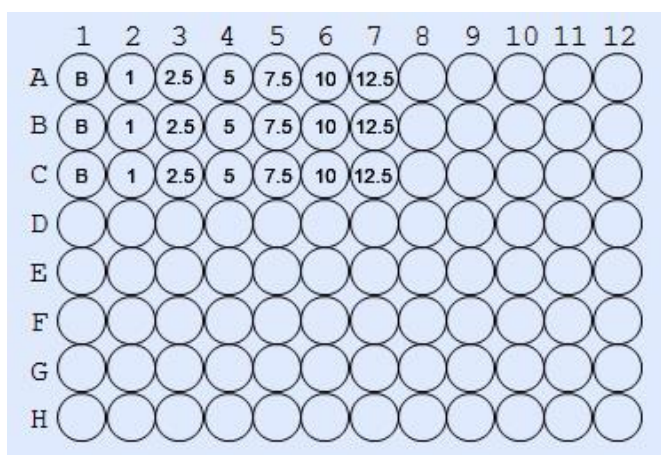
Figure 2.70. 5(6)-FAM-Pro-Ala-Asn-OH (26) arrangement on 96-well plate

As shown in **Figure 2.70**, in each well:

A1~C1 100 μL assay buffer (B)

A2~C2 99 μL assay buffer (B) + 1 μL 100 μM 5(6)-FAM-Pro-Ala-Asn-OH **(26)**

A3~C3 97.5 μL assay buffer (B) + 2.5 μL 100 μM 5(6)-FAM-Pro-Ala-Asn-OH **(26)**

A4~C4 95 μL assay buffer (B) + 5 μL 100 μM 5(6)-FAM-Pro-Ala-Asn-OH **(26)**

239

A5~C5 92.5 μL assay buffer (B) + 7.5 μL 100 μM 5(6)-FAM-Pro-Ala-Asn-OH **(26)**

A6~C6 90 μL assay buffer (B) + 10 μL 100 μM 5(6)-FAM-Pro-Ala-Asn-OH **(26)**

A7~C7 87.5 μL assay buffer (B) + 12.5 μL 100 μM 5(6)-FAM-Pro-Ala-Asn-OH **(26)**

Final assay conditions per well:

- 1μM of 5(6)-FAM-Pro-Ala-Asn-OH **(26)** in A2~C2;

- 2.5μM of 5(6)-FAM-Pro-Ala-Asn-OH **(26)** in A3~C3;

- 5μM of 5(6)-FAM-Pro-Ala-Asn-OH **(26)** in A4~C4;

- 7.5μM of 5(6)-FAM-Pro-Ala-Asn-OH **(26)** in A5~C5;

- 10μM of 5(6)-FAM-Pro-Ala-Asn-OH **(26)** in A6~C6;

- 12.5μM of 5(6)-FAM-Pro-Ala-Asn-OH **(26)** in A7~C7.

2.7.4.3   **AD17 (8), AD20 (9), VG (10) and PN11 (11) Fluorimetric Assay**

AD17 **(8)**, AD20 **(9)**, VG **(10)** and PN11 **(11)** fluorimetric assays were following exactly

the same method for TL11 **(3)** assay.

Final assay conditions per well:

- 10μM of 5(6)-carboxyfluorescein **(5)** in A2~C2 and A5~C5;

- 10μM of probe in A3~C3 and A6~C6;

- 40ng of Legumain in A4~C4, A5~C5 and A6~C6.

2.7.4.4   **FF (6) and MK8 (7) Fluorimetric Assay**

FF **(6)** and MK8 **(7)** fluorimetric assays were following exactly the same method for TL11

(3) assay.

Final assay conditions per well:

- 10μM of FITC **(4)** in A2~C2 and A5~C5;

- 10μM of probe in A3~C3 and A6~C6;

- 40ng of Legumain in A4~C4, A5~C5 and A6~C6.

2.7.4.5   YD103 (43) Fluorimetric Assay

The YD103 **(43)** 96-well plate layout is shown as follows:
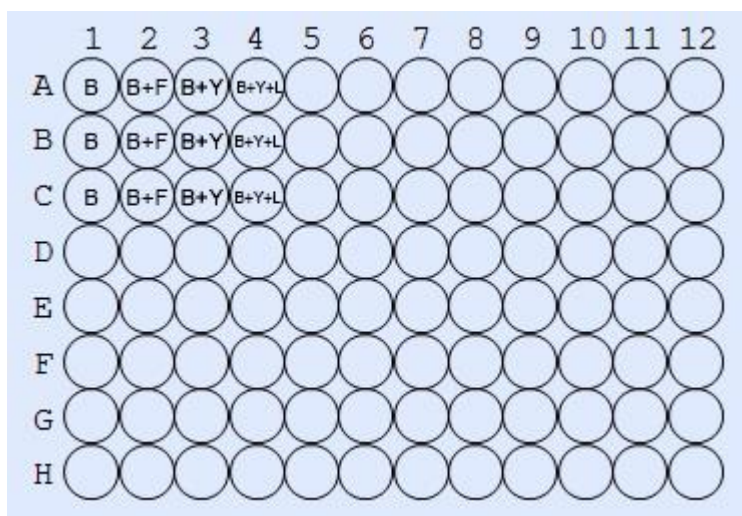
Figure 2.71. YD103 (43) arrangement on 96-well plate

As shown in **Figure 2.71**, in each well:

A1~C1 100 μL assay buffer (B)

A2~C2 90 μL assay buffer (B) + 10 μL 100 μM 5(6)-carboxyfluorescein **(5)** (F)

A3~C3 98.8 μL assay buffer (B) + 1.2 μL 803.9 μM fluorogenic probe YD103 **(43)** (Y)

A4~C4 58.8 μL assay buffer (B) + 1.2 μL 803.9 μM fluorogenic probe YD103 **(43)** (Y) +
    40 μL 1ng/μL Legumain stock solution (L)

Final assay conditions per well:

- 10μM of 5(6)-carboxyfluorescein **(5)** in A2~C2;

- 10μM of YD103 **(43)** in A3~C3 and A4~C4;

- 40ng of Legumain in A4~C4.

2.7.5   TL11 (3), PN11 (11) and VG (10) probes Enzyme Kinetics assay

2.7.5.1   Method

Legumain stock frozen solution, which was kept at -78°C, was incubated at 37°C for two

hours before diluted down to 1ng/μL with assay buffer.

241
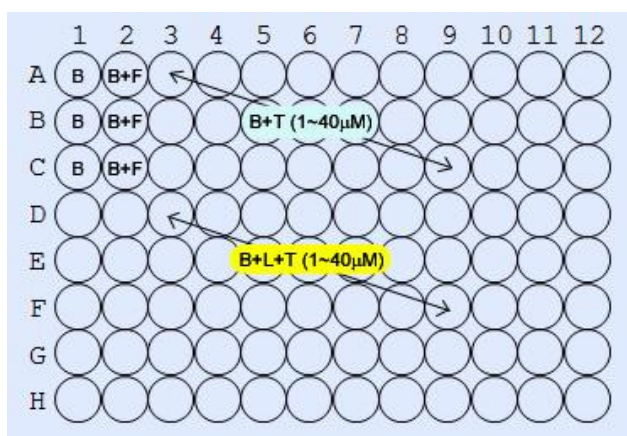
Figure 2.72. TL11 (3) enzyme kinetics assay arrangement on 96-well plate

As shown in **Figure 2.72**, in each well:

A1~C1 100 µL assay buffer (B)

A2~C2 99 µL assay buffer (B) + 1 µL of 100 µM 5(6)-carboxyfluorescein **(5)** (F)

A3~C3 to *A9~C9* in each column, final concentration of TL11 **(3)** (T) was increased from 1 µM, 2.5 µM, 5 µM, 7.5 µM, 10 µM, 20 µM up to 40 µM and assay buffer (B) was applied to top up each well final solution volume to 100 µL.

D3~F3 to *D9~F9* in each column, final concentration of TL11 **(3)** (T) was increased from 1 µM, 2.5 µM, 5 µM, 7.5 µM, 10 µM, 20 µM up to 40 µM, solution and assay buffer (B) was applied to adjust each well solution volume to 60 µL. At last, 40 µL of 1ng/ µL legumain (L) was added into each well of these seven columns just before the 96-well plate was placed into microplate read.

Final assay conditions per well:

• 1µM of TL11 **(3)** in A3~F3; • 2.5µM of TL11 **(3)** in A4~F4; • 5µM of TL11 **(3)** in A5~F5;

• 7.5µM of TL11 **(3)** in A6~F6; • 10µM of TL11 **(3)** in A7~F7;

• 20µM of TL11 **(3)** in A8~F8; • 40µM of TL11 **(3)** in A9~F9;

• 1 µL of 100 µM 5(6)-carboxyfluorescein **(5)** in A2~C2;

• 40µL of 1ng/ µL legumain in D3~F9

• All wells were topped up to 100µL with assay buffer

Methods for PN11 (**11**) and VN (**10**) probes enzyme kinetics assays were very similar to TL11 (**3**) enzyme kinetics assay. When arranging 96-well plates layout for PN11 (**11**) and VN (**10**) probes, they were applied the same as TL11 (**3**) probe on 96-well plate.

2.7.5.2 Enzyme kinetics assay data process by SigmaPlot 12

Data from each enzyme kinetics assay for each probe were processed by using enzyme kinetics wizard under toolbox tag in SigmaPlot 12.

2.7.6 Methods for cytotoxicity and proliferation assays

2.7.6.1 MCF-7 cell culture

ER positive MCF-7 mammary carcinoma cells were cultured in $75cm^2$ flasks containing RPMI-1640 medium (Sigma) (containing phenol red and supplemented with 10% heat inactivated foetal calf serum (FCS), penicillin (50units/mL), streptomycin (50μg/mL) and L-glutamine (2mM)) at 37^oC in 5% CO_2 atmosphere. Cells were supplied with fresh medium every three days and passaged weekly.

To harvest the cells from the flask, medium was poured out and then cells were washed with sterile sodium chloride (30mL) twice to wash out remaining medium in the flask. Then cells were trypsinised by adding 10% trypsin in sterile sodium chloride solution (5mL) in to the flask, which was shaken well and incubated at 37^oC in 5% CO_2 atmosphere for five minutes to release the adherent cells from the flask. Five minutes later, RPMI-1640 medium was added into the flask to quench the action of trypsin and cells were centrifuged for two minutes at 2000rpm to pellet cells before the supernatant

was discarded. Cells were then washed with fresh RPMI-1640 medium again before being resuspended in 30mL of fresh medium.

2.7.6.2   Materials for LDH and MTS assays

ER positive MCF-7 mammary carcinoma cells; RPMI-1640 medium containing phenol red (Sigma); trypsin ($1\times$); Nigrosin; NaCl (sterile); Triton X; MTS kit (Promega); LDH kit (Promega); Stop solution (Promega); PBS buffer; MTT; DMSO; TL3 (16); TL11 (3).

2.7.6.3   Drug preparation for LDH and MTS assays

Stock solutions of TL3 (**16**) and TL11 (**3**) were prepared at 1mM in neat DMSO, filter sterilised and diluted down to 100, 10, 1, 0.1, 0.01μM in phenol red free RPMI (reduced medium) for use.

2.7.6.4   Seeding cells for LDH and MTS assays

Cells were seeded at 2×10^4 cells per well (in 100μL of RPMI medium with phenol red) on a 96-well plates and cultivated for 24h at 37°C in 5% CO_2 atmosphere. Then the usual medium was removed from each well and replaced with 200μL of phenol red free RPMI medium (reduced medium) and treatment drug solutions at concentrations of interest. The 96-well plates were treated for 4h at 37°C in 5% CO_2 atmosphere. Three minutes before the end of drug treatment period, reduced medium was removed from the Triton-X control wells and replaced with 200μL of Triton-X (0.5%).

96-well plate layout was as follows:

	1	2	3	4 to 12
A	Cells + Triton-X			
B	Cells + Medium			
C	Cells + 0.01µM of Drug			
D	Cells + 0.1µM of Drug			
E	Cells + 1µM of Drug			
F	Cells + 10µM of Drug			
G	Cells + 100µM of Drug			
H	Medium only			

A1 to A3: Cells + 200µL of Triton-X;

B1 to B3: Cells + 200µL of phenol red free RPMI medium;

C1 to C3: Cells + 200µL of 0.01µM Drug solution;

D1 to D3: Cells + 200µL of 0.1µM Drug solution;

E1 to E3: Cells + 200µL of 1µM Drug solution;

F1 to F3: Cells + 200µL of 10µM Drug solution;

G1 to G3: Cells + 200µL of 100µM Drug solution;

H1 to H3: 200µL of phenol red free RPMI medium.

2.7.6.4.1 LDH assay

50µL of medium was removed from each of the wells after drug treatment period and placed into a new 96-well plate. 50µL of LDH substrate was added into each well and this new plate was incubated in the dark for 30min at RT. Stop solution (50µL) was applied to each well to stop this reaction. Any large bubbles were popped by using a

syringe needle and then the reaction was read at the absorbance of 492nm within one hour

after the addition of Stop Solution.

2.7.6.4.2   <u>MTS assay</u>

From the wells in the original plate, 50μL of medium was removed from each well, and

then MTS solution (20μL) was added into each well. The 96-well plate was then

incubated for 1h at 37°C in a humidified, 5% CO_2 atmosphere before the reaction was

read at the absorbance of 492nm.

2.8 <u>REFERENCES</u>

Anderson, G. L., McIntosh, M., Wu, L., Barnett, M., Goodman, G., Thorpe, J. D., Bergan, L., Thornquist, M. D., Scholler, N., Kim, N., O'Briant, K. and Drescher, C. (2010) Urban N. Assessing lead time of selected ovarian cancer biomarkers: a nested case-control study. *J. Natl. Cancer Inst.* **102**(1), 26-38.

Chen, J. M., Dando, P. M., Rawlings, N. D., Brown, M. A., Young, N. E., Stevens, R. A., Hewitt, E., Watts, C. and Barrett, A. J. (1997) Cloning, isolation, and characterization of mammalian legumain, an asparaginyl endopeptidase. *J. Biol. Chem.* **272**(12), 8090-8098.

Chen, J. M., Dando, P.M., Stevens, R. A., Fortunato, M. and Barrett, A. J. (1998) Cloning and expression of mouse legumain, a lysosomal endopeptidase. *Biochem. J.* **335**, 111-7.

Chen, J. M., Fortunato, M. and Barrett, A. J. (2000) Activation of human prolegumain by cleavage at a *C*-terminal asparagine residue. *Biochem. J.* **352**, 327-34.

Chen, J. M., Fortunato, M., Stevens, R. A. and Barrett, A, J. (2001) Activation of progelatinase A by mammalian legumain, a recently discovered cysteine proteinase. *Biol. Chem.* **382**(5), 777-83.

Cheung, K. L., Graves, C. R. and Robertson, J. F. (2000) Tumour marker measurements in the diagnosis and monitoring of breast cancer. *Cancer Treat. Rev.* **26**(2), 91-102.

Clegg, R. M. (1995) Fluorescence resonance energy transfer. *Curr. Opin. Biotechnol.* **6**(1), 103-10.

Clerin, V., Shih, H. H., Deng, N., Hebert, G., Resmini, C., Shields, K. M., Feldman, J. L., Winkler, A., Albert, L., Maganti, V., Wong, A., Paulsen, J. E., Keith, J. C. Jr, Vlasuk, G. P. and Pittman, D. D. (2008) Expression of the cysteine protease legumain in vascular lesions and functional implications in atherogenesis. *Atherosclerosis.* **201**(1), 53-66.

Dall, E. and Brandstetter, H. (2012) Activation of legumain involves proteolytic and conformational events, resulting in a context- and substrate-dependent activity profile. *Acta. Crystallogr. Sect. F. Struct. Biol. Cryst.Commun.* **68**, 24-31.

de Jong, J., Klein, I., Bast, A. and van der Vijgh, W. J. (1992) Analysis and pharmacokinetics of *N*-L-leucyldoxorubicin and metabolites in tissues of tumor-bearing BALB/c mice. *Cancer Chemother. Pharmacol.* **31**(2), 156-60.

DiSalvo, A. (2004). Design and synthesis of tumour activated oligopeptide prodrugs that exploit the proteolytic activity of MMP-9. PhD, Edinburgh Napier University.

Edman, P. (1956). Mechanism of the Phenyl Isothiocyanate Degradation of Peptides. *Nature*. **177**, 667-668.

Felding-Habermann, B. and Cheresh, D. A. (1993) Vitronectin and its receptors. *Curr. Opin. Cell Biol*. **5**(5), 864-8.

Hermann, P., Armant, M., Brown, E., Rubio, M., Ishihara, H., Ulrich, D., Caspary, R. G., Lindberg, F. P., Armitage, R., Maliszewski, C., Delespesse, G. and Sarfati, M. (1999) The vitronectin receptor and its associated CD47 molecule mediates proinflammatory cytokine synthesis in human monocytes by interaction with soluble CD23. *J. Cell Biol*. **144**(4), 767-75.

Huang, P.S. and Oliff, A. (2001) Drug-targeting strategies in cancer therapy. *Curr. Opin. Genet. Dev*. **11**(1), 104-10.

Johnson, K. A. and Goody, R. S. (2011) The original Michaelis constant: translation of the 1913 Michaelis-Menten paper. *Biochemistry*. **50**(39), 8264-8269.

Jullian, M., Hernandez, A., Maurras, A., Puget, K., Amblard, M., Martinez, J. and Subra, G. (2009) *N*-terminus FITC labeling of peptides on solid support: the truth behind the spacer. *Tetrahedron Lett.* **50**(3), 260-263.

Kashelikar, D. V. and Ressler, C. (1964) An Oxygen-18 Study of the Dehydration of Asparagine Amide with *N*,*N*'-Dicyclohexylcarbodiimide and *p*-Toluenesulfonyl Chloride. *J. Am. Chem. Soc.* **86** (12), 2467–2473.

Kembhavi, A. A., Buttle, D. J., Knight, C. G. and Barrett, A. J. (1993) The two cysteine endopeptidases of legume seeds: purification and characterization by use of specific fluorometric assays. *Arch. Biochem. Biophys*. **303**(2), 208-213.

Li, D. N., Matthews, S. P., Antoniou, A. N., Mazzeo, D. and Watts, C. (2003) Multistep autoactivation of asparaginyl endopeptidase *in vitro* and *in vivo*. *J. Biol. Chem*. **278**(40), 38980-90.

Liu, C. (2008) Legubicin a Tumor-activated Prodrug for Breast Cancer Therapy. SCRIPPS RESEARCH INST LA JOLLA CA. Available from http://oai.dtic.mil/oai/oai?verb=getRecord&metadataPrefix=html&identifier=ADA4865 31 [accessed 23/10/2013]

Liu, C., Sun, C., Huang, H., Janda, K. and Edgington, T. (2003) Overexpression of legumain in tumors is significant for invasion/metastasis and a candidate enzymatic target for prodrug therapy. *Cancer Res*. **63**(11), 2957-64.

Mathieu, M. A., Bogyo, M., Caffrey, C. R., Choe, Y., Lee, J., Chapman, H., Sajid, M., Craik, C. S. and McKerrow, J. H. (2002) Substrate specificity of schistosome versus human legumain determined by P1-P3 peptide libraries. *Mol. Biochem. Parasitol*. **121**(1), 99-105.

Murthy, R. V., Arbman, G., Gao, J., Roodman, G. D. and Sun, X. F. (2005) Legumain expression in relation to clinicopathologic and biological variables in colorectal cancer. *Clin. Cancer Res*. **11**(6), 2293-9.

Paul, R. and Kende, A. S. (1964) A Mechanism for the *N*,*N'*-Dicyclohexylcarbodiimide Caused Dehydration of Asparagine and Maleamic Acid Derivatives. *J. Am. Chem. Soc.* **86** (19), 4162–4166.

R&D systems (2012) Recombinant Human Legumain/Asparaginyl Endopeptidase. Available from http://www.rndsystems.com/pdf/2199-CY.pdf [accessed 26/03/2013]

Rawlings, N. D., Barrett, A. J. and Bateman, A. (2012) MEROPS: the database of proteolytic enzymes, their substrates and inhibitors. *Nucleic Acids Res.* **40**, D343-D350.

Riss, T. and Moravec, R. (1996) Improved Non-Radioactive Assay to Measure Cellular Proliferation or Toxicity: The CellTiter 96® AQ$_{ueous}$ One Solution Cell Proliferation Assay. *Promega Notes Magazine.* **59**, 19-23.

Sengoku, K., Satoh, T., Saitoh, S., Abe, M. and Ishikawa, M. (1994) Evaluation of transvaginalcolor Doppler sonography, transvaginal sonography and CA 125 for prediction of ovarian malignancy. *Int. J. Gynaecol. Obstet*. **46**(1), 39-43.

Sexton, K. B., Witte, M. D., Blum, G. and Bogyo, M. (2007) Design of cell-permeable, fluorescent activity-based probes for the lysosomal cysteine protease asparaginyl endopeptidase (AEP)/legumain. *Bioorg. Med. Chem. Lett*. **17**(3), 649-53.

Shimada, T., Yamada, K., Kataoka, M., Nakaune, S., Koumoto, Y., Kuroyanagi, M., Tabata, S., Kato, T., Shinozaki, K., Seki, M., Kobayashi, M., Kondo, M., Nishimura, M. and Hara-Nishimura, I. (2003) Vacuolar processing enzymes are essential for proper processing of seed storage proteins in Arabidopsis thaliana. *J. Biol. Chem*. **278**(34), 32292-9.

Stern, L., Perry, R., Ofek, P., Many, A., Shabat, D. and Satchi-Fainaro, R. (2009) A novelantitumor prodrug platform designed to be cleaved by the endoprotease legumain. *Bioconjug. Chem*. **20**(3), 500-10.

Trouet, A., Masquelier, M., Baurain, R. and Deprez-De Campeneere, D. (1982) A covalent linkage between daunorubicin and proteins that is stable in serum and reversible by lysosomal hydrolases, as required for a lysosomotropic drug-carrier conjugate: *in vitro* and *in vivo* studies. *Proc. Natl. Acad. Sci. USA*. **79**(2), 626-9.

Trouet, A., Passioukov, A., Van derpoorten, K., Fernandez, A. M., Abarca-Quinones, J., Baurain, R., Lobl, T. J., Oliyai, C., Shochat, D. and Dubois, V. (2001) Extracellularly tumor-activated prodrugs for the selective chemotherapy of cancer: application to doxorubicin and preliminary *in vitro* and *in vivo* studies. *Cancer Res*. **61**(7), 2843-6.

Turnbull, A. (2003). Design and development of novel DNA topoisomerase inhibitors. PhD, Edinburgh Napier University.

van Haaften-Day, C., Shen, Y., Xu, F., Yu, Y., Berchuck, A., Havrilesky, L. J., de Bruijn, H. W., van der Zee, A. G., Bast, R. C. and Jr, Hacker, N. F. (2001) OVX1, macrophage-colony stimulating factor, and CA-125-II as tumor markers for epithelial ovarian carcinoma: a critical appraisal. *Cancer*. **92**(11), 2837-44.

Van Valckenborgh, E., Mincher, D., Salvo, A. D., Riet, I. V., Young, L., Camp, B. V. and Vanderkerken, K. (2005) Targeting an MMP-9-activated prodrug to multiple myeloma-diseased bone marrow: a proof of principle in the 5T33MM mouse model. *Leukemia*. **19**, 1628-1633.

Wang, L., Chen, S., Zhang, M., Li, N., Chen, Y., Su, W., Liu, Y., Lu, D., Li, S., Yang, Y., Li, Z., Stupack, D., Qu, P., Hu, H. and Xiang, R. (2012) Legumain: A biomarker for diagnosis and prognosis of human ovarian cancer. *J. Cell Biochem.* **113**(8), 2679-86.

Weyermann, J., Lochmann, D. and Zimmer, A. (2005) A practical note on the use of cytotoxicity assays. *Int. J. Pharm*. **288**(2), 369-76.

Wu, W., Luo, Y., Sun, C., Liu, Y., Kuo, P., Varga, J., Xiang, R., Reisfeld, R., Janda, K. D., Edgington, T. S. and Liu, C. (2006) Targeting cell-impermeable prodrug activation to tumor microenvironment eradicates multiple drug-resistant neoplasms. *Cancer Res*. **66**(2), 970-80.

Yamane, T., Takeuchi, K., Yamamoto, Y., Li, Y. H., Fujiwara, M., Nishi, K., Takahashi, S. and Ohkubo, I. (2002) Legumain from bovine kidney: its purification, molecular cloning, immunohistochemical localization and degradation of annexin II and vitamin D-binding protein. *Biochim. Biophys. Acta*. **1596**(1), 108-20.

Contents

Chapter III. DNA Binding Study on Novel Anthracenediones

3.1 <u>INTRODUCTION</u>

In the past two decades, more efforts were focused on the interaction relationship of small molecule compounds with DNA. The study of drug-DNA binding facilitates better understanding of the molecular mechanisms of drug-DNA interaction and affords better ways to design DNA targeted drugs (Li *et al*., 2005). Drug-DNA interaction has two major binding modes: intercalation and groove binding (Chaires, 1998; Palchaudhuri and Hergenrother, 2007). The purpose of studying the DNA-binding properties of compounds in the context of this research project and its relationship to Chapters I and II of this thesis are two-fold. Firstly, several protease substrates (either of MMPs or legumain) contained aminoanthraquinones. The latter are present either as active agents or sometimes 'black-hole' quenchers of fluorophores in FRET pairs. In the former case, amino acid conjugates of spacer-linked anthraquinones might be expected to be cytotoxic based on earlier work (Turnbull, 2003) and it is accepted that whether or not these conjugates bind to DNA can influence their ability to act as topoisomerase inhibitors and their cytotoxic properties. On the other hand, when aminoanthraquinone-spacer compounds have been used as quenchers, it is important from a diagnostic point of view, if probes are to be used *in vivo*, that they are non-toxic or much less toxic than the actives from this series, if and when released as their amino acid conjugates after protease-catalysed cleavage of

oligopeptide substrate precursors. Therefore, this chapter presents the results of DNA-binding studies performed on some earlier-prepared, lead compounds from the cytotoxic series together with some novel analogues prepared here, in an attempt to define structure-activity relationships amongst this closely related group of compounds. The DNA binding properties of anthracenediones related to mitoxantrone (1) have been reported in the early literature (Agbandje *et al.*, 1992).

3.1.1 <u>Intercalating agents</u>

A half century ago, Lerman (1961) and Pritchard *et al.* (1966), hypothesised that the flat shape gave the advantage of polycyclic aromatic ring compounds to insert between two base pairs of the DNA double helix. Van der Waals interaction between base pairs and the π-electron systems of the polycyclic aromatic ring compound are the main binding forces. Their theory was confirmed by others by X-ray crystallographic studies (Lerman, 1961; Pritchard *et al.*, 1966; Nakamoto *et al.*, 2008). Intercalating agents usually have planar structures, normally containing bi/tricyclic ring structures. Once intercalating agents insert between DNA base pairs, which may result in the use of an enormous amount of free energy, they can lead to unwinding and lengthening of the DNA helix (Chaires, 1998; Palchaudhuri and Hergenrother, 2007; Neto and Lapis, 2009) and also cause base-pair deletions or insertions during DNA replication. During lengthening of the DNA, only the axial distance of neighbouring phosphate groups can be increased, the length between neighbouring phosphate groups stays the same (Williams *et al*., 1992). Studies showed that different intercalating agents may have

their own preferred binding sites, and these unique binding site preferences can lead to different pharmacological and cytotoxic activities for different intercalating agents (Nakamoto *et al.*, 2008).

A red-shift of 10nm or more in the visible absorption spectrum can commonly be found during drug-DNA intercalation due to a π-π* electron transition that would be altered in the drug chromophore (Nakamoto *et al.*, 2008).

During DNA intercalation binding, intercalating agents obey the rule of neighbour-exclusion which states that intercalating agents can only bind every other base step. The neighbouring binding sites cannot be occupied by intercalating agents at the same time. The restraint of neighbour-exclusion rule may be caused by the stereochemical structure of the sugar-phosphodiester backbone (Williams *et al*., 1992).

3.1.2 Groove-binding agents

When compared with intercalating agents, groove-binding agents do not cause significant DNA structure changes during drug-DNA interaction and it can be considered as a type of lock-and-key model. Groove-binding compounds commonly have crescent shaped structures and usually bind to the minor groove of DNA, also none or very little free energy is required during drug-DNA binding interaction (Chaires, 1998; Palchaudhuri and Hergenrother, 2007).

3.1.3   Anthracycline Derivatives

Since the first anthracycline, daunorubicin, was introduced as an antineoplastic agent in 1967, more than 200 anthracyclines have been identified and many of them are considered as useful anticancer agents. The most clinically used anthracyclines are: daunorubicin (daunomycin (**2**), rubidomycin), doxorubicin (adriamycin), epirubicin (a semi-synthetic derivative of doxorubicin) and idarubicin. Although they show quite a wide range of efficacy against several types of cancer, due to the risk of irreversible cardiac damage, their clinical efficacy is limited (Smith *et al.*, 2010).
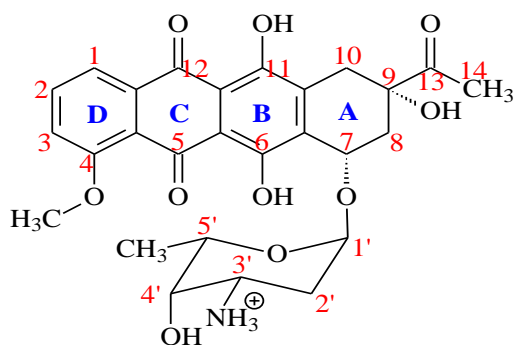
Figure 3.1. Chemical structure of daunomycin (2)

Anti-tumour agent daunomycin (**2**) [**Figure 3.1**] has a planar structure spanning rings B-D that fits well in between base pairs and functions as an intercalator. The nonplanar substituents in ring A interact with the DNA double helix through hydrogen bonding and offer an anchoring function to hold the amino sugar to fit in the minor groove of DNA (Quigley *et al.*, 1980).

3.1.4   Anthracene-9,10-dione Derivatives

The anthracene-9,10-dione series of compounds have been known as more effective for some types of cancer, and less systemically toxic when compared with

254

anthracycline analogues, such as daunomycin (**2**) and doxorubicin (Agbandje *et al*., 1992). Since the late 1970s, numerous aminoalkylaminoanthraquinones have been synthesised in order to reduce cardiotoxic effects caused by doxorubicin in which an aminoalkyl group supplants the amino sugar moiety of the latter. One notable example of this approach, mitoxantrone (**1**) [**Figure 3.2**] (Wallace *et al.,* 1979), has been widely studied and it showed less cardiotoxic effects when compared with anthracyclines doxorubicin and daunorubicin. Although mitoxantrone (**1**) has a planar aromatic structure which is crucial for intercalation, due to the two extended side chains at positions 1 and 4, mitoxantrone (**1**) can only partially intercalate in between base pairs of DNA (Lown *et al.*, 1985). Early structure activity studies indicated that 5,8-dihydroxy-substituition, as present in mitoxantrone's structure, can improve a compound's water solubility and increase cytotoxic potency by approximately 10-fold when compared to the unsubstituted analogue ametrantrone (**2**) [**Figure 3.2**] (Zee-Cheng and Cheng, 1978). Murdock and colleagues pointed out that symmetrical 1,4-bis-substituted side-chains have to be basic, in order to bind to phosphate groups of a DNA chain. Also, 'one-armed' analogues were reported to be less active or inactive (Murdock *et al.,* 1979).
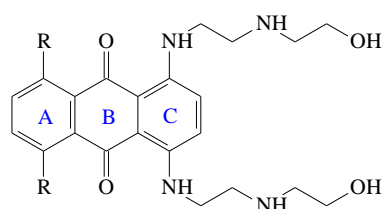
Where: Mitoxantrone: R=OH (**1**)
             Ametantrone: R=H (**3**)

Figure 3.2. Chemical structure of ametantrone (3) and mitoxantrone (1)

255

Cytotoxicity of many topoisomerase II targeting anti-cancer agents, such as mitoxantrone (1), are correlated with their abilities to stabilize DNA-enzyme cleavable complexes in which topoisomerase II enzymes are bound to DNA strands covalently (Osheroff, 1989). These stabilized cleavable complexes are lethal during DNA replication and can lead to mutations, recombination events and cell death (Chen *et al.,* 1996; Willmore *et al.,* 1998). In mitoxantrone derivatives, it had been noticed that there was a good correlation between cytotoxicity and topoisomerase II DNA cleavage. Structure alteration on one side chain did not markedly affect cytotoxic potency or DNA cleavage, however, removing 5,8-dihydroxyl groups from the planar aromatic moiety (ametantrone (3)) significantly reduced the formation of topoisomerase II-DNA-drug cleavable complex in both intact cells and SV40 DNA (De Isabella *et al.*, 1993). Studies showed that mitoxantrone (1) can form drug-stabilized DNA enzyme cleavable complexes with both topoisomerase IIα and topoisomerase IIβ isoforms *in vivo*, in mTOP2β-4 wild-type mouse embryonic fibroblasts, however, topoisomerase IIα is the preferred cytotoxic target of mitoxantrone (1) rather than the topoisomerase IIβ isoform (Errington *et al.,* 1999). During mitoxantrone treatment, topoisomerase IIα cleavable complexes had a half-life of 10 hours and they were 1.7-fold more stable than topoisomerase IIβ cleavable complexes which had a half-life of 6 hours. The longevity of mitoxantrone-stabilized topoisomerase IIα DNA cleavable complex could be related to its cytotoxic properties (Errington *et al.,* 2004).

3.1.5   Competitive Ethidium Displacement
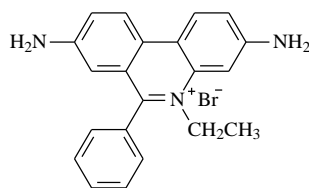
Figure 3.3. Chemical structure of ethidium bromide (4)

Ethidium bromide **(4)** [**Figure 3.3**] is a cationic dye (Olmsted and Kearns, 1977) and a

trypanocidal drug (Newton, 1957) which can intercalate between base pairs in both

double stranded DNA and RNA (Baguley and Falkenhaug, 1978). There are two

modes of site binding for ethidium bromide to interact with DNA. The primary, also

the stronger mode of binding has been defined as intercalation between base pairs. The

second mode of site binding is known as the external binding between ethidium

bromide and the phosphate groups on the DNA surface. Binding of ethidium bromide

to double stranded DNA is saturated when one ethidium bromide molecule is bound

with every four or five base pairs (Nordmeier, 1992). In solution, fluorescence of

ethidium bromide is quenched by aqueous solvent. However, once ethidium bromide

(4) intercalates DNA, the dye molecule is inside the hydrophobic environment which

protects ethidium bromide **(4)** from the aqueous solvent, hence a dramatic fluorescence

release can be detected (Olmsted and Kearns, 1977). The complex of DNA-ethidium

bromide has higher viscosity and higher melting temperature when compared with free

DNA (Nakamoto *et al.*, 2008). The maximum absorbance of ethidium bromide **(4)** is at

480nm, however, once ethidium bromide **(4)** is bound with DNA, the absorption

maximum wavelength shifts to 518nm along with increasing of relative fluorescence

intensity.
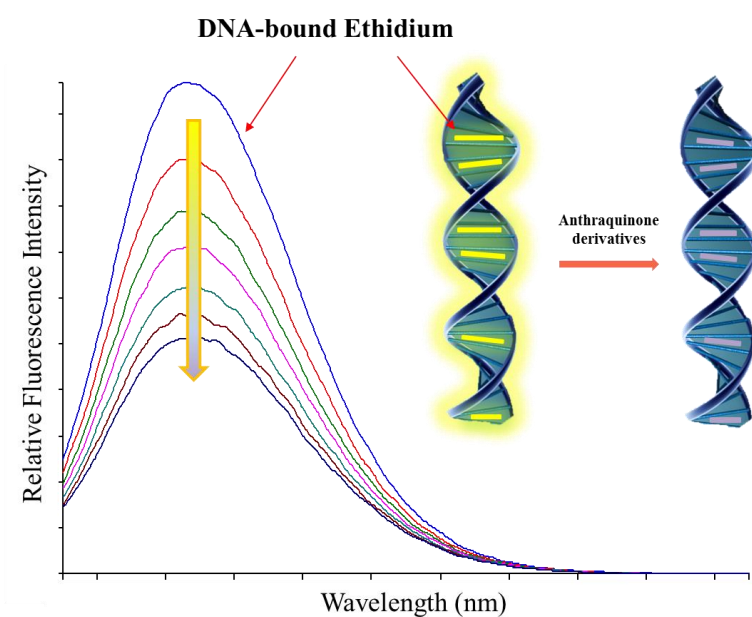
Figure 3.4. Ethidium displacement assay

Ethidium displacement assay **[Figure 3.4]**, an indirect fluorescence based technique,

was first described almost three decades ago (Morgan *et al*., 1979). When ethidium

bromide **(4)** binds to DNA, its fluorescence can be increased by 24-fold (Palchaudhuri

and Hergenrother, 2007). Providing a second DNA binding ligand to DNA-ethidium

complexes can lead to a displacement of ethidium bromide, hence it can cause a

decrease of fluorescence intensity (Baguley *et al*., 1981).

3.2   <u>AIM</u>

Several anthraquinone derivatives had been designed and synthesised in this laboratory. They all have similar chemical structures with various hydroxyl groups at different positions on the anthraquinone basic structure. In order to study their individual DNA binding affinities, measurement of the K_{app} DNA binding constant was introduced as a means of comparison of compounds within closely structurally related series. Hence, how different side chains and different number of hydroxyl groups would affect anthraquinone derivatives' DNA binding affinity can then be calculated and compared. As mitoxantrone (**1**) is the most effective and widely studied anthracene-9,10-dione derivative, so each anthraquinone derivative in this project was compared with the measured mitoxantrone K_{app} value in order to find out how potent these compounds are. Furthermore, the standard cell proliferation MTT assay was applied to NU:UB 21 (**5**), 31 (**6**), 51 (**7**) and YD 4 (**8**) so as to find out the relationships between each compound's DNA binding affinity and cytotoxicity.

3.3 <u>RESULTS AND DISCUSSION</u>

In previous studies on the NU:UB series of aminoanthraquinones and their amino acid conjugates in this laboratory, it was shown that the anthraquinone system has the potential to bind to DNA by intercalation which favours interactions with topoisomerase II, and the extended spacer group or spacer with one amino acid conjugate in the anthraquinone system may favour interactions with topoisomerase I (Turnbull, 2003).

It has been shown that both NU:UB 31 (**6**) and 51 (**7**) are dual topoisomerase I and II inhibitors. The dehydroxylated (anthraquinone), diaminopropane spacer proline conjugate NU:UB 31 (**6**) is able to stimulate topoisomerase I, II α- and II β- mediated DNA cleavage at 5 μM, 25 μM and 25 μM, respectively (optimum concentrations). And the 4, 8-dihydroxylated, diaminopropane spacer glycine conjugate NU:UB 51 (**7**) can stimulate topoisomerase I, II α- and II β- mediated DNA cleavage at 50 μM, 25 μM and 25 μM, respectively (optimum concentrations) (Pettersson, 2004).

The anthraquinone derivatives that have been used in this project for competitive ethidium displacement assay and standard cell proliferation MTT assay all have similar structure which is shown in general form in **Figure 3.5** and details for each derivative are listed in **Table 3.1**:
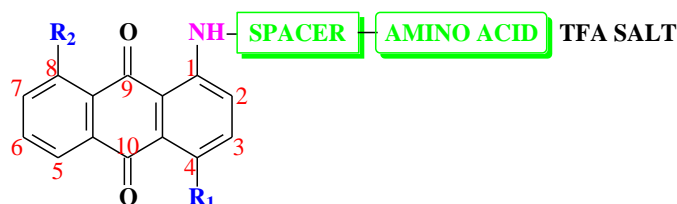
Figure 3.5 General structure of anthraquinone derivatives.

260

Drug	R_1 (C4)	R_2 (C8)	Spacer	Amino acid
NU:UB 83 (9)	OH	OH	$NH(CH_2)_3NH$	Proline
NU:UB 85 (10)	OH	OH	$NH(CH_2)_4NH$	Proline
NU:UB 31 (6)	H	H	$NH(CH_2)_3NH$	Proline
NU:UB 51 (7)	OH	OH	$NH(CH_2)_3NH$	Glycine
YD4 (8)	OH	H	$NH(CH_2)_3NH$	Glycine
YD82 (11)	OH	H	$NH(CH_2)_2NH(CH_2)_2OH$	N/A
NU:UB 466 (12)	H	H	$NH(CH_2)_2NH(CH_2)_2OH$	N/A
YD2 (13)	OH	H	$NH(CH_2)_3NH$	N/A
NU:UB 197 (14)	H	H	$NH(CH_2)_3NH$	N/A
NU:UB 21 (5)	H	H	$NH(CH_2)_3NH$	D-alanine

Table 3.1 Differences in anthraquinone derivatives at the C4 and the C8 positions.

The first nine anthraquinone derivatives shown in **Table 3.1** were compared with mitoxantrone **(1)** in competitive ethidium displacement assay in order to find out if hydroxyl groups at the C4 and/or the C8 positions or different spacers or spacer with different amino acid conjugates would affect DNA binding affinities. Four similar anthraquinone derivatives NU:UB 21 **(5)**, 31 **(6)**, 51 **(7)** and YD 4 **(8)** which all have 1,3-diaminopropane as spacer were also compared in standard cell proliferation MTT assays.

3.3.1 Design and synthesis of anthraquinone DNA-binding agents

Based on the successful synthesis of previous members of the NU:UB series (Turnbull, 2003), YD2 **(13)**, YD4 **(8)**, YD82 **(11)** and NU:UB 466 **(12)** were synthesised by introducing or eliminating one hydroxyl group from similar previous NU:UB compounds in this research project, while the other anthraquinone compounds were prepared previously and given for testing in this research project.

261

3.3.1.1   Synthesis of 4-hydroxy-1-[Propyl Spacer]-AQ TFA salt [YD2] (13)
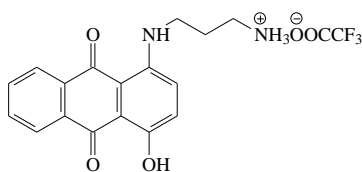
Figure 3.6. Chemical structure of 4-hydroxy-1-[Propyl Spacer]-AQ TFA salt [YD2] (13)

AQ-spacer TFA salt YD2 **(13)** **[Figure 3.6]** is an intermediate compound during the

synthesis of AQ-spacer glycine conjugate TFA salt YD4 **(8)**. When compared with

NU:UB 197 **(14)**, YD2 **(13)** has similar structure with the same diaminopropane spacer

[Propyl Spacer] but having an extra hydroxyl group at the C4 position. Hence, it would

be valuable to determine if an extra hydroxyl group would cause different DNA

binding affinities when comparing YD2 **(13)** and NU:UB 197 **(14)** in the DNA binding

assay.
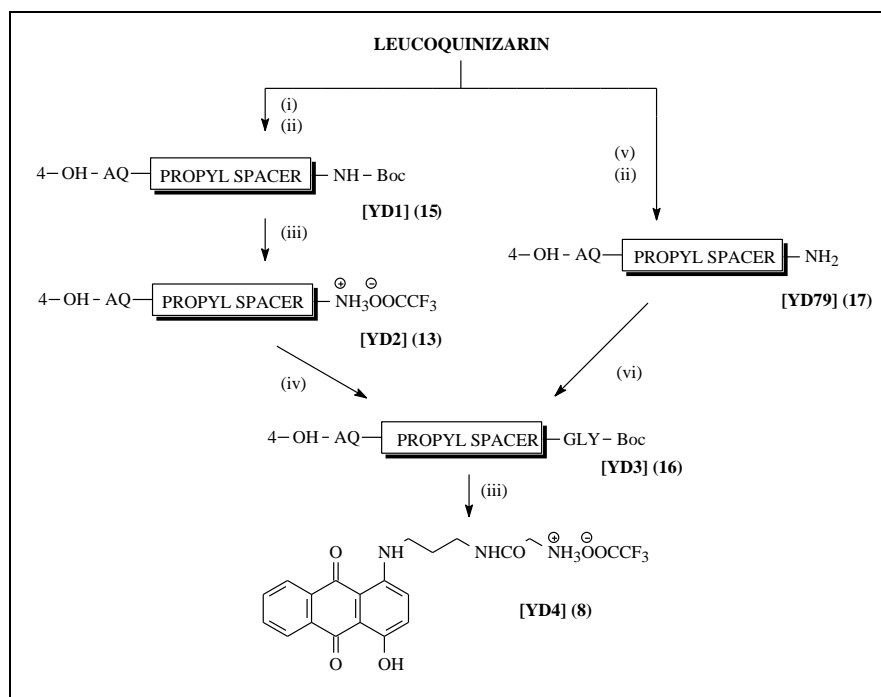
Reagents and conditions: (i) Boc-NH(CH$_2$)$_3$-NH$_2$, EtOH:THF (2:1), water bath, 70min, triethylamine. (ii) O$_2$, 2h. (iii) TFA, RT, 30min. (iv) Boc-Gly-OSu, DMF, triethylamine, RT, 12h. (v) NH$_2$(CH$_2$)$_3$NH$_2$, DCM, water bath 95°C, 60min. (vi) Boc-Gly-OH, HOBt, TBTU, DMF, DIPEA, RT, 12h.

Scheme 3.1. Synthesis of 4-OH-AQ-[Propyl Spacer]-Gly TFA salt [YD4] (8)

The synthesis of 4-hydroxy-1-[Propyl Spacer]-AQ TFA salt, YD2 **(13)**, started with

mixing leucoquinizarin with Boc-NH-$(CH_2)_3$-NH_2 in a mixed solvent of ethanol: THF

(2:1), then this reaction mixture was refluxed for one hour. The colour of this reaction

changed from brown to dark purple. Once the completion of this reaction was

confirmed by TLC, this purple solution was air-bubbled for two hours to oxidize the

first-formed leuco form of the product. After oxidization, 4-hydroxy-1-([Propyl

Spacer]-NH-Boc)-AQ [YD1] **(15)** was purified by column chromatography. Then this

pure (chromatographically homogeneous) purple product was treated with TFA to

remove the Boc-protecting group and form a trifluoroacetate salt YD2 **(13)** **[Scheme

3.1]**. The structure of YD2 **(13)** was confirmed by its electrospray (+) mass spectrum

which had a strong signal at m/z 297 for the cationic species $(RNH_3)^+$.

3.3.1.2   Synthesis of 4-hydroxy-1-(Gly-[Propyl Spacer])-AQ TFA salt [YD4] (8)
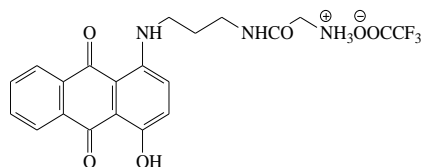
Figure 3.7. Chemical structure of 4-hydroxy-1-(Gly-[Propyl Spacer])-AQ TFA salt [YD4] (8)

Based on the structure of dual topoisomerase I and II inhibitor NU:UB 51 **(7)**, YD4 **(8)**

[Figure 3.7] was designed and synthesised with the objective of 'removing' one

hydroxyl group at the C8 position in NU:UB 51 **(7)** and keeping the same

diaminopropane spacer glycine conjugate in the side chain, to find out whether

eliminating one hydroxyl group at the C8 position would lead to any DNA binding

affinity changes. YD4 **(8)** was prepared by two procedures: via YD2 **(13),** using

mono-Boc-protected diamine (**Method I**), and using free diamine via compound YD79 (**17**) (**Method II**).

Method I of synthesising YD4 (**8**), from YD2 (**13**) route: the trifluoroacetate salt YD2 (**13**) was coupled with Boc-Gly-OSu to give 1-(Boc-Gly-[Propyl Spacer])-4-hydroxy-AQ [YD3] (**16**), then this Boc protected compound YD3 (**16**) was treated with TFA to give the final trifluoroacetate salt YD4 (**8**).

Method II of synthesising YD4 (**8**), from YD79 (**17**) route: leucoquinizatin was reacted with one equivalent of un-protected 1,3-diaminopropane in dichloromethane, then the reaction mixture was oxidized for one hour to give a dark purple intermediate, 4-hydroxy-1-[(3-aminopropyl)amino]anthraquinone [YD79] (**17**). After purification by column chromatography, YD79 (**17**) was coupled with Boc-Gly-OH by using standard peptide coupling methods to form the Boc protected compound YD3 (**16**), which was then purified and treated with TFA to give the final dark purple product YD4 (**8**) [**Scheme 3.1**].

Although YD4 (**8**) can be synthesised by both methods, method I was a better way to synthesise YD 4 (**8**) than method II and this is because in method I, the Boc protected AQ-propylamino spacer YD1 (**15**) was synthesised by using Boc-NH(CH$_2$)$_3$-NH$_2$. Because one end of this diaminopropane is protected by a Boc group, this coupling reaction was quite straightforward and the product was easily purified by running a silica gel chromatography column. In method II, the AQ-propyl spacer YD79 (**17**) was synthesised by using unprotected 1,3-diaminopropane, hence, during the coupling stage, one mole of diaminopropane may react with two moles of leucoquinizarin. Also, the unprotected AQ-propylamino spacer YD79 (**17**) was difficult to dissolve in both

264

dichloromethane and methanol or the mixture of both solvents. So the purification of product YD79 (**17**) on a silica gel chromatography column was more difficult than the purification of the Boc protected product YD1 (**15**) in method I.

3.3.1.2.1 Mass Spectral Characterisation of YD4 (8)

Given YD4 (**8**) is a TFA salt, in order to find signals of both the alkylammonium cation $(RNH_3)^+$ and trifluoroacetate anion, this 4-hydroxy-1-(Gly-[Propyl Spacer])-AQ TFA salt [YD4] (**8**) was analysed by electrospray ionisation in both positive and negative modes.
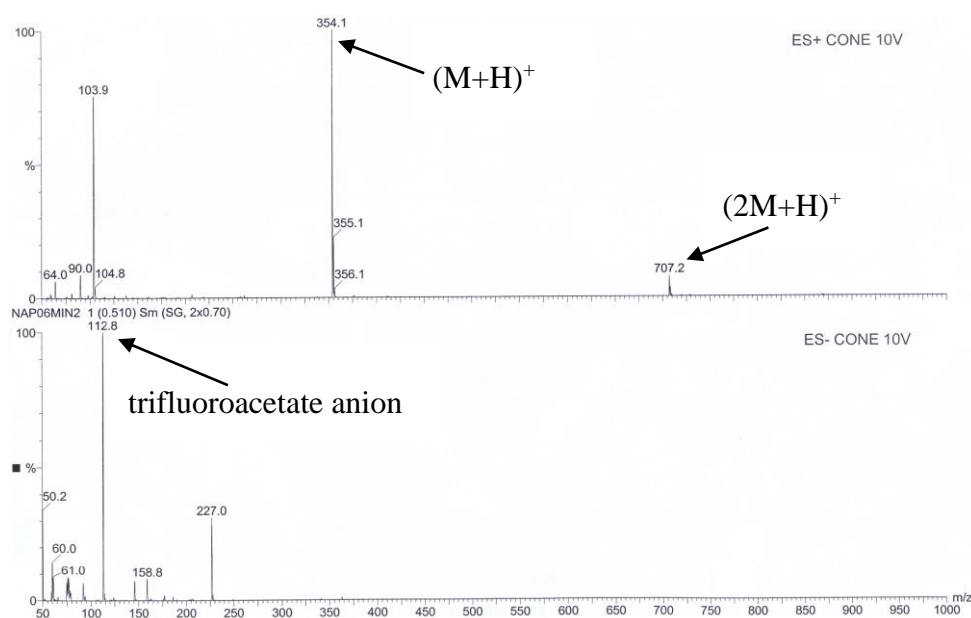
Figure 3.8. ESI(+) Mass spectrum of 4-hydroxy-1-(Gly-[Propyl Spacer])-AQ TFA salt [YD4] (8)

The electrospray (+) mass spectrum showed a strong signal for $(M+H)^+$ at m/z 354.1 (100%), a signal at m/z 707.2 for the species $(2M+H)^+$ and the electrospray (-) mass spectrum had a strong signal at m/z 112.8 (100%) which confirmed the presence of the trifluoroacetate anion [**Figure 3.8**]. Hence, both electrospray positive and negative mass spectra indicated that YD4 (**8**) had the correct structure.

3.3.1.3   Synthesis of YD82 (11)
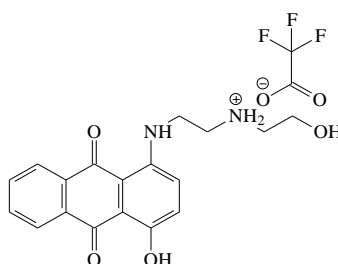
Figure 3.9. Chemical structure of YD82 (11)

YD82 **(11) [Figure 3.9]** shares the same spacer side chain as mitoxantrone **(1)**, and it was designed to have only one spacer side chain at the C1 position instead of two side chains in its structure, and also two hydroxyl groups at the C5 and C8 positions were omitted in YD82 **(11)**. All the structural changes made to YD82 **(11)** were in order to see if removing one of the two spacer side chains from mitoxantrone **(1)** and two additional two hydroxyl groups at the C5 and C8 positions would cause any significant decrease in YD82 DNA binding affinity when compared with mitoxantrone **(1)**; probing the speculation or sometimes assumption that hydroxyl groups augment DNA-binding and that two side-chains is a feature assumed mandatory in mitoxantrone analogues.

Scheme 3.2 illustration of the synthesis of YD82 **(11)**:
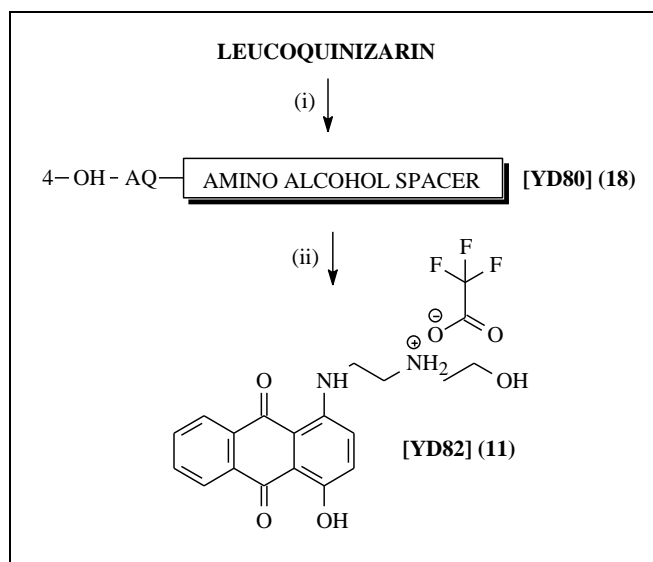
Reagents and conditions: (i) NH$_2$-(CH$_2$)$_2$-NH-(CH$_2$)$_2$-OH, RT, 20min. (ii) TFA, RT.

Scheme 3.2. Synthesis of YD82 (11)

This trifluoroacetate salt YD82 **(11)** was synthesised by treating leucoquinizarin with

2-[(2-aminoethyl)amino]ethanol for 20 minutes, then this purple slurry was extracted

between water and chloroform. After extraction, purple product 4-hydroxy-AQ-amino

alcohol spacer [YD80] **(18)** was purified by flash chromatography and then the

chromatographically pure compound was treated with TFA on ice. Once this purple

compound was completely dissolved in TFA, the solvent was evaporated to dryness

and remaining product was treated with diethyl ether to give a purple precipitate of

final product [YD80] **(18)**.

In the beginning, in order to make this single side-chain substituted compound YD80

(18) instead of 1,4-bis (blue) by-product, a few solvents had been tested for this

reaction, however, the results were not very satisfying. When ethanol: tetrahydrofuran

(THF) (2:1) was used as the reaction solvent (often applicable for this type of

amination), after refluxing for over three hours, the suspension in the round bottomed

267

flask was still brick-red in colour and on the TLC plate, it only showed a very tiny

weak purple spot. Zee-Cheng *et al.* reported in 1979 that they used butanol as the

reaction solvent (Zee-Cheng *et al.*, 1979), so the synthesis of YD80 **(18)** was carried

out again using butanol as reaction solvent. After heating over a water bath for five

hours and leaving at room temperature overnight, the TLC showed quite a lot spots and

also the purple spots were very weak, but this method seemed better than using

ethanol: tetrahydrofuran (2:1) as the reaction solvent. The dark purple compound from

this reaction was then collected and examined by mass spectral and NMR analyses.

However, the results showed the purple compound was not correct, and that cyclisation

on the side chain may have occurred during synthesis.
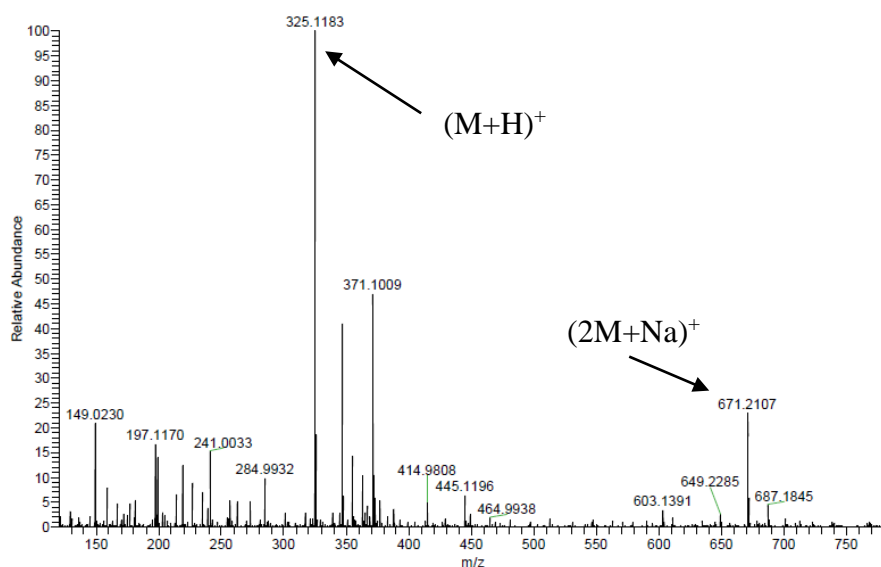
Figure 3.10 Mass spectrum of YD80 (18) cyclisation compound.

In the mass spectrum [**Figure 3.10**], there was a signal at m/z 325.1183 (100%) for the

species $(M+H)^+$, and 671.2107 $(2M+Na)^+$, which indicated that the mass for this

compound was 324Da. However, the expected mass for YD80 **(18)** should have been

326Da. The two missing protons led to the theory that cyclisation occurred during

YD80 **(18)** synthesis. Two possible cyclisation product structures were recognised [**Figure 3.11**]. These would arise from either initial amination at C-1 by the secondary amino group of the amino alcohol aminating reagent, to give A **(19)**, or (preferred) by the primary amino group to give B **(20)**; then, cyclisation onto C-2.
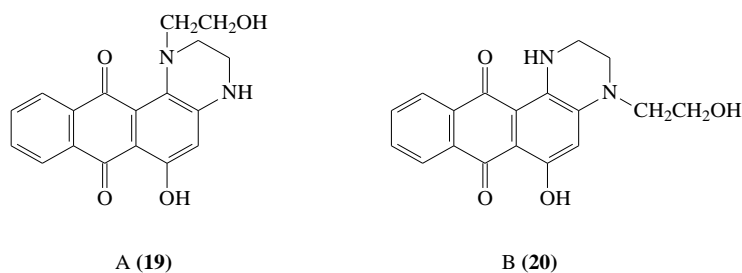
Figure 3.11. Possible cyclisation compounds in YD80 (18) reaction

The NMR spectrum showed clearly that cyclisation happened during reaction (the characteristic and usually well-resolved aromatic proton H-2 peak (typically at 7.2-7.3ppm, doublet) was missing. However, it could not be confirmed whether it was a primary or secondary amine that formed this cyclisation based on the simple ^{1}H NMR spectrum **[Figure 3.11]** (without using NOE experiments or perhaps nitrogen nmr). So, this dried cyclisation compound formed during the YD80 **(18)** reaction was then coupled with (Boc)$_2$O in dry methanol. Three hours later, there was no difference between starting the material and product on TLC plates in a variety of solvent systems, and this may indicate that the cyclisation compound could be structure **B (20)** in **Figure 3.11**. This is because if the cyclisation compound was structure **A (19)**, then it should be able to couple a Boc group onto the available –N<u>H</u>- at C-2, whereas in structure **B (20)**, the C-1 –N<u>H</u>- cannot easily become Boc-protected because of very slow acylation of an NH which is chelated to the quinone oxygen on C-9. Also

269

Zee-Cheng and Cheng reported that the cyclisation in structure **B (20) [Figure 3.11]** was more likely to happen during such reaction (Zee-Cheng and Cheng, 1978). Hence, all evidence supports that the cyclisation compound structure should be structure **B (20)** in **Figure 3.11**.

The ^{1}H NMR spectrum of cyclisation compound **B (20) [Figure 3.11]** showed a 6-proton multiplet signal at 3.56ppm and a 2-proton triplet signal at 3.69 which were assigned to methylene protons in the cyclisation side chain. The alcohol proton was assigned to a one-proton singlet at 4.92ppm. The singlet signal at 6.24ppm was assigned to the H-3 proton. Signals for H-6 and H-7 protons can be found between 7.76 and 7.80ppm. A multiplet signal between 8.19 and 8.22ppm was assigned to H-5 and H-8, and the anthraquinone amino proton was found at 11.06ppm.

During the successful synthesis of YD80 **(18)**, 2-[(2-aminoethyl)amino]ethanol was used neat when mixed with leucoquinizarin without using any solvent or heating. The whole reaction was kept for a quite short time, about 20 minutes, just in order to avoid the reaction starting to form any 1,4-bis blue by-product. Following the isolation of 4-hydroxy-AQ-amino alcohol spacer [YD80] **(18)**, it was converted into its trifluoroacetate salt YD82 **(11)**, which, surprisingly, did not show a difference on TLC between these two compounds (in different solvent systems). Further investigation was carried out, in that YD80 **(18)** was reacted with (Boc)$_2$O in pure methanol. Three hours later, a new blue spot appeared on the TLC plate which was higher-running than the starting YD80 **(18)** spot. This indicated that in YD80's **(18)** chemical structure, there

was likely a secondary amine in the side chain which could be capped with a *t*Boc

protecting group. So, YD80 **(18)** made from mixing leucoquinizarin with amine alone

contained the desired spacer, with a linear side-chain, instead of forming a cyclisation

product and proved the best method for obtaining the target compound.

Both YD80 **(18)** and its TFA salt were analysed by NMR spectroscopy to confirm that

YD82 **(11)**, the TFA salt form of YD80 **(18)**, was correctly formed after treating YD80

(18) with trifluoroacetic acid. Furthermore, the NMR spectrum of YD80 **(18)** showed,

for example, a signal for a one-proton singlet at 2.07ppm confirming the presence of an

amino proton in the side-chain, RN$\underline{H}$(CH$_2$)$_2$OH. The amino proton at the C1 position

of anthraquinone was assigned to a one-proton triplet at 10.52ppm; in YD 82, the

methylene protons for the side-chain were found between 3.03 and 3.77ppm. The

alcohol proton was assigned to a one-proton singlet at 5.29ppm. A signal for a one

proton triplet at 10.20ppm confirming the amino proton at the C1 position of

anthraquinone.

3.3.1.4   <u>Synthesis of NU:UB 466 (12)</u>
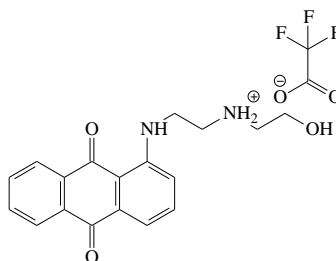
Figure 3.12. Chemical structure of NU:UB 466 (12)

NU:UB 466 (**12**) [**Figure 3.12**] is similar to YD82 (**11**), the only difference between these two compounds is that the hydroxyl group at the C4 position is 'missing' in the NU:UB 466 (**12**). The purpose of designing NU:UB 466 (**12**) was to find out if the missing hydroxyl group at the C4 position would lead to a significant difference between NU:UB 466 (**12**) and YD82 (**11**) DNA binding affinities, as suggested by literature reports on early mitoxantrone analogues (Agbandje *et al.*, 1992).

The synthesis of NU:UB 466 (**12**) is outlined in **Scheme 3.3**:
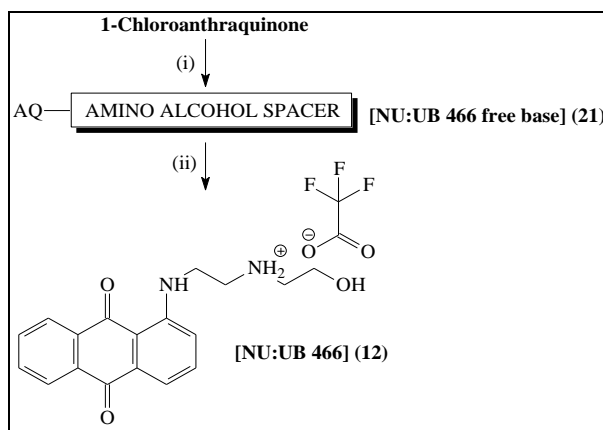
Reagents and conditions: (i) NH$_2$-(CH$_2$)$_2$-NH-(CH$_2$)$_2$-OH, DMSO, water bath, 30min. (ii) TFA, RT

Scheme 3.3. Synthesis of NU:UB 466 (12)

NU:UB 466 (**12**) was synthesised by mixing 1-chloroanthraquinone and 2-[(2-aminoethyl)amino]ethanol in DMSO, then this reaction mixture was heated over a water bath for half an hour. The red NU:UB 466 free base (**21**) was then purified by column chromatography, and dissolved in TFA to give the final trifluoroacetate salt [**Scheme 3.3**].

Both NU:UB 466 free base (**21**) and its TFA salt NU:UB 466 (**12**) were analysed by NMR spectroscopy. For NU:UB 466 free base (**21**), the ^{1}H NMR spectrum (in

d$_6$-DMSO) gave a one proton broad singlet at 1.90ppm confirming the presence of the amino proton in the side-chain. Signals for methylene protons in the side-chain were evidenced between 2.62 and 3.49ppm. A signal of a one proton triplet at 9.75ppm was assigned to the amino proton at the C1 position of the anthraquinone. For NU:UB 466 **(12)**, signals for methylene protons can be found between 3.08 and 3.77ppm. A signal of a one proton triplet was assigned to the alcohol proton at the end of the side-chain at 4.66ppm. The signal at 8.73ppm was assigned to the two (cationic) protons in RNH$_2^+$(CH$_2$)$_2$OH.

The two ^{1}H spectra of NU:UB 466 free base **(21)** and its TFA salt NU:UB 466 **(12)** are quite similar, the only differences are that there was a singlet for two protons at 8.73ppm in the spectrum of NU:UB 466 **(12)** and it was assigned to the cationic amino protons RN$\underline{H}_2^+$(CH$_2$)$_2$OH and there was a small broad signal at 1.90ppm in the NU:UB 466 free base **(21)** ^{1}H spectrum that was assigned to RN$\underline{H}$(CH$_2$)$_2$OH. The amino protons in alkylammonium-type cations of other compounds in the aminoalkylamino-anthraquinones and amino acid conjugates in the NU:UB series had previously been shown to be present in the aromatic region of the spectrum also.

3.3.2   DNA binding assays

During each compound's DNA binding assay, the binding affinity was studied by displacing ethidium bromide from the CT-DNA-ethidium bromide complex by the new potential intercalative agent. During successive additions, the concentration of each compound was increased by 1 μM each time so as to get a reduction of 50% in the

273

fluorescence intensity (of the ethidium-DNA complex). Fluorescence intensity was plotted against compound concentration and QE_{50} values were calculated from the mean value (n=3). The QE_{50} value is the mean concentration of test compound required to effect the 50% reduction in the initial fluorescence of the starting DNA-bound ethidium complex. Thus, the smaller the value, the greater is the DNA binding affinity of the binding ligand.

3.3.2.1 Mitoxantrone (1) DNA binding assay
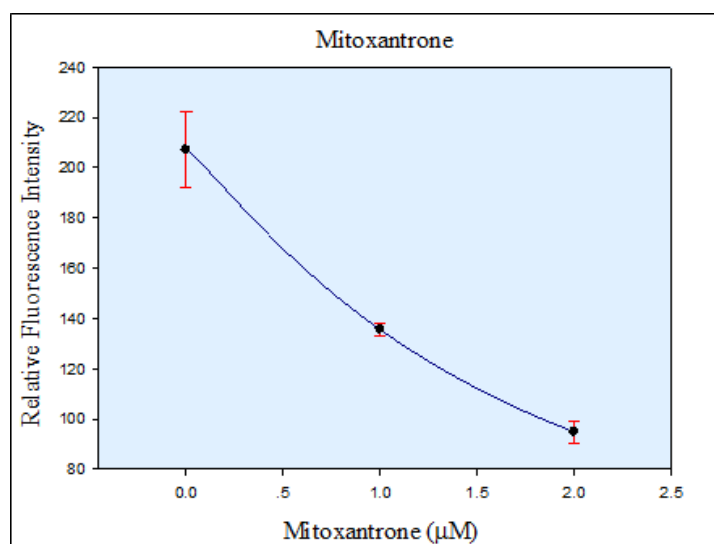
Figure 3.13. Variation of relative fluorescence intensity of CT-DNA (60 μM) with pre-bound EB (4) (30 μM) when treated with different concentrations of mitoxantrone (1) (n=3) in PBS buffer. The excitation wavelength was set at 480nm and maximum emission was observed between 584nm and 589nm.

	Coefficient	Std. Error	t	P
min	-0.0000	0.0000	(+inf)	<0.0001
max	207.0467	5.3015	39.0546	<0.0001
QE_{50}	**1.73**	0.1488	11.6471	<0.0001

When the relative fluorescence intensity reached 50%, the concentration of mitoxantrone **(1)** was 1.73 ± 0.15 μM. In order to calculate the apparent binding constant

(Kapp) for each compound, the binding constant for the CT DNA-ethidium complex was taken from the literature value as reported by Kundu *et al.* (Kundu *et al.*, 2011).

The K_{app} value was calculated according to the equation:

For mitoxantrone (**1**), $K_{app}=(K_{EB}[EB])/[Drug]=(1\times10^7M^{-1}\times30)/1.73=17.34\times10^7M^{-1}$

3.3.2.2   <u>NU:UB 83 (9) DNA binding assay</u>
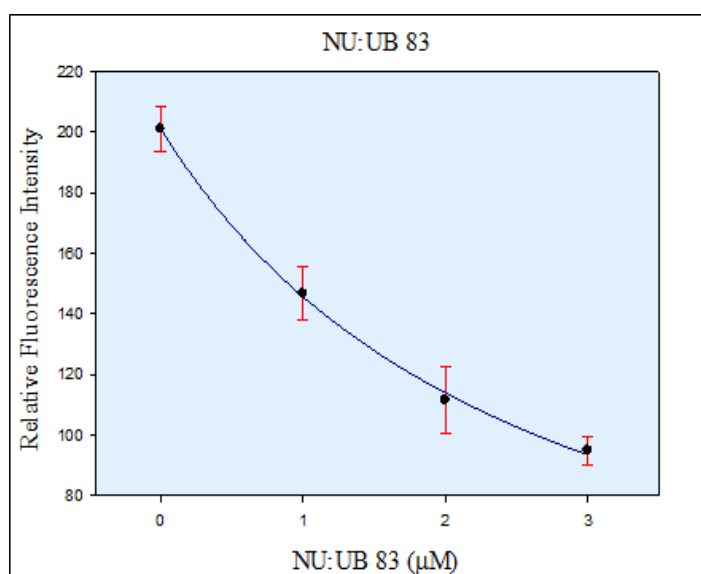
Figure 3.14. Variation of relative fluorescence intensity of CT-DNA (60 μM) with pre-bound EB (4) (30 μM) when treated with different concentrations of NU:UB 83 (9) (n=3) in PBS buffer. The excitation wavelength was set at 480nm and maximum emission was observed between 584nm and 591nm.

	Coefficient	Std. Error	t	P
min	-0.0000	0.0000	(+inf)	<0.0001
max	201.0530	4.6648	43.1002	<0.0001
QE$_{50}$	**2.61**	0.2163	12.0683	<0.0001

When the relative fluorescence intensity reached 50%, the concentration of NU:UB 83 (**9**) was 2.61±0.22μM.

NU:UB 83 (**9**), $K_{app}=(K_{EB}[EB])/[Drug]=(1\times10^7M^{-1}\times30)/2.61=11.49\times10^7M^{-1}$

3.3.2.3 NU:UB 85 (10) DNA binding assay

Figure 3.15. Variation of relative fluorescence intensity of CT-DNA (60 μM) with pre-bound EB (4) (30 μM) when treated with different concentrations of NU:UB 85 (10) (n=3) in PBS buffer. The excitation wavelength was set at 480nm and maximum emission was observed between 584nm and 589nm.

	Coefficient	Std. Error	t	P
min	-0.0000	0.0000	(+inf)	<0.0001
max	211.7459	3.2636	64.8812	<0.0001
QE$_{50}$	**6.43**	0.3105	20.7052	<0.0001

When the relative fluorescence intensity reached 50%, the concentration of NU:UB 85 (10) was 6.43±0.31 μM.

NU:UB 85 (10), $K_{app}=(K_{EB}[EB])/[Drug]=(1 \times 10^7 M^{-1} \times 30)/6.43=4.67 \times 10^7 M^{-1}$
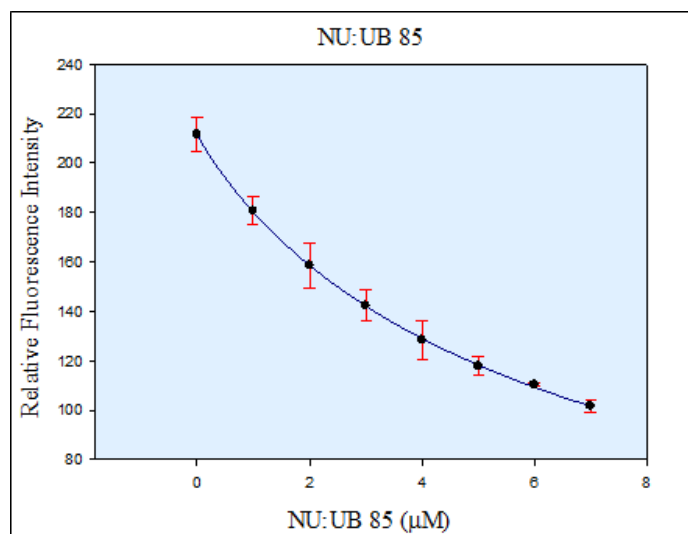
3.3.2.4 NU:UB 31 (6) DNA binding assay

Figure 3.16. Variation of relative fluorescence intensity of CT-DNA (60 μM) with pre-bound EB (4) (30 μM) when treated with different concentrations of NU:UB 31 (6) (n=3) in PBS buffer. The excitation wavelength was set at 480nm (n=3) and maximum emission was observed between 584nm and 591nm.

	Coefficient	Std. Error	t	P
min	-0.0000	0.0000	(+inf)	<0.0001
max	211.2786	2.2639	93.3259	<0.0001
QE$_{50}$	**15.10**	0.4307	35.0585	<0.0001

When the relative fluorescence intensity reached 50%, the concentration of NU:UB 31

(**6**) was 15.10±0.43 μM.

NU:UB 31 (**6**), $K_{app}=(K_{EB}[EB])/[Drug]=(1\times10^7 M^{-1}\times30)/15.10=1.99\times10^7 M^{-1}$

3.3.2.5   <u>NU:UB 51 (7) DNA binding assay</u>

Figure 3.17. Variation of relative fluorescence intensity of CT-DNA (60 μM) with pre-bound EB (4) (30 μM) when treated with different concentrations of NU:UB 51 (7) (n=3) in PBS buffer. The excitation wavelength was set at 480nm and maximum emission was observed between 583nm and 589nm.

	Coefficient	Std. Error	t	P
min	-0.0000	0.0000	(+inf)	<0.0001
max	210.3699	5.1263	41.0377	<0.0001
QE$_{50}$	**5.05**	0.4352	11.6017	<0.0001

When the relative fluorescence intensity reached 50%, the concentration of NU:UB 51 (**7**) was 5.05 ± 0.44 μM.

NU:UB 51 (**7**), $K_{app}=(K_{EB}[EB])/[Drug]=(1 \times 10^7 M^{-1} \times 30)/5.05=5.94 \times 10^7 M^{-1}$

3.3.2.6 YD4 (8) DNA binding assay

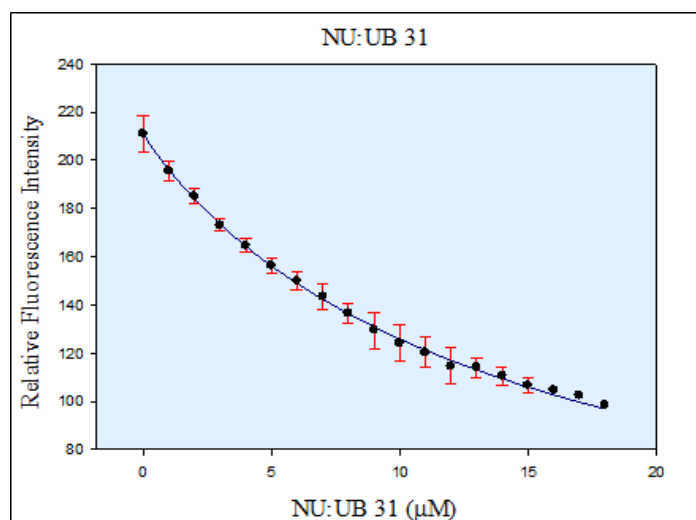**Figure 3.18. Variation of relative fluorescence intensity of CT-DNA (60 μM) with pre-bound EB (4) (30 μM) when treated with different concentrations of YD4 (8) (n=3) in PBS buffer. The excitation wavelength was set at 480 nm and maximum emission was observed between 584 nm and 590 nm.**

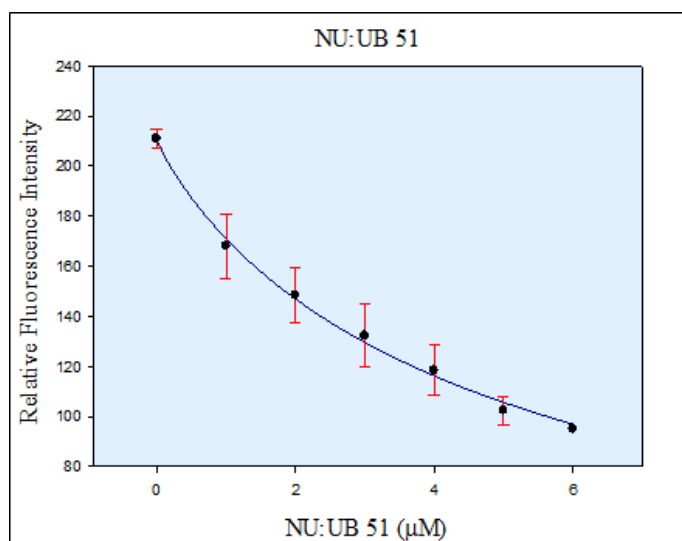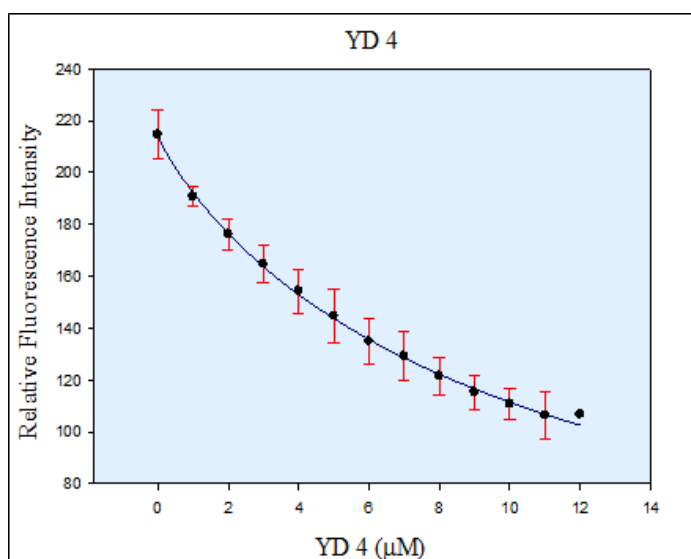|	Coefficient	Std. Error	t	P
min	-0.0000	0.0000	(+inf)	<0.0001
max	214.0050	3.6694	58.3213	<0.0001
QE$_{50}$	**10.95**	0.5518	19.8499	<0.0001

When the relative fluorescence intensity reached 50%, the concentration of YD4 (8) was 10.95±0.55 μM.

YD4 (8), $K_{app}=(K_{EB}[EB])/[Drug]=(1\times10^7M^{-1}\times30)/10.95=2.74\times10^7M^{-1}$

3.3.2.7   <u>YD82 (11) DNA binding assay</u>

Figure 3.19. Variation of relative fluorescence intensity of CT-DNA ($60\,\mu$M) with pre-bound EB (4) ($30\,\mu$M) when treated with different concentrations of YD82 (11) (n=3) in PBS buffer. The excitation wavelength was set at 480nm and maximum emission was observed between 583nm and 590nm.

	Coefficient	Std. Error	t	P
min	-0.0000	0.0000	(+inf)	<0.0001
max	211.3406	0.9483	222.8713	<0.0001
QE$_{50}$	**7.04**	0.0929	75.8328	<0.0001

When the relative fluorescence intensity reached 50%, the concentration of YD82 **(11)** was $7.04 \pm 0.09\,\mu$M.

YD82 **(11)**, $K_{app} = (K_{EB}[EB])/[Drug] = (1 \times 10^7 M^{-1} \times 30)/7.04 = 4.26 \times 10^7 M^{-1}$
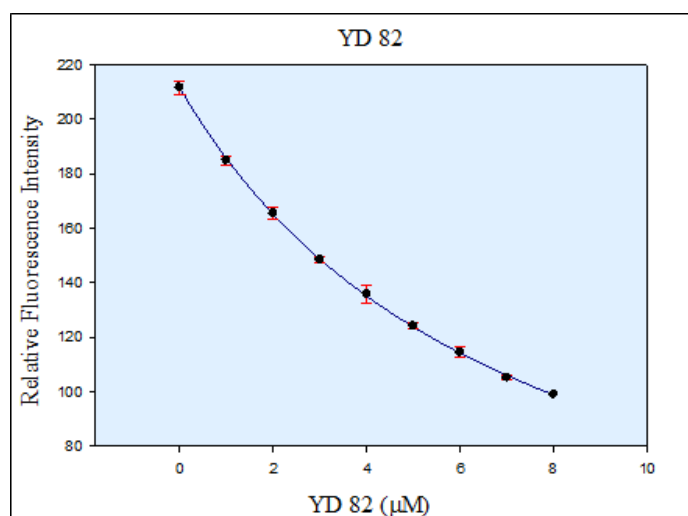
3.3.2.8 NU:UB 466 (12) DNA binding assay

Figure 3.20. Variation of relative fluorescence intensity of CT-DNA (60 μM) with pre-bound EB (4) (30 μM) when treated with different concentrations of NU:UB 466 (12) (n=3) in PBS buffer. The excitation wavelength was set at 480nm and maximum emission was observed between 585nm and 591nm.

	Coefficient	Std. Error	t	P
min	-0.0000	0.0000	(+inf)	<0.0001
max	206.3343	1.5772	130.8217	<0.0001
QE$_{50}$	**14.78**	0.2639	56.0041	<0.0001

When the relative fluorescence intensity reached 50%, the concentration of NU:UB 466 (12) was 14.78±0.26 μM.

NU:UB 466 (12), $K_{app}=(K_{EB}[EB])/[Drug]=(1\times10^7M^{-1}\times30)/14.78=2.03\times10^7M^{-1}$
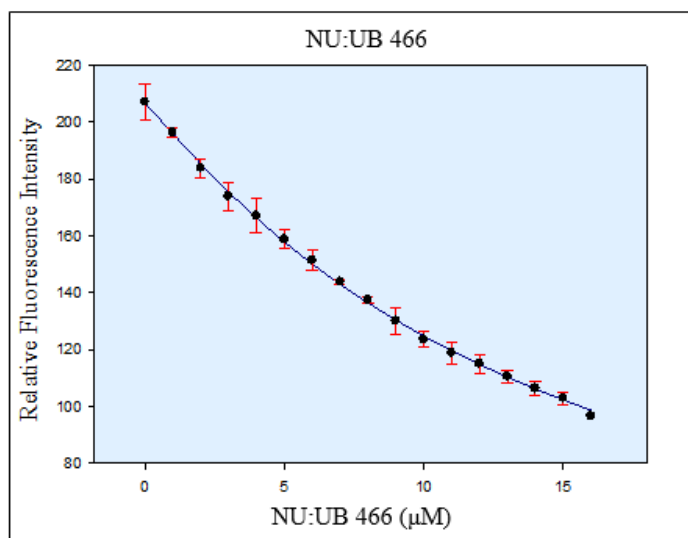
3.3.2.9 YD2 (13) DNA binding assay

Figure 3.21. Variation of relative fluorescence intensity of CT-DNA (60 μM) with pre-bound EB (4) (30 μM) when treated with different concentrations of YD2 (13) (n=3) in PBS buffer. The excitation wavelength was set at 480nm and maximum emission was observed between 589nm and 594nm.

	Coefficient	Std. Error	t	P
min	-0.0000	0.0000	(+inf)	<0.0001
max	542.1397	4.5545	119.0331	<0.0001
QE$_{50}$	**5.08**	0.1319	38.5535	<0.0001

When the relative fluorescence intensity reached 50%, the concentration of YD2 **(13)** was 5.08±0.13 μM.

YD2 **(13)**, $K_{app}=(K_{EB}[EB])/[Drug]=(1\times10^7 M^{-1}\times30)/5.08=5.91\times10^7 M^{-1}$

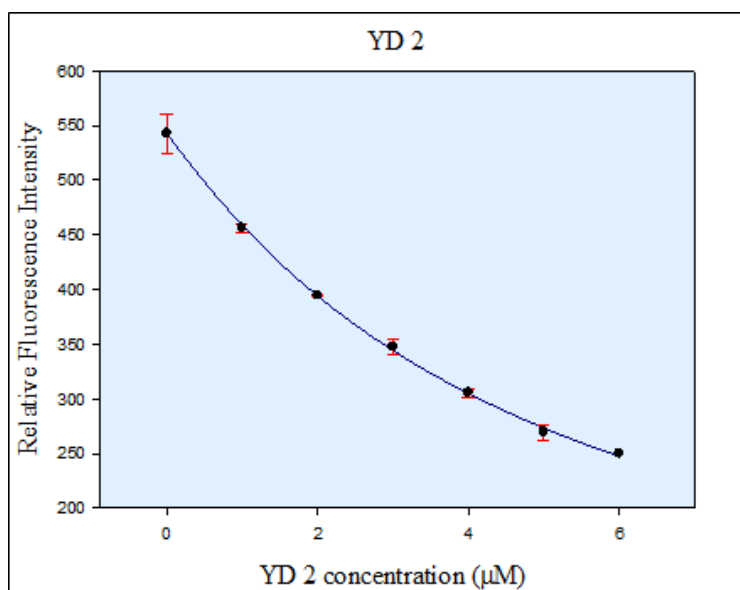### 3.3.2.10   NU:UB 197 (14) DNA binding assay
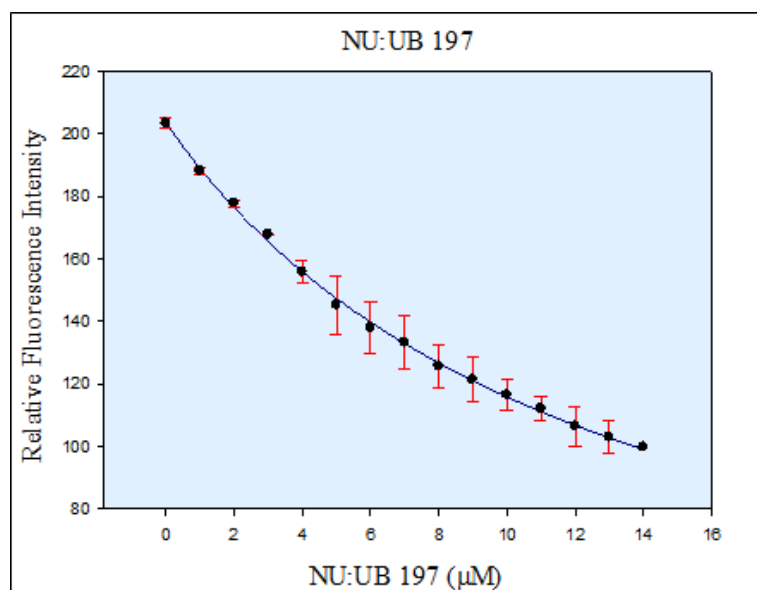
Figure 3.22. Variation of relative fluorescence intensity of CT-DNA (60 μM) with pre-bound EB (4) (30 μM) when treated with different concentrations of NU:UB 197 (14) (n=3) in PBS buffer. The excitation wavelength was set at 480nm and maximum emission was observed between 586nm and 590nm.

	Coefficient	Std. Error	t	P
min	-0.0000	0.0000	(+inf)	<0.0001
max	203.6404	2.7716	73.4749	<0.0001
QE$_{50}$	**13.25**	0.4691	28.2549	<0.0001

When the relative fluorescence intensity reached 50%, the concentration of NU:UB 197 (**14**) was 13.25 ±0.47 μM.

NU:UB 197 (**14**), $K_{app}=(K_{EB}[EB])/[Drug]=(1\times10^{7}M^{-1}\times30)/13.25=2.26\times10^{7}M^{-1}$

All nine anthraquinone derivatives that had been tested in this competitive ethidium displacement assay have a general structure which is shown as in **Figure 3.23**:
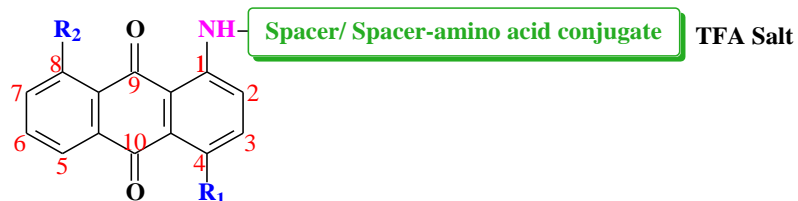
Figure 3.23. General structure of anthraquinone derivatives.

They all have an amine group at the C1 position and it is linked with a spacer, and in the anthraquinone core, hydroxyl group(s) and/or hydrogen at the C4 and/or C8 position.
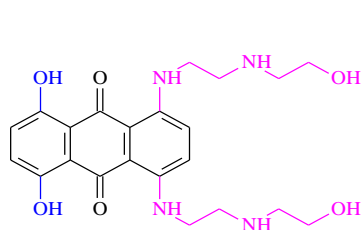
Mitoxantrone (**1**)
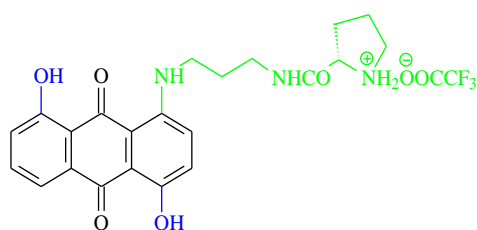
NU:UB 83 (**9**)
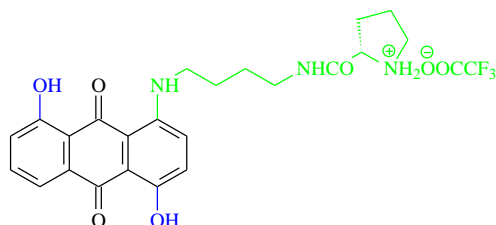
NU:UB 85 (**10**)

NU:UB 31 (**6**)

NU:UB 51 (**7**)

YD4 (**8**)

YD82 (11)   NU:UB 466 (12)

YD2 (13)   NU:UB 197 (14)
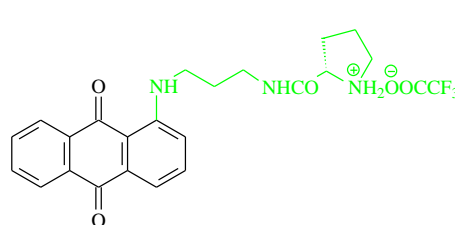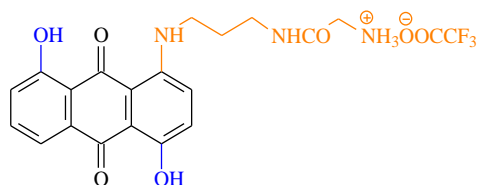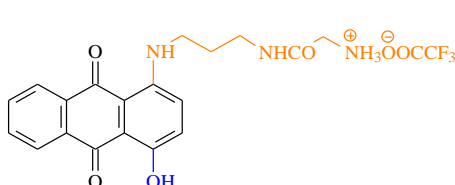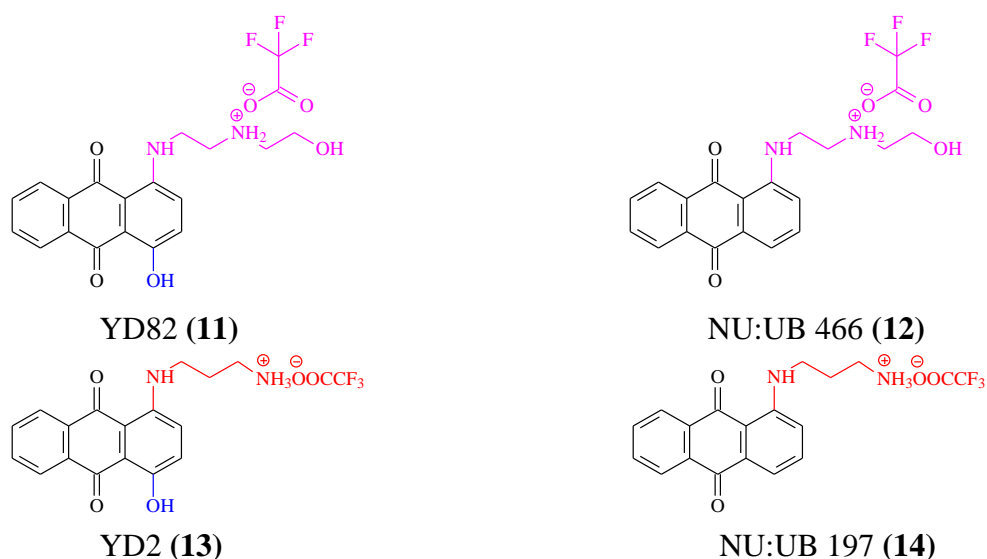
These nine anthraquinone derivatives' structures are quite similar to each other, however, whether the number of hydroxyl groups on the anthraquinone base structure would affect DNA binding constant K_{app} values or whether different lengths or composition of spacer groups or additional amino acid would affect K_{app} were important factors to be determined and will be discussed as follows:

	SPACER/ SPACER AMINO ACID CONJUGATE	R_1	R_2
NU:UB 83 (9)	NH(CH$_2$)$_3$NH-Pro TFA	OH	OH
NU:UB 51 (7)	NH(CH$_2$)$_3$NH-Gly TFA	OH	OH
YD2 (13)	NH(CH$_2$)$_3$NH$_3$ TFA	OH	H
NU:UB 85 (10)	NH(CH$_2$)$_4$NH-Pro TFA	OH	OH
YD82 (11)	NH(CH$_2$)$_2$NH$_2$(TFA)-(CH$_2$)$_2$OH	OH	H
YD4 (8)	NH(CH$_2$)$_3$NH-Gly TFA	OH	H
NU:UB 197 (14)	NH(CH$_2$)$_3$NH$_3$ TFA	H	H
NU:UB 466 (12)	NH(CH$_2$)$_2$NH$_2$(TFA)-(CH$_2$)$_2$OH	H	H
NU:UB 31 (6)	NH(CH$_2$)$_3$NH-Pro TFA	H	H

Table 3.2: Different spacers and functional groups at R1 and R2 positions of anthraquinone derivatives.

Drug	$QE_{50}^{\#}$ (μM)	K_{app} (M^{-1})
Mitoxantrone (1)	1.73±0.15	17.34×10^7
NU:UB 83 (9)	2.61±0.22	11.49×10^7
NU:UB 51 (7)	5.05±0.44	5.94×10^7
YD2 (13)	5.08±0.13	5.91×10^7
NU:UB 85 (10)	6.43±0.31	4.67×10^7
YD82 (11)	7.04±0.09	4.26×10^7
YD4 (8)	10.95±0.55	2.74×10^7
NU:UB 197 (14)	13.25±0.47	2.26×10^7
NU:UB 466 (12)	14.78±0.26	2.03×10^7
NU:UB 31 (6)	15.10±0.43	1.99×10^7

Table 3.3: Anthraquinone derivatives: QE_{50} values and K_{app} binding constants.
 # mean concentration when the CT DNA-EB fluorescence intensity has decreased by 50%.

From **Table 3.2** and **Table 3.3**, the data clearly indicated that among the anthraquinone

derivatives:

1. The more –OH groups at the C4 and/or C8 position(s) on the anthraquinone base

structure, the higher the DNA binding constant K_{app} that the compound would show in

competitive ethidium displacement assays.

- NU:UB 83 (**9**) and NU:UB 31 (**6**) share the same spacer-amino acid conjugate

    -NH(CH$_2$)$_3$NH-Pro trifluoroacetate, but NU:UB 83 (**9**) has two hydroxyl groups

    at the C4 and C8 positions, while NU:UB 31 (**6**) has no hydroxyl group at

    either of those two sites. The results from competitive ethidium displacement

    assay showed that the DNA binding constant K_{app} value for NU:UB 83 (**9**) is

    almost 6-fold greater than the constant K_{app} value for NU:UB 31 (**6**). So,

removing two hydroxyl groups from the structure leads to a dramatic DNA binding affinity decrease.

- NU:UB 51 (**7**) and YD4 (**8**) have the same spacer -NH(CH$_2$)$_3$NH- and are Gly trifluoroacetate salts, however NU:UB 51 (**7**) has two hydroxyl groups on the C4 and C8 sites, and there is only one hydroxyl group at the C4 position in YD4 (**8**). Results of DNA binding constant K$_{app}$ value measurements showed that NU:UB 51 (**7**) can bind onto DNA with almost two-fold stronger affinity than YD4 (**8**).

- Similar results were obtained between YD82 (**11**) and NU:UB 466 (**12**) pair and YD2 (**13**) and NU:UB 197 (**14**) (salt form and free base) pair, K$_{app}$ values for the compound which has one extra hydroxyl group at the C4 position were 2.1 fold and 2.6 fold higher than the other, respectively.

- Compounds YD82 (**11**) and NU:UB 466 (**12**) both contained one single side chain of mitoxantrone (**1**) at the C1 position, and from data shown in **Table 3.3** it clearly showed that the K$_{app}$ values for both compounds were only approximately a quarter and one eighth of mitoxantrone's DNA binding constant K$_{app}$ value, respectively. This may indicate that two -NH(CH$_2$)$_2$NH-(CH$_2$)$_2$OH side chains in mitoxantrone (**1**) are crucial for DNA binding, removing one of these side chains and both hydroxyl groups at the C5 and C8 [NU:UB 466 (**12**)], would lead to a DNA binding affinity decreasing by eight-fold, however, if one hydroxyl group was re-introduced at the C4 position

[YD82 (**11**)], the DNA binding affinity would increase by almost two-fold when compared with NU:UB 466 (**12**) which has no hydroxyl group at all.

2. When compounds have the same amount of hydroxyl groups at the same sites, the structure of the spacer/ spacer-amino acid conjugate that is linked to the amine group at the C1 position can lead to differences in the DNA binding constant K_{app} values as well as the anthraquinone nuclear substitution pattern.

- NU:UB 83 (**9**), NU:UB 51 (**7**) and NU:UB 85 (**10**) all have two hydroxyl groups at the C4 and C8 sites, and share similar but different spacers. NU:UB 83 (**9**) has <u>proline</u>, while NU:UB 51 (**7**) has <u>glycine</u> at the end of the spacer. The K_{app} values showed that NU:UB 83 (**9**) can bind onto DNA with two-fold greater affinity than NU:UB 51 (**7**) did.

- NU:UB 85 (**10**) and NU:UB 83 (**9**) have similar structures. However, in NU:UB 85 (**10**), the *N*-butyl spacer structure has one extra –CH_2 group when compared with the propyl spacer in NU:UB 83 (**9**). Nevertheless, the K_{app} value for NU:UB 85 (**10**) was only one third of the K_{app} value of NU:UB 83 (**9**). This may suggest that the longer spacer in the compound structure, and thus the potential for greater distancing of cationic charge from the chromophore, the less DNA binding affinity the compound would have.

- YD2 (**13**) and YD4 (**8**) each only have one hydroxyl group at the C4 position and share the same spacer. YD2 (**13**) has the aminopropylamino spacer group whereas YD4 (**8**) is the corresponding glycine conjugate. This difference in

side-chain structure leads to the result that YD2 **(13)**, with the shorter distance between the anthraquinone core and the cationic amino group, can bind onto DNA with approximately two fold greater affinity than YD4 **(8)**, its glycine conjugate. This suggests that distancing the positive charge in the side chain from the anthraquinone nucleus leads to decreased DNA-binding properties.

- Both NU:UB 197 **(14)** and NU:UB 31 **(6)** do not have any hydroxyl groups at the C4 and C8 positions. The only difference between these two TFA salts was NU:UB 31 **(6)** is the proline conjugate of NU:UB 197 **(14)**. From the K_{app} values in **Table 3.3**, it suggested that the presence of the proline residue at the end of the propyl spacer can slightly weaken the compound's DNA binding affinity.

From the above results, it was inferred that for compounds that share the same anthraquinone base structure,

1) The DNA binding constant K_{app} value would increase if there were more hydroxyl groups on the anthraquinone base structure. In **Table 3.3** data showed that regardless of the spacer chain, the more hydroxyl groups in the compound structure would increase its' DNA binding affinity (consistent with early reports in the literature on substituted mitoxantrone analogues; section **3.1.4**).

2) When compounds have the same amount of hydroxyl groups at the same positions, the aminopropylamino spacer leads to a higher DNA binding constant, K_{app} value, than the spacer glycine conjugate.

289

3.3.3 **MTT assay**

MTT **(22)**   MTT Formazan **(23)**
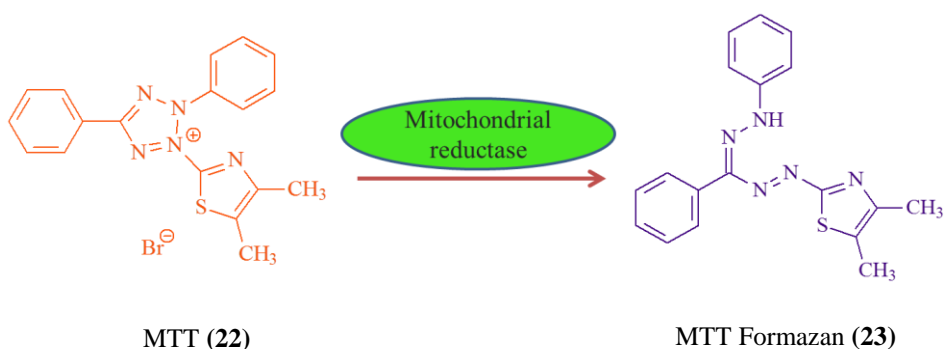
Scheme 3.4, Outline of the MTT assay (the basis of the colourimetric method)

The MTT assay is often used as a method to determine the number of viable cells after exposing to toxic substances. During the MTT assay [**Scheme 3.4**], succinate dehydrogenase in the mitochondria break the tetrazolium ring in the water soluble (pale yellow) tetrazolium salt, 3-[4,5-Dimethylthiazol-2-yl]-2,5-diphenyltetrazolium bromide (MTT) **(22)** thereby converting it to an insoluble dark purple formazan **(23)**, which cannot permeate through the cell membranes and hence it accumulates in the viable cells (Fotakis and Timbrell, 2006).
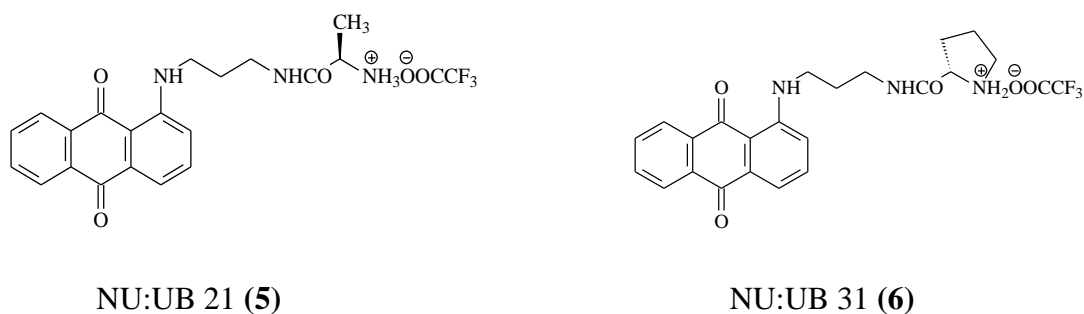
NU:UB 21 **(5)**   NU:UB 31 **(6)**

Figure 3.24. Chemical structures of NU:UB 21 (5) and NU:UB 31 (6).
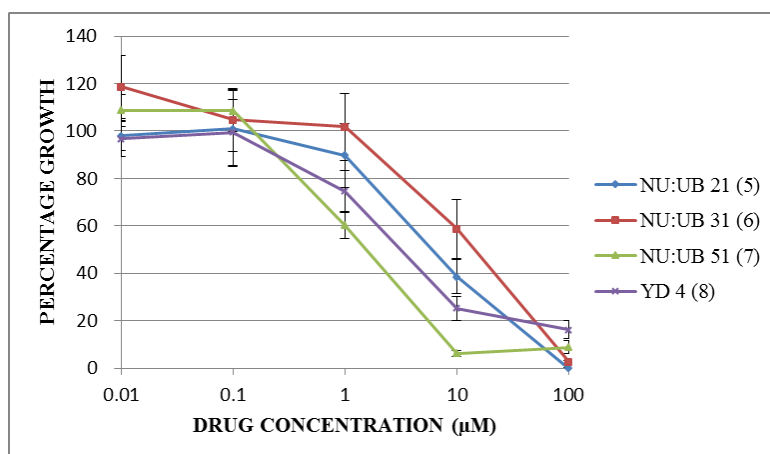
Figure 3.25. Survival rate of MCF-7 breast cancer cells treated with NU:UB 21 (5), NU:UB 31 (6), NU:UB 51 (7) and YD4 (8) for 96h (n=8).

In vitro cytotoxicities of NU:UB 21 **(5)**, NU:UB 31 **(6)**, NU:UB 51 **(7)** and YD4 **(8)** against the MCF-7 breast cancer cell line were measured after 96h incubation by MTT assay (Plumb *et al.*, 1989). MCF-7 cells growth curves against different concentrations of each compound are shown in **Figure 3.25**.

COMPOUND	SPACER SIDE CHAIN	HYDROXYL GROUP POSITION	$IC_{50}(\mu M)$
NU:UB 51 **(7)**	-NH(CH₂)₃NH-Gly TFA	4 & 8	1.2
YD4 **(8)**	-NH(CH₂)₃NH-Gly TFA	4	3.4
NU:UB 21 **(5)**	-NH(CH₂)₃NH-D-Ala TFA	N/A	6.8
NU:UB 31 **(6)**	-NH(CH₂)₃NH-Pro TFA	N/A	10.6

Table 3.4. NU:UB 21 (5), NU:UB 31 (6), NU:UB 51 (7) and YD4 (8) in vitro cytotoxicity against MCF-7 breast cancer cells (96h incubation).

The only difference between NU:UB 21 **(5)** and NU:UB 31 **(6) [Figure 3.24]** is that the terminal amino group of the aminopropylamino spacer, in NU:UB 21 **(5)** links to D-alanine and in NU:UB 31 **(6)** it connects to proline. From the MTT assay results analysed by SigmaPlot 12, it was found that after 96h incubation, NU:UB 21 **(5)** had an IC_{50} value of 6.8 μM whereas NU:UB 31 **(6)** had a value of 10.6 μM. This indicates

that NU:UB 21 **(5)** is approximately 1.5-fold more potent than NU:UB 31 **(6)** (in this cell line).

From their chemical structures, it can easily be noticed that NU:UB 51 **(7)** only has one extra hydroxyl group at position 8 of the anthraquinone when compared with YD4 **(8)**. That extra hydroxyl group makes NU:UB 51 **(7)** (IC_{50} 1.2 μM) almost 3 times more potent than YD4 **(8)** (IC_{50} 3.4 μM).

From **Table 3.4**, the data illustrates that:

1) The more hydroxyl groups on the anthraquinone basic structure, the smaller IC_{50} value obtained (i.e. increased potency) after 96h incubation with MCF-7 breast cancer cells. With two hydroxyl groups at positions C4 and C8, NU:UB 51 **(7)** was 6-fold and 10-fold more potent than NU:UB 21 **(5)** and NU:UB 31 **(6)**, respectively, which do not have any hydroxyl groups on the anthraquinone structure. With one hydroxyl group 'missing' in YD4 **(8)** when compared with NU:UB 51 **(7)**, it showed only a third of the inhibitory activity of NU:UB 51 **(7)**.

2) At the terminus of the aminopropylamino spacer side chain, the smaller the structure of amino acid, the more the potency of that compound. When comparing the methyl group in D-alanine with the five-membered-ring structure of proline, NU:UB 21 **(5)** greater inhibitory potency against MCF-7 cells than NU:UB 31 **(6)**. This may be related to the nature of the amino group; namely, primary in NU:UB 21 **(5)** but secondary in NU:UB 31 **(6)**, or it may simply be

a question of steric hindrance to accessing the amino group in proline by the DNA phosphate backbone. More studies on related compounds are clearly required to determine the consistency of this observation.

3) Having one extra hydroxyl group and the relatively smaller structure of glycine in the aminopropylamino side chain, YD4 **(8)** was determined to be approximately two-fold more potent than NU:UB 21 **(5)** and three times more potent than NU:UB 31 **(6)**.

When comparing DNA-binding data in **Table 3.3**, and *in vitro* cytotoxicity data in **Table 3.4** there appeared to be a direct connection. The stronger DNA-binding affinity a compound shows, the more cytotoxic potency a compound will present. This indicated that there is a good correlation between drug-DNA binding affinity and cancer cell growth inhibitory activity.

3.4 <u>CONCLUSION</u>

From DNA-binding studies, when the anthraquinone series compounds were compared with mitoxantrone (**1**), they indicated the major influencing factor that can affect drug-DNA binding affinities is the number of hydroxyl group in the anthraquinone chromophore. In general, the more hydroxyl groups in the anthraquinone derivative structure, the greater DNA binding affinity a given anthraquinone compound possesses. Also, upon introducing one side chain only into the anthraquinone structure, the DNA binding affinities decreased when compared with mitoxantrone (**1**) which has two side chains at the C1 and C4 positions. For compounds with hydroxyl group(s) at the same position(s) in the anthraquinone compound structure, the length of its side chain may influence its DNA-binding affinity as well, but not as greatly as the presence and number of hydroxyl groups.

Results from DNA-binding studies to determine K_{app} and MTT studies to determine IC_{50} values were consistent. This suggests that the greater DNA binding affinity the anthraquinone compound has, the more cytotoxic potency it will present.

3.5 <u>FUTURE WORK</u>

It has been shown that the different number of hydroxyl groups in the anthraquinone derivative structure can certainly make a major difference to its DNA binding affinity. However, whether alternative substitution patterns of hydroxyl groups in the anthraquinone skeleton would affect the DNA binding constant K_{app} value or whether, for constant number and position of hydroxyl groups in its structure, the composition,

294

such as the number of -(CH$_2$)- groups separating the two amino groups in the side chain (spacer) could lead to different DNA binding affinities? These questions will lead to further study in future work. Because the leading compounds identified in this study (i.e. NU:UB 51 **(7)** and YD4 **(8)**) are both active and good quenchers of fluorescence, they would be good compounds to incorporate into legumain/ MMP activated prodrugs in future studies.

Also, an investigation can be carried out for the new anthraquinone derivatives prepared here to see whether these DNA intercalators can show any DNA-topoisomerase inhibitory activities as well as established members of the NU:UB series.

3.6 STRUCTURE LIBRARY
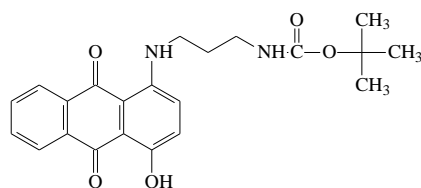
4-hydroxy-1-[Boc-Propyl Spacer]-AQ YD1 **(15)**

4-hydroxy-1-[3-(*N*-tertiarybutoxycarbonylamino)propylamino]anthraquinone
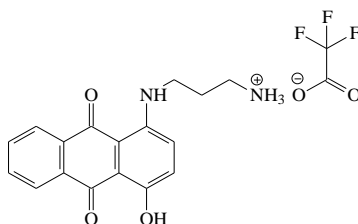
4-hydroxy-1-[Propyl Spacer]-AQ TFA salt YD2 **(13)**

4-hydroxy-1-[(3-aminopropyl)amino]anthraquinone trifluoroacetate

4-hydroxy-1-(Boc-Gly-[Propyl Spacer])-AQ YD3 **(16)**

4-hydroxy-1-[3-(*N*-tertiarybutoxycarbonylglycylamino)propylamino]anthraquinone
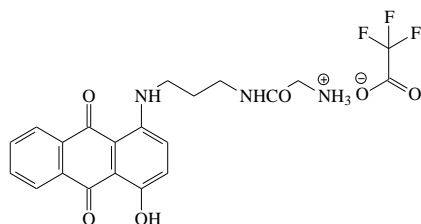
4-hydroxy-1-(Gly-[Propyl Spacer])-AQ TFA salt YD4 **(8)**

4-hydroxy-1-[3-(glycylamino)propylamino]anthraquinone trifluoroacetate
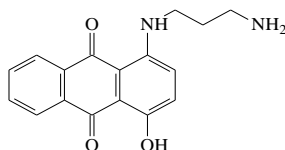
4-hydroxy-1-[Propyl Spacer]-AQ YD79 **(17)**

4-hydroxy-1-[(3-amino)propylamino]anthraquinone
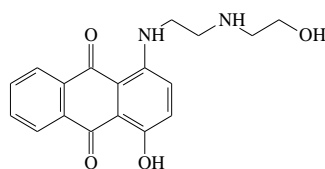
4-hydroxy-1-[Amino Alcohol Spacer]-AQ YD80 **(18)**

4-hydroxy-1-{[2-(2-hydroxyethyl)aminoethyl]amino}anthraquinone
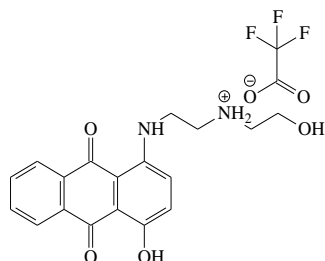
4-hydroxy-1-[Amino Alcohol Spacer]-AQ TFA salt YD82 **(11)**

4-hydroxy-1-{[2-(2-hydroxyethyl)aminoethyl]amino}anthraquinone trifluoroacetate

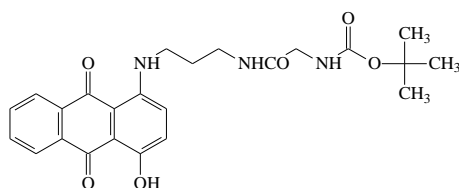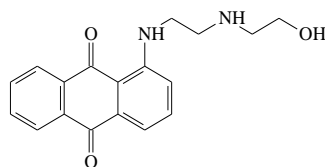1-[Amino Alcohol Spacer]-AQ NU:UB466 free base **(21)**

1-{[2-(2-hydroxyethyl)aminoethyl]amino}anthraquinone
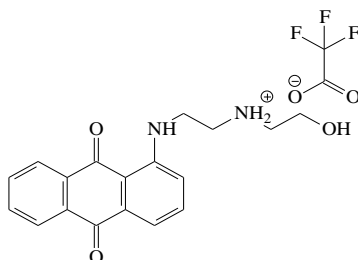
1-[Amino Alcohol Spacer]-AQ TFA salt NU:UB466 **(12)**

1-{[2-(2-hydroxyethyl)aminoethyl]amino}anthraquinone trifluoroacetate
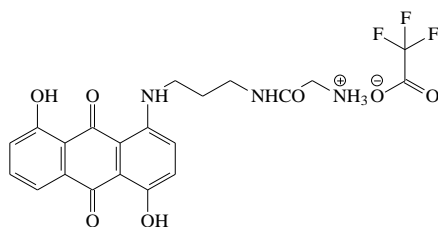
4,8-dihydroxy-1-(Gly-[Propyl Spacer])-AQ TFA salt NU:UB 51 **(7)**

4,8-dihydroxy-1-[3-(glycylamino)propylamino]anthraquinone trifluoroacetate
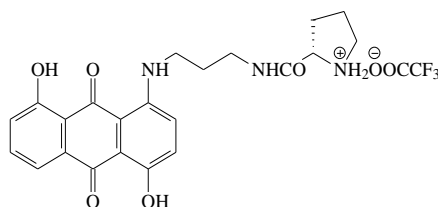
4,8-dihydroxy-1-(Pro-[Propyl Spacer])-AQ TFA salt NU:UB 83 **(9)**

4,8-dihydroxy-1-[3-(L-prolylamino)propylamino]anthraquinone trifluoroacetate
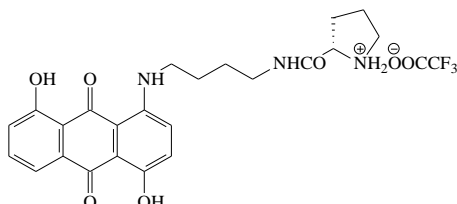
4,8-dihydroxy-1-(Pro-[Butyl Spacer])-AQ TFA salt NU:UB 85 **(10)**

4,8-dihydroxy-1-[4-(L-prolylamino)butylamino]anthraquinone trifluoroacetate
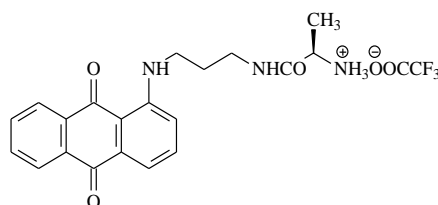
1-(D-Ala-[Propyl Spacer])-AQ TFA salt NU:UB 21 **(5)**

1-(3-[D-alanylamino)propylamino]anthraquinone trifluoroacetate
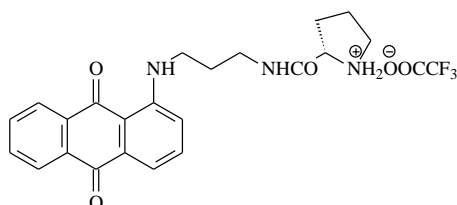
1-(Pro-[Propyl Spacer])-AQ TFA salt NU:UB 31 **(6)**

1-(3-[L-prolylamino)propylamino]anthraquinone trifluoroacetate
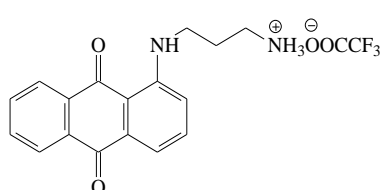
1-[Propyl Spacer]-AQ TFA salt NU:UB 197 **(14)**

1-[(3-aminopropyl)amino]anthraquinone trifluoroacetate

3.7   EXPERIMENTAL

3.7.1   DNA binding assay

3.7.1.1   Materials

Buffer:

PBS buffer was made by dissolving one phosphate buffered saline tablet (Sigma) in 200mL of distilled water to obtain (final concentrations) 0.01M phosphate buffer, 0.0027M potassium chloride, 0.137M sodium chloride, pH 7.4 at 25°C. This buffer solution was stored at 4°C for further use.

Ethidium Bromide:

A stock solution of ethidium bromide 10mg/mL in deionised water was prepared, protected from light and kept at 4°C.

Drug test solutions:

Drug solutions were prepared by making a stock solution of 1mg/mL in DMSO, then further diluted to give a final concentration in the cuvette of 5~20 μM as required.

DNA solution:

One centimetre portion (approximately) of Calf Thymus DNA (Sigma) was dissolved slowly in 5mL of PBS buffer at 4°C for 24h. Any small amount of non-dissolved Calf Thymus DNA residue was filtered off and the concentration of Calf Thymus DNA stock solution was determined by using a Beckman Coulter DU$^{\circledR}$800 UV/Vis Spectrophotometer at 260nm using a molar extinction coefficient of 6600 M^{-1}cm^{-1}.

DNA Quantification:

The analytical wavelength for the spectrophotometer was set at 260nm; the blank reference was PBS alone in a 3mL cuvette. Then 100~300 μL of this unquantified DNA stock solution was placed into the cuvette and diluted with PBS buffer to give a final volume of 3mL. According to the linearity range of the Beer-Lambert Law, the ideal absorbance should fall between 0.5 and 0.7. The absorbance was read three times, the mean value was then used to determine the concentration of this DNA stock solution.

Absorbance (A)=Concentration (C) $\times$ Cell length (L) $\times$ Molar extinction coefficient (Σ)

(The units are: mol/L for C, cm for L, $mol^{-1}dm^3cm^{-1}$ for Σ)

Hence the concentration of DNA solution in the 3mL cuvette can be calculated:

C=Absorbance / (1cm $\times$ 6600$mol^{-1}dm^3cm^{-1}$)

Then by using equation $C_1V_1=C_2V_2$, the concentration of the original DNA stock solution can be determined.

3.7.1.2   **Method**

Excitation and emission wavelengths were set at 480nm and 550-750nm, respectively, for DNA-bound ethidium bromide on a Perkin Elmer Luminescence Spectrometer LS50B to measure the fluorescence intensity. The order of addition of solutions into the 3mL cuvette followed: 1) DNA (final concentration in the cuvette was 60 μM); 2) EtBr (final concentration in the cuvette was 30 μM); 3) PBS buffer, used to top up the

cuvette to give a final volume of 3000 μL. The fluorescence intensity of this solution

mixture was recorded after it came to equilibrium.

A serially diluted drug DMSO solution giving a final concentration in the cuvette of 1

micromolar from its stock solution (1mg/mL) was added into the cuvette, and then the

solution was mixed well and allowed to reach equilibrium for 5min each time. Aliquots

of drug solution were added into the cuvette until the fluorescence intensity dropped to

below half the fluorescence intensity of the original drug free DNA solution. The QE_{50}

value of a drug can be defined by the concentration of this drug that can lead to a 50%

decrease of the fluorescence of original DNA-bound ethidium (Baguley and

Falkenhaug, 1978). From the plot of relative fluorescence intensity against DNA

binding ligand concentration, the apparent DNA binding constant K_{app} can be

calculated by using the equation: $K_{EB}[EB]=K_{app}[DNA$ binding ligand]. The DNA

binding ligand concentration in this equation is defined as the ligand concentration to

cause a 50% decrease of the relative fluorescence intensity of DNA-bound ethidium

bromide, and where $K_{EB}=1.0\times10^{7}M^{-1}$ (Kundu *et al.*, 2011).

3.7.1.3   DNA binding data processing using SigmaPlot 12

The DNA binding QE_{50} values for each substrate were analysed by SigmaPlot 12. The

analysis method chosen was the four parameter logistic curve equation (under the

equation category of standard curves in regression wizard equation which can be found

in nonlinear regression under analysis tab). In the equation options, the minimum Y

value was set as zero.

3.7.2 MTT assay

3.7.2.1 Materials

ER positive MCF-7 mammary carcinoma cells; RPMI-1640 medium containing phenol red (Sigma); trypsin ($1\times$); Nigrosin; NaCl (sterile); Triton X; PBS buffer; MTT **(22)**; DMSO; Test compounds: NU:UB 31 **(6)**; NU:UB 21 **(5)**.

3.7.2.2 Method

In a 96-well plate, in lane 1 (blank), contained RPMI medium only (150μL); in lanes 2 (drug-free control)-12 (with drug), each well was filled up with 150μL of 1.4×10^4cells/mL suspension. Then the 96-well plate was incubated at 37°C in a humidified, 5% CO_2 atmosphere for 24h.

On the next day, Stock solutions of NU:UB 31 **(6)**, and NU:UB 21 **(5)** were prepared at 1mM in neat DMSO, filter sterilised and diluted down to 400, 40, 4, 0.4, 0.04μM in phenol red free RPMI (reduced medium) for use.

Then 50μL of the each drug solution was added to its corresponding well. In order to make sure that the total volume in each well is the same, 50μL of RPMI medium was added into each well in lane 1 and lane 2, blank and control respectively.

The layout of the 96-well plate was:

	1	2	3	4	5	6	7	8	9	10	11	12
A												
B												
C	Blank (RPMI medium only)	Control (Cells only)	0.01μM of Drug 1	0.1μM of Drug 1	1μM of Drug 1	10μM of Drug 1	100μM of Drug 1	0.01μM of Drug 2	0.1μM of Drug 2	1μM of Drug 2	10μM of Drug 2	100μM of Drug 2
D												
E												
F												
G												
H												

Lane 1: Blank (200μL of RPMI medium)

Lane 2: Control (150μL of 1.4×10^4 cells/mL suspension + 50μL of RPMI medium)

Lane 3: 0.01μM drug concentration (150μL of 1.4×10^4 cells/mL suspension + 50μL of 0.04μM drug solution)

Lane 4: 0.1μM drug concentration (150μL of 1.4×10^4 cells/mL suspension + 50μL of 0.4μM drug solution)

Lane 5: 1μM drug concentration (150μL of 1.4×10^4 cells/mL suspension + 50μL of 4μM drug solution)

Lane 6: 10μM drug concentration (150μL of 1.4×10^4 cells/mL suspension + 50μL of 40μM drug solution)

Lane 7: 100μM drug concentration (150μL of 1.4×10^4 cells/mL suspension + 50μL of 400μM drug solution)

Then this 96-well plate was incubated at 37°C in a humidified, 5% CO_2 atmosphere for 96h.

Four days later, the 96-well plate was taken out of the incubator and centrifuged at 1000rpm for 5min. Then 100μL medium was removed from each well with care, and it was replaced with 70μL fresh RPMI medium. The MTT solution was prepared by dissolving 20mg MTT into 4mL 0.01M PBS buffer to give a concentration of 5mg/mL MTT solution. Then 2mL of this 5mg/mL MTT solution was further diluted by adding

into 5mL of RPMI medium. 50μL of this diluted MTT solution was added into each well and the 96-well plate was incubated at 37°C in a humidified, 5% CO_2 atmosphere for 4h. Blue crystals would form in the bottom of the wells. After 4h incubation, the 96-well plate was centrifuged at 1000rpm for 5min again and then all medium was removed from each well without dislodging any of the blue crystals. Then 150μL of DMSO was added into each well on the plate and mixed vigorously with care in order not to create any bubbles in the wells. Before the 96-well plate was read at the absorbance of 550nm, it was left to stand for 30min.

3.7.2.3 IC$_{50}$ calculation

The IC_{50} value for each substrate was calculated from the absorbance data of the MTT product by using SigmaPlot 12. The analysis method chosen was the four parameter logistic curve equation (under the equation category of standard curves in regression wizard equation which can be found in nonlinear regression under analysis tab). In the equation options, the minimum Y value was set as zero.

3.7.3 Chemical synthesis

3.7.3.1 Synthesis of 4-hydroxy-1-[Propyl Spacer]-AQ TFA salt YD2 (13) [4-hydroxy-1-[(3-aminopropyl)amino]anthraquinone trifluoroacetate YD2 (13)]

(Mono) *N*-tertiarybutoxycarbonyl-1,3-diaminopropane (1.024g, 6.02mmol) was added into a suspension of leucoquinizarin (1g, 4.15mmol) in the mixed solvent of ethanol

(60mL) and tetrahydrofuran (30mL), and the reaction mixture was heated over a boiling water bath for 70min. Then, the solution was cooled and aerated for two hours at RT. The oxidised crude product reaction mixture was then partitioned between chloroform and water (1:2, 300mL). The organic phase was dried (Na$_2$SO$_4$), filtered, then purified by flash chromatography on a silica gel column (4.2cm×14cm) which was eluted with dichloromethane first, then dichloromethane: ethyl acetate (19:1).

TLC, toluene: ethyl acetate (4:1), R$_f$ = 0.42 (purple) 4-hydroxy-1-[3-(*N*-tertiarybutoxy carbonyl amino)propylamino]anthraquinone (YD 1) **(15)**. Compound YD 1 **(15)** was chromatographically homogeneous (single spot on TLC).

Yield: 0.345g, 17%. Melting point: 137-138ºC.

Chromatographically pure YD1 **(15)** (300mg, 0.76mmol) was treated with trifluoroacetic acid (10mL) for half an hour, and then excess solvent was evaporated. Diethyl ether (50mL) was added to help to precipitate the title compound. TLC, butanol:acetic acid:water (4:5:1). R$_f$ = 0.6 (purple) product; homogeneous on TLC.

Yield: 0.3g, 96.8%. Melting point: 154-156ºC.

ESMS(-) m/z: 297 (100%).

3.7.3.2   Synthesis of 4-hydroxy-1-(Gly-[Propyl Spacer])-AQ TFA salt [YD4] (8) [4-hydroxy-1-[3-(glycylamino)propylamino]anthraquinone trifluoroacetate YD4 (8)] (method I)

Boc-Gly-OSu (0.332g, 1.22mmol) was dissolved in DMF (8mL), followed by addition of triethylamine (0.17mL, 1.22mmol) as base. The reaction mixture was left at RT for

15min before it was mixed with a solution of YD2 **(13)** (0.25g, 0.61mmol) in DMF (8mL). After keeping at 4°C overnight, the reaction mixture was extracted between chloroform and water (1:2, 300mL). The organic phase was dried (Na$_2$SO$_4$), filtered, then purified by flash chromatography on a silica gel column (4.2cm×12cm) which was eluted with chloroform: ethyl acetate: methanol (4:1:2%). TLC: Butanol: Acetate acid: water (4:5:1). R$_f$ = 0.87 (purple) 1-(Boc-Gly-[Propyl Spacer])-4-hydroxy-AQ [YD3] **(16)**.

Yield: 0.2018g, 73.1%. Melting point: 110-112°C.

ESMS(+) m/z: 476.1 (25%) (M+Na)$^+$.

The pure (chromatographically homogeneous) Boc-protected compound YD3 **(16)** (0.075g, 0.166mmol) was treated with trifluoroacetic acid (3mL) for half an hour. TLC, Butanol: Acetic acid: water (4:5:1), R$_f$ = 0.39 (purple) product. The solvent was evaporated to almost dryness and the residue was treated with diethyl ether to precipitate the title compound.

Yield: 0.0754g, 97.5%.

ESMS(+) m/z: 354.1 (100%) (M+H)$^+$; 707.2 (10%) (2M+H)$^+$; ESMS(-) m/z: 112.8 (100%) trifluoroacetate anion.

3.7.3.3 Synthesis of 4-hydroxy-1-(Gly-[Propyl Spacer])-AQ TFA salt [YD4] (8) [4-hydroxy-1-[3-(glycylamino)propylamino]anthraquinone trifluoroacetate YD4 (8)] (method II)

Leucoquinizarin (1g, 4.13mmol) and 1,3-diaminopropane (0.345mL, 4.13mmol) were mixed in dichloromethane (60mL). This reaction mixture was then heated over a boiling water bath for 1h. The progress of this reaction was monitored by TLC, Butanol: Acetic acid: water (4:5:1), R_f = 0.57 (purple) 4-hydroxy-1-[Propyl Spacer]-AQ [YD79] **(17)**. The crude reaction mixture was aerated for 1h at RT and then purified by flash chromatography on a silica gel column (4.2cm×4cm) which was eluted with dichloromethane: methanol (4:1). When the initial orange and dark brown fractions had eluted, then the solvent system was changed to dichloromethane: methanol (3:1) and chloroform: methanol (4:1, 150mL + 20 drops of acetic acid) to elute all of the required purple compound from the column. All fractions containing the major product were combined together, and then filtered and evaporated to dryness.

Boc-Gly-OH (0.355g, 2.03mmol), HOBt (0.31g, 2.03mmol) and TBTU (0.651g, 2.03mmol) were dissolved in DMF (10mL), then, DIPEA (1.05mL, 6.04mmol) was added and the reaction mixture was left at RT for 15min prior to addition to a stirred solution of 4-hydroxy-1-[Propyl Spacer]-AQ [YD79] **(17)** (0.6g, 2.03mmol) in DMF (10mL). After three hours, chloroform was added and the organic layer was washed with water (2×100mL), saturated sodium bicarbonate solution (2×30mL), water (100mL), dried (Na_2SO_4), filtered and evaporated *in vacuo* to a low volume. The crude

product was purified by silica gel column chromatography (4.2cm×6cm) eluting with chloroform: methanol (19:1). Due to difficulties in discerning bands − because the column turned into a very dark purple colour, small fractions from the column were collected (every 10mL) till no more major purple fraction was evident. Fractions containing the major product were combined, filtered and evaporated to near dryness, then diethyl ether was added to give a precipitate of purple Boc group protected compound YD3 (**16**). Pure (chromatographically homogeneous) YD3 (**16**) was then treated with TFA for 45min and the progress of this deprotection was checked by TLC, chloroform:methanol (9:1), [R_f = 0.1 (purple) final product] for the trifluoroacetate salt YD4 (**8**). Excess solvent was evaporated to dryness and the trifluoroacetate salt was purified by flash chromatography on a silica gel column (4.2cm×4.1cm). In the beginning, elution was conducted with chloroform: methanol (9:1). When the top and middle purple fractions (showing on TLC plates) had eluted, the solvent system was changed to chloroform: methanol (4:1, 150mL + 20 drops of acetic acid). Fractions containing major product were combined, filtered and evaporated to low volume and then diethyl ether was added to help precipitation.

Yield: 0.0841g, 9%. TLC [chloroform:methanol (9:1)]: R_f = 0.1 purple (product).

Both samples of the trifluoroacetate salt YD4 (**8**) from two synthesis methods were compared on TLC, and were shown to be identical by mixed TLC experiments.

3.7.3.4 Synthesis of 4-hydroxy-1-{[2-(2-hydroxyethyl)aminoethyl]amino} anthraquinone trifluoroacetate YD82 (11)

Leucoquinizarin (0.1g, 0.4132mmol) was mixed with 2-[(2-aminoethyl)amino]ethanol (2mL, 19.8mmol) at RT for 20min, and then the reaction slurry was extracted between chloroform and water (1:5, 300mL) immediately. Chloroform layer was dried (Na_2SO_4), filtered and evaporated to a low volume before it was loaded onto a silica gel column (2.1cm×7.5cm) which was eluted with only chloroform at first, when the yellow fraction had eluted, the solvent was changed to ethyl acetate, and finally to chloroform: methanol (4:1) to remove all of the purple compound from the column. Fractions containing the major product were combined, filtered and evaporated to dryness. TLC, chloroform: methanol (4:1), $R_f = 0.24$, (purple) YD80 (18). Then this chromatographically pure purple Boc group protected compound YD80 (18) was dissolved in TFA to form the trifluoroacetate salt YD82 (11), excess solvent was evaporated to afford the title compound.

Yield: 23.1mg, 12.7%.

^{1}H NMR (DMSO-d$_6$, 300 MHz) δ: 3.03 (2H, s, AQ-NHCH$_2$C$\underline{H}_2$), 3.19 (2H, s, RCH$_2$C$\underline{H}_2$OH), 3.65 (2H, s, AQ-NHC$\underline{H}_2$), 3.77 (2H, s, RCH$_2$C$\underline{H}_2$OH), 5.29 (1H, s, R(CH$_2$)$_2$O$\underline{H}$), 7.38 (1H, d, C$_2$-C$\underline{H}$), 7.58 (1H, d, C$_3$-C$\underline{H}$), 7.89 − 7.96 (2H, m, C$_6$-C$\underline{H}$ and C$_7$-C$\underline{H}$), 8.25 -8.29 (2H, m, C$_5$-C$\underline{H}$ and C$_8$-C$\underline{H}$), 10.20 (1H, t, AQ-N$\underline{H}$).

Cyclisation compound B (20) ^{1}H NMR (DMSO-d$_6$, 300 MHz) δ: 3.56 (6H, m, $-NH-(CH_2)_2-N-CH_2-R$), 3.69 (2H, t, -C$\underline{H}_2$OH), 4.92 (1H, s, -CH$_2$O$\underline{H}$), 6.24 (1H, s,

C$_3$-C$\underline{H}$), 7.76 – 7.80 (2H, m, C$_6$-C$\underline{H}$ and C7-C$\underline{H}$), 8.19 – 8.22 (2H, m, C$_5$-C$\underline{H}$ and C$_8$-C$\underline{H}$), 11.06 (1H, s, AQ-N$\underline{H}$-).

3.7.3.5 Synthesis of 1-{[2-(2-hydroxyethyl)aminoethyl]amino}anthraquinone trifluoroacetate NU:UB466 (12)

1-Chloroanthraquinone (0.5g, 0.0021mol) and 2-[(2-aminoethyl)amino]ethanol (3.125mL, 0.0309mol) were mixed together. DMSO (3mL) was added to this reaction mixture to aid dissolution. The reaction mixture was heated over a boiling water bath for 30min. The progress of this reaction was monitored on TLC plates, dichloromethane:methanol (3:2), R$_f$ = 0.34 (red) NU:UB 466 free base **(21)**. Then the reaction mixture was extracted between chloroform and water (1:5, 300mL), dried (Na$_2$SO$_4$), filtered and evaporated to a low volume before it was purified by flash chromatography on a silica gel column (4.2cm×10cm) which was eluted with dichloromethane:methanol (3:2). Fractions containing the major red product were combined, filtered and evaporated. Then NU:UB 466 free base **(21)** was dissolved in TFA for 5min to form a red NU:UB 466 **(12)**, excess solvent was evaporated to almost dryness and then diethyl ether added to precipitate the title compound.

^{1}H NMR (DMSO-d$_6$, 300MHz) δ: 3.08 (2H, dd, AQ-NHCH$_2$C$\underline{H}_2$), 3.22 (2H, m, RC$\underline{H}_2$CH$_2$OH), 3.67 (2H, dd, AQ-NHC$\underline{H}_2$), 3.77 (2H, m, RCH$_2$C$\underline{H}_2$OH), 4.66 (1H, t, R(CH$_2$)$_2$O$\underline{H}$),7.35 (1H, d, C$_2$-C$\underline{H}$), 7.49 (1H, d, C$_4$-C$\underline{H}$), 7.69 (1H, t, C$_3$-C$\underline{H}$), 7.85 – 7.92 (2H, m, C$_6$-C$\underline{H}$ and C$_7$-C$\underline{H}$), 8.13 – 8.20 (2H, m, C$_5$-C$\underline{H}$ and C$_8$-C$\underline{H}$), 8.73 (2H, s, RN$\underline{H}_2^+$(CH$_2$)$_2$OH), 9.72 (1H, t, AQ-N$\underline{H}$).

3.8 <u>REFERENCES</u>

Agbandje, M., Jenkins, T. C., McKenna, R., Reszka, A. P. and Neidle, S. (1992) Anthracene-9,10-diones as potential anticancer agents. Synthesis, DNA-binding, and biological studies on a series of 2,6-disubstituted derivatives. *J. Med. Chem.* **35**(8), 1418-29.

Baguley, B. C., Denny, W. A., Atwell, G. J. and Cain, B. F. (1981) Potential antitumor agents. 34. Quantitative relationships between DNA binding and molecular structure for 9-anilinoacridines substituted in the anilino ring. *J. Med. Chem.* **24**(2), 170-7.

Baguley, B. C. and Falkenhaug, E. M. (1978) The interaction of ethidium with synthetic double-stranded polynucleotides at low ionic strength. *Nucleic. Acids. Res.* **5**(1), 161-71.

Chaires, J. B. (1998) Drug-DNA interactions. *Curr. Opin. Struct. Biol.* **8**(3). 314-320.

Chen, C. L., Fuscoe, J. C., Liu, Q. and Relling, M. V. (1996) Etoposide causes illegitimate V(D)J recombination in human lymphoid leukemic cells. *Blood.* **88**(6), 2210-8.

De Isabella, P., Capranico, G., Palumbo, M., Sissi, C., Krapcho, A. P. and Zunino, F. (1993) Sequence selectivity of topoisomerase II DNA cleavage stimulated by mitoxantrone derivatives: relationships to drug DNA binding and cellular effects. *Mol. Pharmacol.* **43**(5), 715-21.

Errington, F., Willmore, E., Leontiou, C., Tilby, M. J. and Austin, C. A. (2004) Differences in the longevity of topo IIalpha and topo IIbeta drug-stabilized cleavable complexes and the relationship to drug sensitivity. *Cancer Chemother. Pharmacol.* **53**(2), 155-62.

Errington, F., Willmore, E., Tilby, M. J., Li, L., Li, G., Li, W., Baguley, B. C. and Austin, C. A. (1999) Murine transgenic cells lacking DNA topoisomerase IIbeta are resistant to acridines and mitoxantrone: analysis of cytotoxicity and cleavable complex formation. *Mol. Pharmacol.* **56**(6), 1309-16.

Fotakis, G. and Timbrell, J. A. (2006) In vitro cytotoxicity assays: comparison of LDH, neutral red, MTT and protein assay in hepatoma cell lines following exposure to cadmium chloride. *Toxicol. Lett.* **160**(2), 171-7.

Kundu, S., Maity, S., Bhadra, B and Ghosh, P. (2011) Trans-dichlorobis (*N*-p-tolylpyridin-2-amine) palladium (II): Synthesis, structure, fluorescence features and DNA binding. *Indian J. Chem.* **50**, 1443-1449.

Lerman, L. S. (1961) Structural considerations in the interaction of DNA and acridines. *J. Mol. Biol.* **3**(1), 18-30.

Li, N., Ma, Y., Yang, C., Guo, L. and Yang, X. (2005) Interaction of anticancer drug mitoxantrone with DNA analyzed by electrochemical and spectroscopic methods. *Biophys. Chem*. **116**(3), 199-205.

Lown, J. W., Morgan, A. R., Yen, S. F., Wang, Y. H. and Wilson, W. D. (1985) Characteristics of the binding of the anticancer agents mitoxantrone and ametantrone and related structures to deoxyribonucleic acids. *Biochemistry*. **24**(15), 4028-35.

Morgan, A. R., Lee. J. S., Pulleyblank, D. E., Murray, N. L. and Evans, D. H. (1979) Review: ethidium fluorescence assays. Part 1. Physicochemical studies. *Nucleic Acids Res*. **7**(3), 547-69.

Murdock, K. C., Child, R. G., Fabio, P. F., Angier, R. B., Wallace, R. E., Durr, F. E. and Citarella, R. V. (1979) Antitumor agents. 1. 1,4-Bis[(aminoalkyl)amino]-9,10-anthracenediones. *J. Med. Chem*. **22**(9), 1024-30.

Nakamoto, K., Tsuboi, M. and Strahan, G. D. (2008) 'Intercalating drugs' in: Nakamoto, K., Tsuboi, M. and Strahan, G. D. *Drug-DNA interactions structures and spectra.* Hoboken: John Wiley & Sons, Inc., 119-199.

Neto, B. A. and Lapis, A. A. (2009) Recent developments in the chemistry of deoxyribonucleic acid (DNA) intercalators: principles, design, synthesis, applications and trends. *Molecules*. **14**(5), 1725-46.

Newton, B. A. (1957) The mode of action of phenanthridines: the effect of ethidium bromide on cell division and nucleic acid synthesis. *J. Gen. Microbiol*. **17**(3), 718-30.

Nordmeier, E. (1992) Absorption spectroscopy and dynamic and static light-scattering studies of ethidium bromide binding to calf thymus DNA: implications for outside-binding and intercalation. *J. Phys. Chem*. **96**(14), 6045-6055.

Olmsted, J. III and Kearns, D. R. (1977) Mechanism of ethidium bromide fluorescence enhancement on binding to nucleic acids. *Biochemistry*. **16**(16), 3647-3654.

Osheroff, N. (1989) Effect of antineoplastic agents on the DNA cleavage/relegation reaction of eukaryotic topoisomerase II: inhibition of DNA religation by etoposide. *Biochemistry*. **28**(15), 6157-60.

Palchaudhuri, R. and Hergenrother, P. J. (2007) DNA as a target for anticancer compounds: methods to determine the mode of binding and the mechanism of action. *Curr. Opin. Biotechnol*. **18**(6), 497-503.

Pettersson, S. (2004) Biochemistry of topoisomerase inhibition and cellular mechanism of anthraquinone-amino acid conjugates in vitro. PhD, Edinburgh Napier University.

Plumb, J. A., Milroy, R. and Kaye, S. B. (1989) Effects of the pH dependence of 3-(4,5-dimethylthiazol-2-yl)-2,5-diphenyl-tetrazolium bromide-formazan absorption on chemosensitivity determined by a novel tetrazolium-based assay. *Cancer Res*. **49**(16), 4435-40.

Pritchard, N. J., Blake, A. and Peacocke, A. R. (1966) Modified intercalation model for theinteraction of amino acridines and DNA. *Nature*. **212**, 1360-1361.

Quigley, G. J., Wang, A. H., Ughetto, G., van der Marel, G., van Boom, J. H. and Rich, A. (1980) Molecular structure of an anticancer drug-DNA complex: daunomycin plus d(CpGpTpApCpG). *Proc. Natl. Acad. Sci. U S A*. **77**(12), 7204-8.

Smith, L. A., Cornelius, V. R., Plummer, C. J., Levitt, G., Verrill, M., Canney, P. and Jones, A. (2010) Cardiotoxicity of anthracycline agents for the treatment of cancer: systematic review and meta-analysis of randomised controlled trials. *BMC Cancer*. **10**, 337-350.

Turnbull, A. (2003) Design and development of novel DNA topoisomerase inhibitors. PhD, Edinburgh Napier University.

Wallace, R. E., Murdock, K. C., Angier, R. B. and Durr, F. E. (1979) Activity of a novel anthracenedione,1,4-dihydroxy-5,8-bis(((2-[(2-hydroxyethyl)amino]ethyl)amino])-9,10-anthracenedione dihydrochloride, against experimental tumors in mice. *Cancer Res*. **39**(5), 1570-4.

Williams, L. D., Egli, M., Gao, Q. and Rich, A. (1992) DNA intercalation: helix unwinding and neighbour-exclusion. In *Structure & function; Vol. 1: Nucleic Acids* (Sarma, R. H. and Sarma, M. H. Eds.). 107-125, Academic Press.

Willmore, E., Frank, A. J., Padget, K., Tilby, M. J. and Austin, C. A. (1998) Etoposide targets topoisomerase IIalpha and IIbeta in leukemic cells: isoform-specific cleavable complexes visualized and quantified in situ by a novel immunofluorescence technique. *Mol. Pharmacol*. **54**(1), 78-85.

Zee-Cheng, R. K. and Cheng, C. C. (1978) Antineoplastic agents. Structure-activity relationship study of bis(substituted aminoalkylamino)anthraquinones. *J. Med. Chem*. **21**(3), 291-4.

Zee-Cheng. R. K., Podrebarac, E. G., Menon, C. S. and Cheng, C. C. (1979) Structural modification study of bis(substituted aminoalkylamino)anthraquinones. An evaluation of the relationship of the [2-[(2-hydroxyethyl)amino]ethyl]amino side chain with antineoplastic activity. *J. Med. Chem*. **22**(5), 501-505.